TECHNICAL UNIVERSITY OF MOLDOVA

JOURNAL OF ENGINEERING SCIENCE

Technical and applied scientific publication founded on 9 February 1995
Alternative title: Meridian ingineresc

2025
Vol. XXXII (2)

ISSN 2587-3474
eISSN 2587-3482

TECHNICAL UNIVERSITY OF MOLDOVA (PUBLISHING HOUSE)
„TEHNICA UTM" (PRINTING HOUSE)

According to the Decision of the NAQAER No. 12 from 23.02.2024, JES is classified as B+ journal

Main subjects areas of the Journal of Engineering Science:

A. Industrial Engineering

- Mechanical Engineering and Technologies
- Applied Engineering Sciences and Management
- Materials Science and New Technologies
- Electrical Engineering and Power Electronics
- Energy systems
- Light Industry, New Technologies and Design
- Industrial and Applied Mathematics
- Vehicle and Transport Engineering

B. Electronics and Computer Science

- Electronics and Communication
- Microelectronics and Nanotechnologies
- Biomedical Engineering
- Computers and Information Technology
- Automation

C. Architecture, Civil and Environmental Engineering

- Architecture, Urbanism and Cadaster
- Civil Engineering and Management
- Energy Efficiency and New Building Materials
- Environmental Engineering

D. Food Engineering

- Food Technologies and Food Processes
- Food Industry and Management
- Biotechnologies, Food Chemistry and Food Safety
- Equipment for Food Industries

The structure of the journal corresponds to the classification of scientific publications: ***Engineering, Multidisciplinary.***

How to publish a paper:

1. Send the manuscript and information about the author to the **Editorial Board address:** jes@meridian.utm.md
2. Manuscripts are accepted only in English, by e-mail, in template file (www.jes.utm.md)
3. After a review, you will be notified of the editorial board's decision.
4. After the Journal has been published, we will send it to you immediately by mail.

Editor-in-Chief
Dr. hab. prof. univ. Viorel BOSTAN
Technical University of Moldova
viorel.bostan@adm.utm.md

Editorial Board

Responsible Editor
Dr. hab. Rodica STURZA
Editorial Board address: jes@meridian.utm.md

Editorial Production:
Dr. hab. Aliona Ghendov-Moșanu
Dr. Nicolae Trifan
Dr. Svetlana Caterinciuc
Dr. Rodica Cujba

CONTENT

CUPRINS

Journal of Engineering Science *Vol. XXXII, no. 2 (2025), pp. 7 - 25*
Fascicle *Industrial Engineering* *ISSN 2587-3474*
Topic *Applied Engineering Sciences and Management* *eISSN 2587-3482*

https://doi.org/10.52326/jes.utm.2025.32(2).01
UDC 656.11.053.3

ROUNDABOUT – ELEMENT OF SAFETY, ECOLOGY AND ECONOMY

Olivian Pădure *, ORCID: 0000-0002-6024-3763,
Vasile Plămădeală, ORCID ID: 0000-0003-1722-2649,
Vladimir Goian, ORCID: 0000-0002-0031-0389

Technical University of Moldova, 168 Stefan cel Mare Blvd., Chisinau, Republic of Moldova
* Corresponding author: Olivian Pădure, *olivian.padure@tran.utm.md*

Received: 05. 15. 2025
Accepted: 06. 12. 2025

Abstract. Statistical analysis reinforces the conclusion that road accidents are not random and even more unpredictable or unavoidable, although their occurrence is random. The concentration of road accidents at intersections is high, around 25-30% of the total number of road accidents. The intersection itself is an area of concentration of conflict points, where the occurrence of road accidents is both theoretically and practically possible due to the contact of vehicle flows from three different directions: intersecting, separating and merging. Increasing the safety of intersections therefore boils down to taking measures to reduce the number of conflict points and the degree of their potential danger. The article describes the purpose, advantages and disadvantages, conflict points, classification and types of roundabouts. The benefits of roundabout organization in terms of road traffic safety, environmental safety and increasing the road's passing capacity, thus reducing waiting time at intersections, are also analyzed.

Keywords: *roundabout, intersection, conflict points, road accidents, road traffic safety, environmental safety, roundabout capacity.*

Rezumat. Analizele statistice întăresc concluzia, că accidentele rutiere nu sunt întâmplătoare şi cu atât mai mult imprevizibile sau inevitabile, cu toate că apariţia lor este aleatoare. Concentrația accidentelor rutiere la intersecții este una mare, circa 25-30% din numărul total de accidente de circulație. Intersecția prezintă în sine o zonă de concentrare a punctelor de conflict, unde apariția accidentului rutier atât teoretic, cât și practic este posibilă datorită contactului fluxurilor de vehicule din trei direcții diferite: de intersectare, separare și fuzionare. Prin urmare, creșterea siguranței intersecțiilor se reduce la întreprinderea unor măsuri de reducere a numărului punctelor de conflict și gradului de pericol potențial al acestora. În articol sunt descrise destinația, avantajele și dezavantajele, punctele de conflict, clasificarea și tipurile de sensuri giratorii. De asemenea, sunt analizate beneficiile organizării sensului giratoriu privind siguranța traficului rutier, securitatea ecologică și ridicarea capacității de trecere a drumului, astfel reducând timpul de așteptare la intersecții.

Cuvinte cheie*: sens giratoriu, intersecție, puncte de conflict, accidente rutiere, siguranța circulației rutiere, siguranța ecologică, capacitate de trecere a intersecției.*

1. Introduction

In global road traffic management practices, one of the most effective methods of reducing traffic accidents is considered to be roundabout intersections [1]. In many countries in Western Europe, North America and Australia, the effectiveness of using roundabouts is convincingly confirmed by the reduction of all crash indicators, in particular by the reduction in crash severity and the decrease in the number of road traffic accidents with fatalities.

Roundabout intersection or ***roundabout*** is the intersection, where approaching vehicles decelerate and begin to circle around the central „*island*" counterclockwise on roads with traffic on the right side of the road, or clockwise on roads with traffic on the left side of the road, until exiting onto a roundabout arterial (convergence) [2].

Roundabouts are intersections formed by a one-way circular path around a central island. Thus, the roundabout can be compared as a one-way road with a sequence of T-intersections (Figure 1) [3-5].

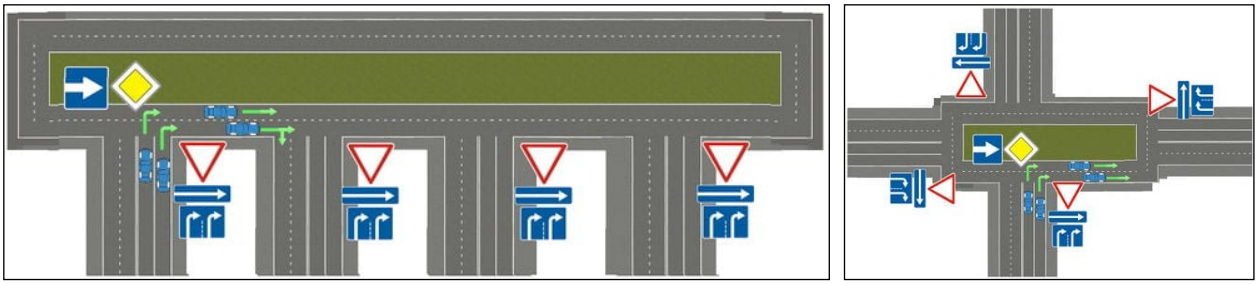

Figure 1. Roundabout intersection shown as a one-way road with a sequence of T-junctions [3,4].

In the literature, roundabouts are attached to a broad class of circular road junctions (circular intersections). However, not every circular road junction is considered to be a roundabout. There are three types of circular road junctions [1].

Rotaries are an old type of circular road junctions, characterized by a large diameter, sometimes exceeding 100 m. The large diameter is due to the high projected traffic speeds, which exceed 50 km/h. Such junctions provide a slight deviation from linear traffic and may operate according to the „*right obstruction*" rule (in countries with right-hand traffic), i.e. traffic entering the circle has priority over traffic moving in the circle.

Neighborhood traffic circles are circular road junctions usually located on local streets in residential areas for traffic calming. The entrances to such junctions may be undirected or accompanied by signs and road markings, which indicate the priority of traffic on the circle. Such intersections are usually not accompanied by flow channelization (i.e. no separation islands are created at the entrance along the roadway axis). Lately, this type of roundabout intersection is becoming more widespread and is used as a means of traffic calming.

Roundabouts are circular road nodes with established geometrical parameters and form of organization of the flow of road traffic, including [1]:

- „*Yield*" or „*Mandatory stop*" road signs at circle entrances [6];
- geometry of the intersection in plan – radii of the roadway side of the circle, of the unimmediate entrances to and exits from the roadway side of the circle, of the approaches to the intersection, which do not allow the development of a speed greater than 50 km/h;
- mandatory canalization of road flows at the entrances to the circle, while the separation islands at the entrances are used as safety islands for pedestrians.

The term ***roundabouts*** originated in the United Kingdom as early as 1929 with the Ministry of Transportation and the Institute of Town and Country Planning. It should be noted that Florida's Roundabout Intersection Guidelines (FRG 1996) introduced a new term ***„modern roundabout"***, which has come to be commonly used in technical literature.

The first roundabout was organized in Paris around the Arc de Triomphe in 1901. Columbus Circle in New York was built in 1904. The first British roundabout followed in 1909 (Letchworth Garden City) – originally planned as a pedestrian island. Later, during 1925-1926 in the UK, several roundabout intersections were built in different parts of London. At that time, when designing intersections, they were guided only by accumulated experience and intuition. Widespread use began in the mid-1960s, when English engineers perfected the system for guiding the flow of cars [1].

In fact, in 1966, the UK adopted a new priority rule – the main road flow moving around the circle has priority over the main road flow entering the circle. With the introduction of this innovation (modification) to roundabouts, the through capacity (by 10-40%, according to a study by the Road Research Laboratory) and traffic safety levels increased significantly. The success of the introduction of modern roundabouts has revived interest in this type of intersections worldwide, especially in Europe.

Since the late 1980s, roundabouts have become a widespread solution for road intersections in several countries, including the Netherlands, Norway, France, Switzerland, Sweden, Switzerland, the United States of America, Australia etc. In the Netherlands, about 400 roundabouts were built in just six years, due to their advantages such as reduced accidents and the absence of the need for traffic lights. In Norway, the number increased significantly between 1990 and 1992, reaching 500 roundabout intersections. France has seen a rapid increase, reaching about 12080 roundabouts at the end of 1994 and more than 27000 in 2005. In Sweden, there has been a significant increase in the number of roundabouts (more than 1000 in 2000), with studies showing that single-lane circles with a central island diameter of 10 to 20 m are the safest, reducing speed and accidents, especially those involving cyclists. The United States began building modern roundabouts in the 1990s with excellent results in reducing accidents, and by 2002 the number had exceeded 600. In the meantime, roundabouts have become very popular in many countries. In Australia, for example, the number has risen to over 10000, in the UK to over 25000 and in France to over 32000 [7].

At busy intersections, waiting times for yielding transportation can be quite long. This would create opportunities for some road users to use all sorts of time-saving tricks. Intersection points and frequent turning conditions create dangerous situations, thus the overall traffic picture becomes seemingly uncontrollable.

The traffic conditions at an intersection have a specific character, due to the existence of points where vehicle flows intersect with each other and vehicle flows with pedestrian flows. These points of contact are called „*conflict points*", as they are where collisions are most likely to occur. In the case of the intersection of two roads with X-shaped two-way traffic (Figure 2a), 32 possible „*vehicle-vehicle*" conflict points can be determined [5-11], of which 16 intersection points (red color), 8 separation points (green color) and 8 merging points (blue color), as well as 8 possible „*vehicle-pedestrian*" conflict points (white color) [12].

As a rule, intersection points represent the greatest potential hazard, since the severity of the consequences of a road accident is greater than in the case of a road accident at the

points where the flows separate or merge. The number of conflict points and the potential danger of the intersection increases [12]:

- as traffic intensity increases;
- in the absence of direction restrictions;
- when the number of traffic lanes increases;
- when the width of the roadway increases;
- in the absence of restrictions on the choice of lanes for the intersection of vehicle and pedestrian flows etc.

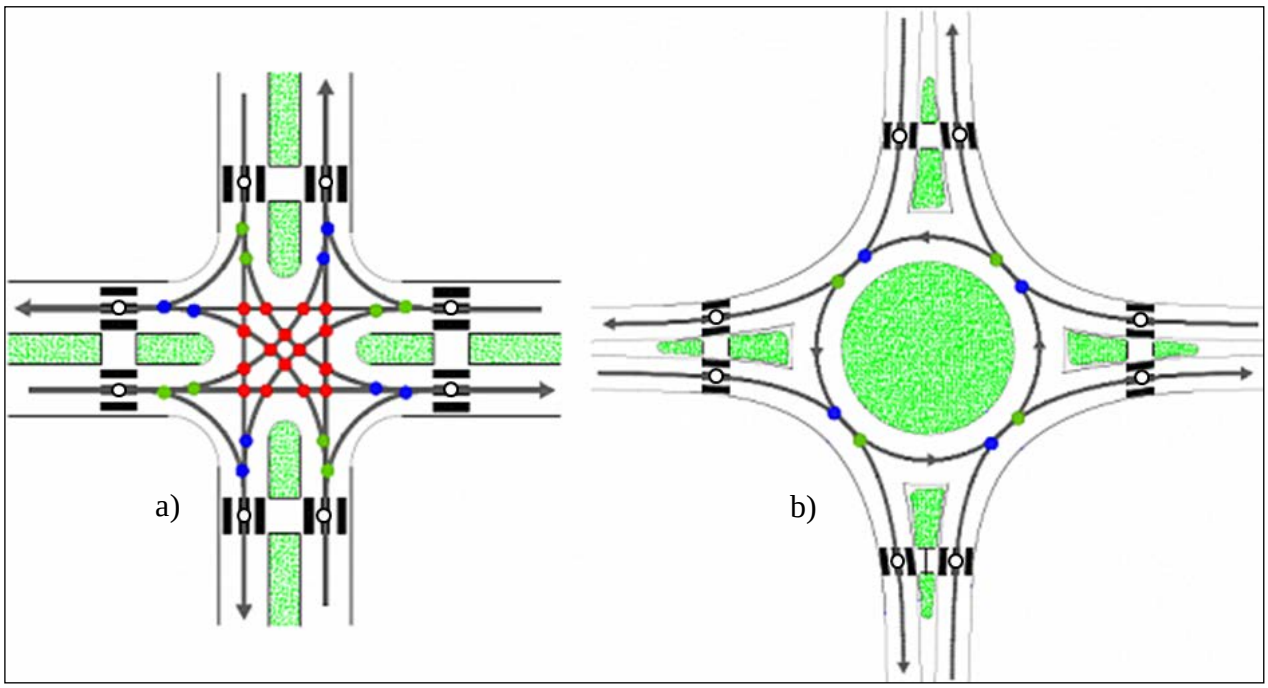

Figure 2. Possible conflict points in an intersection [8]:
a) X-shaped intersection; b) roundabout intersection.

Frequent intersections and junctions of secondary roads with the main road hinder the smooth flow of traffic on the main road, increasing the potential risk of road accidents along its entire length.

The risk of a traffic accident increases, in particular, when traffic intensity on secondary roads increases. In the absence of means of directing traffic, the waiting time at the entrance from the secondary road to the main road can be quite long. This causes drivers on the secondary road to take dangerous actions to reduce the waiting time, e.g. speeding up in order to „*squeeze through*".

Multi-lane roundabouts, although they can increase traffic handling capacity, can create new conflict points between traffic participants (Figure 3). When a roundabout has only one traffic lane, traffic usually flows smoothly. However, in the case of multi-lane roundabouts, vehicles choose different paths based on their intentions to accelerate, which can lead to path intersections.

At the same time, drivers crossing a roundabout tend to travel in the most direct and shortest path. These intersections are not always foreseen in the original design and can create conflicts which, during periods of freer traffic, can be even more frequent, thus increasing the risk of accidents.

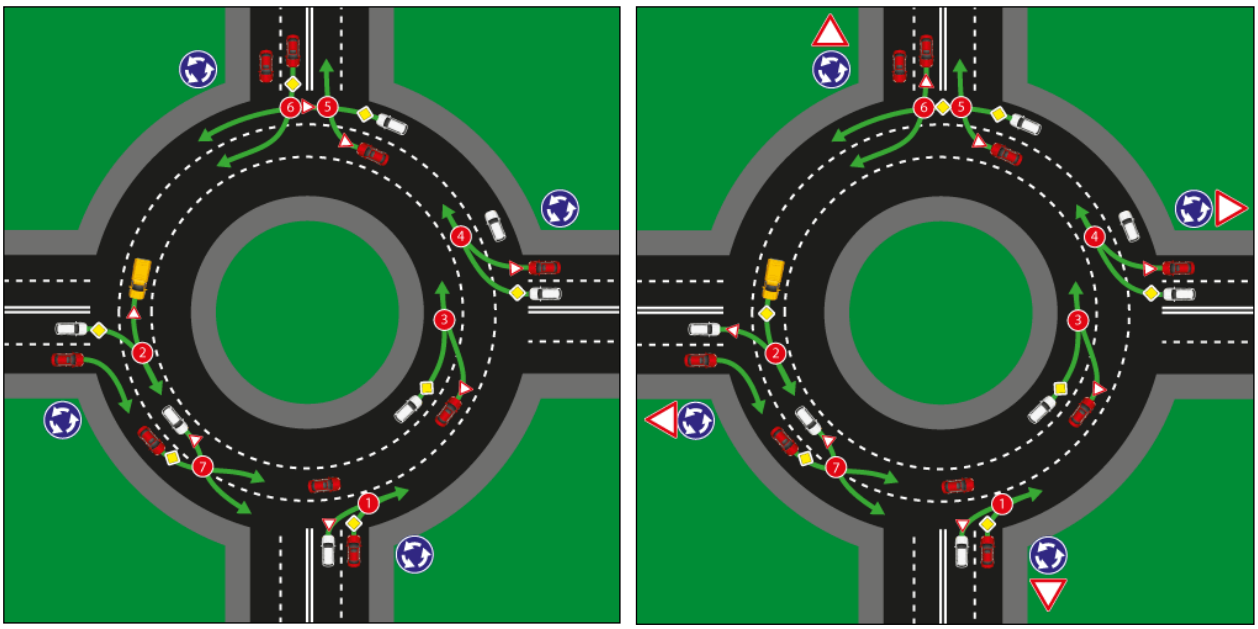

a) b)

Figure 3. Possible conflict points at a roundabout intersection multi-lane roundabout [13]: a) equivalent intersection; b) non-equivalent intersection.

Another negative aspect is that widening the roundabout does not always bring a proportional increase in traffic capacity. In multi-lane roundabouts, the center lanes are often less used, which leads to an inefficient use of the whole infrastructure and can cause congestion in the peripheral sections with a higher flow of vehicles. Thus the total capacity of the roundabout does not always align with traffic requirements.

2. Solutions to improve road traffic flow and safety

In order to improve traffic flow and reduce the risk of road accidents on high-traffic priority roads, it is usually recommended to design intersections in two or more levels. Various variants of such intersections are used, but they require large capital investments.

The rich experience of some countries shows that less costly solutions can be used on public roads with low traffic intensity, which successfully improve traffic flow and safety. Proven and effective solutions include [9-11]:

- dividing the X-shaped intersection into two T-shaped ones;
- application of speed limiting measures by raising the intersection area, pedestrian crossing or applying artificial speed bumps;
- channelization (routing) through the space in the form of markings of separating and merging flows;
- channelization of flows by means of graded spaces (islands);
- the organization of additional lanes in order not to hinder the movement of vehicles entering and exiting the intersection when turning right;
- organization of the additional lanes in order not to hinder traffic in the intersection by vehicles turning left;
- organization of the left-turn manoeuvre at right-turning intersections;
- reorganizing the Y- or X-shaped intersection into a roundabout intersection etc.

It is often proposed to build additional traffic lanes to increase the through capacity of busy intersections. Practice in many countries shows that increasing the number of lanes

at intersections leads to an increase in the number of road accidents. Norwegian studies show that after widening the intersection, the number of road accidents with injuries increases on average by 10% and the number of road accidents with property damage doubles. This phenomenon is explained by the following [11]:

- the wider road in the intersection causes drivers to increase speed to cross the intersection faster;
- the wider roadway increases the length of the pedestrian crossing, therefore also the length of time pedestrians is on the roadway side;
- additional traffic lanes increase the willingness and possibilities to change lanes in the vicinity of the intersection, which increases the risk of road accidents not only at the intersection itself but also in the vicinity of the intersection.

Therefore, in order to increase the passing capacity of congested intersections, nowadays more and more often, the reorganization of these intersections into roundabouts is applied. The aim and purpose of roundabout intersections are the following [14]:

- distribution of road flows in nodes with a complex structure and a large number of intersecting roads;
- increasing the through capacity of the intersection and reducing waiting time in front of the intersection;
- increase road traffic safety;
- traffic calming;
- creating an architectural style specific to the urban environment;
- introducing convenient forms of traffic management for left-turning and turning traffic flows;
- reducing noise and traffic speed when locating junctions in close proximity to medical and educational institutions etc.

The organization of roundabouts is not recommended: on road sections with a longitudinal gradient of more than 4%; at the beginning and end of road sections with long slopes and ramps; in the immediate vicinity of railway level crossings; when vehicles with an increased gauge size of more than 25% are present in the traffic flow.

3. Advantages and disadvantages of organizing roundabouts

Roundabout organization has the following advantages [3,7,11,14,15]:

✓ reducing the theoretical number of „*vehicle-vehicle*" conflict points from 32 to 8 (Figure 2b), of which 4 separation points (green color) and 4 merging points (blue color), as well as 8 possible vehicle-pedestrian conflict points (white color);

✓ eliminating the area, where the most serious road accidents occur, with the help of the central island, which „*covers*" the area of the most dangerous intersection conflict points;

✓ the complete elimination of the risk of serious head-on collision road crashes, with only the less dangerous conflict points of separation and merging of road flows, which reduce the likelihood and severity of road crashes;

✓ low speed forcing by design, which forces drivers to slow down on entry, reducing the risk of serious crashes;

✓ achieving the self-regulating property inherent to roundabouts, which ensures a constant uninterrupted flow of traffic at low speed, as opposed to traffic light routing;

✓ one-way routing of traffic inside the circle, which does not cause psychological stress on the driver's part due to the need to monitor traffic from other directions when waiting for the intersection entry interval;

✓ exclusion of left-turn situation and turning maneuver from oncoming traffic;

✓ low traffic speed, due to the smooth and calm rotation around the center island, which allows drivers to adequately assess the traffic situation and respond quickly, and in case of a road accident, the consequences, as a rule, do not become serious for the occupants of the car, being limited only to damage to the vehicle body;

✓ the slow deceleration of the traffic flow on the circle, which reduces the number of braking – stopping – acceleration, helps to reduce the negative impact of transport on the environment (emissions, noise);

✓ achieving more efficient traffic organization when passing through a junction with 4 or more roads;

✓ reduced capital costs compared to multi-level junctions;

✓ reduced maintenance compared to signalized intersections, which require constant electricity, repairs and calibration;

✓ lower long-term costs; once built, a roundabout can operate for decades with minimal intervention;

✓ adaptability, which allows the effective use of roundabouts in various types of intersections: from urban, moderately trafficked intersections to major highway intersections;

✓ increase traffic safety by 1.5-3 times compared to other types of intersections at the same level;

✓ the organization of roundabouts helps to reduce the number of road accidents and the severity of their consequences etc.

Among the disadvantages of the roundabout are [3,14,15]:

➢ need in large areas of land compared to classic intersections, which can be a problem in dense urban areas with old infrastructure or buildings close to intersections;

➢ reduced average traffic speed;

➢ difficulties in organizing the crossing of pedestrians and cyclists in the absence of special infrastructure;

➢ waiting time at the entrance to the circle during rush hours, when priority is given to vehicles traveling on the circle;

➢ difficulties in organizing priority for passing vehicles;

➢ confusion for inexperienced or unfamiliar drivers, roundabouts, which can cause uncertainty or hesitation;

➢ inefficiency in heavy traffic when roundabouts can become congested, requiring additional interventions such as temporary traffic lights;

➢ high upfront costs for design, construction and relocation of existing infrastructure;

➢ increased risk of tipping of vehicles with high center of gravity as traffic speeds increase;

➢ maneuvering difficulties for large vehicles, particularly at small roundabouts, requiring special solutions such as traversable center islands;

➢ the need to create a fairly complex system of information assistance for drivers on traffic conditions etc.

4. Types of roundabouts

In order to ensure a unified approach to the purpose, scope, geometric parameters, design and traffic organization, roundabout intersections are classified as follows [3,12,14]:

Large roundabouts. They are primarily used on roads outside settlements with high design speeds. Entering the roundabout is performed with right turn, driving on the roundabout forward and exiting the roundabout with right turn. The outer diameter of the middle island of these circles is 100-120 m (Figure 4a), the estimated design speed – 50 km/h, the number of converging roads ⩽ 4, the estimated intensity – up to 70 thousand vehicles/24 h, the number of lanes on the entrance/exit – 2/2-3/3 and the number of lanes on the circle roadway – 2-3.

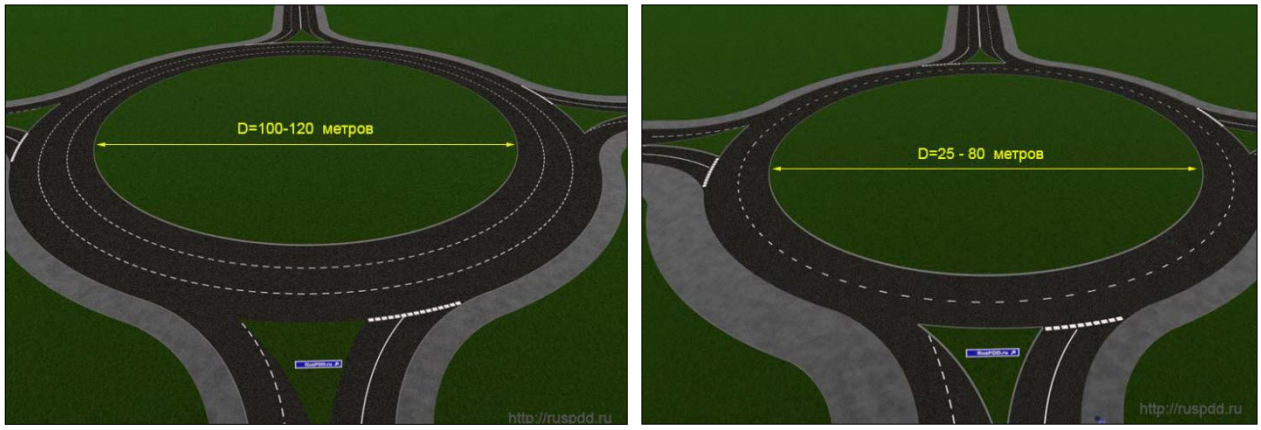

a) b)

Figure 4. Roundabout intersection [3, 12]:
a) large roundabout; b) medium roundabout.

Medium roundabouts. These are the most common intersections of this type for urban and non-urban roads. They possess a fairly high through capacity at a small node area. The outer diameter of the middle island of these circles is 25-80 m (Figure 4b), estimated design speed – 35-40 km/h, number of converging roads ⩽ 5, estimated intensity – up to 35-40 thousand vehicles/24 h, number of lanes on the entrance/exit – 2/2-3/3 and number of lanes on the circle roadway – 2-3.

Small roundabouts. Abroad, this type of intersection is called compact. It is recommended to be used at the nodes of the local road network and trunk road network of regional significance. The outside diameter of the middle island of such circles is 20-25 m (Figure 5a), the outside diameter of the roadway – not more than 30 m, the width of the 4,5-5,5 m, design speed – 25 km/h, number of convergent roads ⩽ 4, estimated intensity – up to 20-25 thousand vehicles/24 h, number of lanes on entry/exit – 1/1 and number of lanes on the circle – 1.

At intersections with small roundabouts it is possible to organize a marginal lane of the middle island for large vehicles (Figure 5b). At such intersections it is no longer logical to apply the „*classical*" maneuvering scheme to the roundabout. Here, the right turn is passed through the circle in a single maneuver, and the entry onto the circle takes place from the steering island tangentially to the middle island.

Mini roundabouts. These are used on local road networks for traffic calming. The outside diameter of the middle island of these circles is 13-18 m (Figure 6a), estimated design speed – 15-25 km/h, number of converging roads ⩽ 4, estimated intensity – up to 15-20

thousand vehicles/24 h, number of lanes on the entry/exit – 1/1 and number of lanes on the circle roadway – 1.

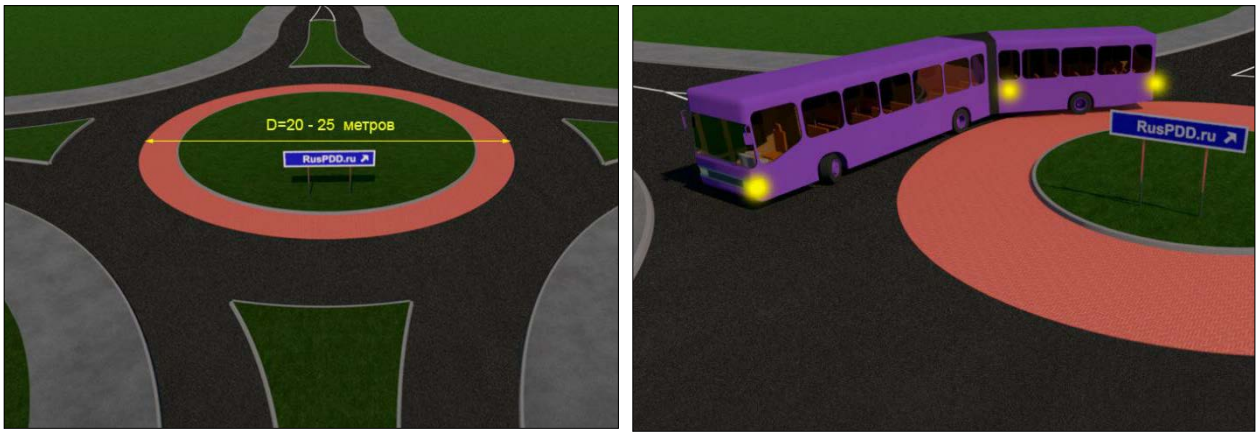

a) b)

Figure 5. Roundabout [3, 12]:
a) small roundabout; b) marginal lane of the middle island for large vehicles.

At intersections with mini roundabouts, as well as at intersections with small roundabouts, a marginal lane of the middle island is organized for large vehicles (Figure 4b). The right turn and the entrance to the circle are identical.

Roundabout road surfaces. These (Figure 6b) represent nodes formed in the process of historical development and organized for roundabout traffic. Road surfaces, when organizing the roundabout on them, are not subject to systematization and classification. The parameters of these intersections are determined by calculation or modeling methods.

The main initial data, in this case, are the dimensions of the road surface, the intensity and composition of road flows, the correspondence matrix, the traffic management schemes on converging streets. At these intersections also the „classical" circular movement does not fit. Traveling in the circle at some exits might continue straight ahead in the right direction, at others go left. The entry on the circle, too, can be performed both in the forward direction and turning right. Estimated design speed – 20-40 km/h, number of converging roads ⩾ 3, estimated intensity – up to 60 thousand vehicles/24 h, number of lanes on the entrance/exit – 1/1-3/3 and number of lanes on the circle roadway – 2-3.

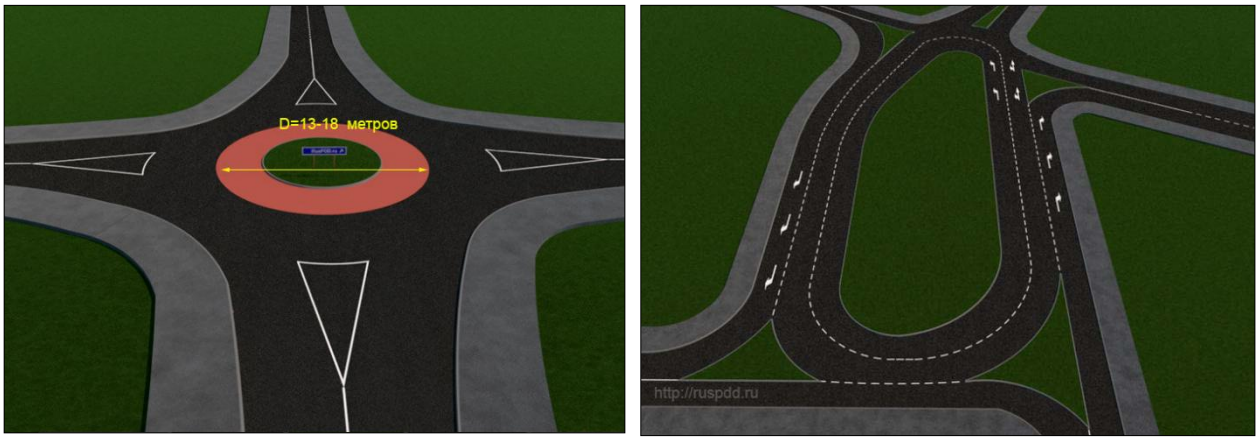

a) b)

Figure 6. Roundabout [3,12]:
a) mini roundabout; b) road surface with roundabout.

Simple roundabout intersections. Undirected intersections and junctions of local roads shall be equipped only with a guide island in the middle with a particularly small diameter, without changing the geometric parameters of the intersection. Travel in the intersection is carried out on the circle, which is provided with priority. It is applied in priority localities for the purpose of traffic calming. The use of central guide islands for traffic guidance is permitted. Simple roundabout intersections are organized under restricted traffic conditions. The central guiding island shall be in the form of a marker or construction with a slight bump for the passage of large vehicles (Figure 7). The outer diameter of the middle island of such circles is 4-10 m, the estimated design speed – 10-15 km/h, the number of converging roads ⩽ 4, the estimated intensity – up to 15 thousand vehicles/24 h, the number of lanes on the entrance/exit – 1/1 and the number of lanes on the circle roadway – 1. Such a roundabout can be organized practically at any intersection of two-lane roads without changing the intersection boundaries.

Figure 7. Simple junction with roundabout [3, 12].

Auxiliary and incomplete roundabout intersections. This category includes intersections with roundabout elements, nodes with a transverse-circular circulation pattern. This type of intersections are designed as traffic nodes (Figure 8). Estimated design speed – 15-30 km/h, number of converging roads ⩽ 5, the estimated intensity – up to 50 thousand vehicles/24 h, the number of lanes on the entry/exit – 1/1-3/3 and the number of lanes on the circle road – 1-3. Roundabouts with complex (non-standard) planning.

Figure 8. Auxiliary and incomplete roundabout intersections [3,16,17].

Turbo-turn intersections, intersections with dual center-guide island, intersections with mini-islands at entrances, intersections with central divided and segmented guide islands. Estimated design speed – 10-20 km/h, number of converging roads ⩽ 5, estimated intensity – 15-50 thousand vehicles/24 h, number of lanes on the entrance/exit – 1/1-3/3 and number of lanes on the circle road – 1-3.

5. Roundabouts with complex planning

Turbo-turned intersections (Figure 9) are multi-lane signalized intersections highlighted by a low curb stone in a spiral. They are formed by the arrangement of a central guiding island with a particularly complex shape and channelization of traffic. Their organization is due to the need to exclude additional conflict points at the intersection of vehicle traffic paths in the case of a two-lane roundabout. The throughput capacity of turbo-roundabout intersections is 3 to 5.5 thousand vehicles/h.

Pioneers in the development and implementation of turbo-turns are traffic engineers from the Netherlands. The main reason for the implementation of the new type of roundabout is the unsatisfactory traffic safety results in multi-lane roundabouts under high traffic intensity conditions**.**

In the Netherlands, multi-lane roundabouts are no longer built and those that are built are reorganized as turbo-roundabouts. The application of turbo-roundabouts is permitted by British design standards and it is recommended that the management of vehicle flows in the roundabout should be achieved by road markings only. In the Netherlands low kerbs are used to separate the lanes of the roundabout. Roundabouts have become the subject of research and analysis in Germany.

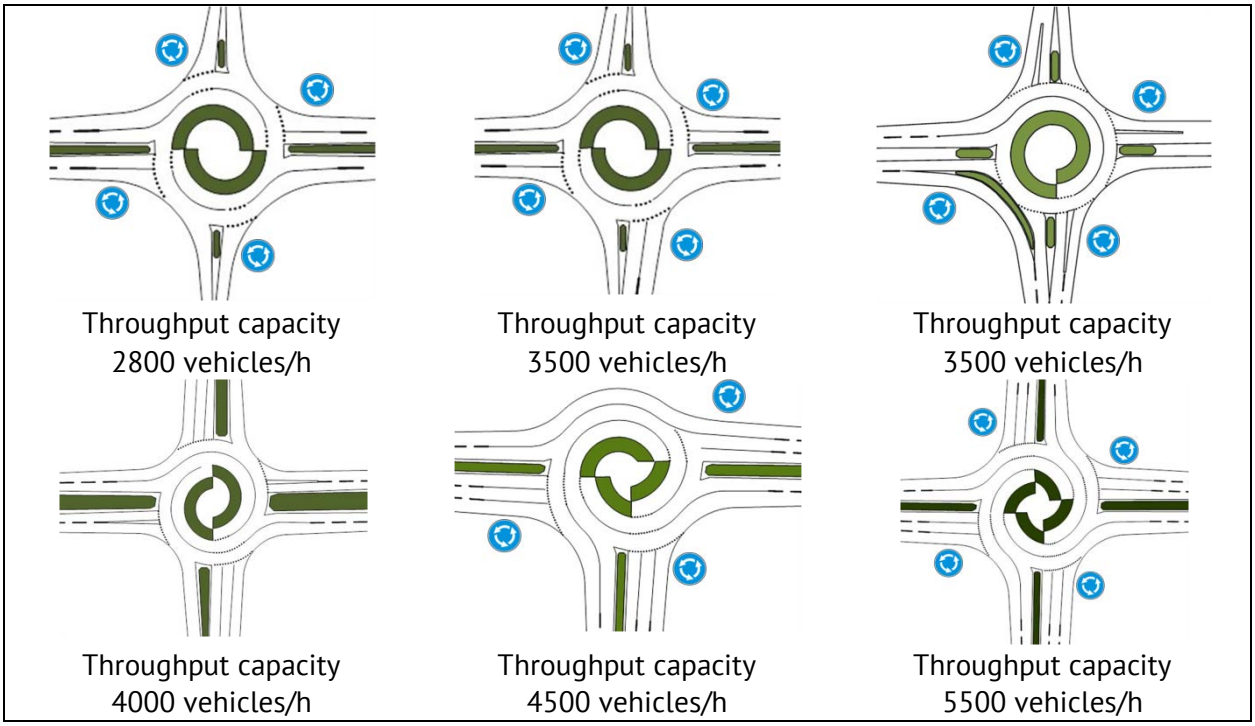

Figure 9. Turbo-turn junctions [3,14].

Turbo-turn intersections work on the principle of an uncoiled spiral, which extends outwards. Entering the outer ring of the turbo-turn, the vehicle moves in the same way as in a normal roundabout. The innovative element of the roundabout is the principle of moving

the vehicle, which has entered the roundabout on the inside lane. Travelling in the inside lane, the vehicle travels in a very clearly delimited strip by curbs, so that on exiting it will be on the outer ring, without colliding with vehicles in other lanes.

The main features of turbo-turn are the following [18]:

- two or more traffic lanes are organized, arranged by separation with a spiral curb;
- the required lane must be chosen before entering the roundabout, consulting the signs and road markings;
- when entering the roundabout, the driver shall give priority to vehicles in the roundabout and, if necessary, cross one or two traffic lanes;
- in the turbo roundabout, flow crossings or lane-to-lane maneuvers are not permitted and are not possible because of the curb.

The advantages of turbo-turn are the following:

✓ simple and clear roundabout entry situation, when the driver gives priority to the vehicles traveling in the roundabout;

✓ traffic fluidity and prevention of bottlenecks due to better organized traffic flow, thus reducing the risk of congestion;

✓ the risk of road accidents due to lane changing is excluded;

✓ the need for careful speed control due to lane dividers etc.

The traffic lanes in turbo-turn roundabouts are separated by a low kerb. Thanks to this separation, the vehicle moves only within its own separate lane without the risk of colliding with another vehicle while maneuvering.

At present, specialists in the Netherlands distinguish five types of four-input turbo-turns (Figure 9). The Dutch classification of the roundabout is based on the criterion of the number of lanes into and out of the roundabout. The need to change the number of entry/exit lanes is determined by the actual traffic distribution picture in the roundabout. The safety of traffic flow at intersections is determined not only by the number of conflict points but also by the type of conflict. In turbo-roundabout roundabouts there are no intersection and narrowing conflicts, the only conflict is generated by the need to give priority to the vehicles on the roundabout. In this situation driver behavior is easily

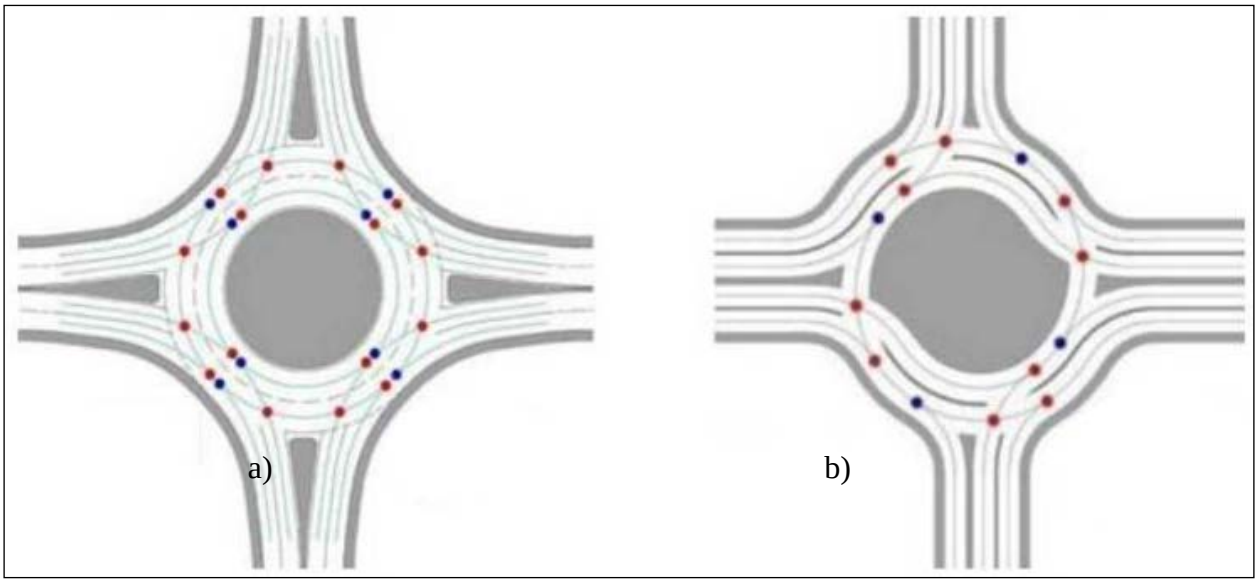

Figure 10. Points of conflict in a roundabout intersection [3, 19]:
a) classic; b) turbo-turn.

predictable as the vehicles travel in separate lanes. The separation of the traffic lanes helps to reduce the traveling speed, which reduces the risks.

The reorganization of the four-entry multi-lane roundabout into a turbo-roundabout reduces the number of conflict points from 24 to 14 (Figure 10), where the red marked points are the points of merging or intersection of road flows, and the blue marked points are the points of separation of road flows.

The problem of organization of roundabouts with turbo-roundabouts is more complex than the design of modern classical roundabouts. However, even if the costs of arranging roundabouts with turbo-turns are slightly higher than in the case of ordinary roundabouts, these investments are operationally recovered due to the significant increase in traffic safety and minimization of the number of road accidents, including financial and material losses, as well as saving lives.

On the local road network, where it is not possible to create regular intersections, it is recommended to use roundabout intersections, using a number of organizational solutions (Figures 11a and 11b), in order to ensure the self-regulation of the traffic process. In order to facilitate the passage of other types of vehicles, e.g. trams and other routing vehicles on the lane specially reserved for them, intersections with split and segmented central guide islands are organized (Figure 11c) [14].

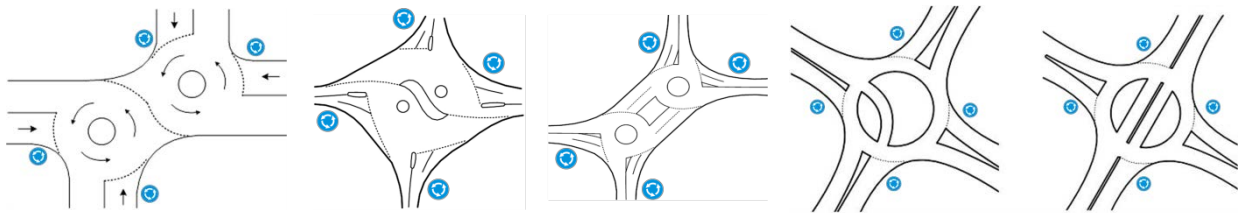

a) b) c)

Figure 11. Roundabout intersections with complex planning [3, 14]:
a) roundabout at a displaced intersection; b) roundabout at a complex junction with sewers; c) intersections with split and segmented central guidance islands.

Technical solutions, which considerably reduce the number of conflict points and increase the crossing capacity of the intersection, but require huge capital investments, are roundabout intersections with turbine-turn (Figure 12a). A simpler and lower-cost solution are turbo-turn intersections of a special design (Figure 12b).

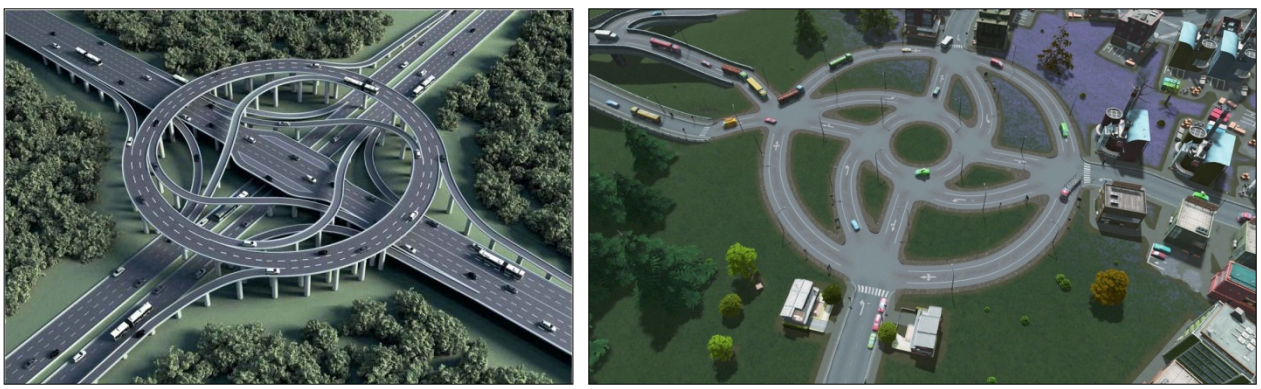

a) b)

Figure 12. Intersections with turbo and turbo-turn [3, 20]:
a) with turbo-spin; b) with turbo-spin.

„Magic roundabout" intersections. This complex intersection (Figure 13) consists of five smaller roundabouts that direct traffic clockwise around a central circle that operates counter-clockwise [21]. Despite its strange appearance, this configuration is much more efficient than the classic roundabouts. Each of the outer circles serves for the entry and exit of cars on the corresponding road.

Experienced drivers can cross the intersection more efficiently (yellow line), thus saving time, and less experienced drivers can go with the flow, bypassing the edges on the large outer circle (red line).

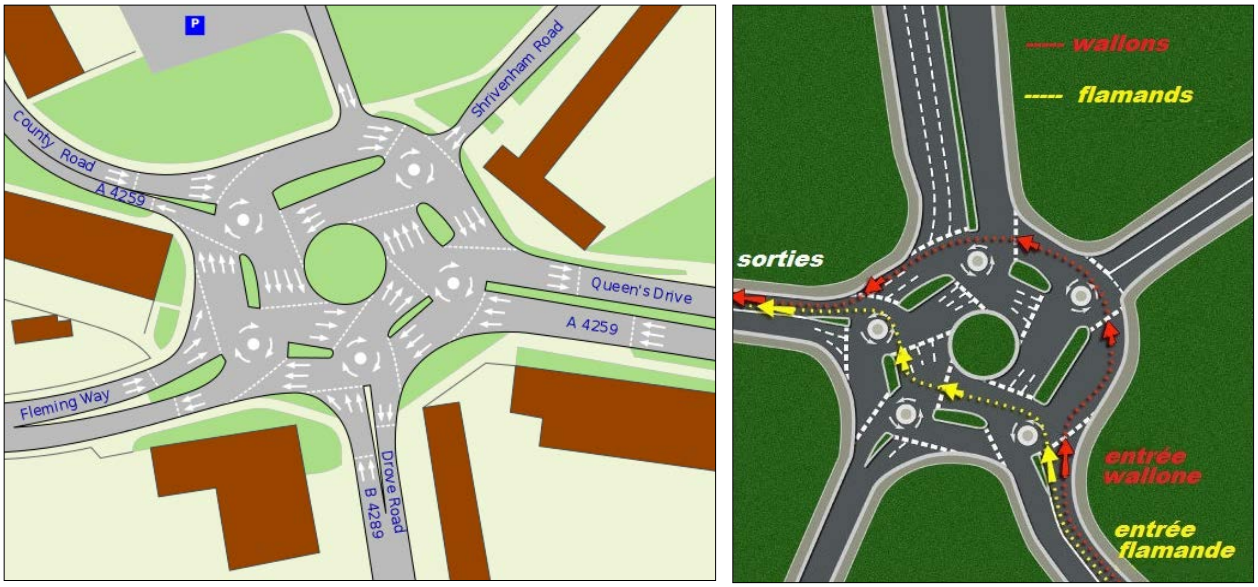

Figure 13. Intersection with „magic roundabout" [3,21].

The junction was designed by engineer Frank Blackmore, who worked at the British Transportation and Road Research Laboratory. Swindon's famous junction came into being in 1972. It was originally called the County Isles, but was quickly renamed the „*magic roundabout*", eventually becoming the official name.

Despite negative comments in the press, the Swindon junction has surprisingly good safety and efficiency indicators. The main property of the junction is the simplicity of the rules. Efficiency is achieved by reducing traffic speeds and increasing driver attention.

6. Benefits of roundabout organization

The roundabout intersection with regard to traffic safety occupies an intermediate position between a simple undirected and a directed intersection. Research in the UK, Denmark, Sweden, Norway, Australia, the Netherlands, Switzerland, Germany, the Netherlands, Norway, Australia, Switzerland etc. has shown the following [14,21,22]: roundabout intersections generally reduce total road accidents by 35%, road accidents with fatalities by 90%, road accidents with injuries by 75%, road accidents involving pedestrians by 35% and road accidents involving cyclists by 10%. According to the road accident severity index, roundabout intersections are more effective on roads outside settlements, where the number of road fatalities is reduced by more than 2 times. At roundabout intersections in built-up areas this index is 18-20%.

Roundabout intersections provide a higher through capacity than regular X-shaped intersections, both directed and undirected. This is explained, by transforming the flow of

intersecting or turning flows, which are usually related to waiting periods and can create obstacles to other flows, into decelerated traffic on the circle. Although, the circular path reduces the speed of movement, the total intersection crossing time decreases, as the need for a complete stop of vehicles occurs quite rarely.

The magnitude of the time gain depends on the traffic intensity, the variations in traffic intensity during the day and the distribution of transportation flows on the side roads entering the circle, therefore it is difficult to present general figures. In a study in Germany it was observed that the waiting time for a car at a roundabout intersection is on average 15 s shorter than at a traffic-light controlled intersection with a traffic intensity of 500 to 2000 cars/h. A study in Sweden of 20 non-equivalent undirected intersections that were reorganized into roundabout intersections showed that cars entering from the main road lost an average of 2.3 s/car, while cars entering from the secondary road gained 4.4 s/car [21].

Recently, in Western European countries (especially Germany and France), active X-shaped intersections are being actively replaced by roundabout intersections. Prerequisites for the implementation of such measures, serve the high content of toxic gases in the area of intersections and their reduced passing capacity. The controlled traffic flow requires the transport flow to move in a stop-brake-accelerate mode. This traffic regime is accompanied by an increase in harmful emissions into the atmosphere. The reorganization of the X-shaped intersection transforms the polluting transport flow regime into a cleaner and more fluidized regime of continuous circular motion.

In a study in Denmark it was observed that the emission of hydrocarbons (HC), carbon oxides (CO) and nitrogen oxides (NO_x), calculated in grams/km travelled, is on average 5-10% lower when driving through a roundabout than when driving through a traffic light controlled intersection. A study in Sweden showed a 29% reduction in carbon monoxide emissions and a 21% reduction in nitrogen oxides emissions after reorganizing the traffic-light controlled intersection into a roundabout [20].

A group of researchers at Kansas State University (USA) carried out an experiment, recording vehicle emissions at six locations: three classic intersections and three roundabouts. Twice a day (morning and evening), the scientists measured the amount of pollutants in the air and recorded them. The results confirm that vehicles at roundabouts emit significantly less harmful substances than vehicles at regular intersections. On average, carbon monoxide emissions fell by 33% and carbon dioxide, which is America's most polluting pollutant, by 46%. Other gases, such as nitrogen oxides and hydrocarbons, fell by a third and a half respectively.

The social and aesthetic benefits are to improve the pedestrian appearance and can serve as community landmarks. Roundabouts can be landscaped with green spaces, fountains or works of art, contributing to the aesthetics of the city. They can also be used at urban and rural intersections, highways and parking lots. Mini and turbo roundabouts are ideal for improving safety and flow in busy neighborhoods.

While roundabout intersections offer many advantages, they are not without their critics and challenges. One of the main complaints is related to driver confusion, especially among inexperienced drivers and those unfamiliar with the rules of the road at such intersections.

Another aspect criticized is the space needed to build a roundabout. In densely populated urban areas, the creation of such a roundabout may require the demolition of

buildings or significant changes to existing road infrastructure. These modifications can be costly and may be resisted by the local community.

Also, roundabouts are not always the best solution for all intersections. In the case of extremely busy intersections, they can become overloaded and cause bottlenecks, especially during rush hours. In such situations, alternative solutions, such as intelligent traffic lights or zebra crossings, may be more effective.

7. International road accident statistics after roundabout implementation [1]

Australia. In 1981 the results of the implementation of 73 roundabouts were evaluated. There was a 74% decrease in the rate of road accidents, while property damage from road accidents decreased by 32% and the number of road accidents involving pedestrians decreased by 68%. For 3 years there were no fatal road accidents.

In 1990, at the 15th Australian Road Research Board conference, an analysis of road accident statistics at 230 intersections in New Wales before and after their conversion to roundabouts was presented. The average number of road accidents at an intersection per year fell by 41.5% from 3.910 to 2.289, the average number of road accidents with persons injured at an intersection per year – by 45.4% from 1.045 to 0.571 and the average number of persons killed at an intersection per year – by 62.5% from 0.024 to 0.009.

Belgium. In Wallonia in the 90s of the last century, the number of roundabouts increased 10-fold, while the total number of road accidents at roundabouts increased only 2-fold. In the period 1992-2000, the experience of converting 122 undirected intersections into roundabouts was studied, while it was found that:

✓ the average number of road accidents with traumatized persons at an intersection per year after the transformation was reduced by 41.6%, from 1.352 to 0.789;

✓ the average number of serious road crashes at an intersection per year was reduced by 48% from 0.373 to 0.194.

UK. During research in 1984, it was found that the annual number of road accidents at roundabout intersections averaged 3.31, of which only 16% were road accidents with injuries and fatalities, and the average number of road accidents per 100 million vehicles passing through roundabouts was 27.5. Studies carried out in this country indicate that roundabouts have led to a decrease in waiting times by up to 20% and a reduction in road accidents by up to 50% in some regions [23].

Repeated studies on the evaluation of road accidents at different roundabouts have been carried out between 1999 and 2003. It was established, that the average number of road accidents at a roundabout per year was 1.77, of these only up to 7% were road accidents with traumatized and fatalities. Compared to 1984, the rate of road accidents at roundabouts has decreased by 46.5%.

Netherlands. At the end of 1992, 181 roundabouts were surveyed in the Netherlands. The intersections were previously undirected, but due to the high rate of traffic accidents, they were converted into roundabouts as a result:

✓ the average number of road traffic accidents at an intersection per year after the transformation was reduced by 51% from 4.9 to 2.4;

✓ the average number of people traumatized at one intersection per year has been reduced by 71.5% from 1.3 to 0.37.

USA. According to a report by the Federal Highway Administration, there are more than 7000 roundabouts in the United States and the number is growing. This expansion is

supported by data showing that, on average, roundabouts reduce fatal crashes by 90% and total crashes by 75% compared to traditional signalized intersections [23].

According to a federal source in 2000 a study was conducted at 24 intersections converted to modern roundabouts in the states: California, Colorado, Florida, Kansas, Kansas, Maryland, South Carolina and Vermont. The effect was as follows: reduction in the number of road accidents – 39%; reduction in the number of road accidents with injured persons – 76%.

The above-mentioned source reported that a study of 15 small, single-lane roundabouts on the roadway side of a circle in Maryland (2002) showed their exceptional effectiveness. The following results were obtained: reduction in the number of accidents road accidents – 60%; reduction in the number of road accidents with traumatized persons – 82%; number of fatalities – 100%; reduction in property damage only – 27%.

A more recent study of 8 intersections in Maryland published the following data:

✓ the average number of traffic crashes at an intersection per year after the transformation was reduced by 75.8%, from 5.9 to 1.43;

✓ the average number of traffic crashes per 100 million vehicles passing through the intersection decreased by 76.7%, from 1.59 to 0.37 after the transformation.

Another interesting fact: 60 roundabouts have been built in the city of Carmel, Indiana (more than in any other city in the United States) and, as a result, there has been an 80% reduction in injuries and a 40% reduction in road accidents [7].

According to the Institute for Highway Safety, modern roundabouts generally show a reduction in American practice:

- of road accidents with fatalities of 90%;
- 76% of road accidents with trauma;
- 30-40% of road accidents involving pedestrians;
- 10% of road accidents involving cyclists.

A 2004 study estimated that converting 10% of classic intersections in the US to roundabouts would have prevented 51000 traffic crashes in 2018, including 231 fatalities and approximately 34000 road crashes with trauma. It notes that the study covers single-lane intersections. Meanwhile, a 2019 Insurance Institute for Highway Safety study also found that the safety of two-lane roundabouts also improves over time as drivers get used to the new roundabout. Researchers analyzed roundabout intersections built in Washington State between 2009-2015 and found that traffic crashes at two-lane roundabouts decreased by an average of 9%/year [24].

***France*.** An analysis of the results of the implementation of 83 roundabout intersections in France in 1986 showed the following indicators:

✓ the average number of road accidents with traumatized persons at an intersection per year after the conversion was reduced by 78.2%, from 1.42 to 0.31;

✓ the average number of fatalities per intersection per year has decreased by 82.4% from 2.78 to 0.49;

✓ the average number of persons killed at an intersection per year decreased by 87.5% from 0.16 to 0.02.

***Germany*.** In 1995, an experiment was carried out in Germany in which 13 ordinary undirected intersections were converted into mini roundabouts. It was established that the use of a mini roundabout instead of a regular intersection in an urban environment leads to a significant reduction in accidents and average road accident damage:

✓ The average number of road accidents per 1 million vehicles passing through the intersection decreased by 29.1% from 0.79 to 0.56 after the transformation;

✓ The average number of serious road accidents per intersection per year decreased by 48% from 0.373 to 0.194.

8. Conclusion

According to road accident statistics at roundabout intersections, unlike traditional roundabouts, there are almost no head-on, right-turn and left-turn collisions. The reasons are speed reduction and one-way traffic. These characteristics of roundabouts generally reduce total road crashes by 35%, road crashes with fatalities by 90%, road crashes with injuries by 75%, road crashes involving pedestrians by 35% and road crashes involving cyclists by 10%.

In conclusion, it is safe to say that, with the stated aim of increasing road traffic safety, improving environmental safety and increasing road capacity, which reduces waiting times at intersections and subsequently translates into savings, roundabout intersections are a great solution. The organization of roundabouts from every technical and architectural point of view is of major practical interest for many countries, including the Republic of Moldova.

Conflicts of Interest: The author declares no conflict of interest.

References

1. Modern roundabouts, Irkutsk, 2009. Available online: http://transport.istu.edu/downloads/books/deponent_3.pdf (accessed on 24.09.2024) [in Russian].
2. Ukaderov, V.V. Improving the organization of traffic through intersections. Master's thesis, Krasnoyarsk, 2022, 80 p. [in Russian].
3. Goian, V.; Plămădeală, V.; Beiu, I. Organization and safety of road traffic. Volume 4. Organization and safety of vehicle traffic in various conditions and traffic situations. University course. Tehnica-UTM, Chisinau, RM, 2021, 306 p. ISBN 978-9975-45-721-7, ISBN 978-9975-45-724-8 (PDF) [in Romanian].
4. Intersections. Roundabouts. Available online: https://wiki.zr.ru/Перекрестки._Круговое_движение (accessed on 26.09.2024) [in Russian].
5. Onceanu, V.; Voleac, P. Roundabout design considerations. Available online: https://ibn.idsi.md/sites/default/files/imag_file/352-359_2.pdf (accessed on 26.09.2024) [in Romanian].
6. Plămădeală, V.; Goian, V.; Beiu, I. *Organization and safety of road traffic. Technical means of organizing and directing road traffic*. Volume 3. University course. Tehnica-UTM, Chisinau, RMN, 2021, 450 p. ISBN 978-9975-45-721-7, ISBN 978-9975-45-728-6 (PDF) [in Romanian].
7. Road Usability: Roundabouts. Available online: https://lpgenerator.ru/blog/2015/12/21/yuzabiliti-dorozhnogo-dvizheniya-krugovye-razvyazki/ (accessed on 26.09.2024) [in Russian].
8. Goian, V.; Plămădeală, V.; Beiu, I. Organization and safety of road traffic. Normative acts, safety elements and characteristics of road traffic. Volume 1. University course. Tehnica-UTM, Chisinau, RM, 2021, 341 p. ISBN 978-9975-45-721-7, ISBN 978-9975-45-722-4 (PDF) [in Romanian].
9. Onceanu, V. *Organization and safety of road traffic*. Elena VI, Chisinau, Republic of Moldova, 2006, 273 p. ISBN 978-9975-935-94-4 [in Romanian].
10. Onceanu, V.; Armașu, S. *Road traffic safety management and audit*. Tehnica-UTM, Chisinau, Republic of Moldova, 2011, 240 p. ISBN 978-9975-45-175-8 [in Romanian].
11. Operating principles of a roundabout and its advantages over an X-shaped intersection. Available online: http://www.ador.ru/data/files/static/audit_16.pdf (accessed on 26.09.2024) [in Russian].
12. Roundabouts in the Russian Federation. Available online: https://zen.yandex.ru/media/ruspdd/krugovoe-dvijenie-v-rf-5c1bd62bb7cd5100aad3a9d2 (accessed on 27.09.2024) [in Russian].
13. How to determine priority at a roundabout? Available online: https://ruspdd.ru/journal/62-krugovoe-dvizhenie-prioritet/ (accessed on 27.09.2024) [in Russian].
14. Methodological recommendations for the development and implementation of measures to organize traffic. Increasing the efficiency of using roundabouts. Available online: https://files.stroyinf.ru/Data2/1/4293734/4293734704.pdf (accessed on 28.09.2024) [in Russian].

15. Roundabouts: pros, cons, accident statistics. Available online: https://avtoshkolamost.ru/articles/krugovye-perekrestki (accessed on 28.09.2024) [in Russian].
16. The second stage of the Piskarevskaya interchange has opened in St. Petersburg. Available online: https://topdialog.ru/2014/11/29/v-peterburge-otkrylas-vtoraya-ochered-piskarevskoj-razvyazki/ (accessed on 28.09.2024) [in Russian].
17. The Hippodrome intersection has taken away the Haabersti Circle's title as a traffic jam magnet. Available online: https://rus.postimees.ee/6244032/perekrestok-u-ippodroma-otobral-u-kruga-haabersti-titul-magnita-probok (accessed on 27.09.2024) [in Russian].
18. Ambrosi, Gr.; Ambrosi, E. Turbo-gyration as a method of improving road traffic safety. In: *Materials of the national scientific-practical conference „Transport: engineering, economics and management"*, Chisinau TUM, 2017, p. 59-62. ISBN 978-9975-45-511-4 [in Romanian].
19. Draft new standard for roundabouts. Available online: http://transspot.ru/2017/09/25/proekt-novogo-standarta-na-kolcevye-peresecheniya/ (accessed on 25.09.2024) [in Russian].
20. Turbine-ring interchanges: the end of traffic jams! Available online: https://hodor.lol/post/159468/ (accessed on 30.09.2024) [in Russian].
21. England's „Magic Roundabout" lets cars navigate six circles. Available online: https://cfts.org.ua/news/2016/08/05/volshebnaya_krugovaya_razvyazka_v_anglii_propuskaet_avtomobili_cherez_shest_kolets_video_35620 (accessed on 30.09.2024) [in Russian].
22. Capsky, D.V. *Traffic management. Accident rate: analysis, assessment, forecasting. Study guide for students majoring in 1-44 01 02*. Traffic management, Minsk, Belarus, 2023, 439 p. ISBN 978-985-583-849-5 [in Russian].
23. Roundabout speed limit. Available online: https://www.topgear.ro/sens-giratoriu-viteza-legala/?utm_source=chatgpt.com (accessed on 30.09.2024) [in Romanian].
24. Why we need roundabouts: studying accident statistics. Available online: https://110km.ru/art/krugovye-perekrestki-udobno-voditelyam-bezopasno-peshehodam-134693.html (accessed on 26.09.2024) [in Russian].

Citation: Pădure, O.; Plămădeală, V.; Goian, V. Roundabout – element of safety, ecology and economy. *Journal of Engineering Science*. 2025, XXXII (2), pp. 7-25. https://doi.org/10.52326/jes.utm.2025.32(2).01.

Submission of manuscripts: jes@meridian.utm.md

Journal of Engineering Science *Vol. XXXII, no. 2 (2025), pp. 26 - 34*
Fascicle *Electronics and Computer Science* *ISSN 2587-3474*
Topic *Electronics and Communication* *eISSN 2587-3482*

https://doi.org/10.52326/jes.utm.2025.32(2).02
UDC 519.2:621.3.076.52

THE LIKELIHOOD FUNCTION BASED ON UNCENSORED/ CENSORED STATISTICAL DATA FOR MIN-PSD(MAX-PSD) AND MAX-PSD(MIN-PSD) AS LIFETIME DISTRIBUTIONS IN NETWORK RELIABILITY

Alexei Leahu *, ORCID: 0000-0002-1670-0111,
Veronica Andrievschi-Bagrin, ORCID: 0000-0001-8364-9873,
Maria Rotaru, ORCID: 0000-0002-3198-0297

Technical University of Moldova, 168 Stefan cel Mare Blvd., Chisinau, Republic of Moldova
* Corresponding author: Alexei Leahu, a*lexei.leahu@ati.utm.md*

Received: 03. 11. 2025
Accepted: 04. 18. 2025

Abstract. In this paper general formulas for the likelihood function have been derived in the case when uncensored/censored statistical data refer to the lifetime of serial-parallel and parallel-serial type networks when the lifetimes of the system units are independent, identically distributed random variables, the number of subsystems and the number of units in each subsystem are random variables with power series type distribution. The formulas can be applied to obtain maximum likelihood estimators for the parameters of the lifetime distribution of the mentioned networks. The results are illustrated by examples of concrete probabilistic models.

Keywords: *lifetime distributions, Power Series Distribution, serial-parallel and parallel-serial networks, likelihood function, maximum likelihood estimator.*

Rezumat. În lucrare au fost deduce formule generale pentru funcția de verosimilitate în cazul în care datele statistice necenzurate/cenzurate se referă la durata de viață a rețelelor de tip serial-paralel și paralel-serial, când duratele de viață ale unităților sistemului sunt variabile aliatoare independente, distribuite identic, numărul de subsisteme și numărul de unități din fiecare subsistem sunt variabile aliatoare cu distribuție de tip serie de puteri. Formulele pot fi aplicate pentru a obține estimatori de verosimilitate maximă pentru parametrii distribuției duratelor de viață ale rețelelor menționate. Rezultatele sunt ilustrate prin exemple de modele probabilistice concrete.

Cuvinte cheie: *distribuția duratei de viață, Distribuție de tip Serie de Puteri, rețele serial-paralelele și paralel-seriale, funcția de verosimilitate, estimator de verosimilitate maximă.*

1. Introduction

The problem of obtaining maximum likelihood estimators for the lifetime distribution parameters of serial-parallel and parallel-serial networks first requires knowledge of the likelihood function based on both uncensored and censored statistical data. Since dynamic probabilistic models have already been launched and researched for the mentioned networks,

following which the most general analytical formulas were obtained [1], it is natural that they have a similar continuity in the case of the likelihood function.

2. Auxiliary notions and results

Here are the results from [1] that we will continue to rely on. It is about the two networks type *A*, serial-parallel and type *B*, parallel-serial [1], [2], according to Figure 1.

The general probabilistic model, in the case of both networks, assumes the following:

-the lifetimes of the network units are non-negative, independent, identically distributed random variables (i.i.d.r.v.) with the cumulative distribution function (c.d.f.) *F (x)= F_X (x, λ),* where parameter $\lambda \in \not\subseteq \mathbf{R}^k$;

-the number *M* of subnets is a r.v. with possible values from the set of natural numbers, of the Power Series Distributions class *(*PSD) [3], [4} with the power series function $B(\omega) = \sum_{m\geq 1} b_m \omega^m$, with the radius of convergence, τ > 0, i.e., $P(M = m) = \frac{b_m \omega^m}{B(\omega)}, b_m \geq 0, m = 1,2, \dots, \omega \in (0, \tau)$;

- the numbers N_k of units in the subnets k = 1, 2, . . . , M are *0*-truncated , i.i.d.r.v., of class *PSD*, with power series function, $A(\theta) = \sum_{n\geq 1} a_n \theta^n$, with the radius of convergence, τ > 0, i.e., $P(N_k = n) = \frac{a_n \theta^n}{A(\theta)}, a_n \geq 0, n = 1,2, \dots, \theta \in (0, \tau)$;

-the lifetimes of the network units and the numbers *M, N_k, k =1, 2, . . . , M* are completely independent r.v.

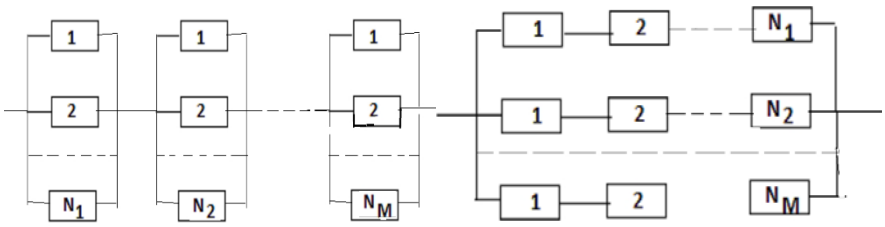

Figure 1. Schematic representation of serial- parallel and parallel-serial networks: a) Serial-Parallel Network scheme; b) Parallel-Serial Network scheme [1].

From [1] we will call on the following:

Propositon. *The cumulative distribution functions* $U(x;\ \lambda, \propto, \omega))$ *and* $V(x;\ \lambda, \propto, \omega))$ *of the lifetimes of the networks, respectively, of serial-parallel type and parallel-serial type, can be calculated according to the formulas:*

$$\boldsymbol{U(x;\ \lambda, \propto, \omega)} = \mathbf{1} - \frac{\boldsymbol{B(\omega(1 - A(\theta F(x;\lambda)) / A(\theta))}}{\boldsymbol{B(\omega)}} \quad (1)$$

$$\boldsymbol{V(x;\ \lambda, \propto, \omega)} = \frac{\boldsymbol{B(\omega(1 - A(\theta(1 - F(x;\lambda))) / A(\theta))}}{\boldsymbol{B(\omega)}} \quad (2)$$

Remark. Because c.d.f. $U(x;\ \lambda, \propto, \omega))$, as the lifetime distribution of serial-parallel network,

coincides with c.d.f. of the r.v. $min(\max\limits_{1\leq i\leq N_1} X_{i1}, \max\limits_{1\leq i\leq N_2} X_{i2}, \dots, \max\limits_{1\leq i\leq N_M} X_{iM})$ and $V(x;\ \lambda, \propto, \omega))$, as the lifetime distribution of the parallel-serial network, coincides with c.d.f. of the r.v. $max(\min\limits_{1\leq i\leq N_1} X_{i1}, \min\limits_{1\leq i\leq N_2} X_{i2}, \dots, \min\limits_{1\leq i\leq N_M} X_{iM})$, where X_{ij} , *i=1, ..., Nj , j=1, ..., M* are lifetimes of all units, r.v. *M ∈ PSD* with power series function *B(ω)* and $N_1, N_2, \dots, N_M$ are i.i.d.r.v. as r.v. *N ∈ PSD*

with power series function $A(\vartheta)$, the distributions $U(x;\ \lambda, \propto, \omega)$) and $V(x;\ \lambda, \propto, \omega)$) will be called, respectively, *Min-PSD(Max-PSD)* and *Max-PSD(Min-PSD)* lifetime distributions in network reliability [1].

These general formulas allow us to determine, in practice, the likelihood function for any concrete serial-parallel or parallel-serial type network model, considered as a particular case of the models described above. We note, that from the Ec. (1)-(2) we have the following result [1].

Consequence. *If the lifetime of each unit is a r.v. of (absolutely) continuous type, then the lifetimes of the respective networks will be r.v. of (absolute) continuous type too. At the same time, if the lifetime of each unit is a r.v. of discrete type, then the lifetimes of the respective networks will be r.v. of discrete type too.*

3. Likelihood function based on uncensored data

Let us consider the sample of size *n* of uncensored data $(x_1, x_2, ..., x_n)$ of the lifetimes of a network of type *A* or *B*. The fact that the data are uncensored means that the values $x_1, x_2, ..., x_n$ represent the results of *n* observations made on the lifetime of the network from the start of its operation until its failure. The likelihood function is defined based on the Maximum Likelihood Principle, according to which: if a random event has occurred, then it means that this is the event with the highest probability to occur.

In the assumption that c.d.f. of the lifetime of each unit of the network depends on a parameter, let's say, λ, i.e., $F(x) = F(x; \lambda)$. Then Ec. (1) – (2) show that the distributions of network lifetimes, generally, depend on 3 parameters, λ, θ, ω.

Case1. ***The lifetime of each units is a r.v. of (absolute) continuous type***

Most of the probabilistic models that aim at the lifetime of the networks we approach start from the assumption that the lifetime of each unit is a r.v. of absolute continuous type. So, according to our Consequence, the lifetime of the network will also be a r.v. of absolute continuous type. This means that, having the Ec. (1) – (2) at our disposal, we can determine the probability density function (p.d.f.) of the lifetimes for serial-parallel networks and serial-parallel networks, respectively, according to the formulas:

$$u(x;\ \lambda, \propto, \omega\ ) = \frac{dU(x;\lambda,\propto,\omega\ )}{dx}, \quad v(x;\ \lambda, \propto, \omega\ ) = \frac{dV(x;\lambda,\propto,\omega\ )}{dx}.$$

This means that the respective likelihood functions will be written as follows:

$$\boldsymbol{L_U(x_1, x_2, \ldots, x_n;\ \lambda, \propto, \omega\ ) = \prod_{k=1}^{n} u(x_k; \lambda, \propto, \omega\ )} \tag{3}$$

$$\boldsymbol{L_V(x_1, x_2, \ldots, x_n;\ \lambda, \propto, \omega\ ) = \prod_{k=1}^{n} v(x_k; \lambda, \propto, \omega\ )} \tag{4}$$

Example 1. We will take as a special case of the models described by us, the case when the number of subnetworks *M* is not random, but is constant, being equal with natural number *M* , and the number of units N_i in the subnetwork number $i = 1, ..., M$ is also constant , being known and equal to a natural number *N*. Therefore, formally, we can consider that *M* is of the *PSD* class with the power series function $B(\omega) = \omega^M$, but also that *N* is of the *PSD* class with the power series function $A(\vartheta) = \vartheta^N$. We assume, for example, that the lifetime of each unit is exponentially distributed r.v. with parameter λ > 0, i.e., with c.d.f. $F(x)=(1-e^{-\lambda x})I_{[0,+\infty]}(x)$.

The problem arises of constructing a maximum likelihood estimator (m.l.e.) for this parameter, having available the experimental data of the lifetimes *(x_1, x_2, ..., x_n)* aimed at the results of the operation of *n* identical serial -parallel or parallel-serial networks.

Solution. Substituting in the Ec. (1)-(2) the concrete expressions of the functions *F(x), A(ϑ)* and *B(ϑ)*, we deduce that in this case the lifetime c.d.f. of the serial-parallel and parallel-serial network are, respectively,

$$\boldsymbol{U(x;\lambda,N,M)} = \mathbf{1} - \left(\mathbf{1} - \left(\boldsymbol{F}(\boldsymbol{x})\right)^{\boldsymbol{N}}\right)^{\boldsymbol{M}} = \mathbf{1} - \left(\mathbf{1} - \left(\mathbf{1} - \boldsymbol{e}^{-\lambda x}\right)^{\boldsymbol{N}}\right)^{\boldsymbol{M}} \boldsymbol{I}_{[\mathbf{0},+\infty)}(\boldsymbol{x}) \qquad (5)$$

$$V(x;\ \lambda, N, M) = \left[1 - \left(1 - F(x)\right)^{N}\right]^{M} = (1 - e^{-\lambda N x})^{M} I_{[0,+\infty)}(x) \qquad (6)$$

According to the above Consequence, because the lifetime of each unit is (absolutely) continuous r.v., we deduce that the lifetimes of our networks are (absolutely) continuous r.v. with, respectively, probability density functions

$$u(x;\lambda,N,M) = \frac{dU}{dx} = (\mathrm{MN}\lambda)e^{-\lambda x}(1-e^{-\lambda x})^{N-1}\,(1 - (1-e^{-\lambda x})^{N})^{M-1} I_{[0,+\infty]}(x)$$

$$v(x;\lambda,N,M) = \frac{dV}{dx} == \mathrm{MN}\lambda e^{-\lambda N x}\left(1 - e^{-\lambda N x}\right)^{\mathrm{M}-1} I_{[0,+\infty]}(x)$$

So, Likelihood function, corresponding to the continuous data, for serial-parallel network is

$$L_U(x_1, x_2, \ldots, x_n;\ \lambda, N, M) = \prod_{k=1}^{n} u(x_k;\lambda,N,M) =$$

$$(MN\lambda)^n e^{-\lambda N \sum_{k=1}^{n} x_k} * \prod_{k=1}^{n} \left(1 - e^{-\lambda x_k}\right)^{N-1} ((1 - (1-e^{-\lambda x_k})^{N})^{M-1}$$

and for parallel-serial network is

$$L_V(x_1, x_2, \ldots, x_n;\ \lambda, N, M) = \prod_{k=1}^{n} v(x_k;\lambda,N,M) =$$

$$(MN\lambda)^n e^{-\lambda N \sum_{k=1}^{n} x_k} \prod_{k=1}^{n} \left(1 - e^{-\lambda N x_k}\right)^{M-1}$$

By the definition, the maximum likelihood estimator (m.l.e.) for the parameter λ, parameters *M, N* being known, represents that value $\hat{\lambda}$ for which the likelihood function takes its maximum value (see Maximum Likelihood Principle) [5]. For *M > 1, N>1* , our likelihood functions can be maximized using numerical methods only, but for *M = 1,* otherwise, when the parallel-serial network is always more reliable than the serial-parallel network, this problem can be explicitly solved for the parallel-serial network. Indeed, in this case, the maximum likelihood estimator (m.l.e.) $\hat{\lambda}$ for the parameter λ, our likelihood function can be maximized, solving likelihood equation:

$$\frac{d}{d\lambda} ln L_V(x_1, x_2, \ldots, x_n;\ N, \lambda) = 0$$

i.e., equation

$$\frac{d}{d\lambda}[n(lnN + ln\lambda) - \sum_{k=1}^{n} \lambda N x_k] = 0 \quad \text{i.e.,}$$

$$\frac{n}{\lambda} - N \sum_{k=1}^{n} x_k = 0$$

In this way, for paralel-serial network, we find that

$$m.l.e.\hat{\lambda} = \frac{n}{N \sum_{k=1}^{n} x_k}$$

Case 2. ***The lifetime of each units is a r.v. of discrete type***

The Ec. (1) - (2) being valid also when the lifetime of the network units is r.v. of discrete type, then, according to our Consequence, the lifetimes of the networks will of discrete type too. More precisely, if the lifetime *X* of each unit is this, for example, a r.v. with values from the set {0,1,2, ..., k, ...} given by the parametric probabilistic distribution $P_\lambda\ (X = k)$, where $P_\lambda\ (X = k) \geq 0,\ k = 0,1,2,\ldots,\ \sum_{k\geq o} P_\lambda\ (X = k) = 1$, then the lifetimes *U* and *V* of our networks will also be r.v. of discrete type too, with the possible values from the same set. Because for any integer value *x* from the set of possible values, for example, for r.v. *U*, we have that c.d.f. is equal with $U(x;\ \lambda, \propto, \omega) = \sum_{k:k\leq x} P_{\lambda,\propto,\omega}\ (U = k)$, it turns out that for the lifetime *U* of the serial-parallel network

$$P_{\lambda,\propto,\omega}\ (U = 0) = \mathrm{U}(0;\ \lambda, \propto, \omega), \quad \textbf{\textit{and}}$$
$$P_{\lambda,\propto,\omega}\ (U = k) = U(k;\ \lambda, \propto, \omega) - U(k-1;\ \lambda, \propto, \omega), for\ k \geq 1 \tag{7}$$

Analogously, for the lifetime *V* of the parallel-serial type network

$$P_{\lambda,\propto,\omega}\ (V = 0) = V(0;\ \lambda, \propto, \omega), \quad \textbf{\textit{and}}$$
$$P_{\lambda,\propto,\omega}\ (V = k) = V(k;\ \lambda, \propto, \omega) - V(k-1;\ \lambda, \propto, \omega), for\ k \geq 1 \tag{8}$$

According to the Maximum Likelihood Principle in Case 2, using Ec. (7) - (8), the respective functions for serial-parallel and parallel-serial networks will be written as follows:

$$L_U(x_1, x_2, \ldots, x_n;\ \lambda, \propto, \omega) = \prod_{k=1}^{n} P_{\lambda,\propto,\omega}\ (U = x_k). \tag{9}$$

$$L_V(x_1, x_2, \ldots, x_n;\ \lambda, \propto, \omega) = \prod_{k=1}^{n} P_{\lambda,\propto,\omega}\ (V = x_k) \tag{10}$$

where $P_{\lambda,\propto,\omega}\ (U = x_k)\ and\ P_{\lambda,\propto,\omega}\ (V = x_k)$ are calculated according to the Ec. (7) – (8).

Example 2. We will consider the same model as in Example 1, with the difference that the lifetimes are random variables, independent, identically distributed geometrically with the parameter λ, 0<λ<1, i.e., lifetime is a r.v. given by distribution

$$P_\lambda\ (X = k) = \lambda(1-\lambda)^k, k = 0,1,2, \ldots$$

So, for each *x, x=0,1,2,* ..., c.d.f.

$$F(x;\ \lambda) = \sum_{k=0}^{x} \lambda(1-\lambda)^k = 1 -\ (1-\lambda)^{x+1}$$

Using Ec. (5) – (6) we find that

$$P_{\lambda,,N,M}\ (U = k) = (1-(1-(1-\lambda)^k)^N)^M - (1-(1-(1-\lambda)^{k+1})^N)^M, for\ k \geq 0$$

Replacing these probabilities, respectively, in the Ec. (9) – (10), we obtain the corresponding Likelihood Functions for serial-parallel and parallel-serial networks. As they show, $m.l.e.\hat{\lambda}$ can only be found by numerical methods.

4. Likelihood function based on censored data

In Statistics data are called censored when the value of an observation is partially known. This is usually the case in survival/reliability analysis, where the time to a certain event is of interest, but for some studies, the event has not yet occurred at the time of analysis. For example, if we are studying the lifetime of a product, the censored data would be cases where the product is still working at the end of the study period, so we do not have an exact value for lifetime.

There are several types of censorship [6,7]:

- ✓ **Right-censoring.** We don't know what happens after a certain point.

- ✓ **Left censoring.** Left-censored observations occur in life test applications when a system has failed at the time of its first inspection; all that is known is that the unit failed before the inspection time. We have no information about what happened before a certain point.
- ✓ **Interval censoring.** We know that the event occurred within a certain interval, but we do not know the exact time.

Censoring is important because it affects how we analyze and interpret data. Statistical methods must be adapted to account for the incomplete information provided by censored data. It is important for us to know that in the case of censored data, the Likelihood Function is written more simply, because regardless of the type of data (discrete or (absolutely) continuous), we only need the c.d.f. of the observed variable.

Regarding our case, when the lifetime *Y*, given by c.d.f. $F_Y(x)$, targets serial-parallel or parallel-parallel networks, the censored data is represented by random events of the form: $\{Y \leq a\}$, i.e., *the data is left censored*; $\{a < Y \leq b\}$, i.e., *the data is interval censored*, $\{Y > b\}$, i.e., *the data is right censored*, where $0<a<b<+\infty$. Otherwise, since the lifetime is a non-negative r.v., we note that both left censoring and right censoring can be considered special cases of interval censoring. Indeed: probabilities of these events are equals to

$$P\{Y \leq a\} = F_Y(a),\ P\{a < Y \leq b\} = F_Y(b) - F_Y(a), P\{Y > b\} = 1 - F_Y(b).$$

So, we may solve the problem of writing the Likelihood Function. For this, it is sufficient to know the following information:

(1) the *a* and *b*, as the values that determine the 3 types of data censoring;

(2) the c.d.f. $F_Y(x)$ of the lifetime *Y*, also known as a function, that depends on 3 parameters, more exactly, $F_Y(x) = F_Y(x;\ \lambda, \propto, \omega)$;

(3) the probabilities $P\{Y \leq a\}, P\{Y > b\}, P\{a < Y \leq b\}$;

(4) the sample size *n* of data and the numbers n_1, n_2 and n_3, respectively, of the left, interval and right censored data, where $n_1+n_2+n_3=n$.

Then, according to the Maximum Likelihood Principle, Likelihood Function corresponding to the censored data of lifetime *Y* is done by the formula:

$$L_Y(n_1, n_2, n_3\,; \lambda, \propto, \omega) =$$
$$[F_Y(a;\ \lambda, \propto, \omega)]^{n_1}] * [1 - F_Y(a;\ \lambda, \propto, \omega)]^{n_2} * [F_Y(\mathrm{b};\ \lambda, \propto, \omega) - F_Y(\mathrm{a};\ \lambda, \propto, \omega)]^{n_3}.$$

Replacing in this formula c.d.f. $F_Y(x;\ \lambda, \propto, \omega)$ with c.d.f. $U(x;\ \lambda, \propto, \omega)$ or c.d.f. $V(x;\ \lambda, \propto, \omega)$, given by the Ec. (1)-(2), we obtain Likelihood Functions for serial-parallel and parallel-serial networks.

Remark. The above likelihood function represents the case when the data are censored on 3 intervals, but it can be extended, similarly, to the case when the number of censoring intervals is greater than 3. This will be illustrated in Exemple 3.

Example 3. We will consider the same model as in Example 1, with the difference that we have *n* cenzored data, where number of left cenzored data with the threshold *a* is equal with n_1, the number of censored data by interval *(a,b]* is equal with n_3 and number of right cenzored data with the threshold *b* is equal with n_3, $a>0$, $a<b<+\infty$, $n_1+n_2+n_3=n$. Then, on the base of Ec. (11), using, respectively Ec. (5)-(6), the Likelihood Functions for serial-parallel and parallel networks may by write, respectively, as

$$L_U(n_1, n_2, n_3\,;\ \lambda, N, M =$$

$$\left(\frac{\boldsymbol{n!}}{\boldsymbol{n_1!\,n_2!\,n_3!}}\right) * \left\{\mathbf{1}-\left(\mathbf{1}-\left(\mathbf{1}-\boldsymbol{e}^{-\lambda a}\right)^{N}\right)^{M}\right\}^{n_1}\left\{\left[\left(\mathbf{1}-\left(\mathbf{1}-\boldsymbol{e}^{-\lambda a}\right)^{N}\right)\right]^{M} - \left[\left(\mathbf{1}-\left(\mathbf{1}-\boldsymbol{e}^{-\lambda b}\right)^{N}\right)\right]^{M}\right\}^{n_2} * \left\{\left[\left(\mathbf{1}-\left(\mathbf{1}-\boldsymbol{e}^{-\lambda b}\right)^{N}\right)\right]^{M}\right\}^{n_3} \tag{11}$$

$$\boldsymbol{L_V(n_1,n_2,n_3;\,\lambda,N,M)} = \left(\frac{\boldsymbol{n!}}{\boldsymbol{n_1!\,n_2!\,n_3!}}\right)\left[\left(\mathbf{1}-\boldsymbol{e}^{-\lambda N a}\right)^{M}\right]^{n_1} * \left[\left(\mathbf{1}-\boldsymbol{e}^{-\lambda N b}\right)^{M}-\left(\mathbf{1}-\boldsymbol{e}^{-\lambda N a}\right)^{M}\right]^{n_2} * \left[\mathbf{1}-\left(\mathbf{1}-\boldsymbol{e}^{-\lambda N b}\right)^{M}\right]^{n_3} \tag{12}$$

To find out the m.l.e. $\hat{\lambda}$ for the parameter λ we will take the case when the parallel-serial networkis more reliable than serial parallel, i.e., the case when, according to the work [1], *N<M*. For example: *N=2, M=3*, and as the unit of lifetime we will take *1* year. To test the algorithm for obtaining a maximum likelihood estimate for the parameter λ, we simulate Monte Carlo [8]-[15], using Chat GPT 4, values of the lifetime of our network in the case, for example, when λ =0.2, i.e., when the lifetime . of each unit in the network has an average value equal to 1/ λ =5 years. Here are the simulated values written as a variational string in ascending order:

(1.23,1.67,1.89, 2.34,2.56,2.78,2.89,3.12,3.45,3.78,4.01,4.23,4.56,5.01,5.34,5.67,5.89, 6.12,6.45,6.78).

We assume that these data are censored according to the values *a=2 years* and *b=4 years*. So, we assume that we have at our disposal, from a total number of *n = 20* data, n_1*=3* data censored on the left, n_2*=7* data censored on the interval (2,4] and n_3*=10* data censored on the right. Then the Likelihood Function is

$$L_V(3,7,10;\,\lambda,2,3) = \frac{20!}{3!\,7!\,10!} * ((1-e^{-4\lambda})^3)^3 * [\left(1-e^{-8\lambda}\right)^3 - \left(1-e^{-4\lambda}\right)^3]^7 * [1-\left(1-e^{-8\lambda}\right)^3]^{10}$$

By means of the Mathematica 14.0 we find that value of λ for which the Likelihood Function takes its global maximum, that is, we find that m.l.e. $\hat{\lambda}$=0.0882487. Comparing it with the true value of λ=0.2, we find that the approximation is not so good. So it's a problem related to the nature of censorship.

Now, on the base of the above simulated data, we assume that these data are censored according to the values *a=2 years*, *b=4 years* and *c=6 years*. That means we assume that we have at our disposal, from a total number of *n = 20* data, n_1*=3* data censored on the left, n_2*=7* data censored on the interval (2,4], n_3*=7* data censored on the interval (4,6], and n_4*=3* data censored on the right. If in the previous case we had data censored on 3 intervals, now we will have to deal with data censored on 4 intervals. The method of calculating the Likelihood Function being similar, we find that

$$L_V(3,7,7,3;\,\lambda,2,3) = \frac{20!}{3!7!7!3!} * ((1-e^{-4\lambda})^3)^3 * ((1-e^{-8\lambda})^3 - \left(1-e^{-4\lambda}\right)^3)^7 * * (1-\left(1-e^{-12\lambda}\right)^3)^3$$

Now, also by means of Mathematica 14.0, we find that value of λ for which the Likelihood Function takes its global maximum, i.e., we find that m.l.e. $\hat{\lambda}$ =0.214796 satisfactorily approximates the true value of the parameter λ=0.2.

5. Conclusions

General formulas in Eq. (1)-(2) for determining c.d.f. of lifetimes is a large source of dynamic probabilistic models for serial-parallel or parallel-serial networks, but also a basis for writing the Likelihood Function, when the data are uncensored or censored. Writing the likelihood function for censored data becomes simpler, because it does not depend on the type of lifetime as r.v. (discrete or continuous), using only c.d.f. But the problem of finding an m.l.e. which approximates as well as possible the true value of the unknown parameter is complicated, because it is difficult to match the censoring intervals. The fact that matching the censoring intervals is difficult, even when we rely on simulation data, shows us that in the case of real problems the use of maximum likelihood estimators must be done with great caution if the choice of censoring intervals does not have a mathematical reasoning. However, this is a problem that deserves to be researched more deeply. The examples given show that finding the maximum likelihood estimators becomes a maximization problem that can be solved, as a rule, by numerical methods.

These results were presented at the International Conference on Electronics, Communications and Computing, ECCO 2024, 17-18 October, Chisinau, Republic of Moldova.

Acknowledgments: The results were obtained within the Institutional Research Project 020404 concluded with the Ministry of Education and Research of the Republic of Moldova.

Conflicts of Interest: The authors declare no conflict of interest.

References

1. Leahu, A.; Andrievschi-Bagrin, V.; Ciorbă, D.; Fiodorov, I. On dynamic probabilistic models in network reliability. In: *Changes and Innovations in Social Systems,* Hoscova-Mayerova, S.; Flaut, C.; Flaut, D.; Rascova, P. (Eds); Springher Nature, Cham, Switzerland, 2025, 657 p.
2. Kapur, K.C.; Lamberson, L.R. *Reliability in engineering design*. Wiley India Pvt. Limited, New Delhi, India, 2009, 608 p.
3. Noack, A. A class of random variables with discrete distributions. *Annals of Mathematical Statistics* 1950, 21, pp. 127–132.
4. Leahu, A.; Andrievschi-Bagrin, V.; Ciorbă, D., Fiodorov, I. Once again about the reliability of serial-parallel and parallel-serial networks. In: *International Conference on Electronics, Communications and Computing*, 21-22 October, 2021, Chisinau, Republic of Moldova, pp. 170-173.
5. Barlow, R.; Proshan, F. *Statistical Theory of Reliability and Life testing: Probability Models*. Holt, Rinehart & Winston Inc., NY, USA, 1974, 290 p.
6. Meeker, W. Q.; Escobar, L.A. *Statistical Methods for Reliability Data*. John Wiley & Sons, Inc., NY, SUA, 1989, 680 p.
7. Lee, E. T.; Wang, J. W. Statistical Methods for Survival Data Analysis, 3rd Edition. John Wiley&Sons, New Jersey, USA 2003, 513 p.
8. Gertsbakh, I.; Spungin Y. *Models of Network Reliability: Analysis, Combinatorics and Monte Carlo*, CRC Press, Boca Raton, USA, 2012, 217 p.
9. Gertsbakh, I. *Reliability Theory with Applications to Preventive Mentenance*. Springer-Verlag Berlin Heidelberg, Germany, 2005, 215 p.
10. Kroese, D.; Taimre, T.; Botev, Z. I. *Handbook of Monte Carlo Methods*. John Wiley & Sons, Inc., New Jersey, USA, 2011, 727 p.
11. Ross, S. M. *Introduction to Probability Models*. 10 th Edition. Elsevier, Amsterdam, Netherlands, 2010, 784 p.
12. Faulin, J.; Juan, A.A.; Martorell, S.; Ramires-Marquez, J.-E. *Simulation Methods for Reliability and Availability of Complex Systems*. Springer-Verlag London Limited, London, UK, 2010, 315 p.
13. Hoang Pham (Editor). *Handbook of Reliability Engineering*. Springer-Verlag London, London, UK, 2003, 663 p.
14. O'Connor, P.T.D.; Kleyner, A. *Practical Reliability Engineering*, 5th Editions. John Wiley&Sons, New Delhi, India, 2012, 484 p.
15. Barbu, A.; Song-Chun Zhu. *Monte Carlo Methods*. Springer Nature, Singapore Pte Ltd, Singapore, 2020, 422 p.

Citation: Leahu, A.; Andrievschi-Bagrin, V.; Rotaru, M. The likelihood function based on uncensored/ censored statistical data for Min-PSD(Max-PSD) and Max-PSD(Min-PSD) as lifetime distributions in network reliability. *Journal of Engineering Science*. 2025, XXXII (2), pp. 26-34. https://doi.org/10.52326/jes.utm.2025.32(2).02.

Submission of manuscripts: jes@meridian.utm.md

Journal of Engineering Science *Vol. XXXII, no. 2 (2025), pp. 35 - 45*
Fascicle *Electronics and Computer Science* *ISSN 2587-3474*
Topic *Microelectronics and Nanotechnologies* *eISSN 2587-3482*

https://doi.org/10.52326/jes.utm.2025.32(2).03
UDC 539.2:543.42:621.3.049.77

IN-DEPTH PROPERTIES ANALYSIS OF $ZnAl_2O_4$/ZnO MICRO-NANOSTRUCTURES

Cristian Lupan *, ORCID: 0000-0003-2268-6181

Technical University of Moldova, 168, Stefan cel Mare Blvd., Chisinau, Republic of Moldova
* Corresponding author: Cristian Lupan, cristian.lupan@mib.utm.md

Received: 04. 08. 2025
Accepted: 05. 14. 2025

Abstract. This manuscript presents characterization of $ZnAl_2O_4$/ZnO micro-nanostructures of their morphological, chemical, structural and sensing properties. The ZnO micro-nanostructures obtained using flame transport synthesis were covered with $ZnAl_2O_4$ nanodots by chemical approach. Morphological, chemical and structural properties have been investigated using SEM, EDX and XRD, respectively. Scanning electron microscopy investigation shows the formation of micro-nanostructures of different morphologies, namely tetrapods and nanowires, covered with nanodots. The EDX study revealed the chemical composition of the micro-nanostructures, confirming the presence of Al on the micro-nanostructures' surfaces too. The XRD pattern of the studied micro-nanostructures shows the presence of ZnO and $ZnAl_2O_4$ crystalline phases in the grown material. A single $ZnAl_2O_4$/ZnO nanostructure was integrated into a device by FIB/SEM and tested to a series of gases at different operating temperatures, demonstrating selectivity to 100 ppm hydrogen gas and response value of ~1.2 up to ~3.65 at 20 °C and 150 °C, respectively. A sensing mechanism to hydrogen gas was proposed, involving free electrical charge transfer between ZnO wire and $ZnAl_2O_4$ nanodots. Based on the knowledge gained, optimization of hydrogen gas sensors using the methods and nanomaterials presented herein is envisioned.

Keywords: *nanodots, energy-dispersive X-ray spectroscopy, scanning electron microscope, Rigaku X-ray diffraction, spinel, ternary, $ZnAl_2O_4$, gas sensor.*

Rezumat. În această lucrare sunt prezentate proprietățile morfologice, chimice, structurale și senzoriale ale micro-nanostructurilor $ZnAl_2O_4$/ZnO. Micro-nanostructurile de ZnO obținute prin metoda sintezei prin transport de flacără au fost acoperite cu nanopuncte de $ZnAl_2O_4$ prin metoda chimică. Proprietățile morfologice, chimice și structurale au fost investigate utilizând SEM, EDX și XRD. Investigația prin microscopie electronică de scanare arată formarea de micro-nanostructuri de diferite morfologii, și anume tetrapozi și nanofire, acoperite cu nanopuncte. Studiul EDX a relevat compoziția chimică a micro-nanostructurilor, confirmând prezența Al și pe suprafețele micro-nanostructurilor. Difractograma XRD a micro-nanostructurilor studiate arată prezența fazelor cristaline ZnO și $ZnAl_2O_4$ în materialul obținut. Prin intermediul FIB/SEM a fost integrată o singură nanostructură $ZnAl_2O_4$/ZnO într-un dispozitiv și testată la o serie de gaze la diferite temperaturi de operare, demonstrând selectivitate la 100 ppm hidrogen cu valoarea răspunsului de ~1.2 la 20 °C până la ~3.65 la 150 °C. A fost propus un mecanism de detecție a hidrogenului, care implică transferul

sarcinilor electrice libere dintre firul de ZnO și nanopunctele de $ZnAl_2O_4$. Pe baza rezultatelor obținute, se preconizează optimizarea senzorilor de hidrogen utilizând metodele și nanomaterialele prezentate.

Cuvinte-cheie: *nanopuncte, spectroscopie cu raze X cu dispersie de energie, microscop electronic cu scanare, difracție de raze X Rigaku, spinel, ternar, $ZnAl_2O_4$, senzor de gaz.*

1. Introduction

Metal oxides (CuO, ZnO, MoO_3, In_2O_3, etc.) are a group of materials that can be used in various applications, due to their properties and various methods of synthesis [1–6]. For sensing applications, a great interest is in developing devices capable of detecting reliably and accurately a target gas in ambient conditions and mixtures of gases [2]. Pristine semiconductor metal oxides lack selectivity, high response and require high operating temperatures devices [7]. These drawbacks can be improved by fine tuning the material characteristics and performances via additives, crystalline phase control or mixing different materials [7].

ZnO can be used for diverse types of applications, due to a multitude of morphology and cost-efficient methods of obtaining [3,8]. Considering its properties (bandgap ~3.37 eV, chemical and thermal stability, high mobility of electrons, large exciton binding energy ~60 meV, etc.), zinc oxide can be used for sensing applications, such as UV and gas sensors [9-11]. Previous results showed that pure ZnO has low selectivity and high working temperatures, showing response to a wide range of VOC vapors (formaldehyde, benzene, acetone, ethanol, methanol, etc.) at 200 – 400 °C [11,12]. Different methods to improve sensing devices based on this material were reported before, including doping [10], functionalization [11,13], formation of junctions [8,9,14], and of heterostructures [15] etc.

Oxide spinel compounds (AB_2O_4) can be used for various types of applications, including gas sensing [16]. For example, Zn_2SnO_4 was used as ethanol, acetone and nitrogen dioxide sensor at operating temperatures of 200-400 °C [17]. A carbon monoxide sensor based on $ZnCo_2O_4$ was presented before, capable of detecting 300 ppm of test gas at 200 °C [18]. Lowering the working temperature of sensors is an important task in decreasing power consumption and complexity of devices [19].

$ZnAl_2O_4$ (bandgap ~3.8 eV) is a promising material for use in different applications, as catalyst, optoelectronic, etc., due to its thermal stability, electronic and chemical properties [16,20–22]. There are various methods for obtaining spinel type metal oxide nanostructures such as hydrothermal, co-precipitation, sol-gel, biological, calcination etc. [16,21-23]. Another method for synthesizing $ZnAl_2O_4$ is the solution combustion synthesis method, obtaining spherical and well crystalline particles [24]. Previous works showed the possibility of using $ZnAl_2O_4$ or ZnO/$ZnAl_2O_4$ combination as sensing material for different types of gases: hydrogen, propane, carbon monoxide, etc. [16,22,25,26].

Hydrogen is a versatile gas that can be used in various applications from automotive, material synthesis, heating, up to treatment of diseases [22,27]. Due to its explosive nature and the lack of color, odor and taste, which makes it difficult to detect by human senses, this gas poses a significant hazard during its use and storage, leading to the necessity of small, accurate and reliable devices that are capable of detecting it [28].

The main goal of this work is to present a method of obtaining $ZnAl_2O_4$/ZnO micro-nanostructures and to study in detail its properties, in order to use this material combination

as sensing material. Morphological, chemical, structural and sensing properties have been investigated in detail, with the results summarized in this paper.

2. Materials and Methods

Zinc oxide (ZnO) micro-nanostructures obtained by flame transport synthesis (FTS) method were used as base material, using Zn metal microparticles as precursor and polyvinyl butyral powder as a sacrificial polymer, with the process described in details in paper [29]. Chemical method was used to cover ZnO with zinc aluminate ($ZnAl_2O_4$), using aluminum acetate basic hydrate ($AlC_4H_7O_5 \cdot H_2O$, purity >98%) mixed with diluted ethanol (100%) in a glass container as precursors, with the process described in detail in work [16]. Ethanol was evaporated by placing the sample on a plate heated to 90 °C for 14h. At the end the nanostructures were thermally annealed on quartz substrate at 1000 °C for 3h in air.

The morphology and chemical composition of obtained micro-nanostructures was studied using scanning electron microscope (SEM) and energy-dispersive X-ray spectroscopy (EDX) using Zeiss Supra 55VP. Structural properties have been investigated using Rigaku X-ray diffraction (XRD).

In order to obtain electrical devices, a single $ZnAl_2O_4$/ZnO nanostructure was placed on a Si/SiO_2 (525 μm/800 nm) substrate with two prepatterned Cr/Au (11 nm/170 nm) electrodes and connected using focused ion beam scanning electron microscope (FIB-SEM, FEI Helios Nanolab 600) for depositing Pt contacts [30,31].

Gas sensing and electrical properties of the developed devices were investigated using two-probe approach and a Keithley 2400 source meter, controlled via LabView software [31]. Samples were tested to a series of gases with concentration of 100 ppm at different operating temperatures from room temperature (20 °C) up to 150 °C. The relative humidity was monitored and controlled at 10% during all measurements.

The gas response (S) was determined using the ratio of current in air (I_{air}) and during gas exposure (I_{gas}):

$$S = \frac{I_{gas}}{I_{air}} \quad (1)$$

3. Results and discussion

SEM was used to investigate morphological properties of obtained micro-nanostructures using FTS and chemical method, with the results presented in Figure 1. In Figure 1a and 1b are shown low and high magnification SEM images of as-grown ZnO, observing interconnected nanostructures, namely tetrapods and nanowires, with various sizes. Interconnected nanostructures or individual tetrapod/nanowire can be potentially used for sensing devices used for ultraviolet light or gas sensing [29,32].

The wrinkles visible on the ZnO surface at high magnification (Figure 1b) are due to the high temperature of 900 °C during flame transport synthesis [23]. The tetrapod arm diameters, determined from Figure 1b, is ~0.5 – 2.5 μm. Previous studies using ZnO obtained via FTS showed that the synthesis temperature has a major effect on the size and diameter of the obtained nanostructures [32].

Figure 1c represents higher magnification SEM images of $ZnAl_2O_4$/ZnO micro-nanostructures obtained using chemical method followed by 3h thermal annealing at 1000 °C, observing that micro-nanostructures have tetrapodal or nanowires morphology with various diameters and lengths. Diameter of nano-microstructures, determined from Figure 1c, is ~0.5 – 2.5 μm, which is similar to as-deposited ZnO, showing that 3h annealing at 1000 °C

has no visible effect on the size after initial deposition using FTS. The investigated tetrapods and nanowires have higher surface roughness compared to ZnO structures. Small nanodots of $ZnAl_2O_4$ are visible on the surface of deposited micro-nanostructures after thermal annealing (see Figure 1c).

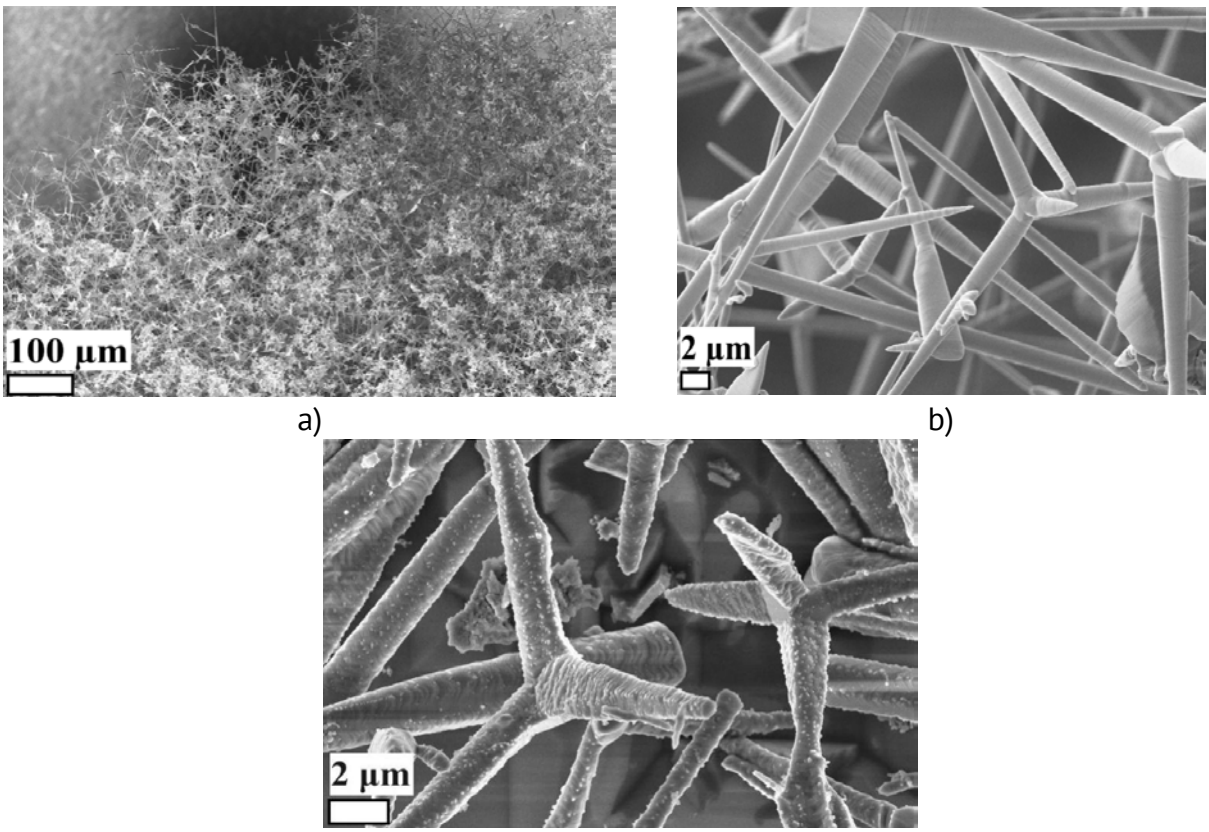

a) b)

c)

igure 1. SEM images of: a) and b) ZnO micro-nanostructures at low and high magnification; c) $ZnAl_2O_4$/ZnO micro-nanostructures annealed at 1000 °C for 3 h.

Using high-magnification SEM image and microscope software tools, the size of the deposited $ZnAl_2O_4$ nanodots was determined, as presented in Figure 2. The average nanodot size is ~65-75 nm and are spread randomly on the surface of the nanowire. The nanodots size is similar to $ZnAl_2O_4$ nanocrystals, with grain size of ~50 nm, reported in previous work [21].

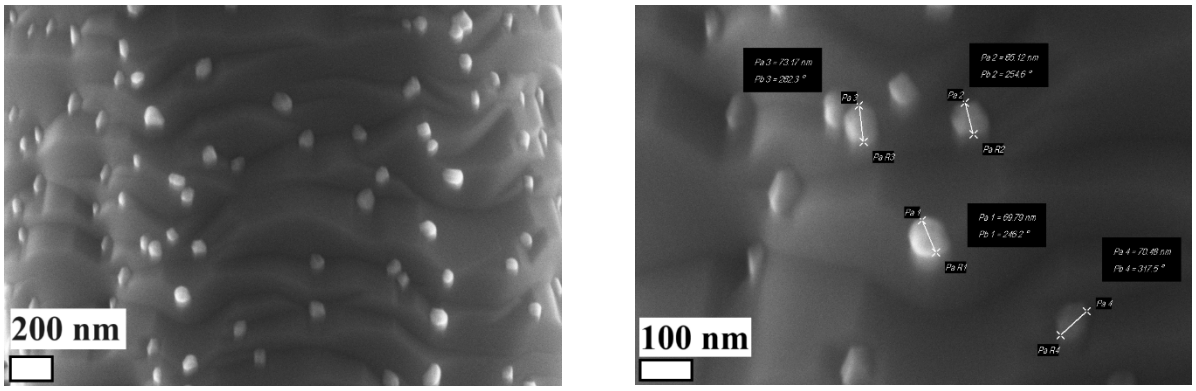

a) b)

Figure 2. SEM image of surface of $ZnAl_2O_4$/ZnO micro-nanostructures annealed at 1000 °C for 3h in air and measured at different magnifications: a) 200 nm scale bar; and b) 100 nm scale bar.

EDX mapping was used to investigate the chemical properties of grown micro-nanostructures in a target area (Figure 3a). EDX results are presented in Figure 3b-d, detecting three elements: Zn, O and Al, distributed on the surface of sample.

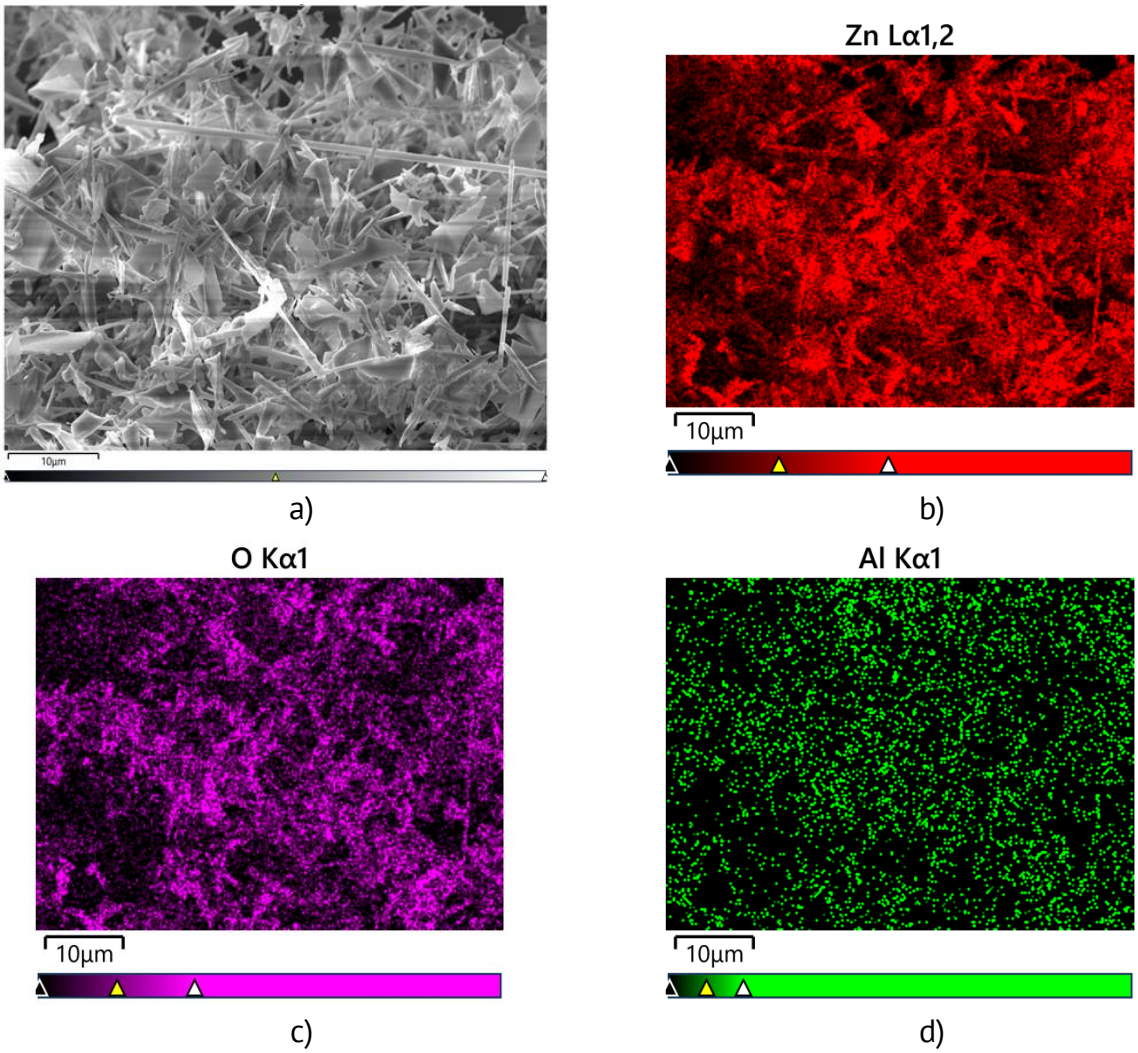

Figure 3. EDX mapping of $ZnAl_2O_4$/ZnO micro-nanostructures annealed at 1000 °C for 3h: a) scanned area; b) distribution of Zn; c) distribution of O; d) distribution of Al.

A quantitative analysis of elements in the studied $ZnAl_2O_4$/ZnO micro-nanostructures is presented in Table 1, observing smaller presence of Al (0.27 at.%), compared to Zn (50.18 at.%) and O (49.55 at.%).

Table 1

EDX results for atomic % of elements present in micro-nanostructures

Element	Atomic %
O	49.55
Al	0.27
Zn	50.18

The results for EDX scan for a single nanowire are presented in Figure 4, where Zn, O and Al elements were detected. As can be seen, Zn and O are present in the nanowire, while Al covers measured surface, due to the use of the chemical method of deposition.

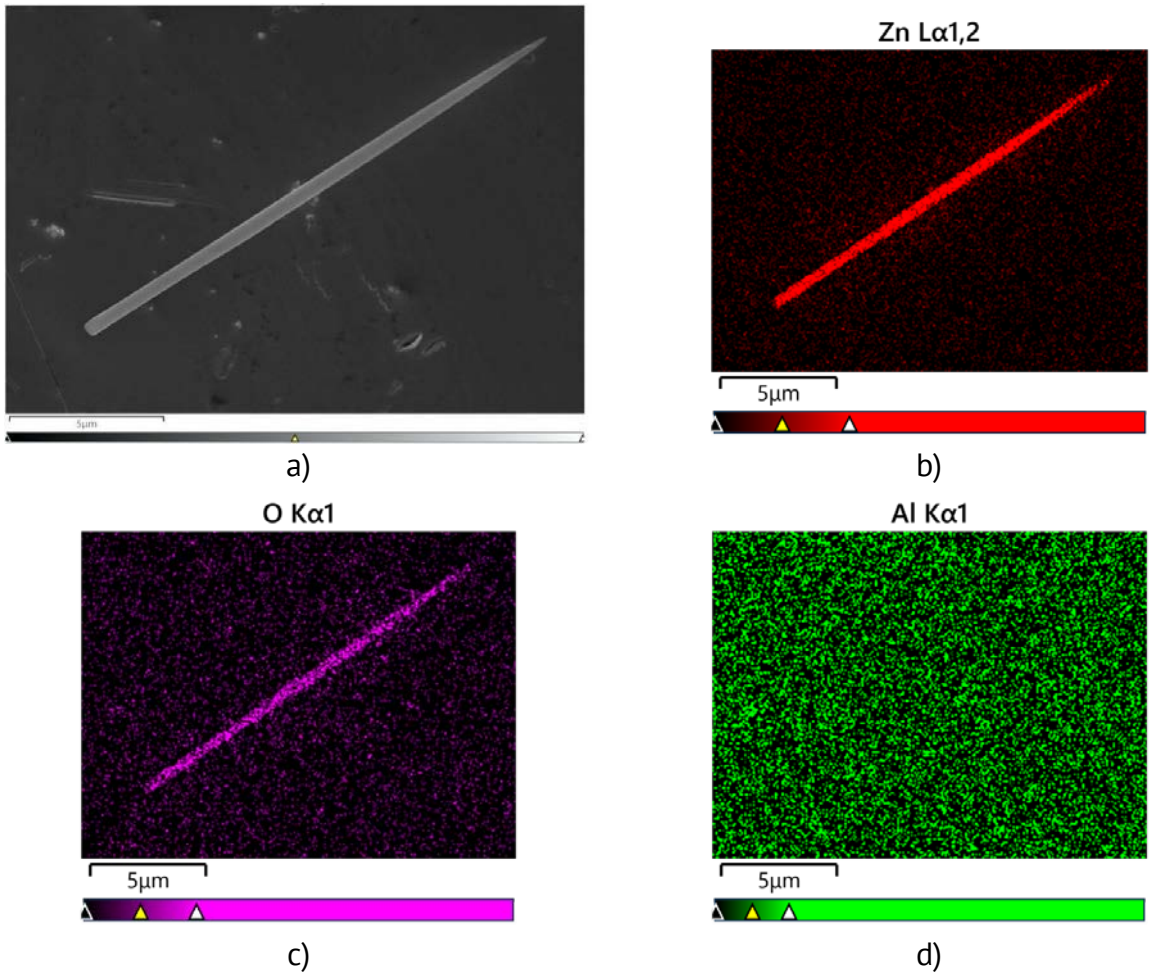

Figure 4. EDX mapping of $ZnAl_2O_4$/ZnO single nanowire annealed at 1000 °C for 3 h: a) scanned area; b) distribution of Zn; c) distribution of O; d) distribution of Al.

EDX line scan at high magnification where nanodots are visible, is presented in Figure 5. EDX line scan technique allows chemical analysis of elements in the predominance area to be seen and measured. Y-axis presenting counts of the chemical element or relative concentration in the scanned line [33].

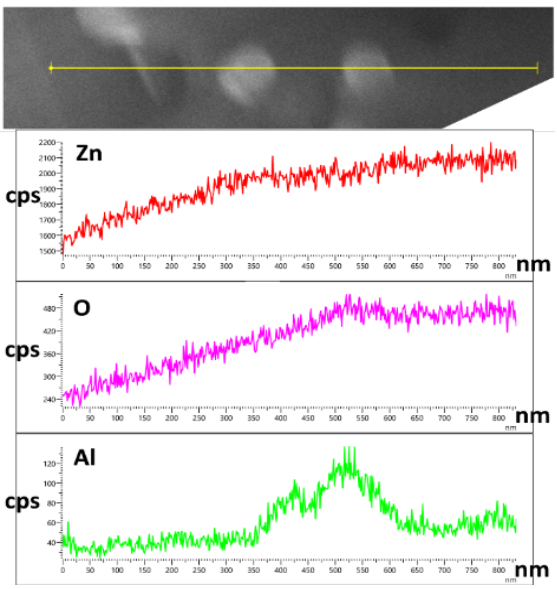

Figure 5. EDX line scan crossing nanodots of $ZnAl_2O_4$/ZnO single nanowire annealed at 1000 °C for 3h.

The presence of individual elements of Zn, Al and O is confirmed by measurement, with a low quantity of Al, as observed in investigated micro-nanostructures. Appearance of Al peak is coincident with the position of nanodots, showing presence of this element in those nanostructures, indicating that is mostly present on the newly formed nanodots.

XRD was used to confirm chemical composition, phase and structure of the obtained micro-nanostructures. The results for the XRD measurement in the 60-80° 2θ values are presented in Figure 6. Detected XRD reflections were attributed according to standard cards PDF #031161 ($ZnAl_2O_4$) and PDF #0361451 (ZnO).

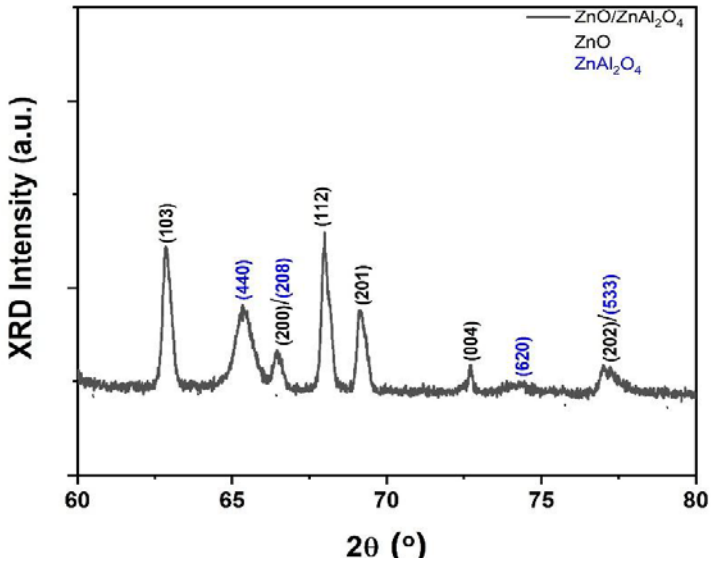

Figure 6. XRD pattern of $ZnAl_2O_4$/ZnO micro-nanostructures annealed at 1000 °C for 3h in air.

Multiple ZnO and $ZnAl_2O_4$ diffractions peaks were attributed in this range, with highest intensity for (103) and (112) ZnO planes. The highest intensity for $ZnAl_2O_4$ peak was observed for (440) plane. Some overlapping ZnO and $ZnAl_2O_4$ peaks were detected. No diffraction peaks corresponding to other materials were detected in the investigated samples.

Average crystallite size (*D*) for $ZnAl_2O_4$ (440) plane was determined using the Scherrer formula [34]:

$$D = \frac{k \cdot \lambda}{\beta \cdot cos\theta} \quad (2)$$

where: *k* – shape factor (*k* = 0.9), *λ* – wavelength of the radiation (*λ* = 1.5406 Å), *β* – full-width half maximum intensity of the reflection.

The calculated *D* is ~70.65 nm, which is similar to the measured $ZnAl_2O_4$ nanodot size from the SEM images. The sensing device based on a single $ZnAl_2O_4$/ZnO nanostructure was tested to a series of gases with concentration of 100 ppm (acetone, n-butanol, methane, ethanol, hydrogen, ammonia and 2-propanol) at different operating temperatures from 20 °C up to 150 °C, with the results presented in Figure 7.

As can be seen, response was observed only for 100 ppm hydrogen gas at all operating temperatures, meaning that sensor is selective to this gas. Response value (*S*) increased from ~1.2 up to ~3.65 with the rise of operating temperature from 20 °C to 150 °C, respectively.

Gas response and selectivity to hydrogen for $ZnAl_2O_4$/ZnO based device can be attributed to the formation of *n-n* heterostructure and use of Pt contacts for the nanostructure, which can act as catalysts too [16,22]. Increased response at 100-150 °C compared to room temperature, can be attributed to the presence of more reactive oxygen species (O^-) on the surface of the material [22].

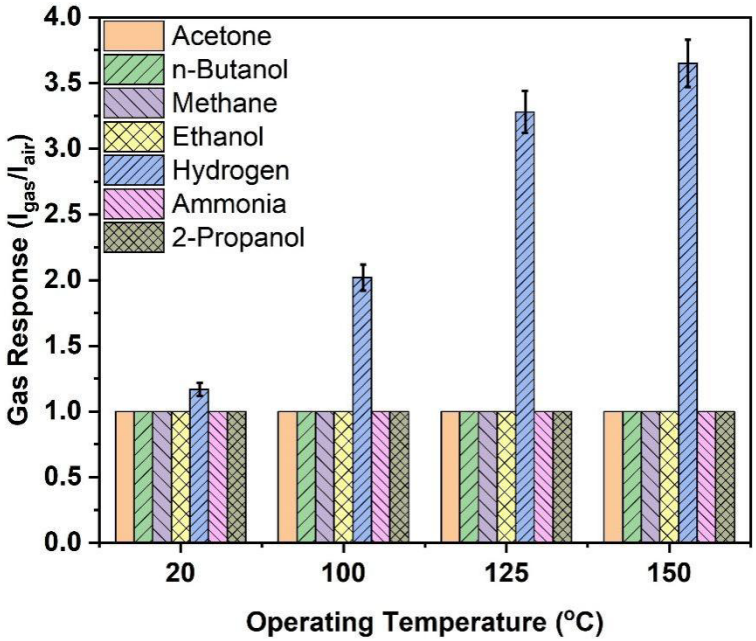

Figure 7. Gas response to a series of gases with concentration of 100 ppm at different operating temperatures for device based on a single $ZnAl_2O_4$/ZnO nanostructure annealed at 1000 °C for 3 h in air.

In Figure 8 is presented schematic representation of proposed hydrogen gas sensing mechanism for $ZnAl_2O_4$/ZnO based device. When the device is in air atmosphere (Figure 8a), oxygen species are adsorbed on the surface of the material, in this case O^- at 100-150 °C [35,36]. An electron flow between $ZnAl_2O_4$ nanodots and ZnO takes place, leading to higher concentration of free-electrons in conduction band of ZnO, which in turn increases oxygen coverage in air environment [16,37].

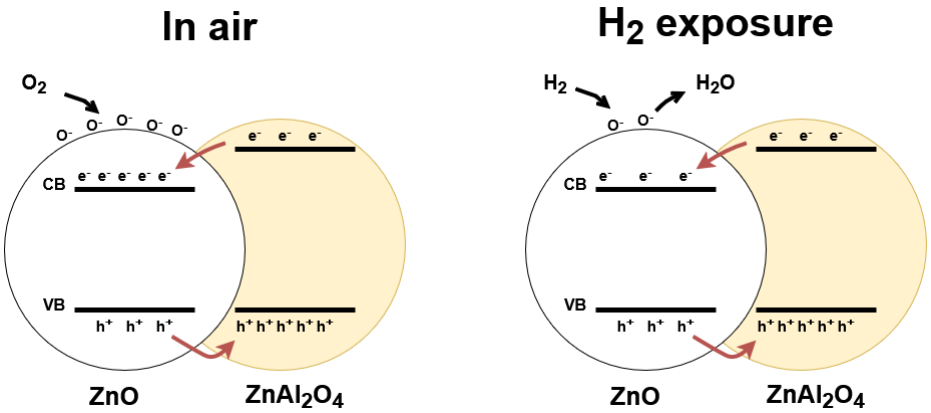

Figure 8. Schematic representation for proposed sensing mechanism for device based on single ZnO/$ZnAl_2O_4$ nanostructure: a) in air and b) during H_2 exposure.

The following reaction during hydrogen exposure takes place with the oxygen species on the surface (Figure 8b) [37]:

$$H_2 + O^- \rightarrow H_2O + e^- \quad (3)$$

The reaction leads to the release of H_2O in the environment and the captured electrons to the conduction band, increasing current. Faster oxidizing processes and increased response during hydrogen gas exposure are possible due to the free charge transfer from $ZnAl_2O_4$ to

ZnO, which was also previously reported by other authors when adding different nanoparticles on the surface of the base material [16,38].

5. Conclusions

ZnO micro-nanostructures obtained using flame transport synthesis were covered with $ZnAl_2O_4$ nanodots using chemical method, followed by annealing at 1000 °C for 3h in air. Morphological investigation shows the formation of tetrapods and nanowires, covered with small nanodots with ~65-75 nm diameter.

EDX study presented chemical composition of the sample, confirming the presence of Al, with at.% of ~0.27%. By comparing EDX results from multiple interconnected micro-nanostructures and single nanowire, it was detected that Al covers entire surface of the sample, while Zn and O is mostly present in the nanowire/tetrapod. EDX line scan indicate that appearance of Al peak is coincident with the position of nanodots, showing its presence on the newly formed nanodots.

The XRD pattern of the investigated micro-nanostructures shows presence of ZnO and $ZnAl_2O_4$ in the sample, by attributing peaks according to PDF cards of the materials.

Sensing study presented insights on the behavior of the $ZnAl_2O_4$/ZnO based device to a series of test gases at different operating temperatures, observing selectivity to 100 ppm hydrogen and a response value of ~1.2 up to ~3.65 at operating temperatures of 20 °C and 150 °C, respectively. A sensing mechanism was proposed, based on the free charge transfer between ZnO and $ZnAl_2O_4$.

The results obtained and presented in this study can be used for further enhancement of hydrogen gas sensing properties of devices based on this material, which can be potentially integrated and used in personal, industrial, environmental monitoring devices.

The results were presented and discussed at the 13th International Conference on Electronics, Communications and Computing (IC ECCO 2024), Chisinau, Republic of Moldova, 17-18 October, 2024.

Acknowledgments: This paper was supported by project code 24.80012.5007.15TC by National Agency for Research and Development of Moldova at Technical University of Moldova.

Cristian Lupan gratefully acknowledges: Kiel University, Germany, Department of Materials Science, Chair for Multicomponent Materials and Chair of Functional Nanomaterials; PSL Université, Chimie-ParisTech IRCP, Paris, France; Twente University, Enschede, the Netherlands for collaboration in 2023 – 2025 and Technical University of Moldova for constant support. C. Lupan would like to express special appreciation and thanks to Ph.D. scientific adviser Professor, dr. hab. Artur Buzdugan (TUM) and assoc. prof. dr. Nicolai Ababii (TUM) for their support, comments and discussions on this work.

Conflicts of Interest: The author declares no conflict of interest.

References

1. Wang, C.; Yin, L.; Zhang, L.; Xiang, D.; Gao, R. Metal oxide gas sensors: Sensitivity and influencing factors. *Sensors* 2010, 10, pp. 2088–2106.
2. Schröder, S.; Ababii, N.; Brînză, M.; Magariu, N.; Zimoch, L.; Bodduluri, M. T.; Strunskus, T.; Adelung, R.; Faupel, F.; Lupan, O. Tuning the Selectivity of Metal Oxide Gas Sensors with Vapor Phase Deposited Ultrathin Polymer Thin Films. *Polymers* (Basel) 2023, 15, 524.
3. Mishra, Y. K.; Kaps, S.; Schuchardt, A.; Paulowicz, I.; Jin, X.; Gedamu, D.; Wille, S.; Lupan, O.; Adelung, R. Versatile fabrication of complex shaped metal oxide nano-microstructures and their interconnected

networks for multifunctional applications. *KONA Powder Part J* 2014, 31, pp. 92–110.
4. Paulowicz, I.; Postica, V.; Lupan, O.; Wolff, N.; Shree, S.; Cojocaru, A.; Deng, M.; Mishra, Y. K.; Tiginyanu, I.; Kienle, L.; Adelung, R. Zinc oxide nanotetrapods with four different arm morphologies for versatile nanosensors. *Sensors Actuators, B Chem* 2018, 262, pp. 425–435.
5. Lupan, O.; Chow, L.; Chai, G.; Heinrich, H.; Park, S.; Schulte, A. Growth of tetragonal SnO_2 microcubes and their characterization. *J Cryst Growth* 2008, 311, pp. 152–155.
6. Khallaf, H.; Chen, C. T.; Chang, L. B.; Lupan, O.; Dutta, A.; Heinrich, H.; Haque, F.; Del Barco, E.; Chow, L. Chemical bath deposition of SnO_2 and Cd_2SnO_4 thin films. *Appl Surf Sci* 2012, 258, pp. 6069–6074.
7. Degler, D.; Weimar, U.; Barsan, N. Current Understanding of the Fundamental Mechanisms of Doped and Loaded Semiconducting Metal-Oxide-Based Gas Sensing Materials. *ACS Sensors* 2019, 4, pp. 2228–2249.
8. Newton, M. C.; Shaikhaidarov, R. ZnO tetrapod p-n junction diodes. *Appl Phys Lett* 2009, 94, pp. 20–23.
9. Khan, R.; Ra, H. W.; Kim, J. T.; Jang, W. S.; Sharma, D.; Im, Y. H. Nanojunction effects in multiple ZnO nanowire gas sensor. *Sensors Actuators, B Chem* 2010, 150, pp. 389–393.
10. Lupan, C.; Khaledialidusti, R.; Mishra, A. K.; Postica, V.; Terasa, M. I.; Magariu, N.; Pauporté, T.; Viana, B.; Drewes, J.; Vahl, A.; Faupel, F.; Adelung, R. Pd-Functionalized ZnO:Eu Columnar Films for Room-Temperature Hydrogen Gas Sensing: A Combined Experimental and Computational Approach. *ACS Appl Mater Interfaces* 2020, 12, pp. 24951–24964.
11. Chai, G. Y.; Lupan, O.; Rusu, E. V.; Stratan, G. I.; Ursaki, V. V.; Sontea, V.; Khallaf, H.; Chow, L. Functionalized individual ZnO microwire for natural gas detection. *Sensors Actuators, A Phys* 2012, 176, pp. 64–71.
12. Teimoori, F.; Khojier, K.; Dehnavi, N. Z. Investigation of sensitivity and selectivity of ZnO thin film to volatile organic compounds. *J Theor Appl Phys* 2017, 11, pp. 157–163.
13. Lupan, O.; Postica, V.; Hoppe, M.; Wolff, N.; Polonskyi, O.; Pauporté, T.; Viana, B.; Majérus, O.; Kienle, L.; Faupel, F.; Adelung, R. PdO/PdO_2 functionalized ZnO:Pd films for lower operating temperature H_2 gas sensing. *Nanoscale* 2018, 10, pp. 14107–14127.
14. Kumar, V.; Rawal, I.; Kumar, V. Fabrication of n-ZnO/p-Si++ Hetero-junction Devices for Hydrogen Detection: Effect of Annealing Temperature. *Silicon* 2022, 14, pp. 7711–7723.
15. Kaur, N.; Zappa, D.; Ferroni, M.; Poli, N.; Campanini, M.; Negrea, R.; Comini, E. Branch-like NiO/ZnO heterostructures for VOC sensing. S*ensors Actuators, B Chem* 2018, 262, pp. 477–485.
16. Hoppe, M.; Lupan, O.; Postica, V.; Wolff, N.; Duppel, V.; Kienle, L.; Tiginyanu, I.; Adelung, R. $ZnAl_2O_4$-Functionalized Zinc Oxide Microstructures for Highly Selective Hydrogen Gas Sensing Applications. *Phys Status Solidi Appl Mater Sci* 2018, 215, pp. 1–13.
17. Hemmatzadeh Saeedabad, S.; Baratto, C.; Rigoni, F.; Rozati, S. M.; Sberveglieri, G.; Vojisavljevic, K.; Malic, B. Gas sensing applications of the inverse spinel zinc tin oxide. *Mater Sci Semicond Process* 2017, 71, pp. 461–469.
18. Morán-Lázaro, J. P.; López-Urías, F.; Muñoz-Sandoval, E.; Blanco-Alonso, O.; Sanchez-Tizapa, M.; Carreon-Alvarez, A.; Guillén-Bonilla, H.; Olvera-Amador, M. de la L.; Guillén-Bonilla, A.; Rodríguez-Betancourtt, V. M. Synthesis, characterization, and sensor applications of spinel $ZnCo_2O_4$ nanoparticles. *Sensors* (Switzerland) 2016, 16, 2162.
19. Lupan, O.; Postica, V.; Labat, F.; Ciofini, I.; Pauporté, T.; Adelung, R. Ultra-sensitive and selective hydrogen nanosensor with fast response at room temperature based on a single Pd/ZnO nanowire. *Sensors Actuators, B Chem* 2018, 254, pp. 1259–1270.
20. Zhang, D.; Du, C.; Chen, J.; Shi, Q.; Wang, Q.; Li, S.; Wang, W.; Yan, X.; Fan, Q. Improvement of structural and optical properties of $ZnAl_2O_4:Cr^{3+}$ ceramics with surface modification by using various concentrations of zinc acetate. *J Sol-Gel Sci Technol* 2018, 88, pp. 422–429.
21. Padmapriya, G.; Amudhavalli, M. Synthesis and characterization studies of spinel $ZnAl_2O_4$ nanoparticles prepared by Aloe vera plant extracted combustion method. *Malaya Journal of Matematik* 2020, 2, pp. 2089–2091.
22. Lupan, C.; Kohlmann, N.; Petersen, D.; Teja, M.; Buzdugan, A.; Jetter, J.; Quandt, E.; Kienle, L.; Adelung, R. Hydrogen nanosensors based on core/shell ZnO/Al_2O_3 and $ZnO/ZnAl_2O_4$ single nanowires. *Mater Today Nano* 2025, 29, 100596.
23. Rodrigues, J.; Hoppe, M.; Ben Sedrine, N.; Wolff, N.; Duppel, V.; Kienle, L.; Adelung, R.; Mishra, Y. K.; Correia, M. R.; Monteiro, T. $ZnAl_2O_4$ decorated Al-doped ZnO tetrapodal 3D networks: microstructure, Raman and detailed temperature dependent photoluminescence analysis. *Nanoscale Adv* 2020, 2, pp. 2114-2126.
24. Mirbagheri, S. A.; Masoudpanah, S. M.; Alamolhoda, S. Structural and optical properties of $ZnAl_2O_4$ powders synthesized by solution combustion method: Effects of mixture of fuels. *Optik* (Stuttg) 2020, 204, 164170.
25. Huízar-Padilla, E.; Guillén-Bonilla, H.; Guillén-Bonilla, A.; Rodríguez-Betancourtt, V. M.; Sánchez-Martínez, A.; Guillen-Bonilla, J. T.; Gildo-Ortiz, L.; Reyes-Gómez, J. Synthesis of $ZnAl_2O_4$ and evaluation of the response in

propane atmospheres of pellets and thick films manufactured with powders of the oxide. *Sensors* 2021, 21, 2362.
26. Iaiche, S.; Djelloul, A. ZnO/$ZnAl_2O_4$ nanocomposite films studied by X-Ray diffraction, FTIR, and X-Ray photoelectron spectroscopy. *J Spectrosc* 2015, 836859.
27. Zhai, X.; Chen, X.; Ohta, S.; Sun, X. Review and prospect of the biomedical effects of hydrogen. *Med Gas Res* 2014, 4, pp. 19–22.
28. Gu, H.; Wang, Z.; Hu, Y. Hydrogen gas sensors based on semiconductor oxide nanostructures. *Sensors* 2012, 12, pp. 5517-5550.
29. Mishra, Y. K.; Modi, G.; Cretu, V.; Postica, V.; Lupan, O.; Reimer, T.; Paulowicz, I.; Hrkac, V.; Benecke, W.; Kienle, L.; Adelung, R. Direct Growth of Freestanding ZnO Tetrapod Networks for Multifunctional Applications in Photocatalysis, UV Photodetection, and Gas Sensing. *ACS Appl Mater Interfaces* 2015, 7, pp. 14303–14316.
30. Lupan, O.; Chai, G.; Chow, L. Fabrication of ZnO nanorod-based hydrogen gas nanosensor. *Microelectronics J* 2007, 38, pp. 1211–1216.
31. Lupan, O.; Magariu, N.; Khaledialidusti, R.; Mishra, A. K.; Hansen, S.; Krüger, H.; Postica, V.; Heinrich, H.; Viana, B.; Ono, L. K.; Cuenya, B. R.; Chow, L.; Adelung, R.; Pauporté, T. Comparison of Thermal Annealing versus Hydrothermal Treatment Effects on the Detection Performances of ZnO Nanowires. *ACS Appl Mater Interfaces* 2021, 13, pp. 10537–10552.
32. Shree, S.; Postica, V.; Voß, L.; Lupan, C.; Mishra, Y. K.; Kienle, L.; Adelung, R.; Lupan, O. Optimization of T-ZnO Process for Gas and UV Sensors. *ACS Appl Electron Mater* 2025, 7, pp. 3848–3863.
33. Mijangos, F.; Celaya, M. A.; Gainza, F. J.; Imaz, A.; Arana, E. SEM–EDX linear scanning: a new tool for morpho-compositional analysis of growth bands in urinary stones. *J Biol Inorg Chem* 2020, 25, pp. 705–715.
34. Khorsand Zak, A.; Abd. Majid, W. H.; Abrishami, M. E.; Yousefi, R. X-ray analysis of ZnO nanoparticles by Williamson-Hall and size-strain plot methods. *Solid State Sci* 2011, 13, pp. 251–256.
35. Yamazoe, N.; Fuchigami, J.; Kishikawa, M.; Seiyama, T. Interactions of tin oxide surface with O_2, H_2O and H_2. *Surf Sci* 1979, 86, pp. 335–344.
36. Chang, S. C. Oxygen Chemisorption on Tin Oxide: Correlation Between Electrical Conductivity and Epr Measurements. *J Vac Sci Technol* 1979, 17, pp. 366–369.
37. Barsan, N.; Rebholz, J.; Weimar, U. Conduction mechanism switch for SnO_2 based sensors during operation in application relevant conditions; Implications for modeling of sensing. *Sensors Actuators, B Chem* 2015, 207, pp. 455–459.
38. Kim, H. J.; Jeong, H. M.; Kim, T. H.; Chung, J. H.; Kang, Y. C.; Lee, J. H. Enhanced ethanol sensing characteristics of In_2O_3-decorated NiO hollow nanostructures via modulation of hole accumulation layers. *ACS Appl Mater Interfaces* 2014, 6, pp. 18197–18204.

Citation: Lupan, C. In-depth properties analysis of $ZnAl_2O_4$/ZnO micro-nanostructures. *Journal of Engineering Science*. 2025, XXXII (2), pp. 35-45. https://doi.org/10.52326/jes.utm.2025.32(2).03.

Submission of manuscripts: jes@meridian.utm.md

Journal of Engineering Science *Vol. XXXII, no. 2 (2025), pp. 46 - 57*
Fascicle *Electronics and Computer Science* *ISSN 2587-3474*
Topic *Biomedical Engineering* *eISSN 2587-3482*

https://doi.org/10.52326/jes.utm.2025.32(2).04
UDC 615.47:611.7/.8

INTERFACE ADAPTATION DESIGN FOR EXTRACELLULAR RECORDINGS FROM EXCITABLE TISSUE

Constantin-Daniel Oancea *, ORCID: 0000-0002-6138-4779

National University of Science and Technology Politehnica, Independentei 313, Bucharest, Romania
* Corresponding author: Constantin-Daniel Oancea, *daniel.oancea@upb.ro*

Received: 05. 12. 2025
Accepted: 06. 21. 2025

Abstract. For a clear and almost exhaustive perspective on the physiology of living organisms, it is important to use the best method to sample the signal and to process it correctly, without affecting the content of information. Therefore, the method must ensure the best possible sensitivity and selectivity. In this work, a device for processing physiological signals is designed. The main component will be an instrumentation amplifier, whose characteristics meet specific requirements. This is an amplifier suitable for high-quality recording of extracellular signals from muscle and nervous tissue. Its characteristics are related to the fact that it has a gain and bandwidth for the signals of interest, a common mode rejection rate, filtering and low internal noise. The input impedance is high, and the consumption is low are other key features of this device. In addition, the component costs are very low, and the design is very compact. Due to the high input impedance of the amplifier, it adapts very easily to different signals. The final experimental results show the viability of the solution chosen by design.

Keywords: *tissue, recording, conditioning, instrumentation amplifier.*

Rezumat. Pentru o perspectivă clară și aproape exhaustivă asupra fiziologiei organismelor vii, este important să se utilizeze cea mai bună metodă de eșantionare a semnalului și de procesare corectă a acestuia, fără a afecta conținutul informației. Prin urmare, metoda trebuie să asigure o sensibilitate și o selectivitate cât mai bună. În cadrul acestei lucrări se proiectează un dispozitiv pentru prelucrarea semnalelor fiziologice. Componenta principală va fi un amplificator de instrumentație, ale cărui caracteristici îndeplinesc cerințe specifice. Acesta este un amplificator potrivit pentru înregistrarea de înaltă calitate a semnalelor extracelulare din țesutul muscular și nervos. Particularitățile lui sunt legate de faptul că are un câștig și o lățime de bandă pentru semnalele de interes adecvat, o rată de rejecție a modului comun, filtrare și zgomot intern mic. Impedanța de intrare este mare și un consum redus sunt alte caracteristici cheie ale acestui dispozitiv. În plus, costurile componentelor sunt foarte mici și design-ul este foarte compact. Datorită impedanței mari de intrare a amplificatorului, se adaptează foarte ușor la semnale diferite. Rezultatele experimentale finale arată viabilitatea soluției alese prin proiectare.

Cuvinte-cheie: *țesut, înregistrare, condiționare, amplificator instrumentațional.*

1. Introduction

To design this kind of device, we must look to three basic functions of any biopotential amplifier: amplifier gain, signal filtering, and which is important when is used to live organisms, protection regarding dangerous potentials. This method can be used as an invasive or non-invasive method. An example of biopotential measurement systems is presented in Figure 1. Main components are electrodes, amplifier, oscilloscope, interface and conversion to connect to a computer. As seen in Figure 1 the performance of this measurement system depends by amplifier stage.

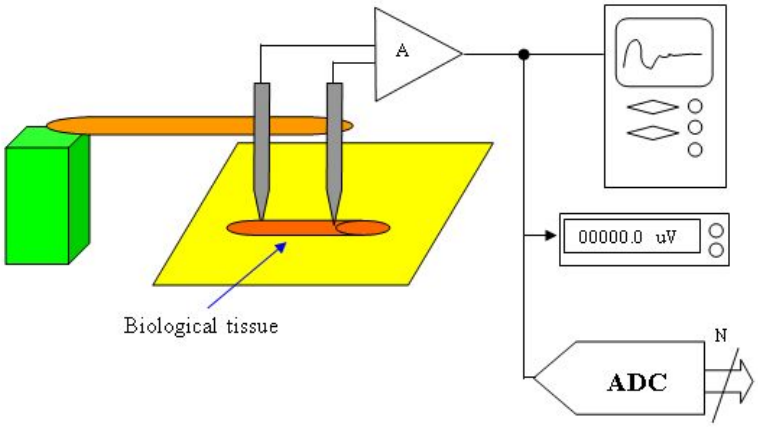

Figure 1. Measurement system for physiological pulses.

Signals can be different types starting with extracellular signals, neuro-physiological signals and brain signals or from muscular activities [1].

On the market are some examples of amplifiers used for physiological signals, like Microelectrode Amplifier (MEA) type 695, COMPEX device and various ECG devices.

The PLUGSYS MEA device is a universal amplifier that samples the signal through microelectrodes, used for physiological and pharmacological research. Using a separate preamplifier (for the first stage), it allows direct measurement of intracellular or extracellular potentials. The PLUGSYS device, even if limited to a single input channel, incorporates advanced technology that requires, in addition to the high performance of the amplifier, other modern additional facilities, such as adjustable output filter, generator for performing a calibration, audio and graphic LED indicators for monitoring the sound and visual signal. The operation of the microelectrodes can also be tested (by measuring contact resistance), tissue capacitance compensation and zero adjustment. Additionally, the PLUGSYS MEA can be equipped with special input stages and a proprietary multifunctional clamp amplifier module for current clamp and voltage clamp applications. The output is made externally via the Bayonet Neill-Concelman (BNC) jack on the front panel, which ensures firm contact and protection against interference. The bandwidth is from DC to 30 kHz (-3 dB). The output signal is ±10 V for an input signal of ±1 V. The low-pass filter has 7 steps, from 30 Hz to 30 kHz (-3 dB). The gain is fixed at 10, and the input offset compensation is ±400 mV [2].

Electrocardiogram (ECG) is an electrical signal present in living organisms with a typical amplitude of 500 μV and a frequency range of 0.01 to 250 Hz. The desired output signal from the amplifier for the ECG signal is a maximum amplitude signal of 5V, with a frequency range of 0.5 to 100 Hz. Therefore, this amplifier has a gain of 1000, and the filter will have a passband of 0.5 to 100 Hz. Three important and basic functions of any biopotential amplifier must be considered when studying this type of amplifier: patient protection from

non-compliant electrical voltages, signal amplification, and signal filtering. The biopotential amplifier requires an appropriate amplification range, as well as an appropriate frequency range. Noise reduction is another constraint of this amplifier. The basic components of biopotential amplifiers are differential topology amplifiers and instrumentation amplifiers.

COMPEX device is a typical example for a device used to record biological pulses. The basic unit contains an IEEE-488 interface and thus is connected to any computer that is also fitted to this standard. High transfer rates (1 Mb/s) ensure us to be able to connect simultaneously several (up to 16) basic units. Every basic unit is equipped with its own microcontroller that organizes the data exchange with the computer. COMPEX module for analog measurements allows the two-channel recording of extremely fast analog signals. The sampling frequency is 300 kHz maximum, so in this case a resolution of 10 measuring points signals of up to 30 kHz can be recorded per period. To avoid couplings of the earth cables the inputs are designed as earth-free differential voltage inputs so that in each case only the exact voltage difference between two freely selected points is measured and displayed. Therefore, this plug-in module is extremely suitable for representing nerve and sensory, physiological values. It is not necessary to buy and operate a recorder or an expensive storage oscilloscope. The inputs are differential, input resistance is 1MΩ, sensitivity have many values (100 mV, 200 mV, 500 mV, 1 V, 2 V, 5 V, 10 V), sampling frequency: software controlled, 30 Hz, 100 Hz, 300 Hz, 1 kHz, 10 kHz, 30 kHz, 100 kHz, 300 kHz, resolution has 8biţi and triggering point of time: software controlled: 0-90 % [3, 4].

From the example above we must take into consideration some aspects regarding proposed device. Briefly, it is about properties that they must fulfill.

Signal amplification is important because of its very low amplitude of its. For signals like EMG, 0,1 mV value can be found. Entire range is around from 10 μV to 5 mV. Signal output value is around 5 V. Necessary gain is x5000. At the same time, with our signal it is other interference signals [5].

Amplifier stages not limited only to simple amplification, but it must be accomplishing others things like accuracy of gain and linearity of signal, current – voltage conversion, decrease noise by increasing signal to noise ratio, and filtering capabilities.

For amplification only function it is thought that we have the following: noise, gain/sensitivity, domain, input signal type (differential or single-ended), common mode rejection rate, input impedance, filtering performance [5].

Noise sources can be from amplifier itself, environment itself (bioelectric sources, heartbeat), cabling effects (power supply at 50Hz), and movement artifact 30Hz. Rejection and attenuation of these noise signals can be done by shielded cable and pre-amplified electrodes.

Gain and sensitivity must vary in a wide range and linearity and gain accuracy must be within reasonable limits.

If it is not choosing an optimal range, for great signals, the device can go in clipped mode and distort the signal. To avoid clipped conditions, there must be the proper gain [5].

Input in amplifier can be done referenced to ground (one working electrode and one reference electrode), differential (two working electrodes and one reference electrode) or double differential (three working electrodes and one reference electrode). The last two electrodes can give better signals and minimum disturbance from common mode signals.

Common Mode Rejection Ratio (CMRR) represents a coefficient which shows how good the amplifier is in eliminating common artifacts regarding useful signals. The great value of

it denotes a very good amplifier. For example, if we have a CMRR ratio ⩾ 10000:1 (or 80 dB) then 99.99% from common signal is rejected or difference of electrode potentials (working electrode and reference electrode) is increased for 10000 times greater than both electrodes common potentials [6].

Input impedance means a quantitative meaning of resistance against current flow. Important is electrodes/site preparation impedance but amplifier input impedance, also. The mutual impact of these both impedances can be reduced to minimum by adaptation.

Practical input impedance of amplifier must be greater than surface contact to avoid signal attenuation. Input impedance can be optimized by setting the place (shave region, abrade, clean with alcohol, use electrolytic gel) and circuit design. For better results, the electrode impedance and surface impedance should be reduced as much as possible, or the input impedance of the amplifier should be increased. Noise reduction is closely correlated with electrode impedance.

Another way to decrease the noise is to shield with a metallic case, the entire measurement system. Using electrochemical batteries, it is a good way to reduce costs of power supply.

Filter types used can be low-pass, notch filter and high-pass. The low-pass filter allows signals with a frequency lower than an upper limit to pass (800-1000 Hz for EMG). Notch filter eliminates a narrow frequency band (50 Hz). The high-pass filter does not allow signals with a frequency lower than a limit to pass (2 Hz for EMG).

Some amplifier has selectable output modes: original signal, RMS: "root mean square" processed signal, and filtered signal. It is recommended to collect raw signals and post-process as needed, to avoid losing information.

The main objective of this work is to develop, with minimal cost, a high-performance amplifier that can bring the low-level signals present in the human body to a convenient level. The output signal of this device can be used, for example, as an input for an acquisition board. This way, the advantages of data processing using a computer system can be used. The fact that the scheme can be easily adapted (by gain and filter options) to any signal is an advantage, ensuring versatility. Avoiding noise that can affect the original signal is done by using shielded cables and protecting the entire device with a metal box.

2. Materials and Methods

The proposed device is a combination of amplifiers-filters, that main purpose is to adapt physiological signal to easy follow by classical measurement methods. This is important when want to connect this device to a data acquisition system for post processing and memorizing them. For the current situation, we have the following parameters considered for the designed device [7]:

- A very high input impedance
- Gain range: 100 - 1000
- Bandwidth, controlled by filtering: 1 Hz – 5 kHz (20 kHz)
- CMRR ~ 100 dB

The general block diagram for this type of measurement system is shown in Figure 2. Components are IA – instrumentation amplifier, A – signal amplification, F – filters.

If the main role of first two stages is to amplifier and to convert from differential signal to ground referenced signal, the filtering stage rejects useless signal (industrial power supply

– 50 Hz) and to superior limiting to avoid overlapping signal spectral components. This last thing is important when it is used an analog to digital converter [8].

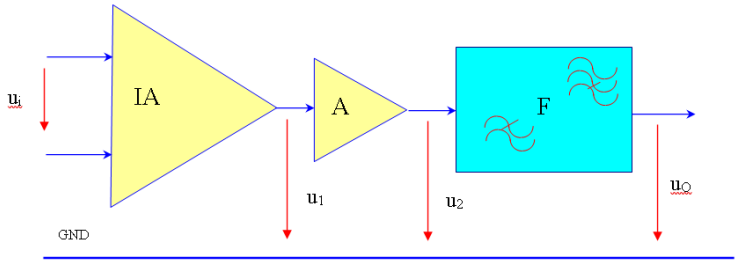

Figure 2. Block diagram of amplification-filtering device.

There are two types of filters: notch filters and low-pass filters. The block diagram is a minimal configuration. Special restrictions must be made to shield the device.

The first stage of this device must be an instrumentation amplifier. The main advantage is common mode rejection rate, very high input impedance and a single adjustable resistor for gain. At the first look, the amplification can be solved from one amplification stage. But it is important to know that the amplification is not constant to any frequency. Here were used LT1920, by Linear Technologies. Two operational amplifiers do the next two amplifier stages from integrated quad circuit LT1079. The preferable solution is this because the interest is to maintain enough bandwidth. The gain and frequency bandwidths are antagonist behavior [9].

A double T network can do a high-quality notch filter. Double T network is one of the RC filtering networks who has a very good characteristic. This RC network is working together with a repeater, which ensures a segregate of output versus network and low output impedance. The high input impedance of repeaters made by operational amplifier has a result in double T network resistor dimensions [10]. Therefore, the capacitors have very low capacitance and low physical dimensions, even if there are low frequency [11]. Quality factor, Q, is about 50. Repeater does not affect double T network parameters, slope and frequency. Figure 3 shows an example of a notch filter [12].

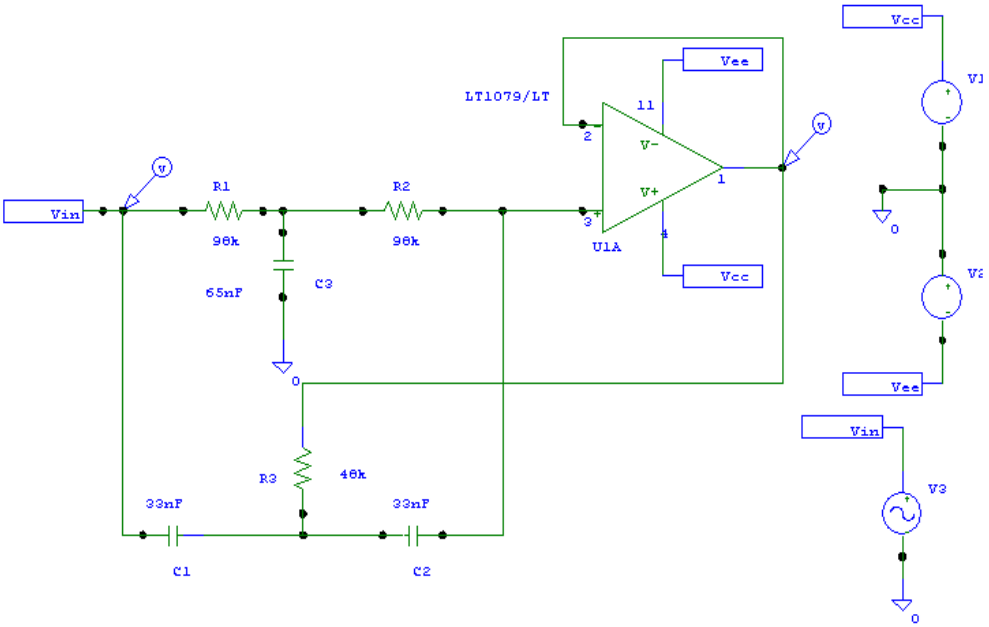

Figure 3. Example of notch filter schematics.

The relationship between capacitor C3 and resistor R3, which usually are linked to ground, is connected to the output of the repeater. This case does not affect the entire functionality of filters because of the very low impedance of output [13].

For interested frequency, ft=50 Hz, the results are pair value: R1=98 kΩ and C1=33 nF or R1=318 kΩ and C1=10 nF. These quantities are for industrial frequency, 50Hz in European countries, rejection.

$$f_0 = \frac{1}{2 \cdot \pi \cdot R1 \cdot C1}$$
$$R1 = R2 = 2 \cdot R3 \quad (1)$$
$$C1 = C2 = \frac{C3}{2}$$

The characteristic of the studied notch filter (for 50 Hz) is very well outlined, Figure 4.

If this device is used in a computer aided system, it is not necessary because the industrial frequency is easy to reject by digital filtering. In this case we must use an anti-aliasing filter to avoid false artefacts in signal [14].

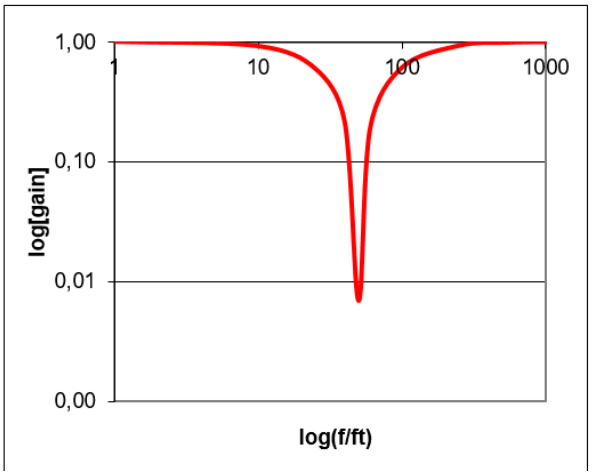

Figure 4. The characteristic of the studied notch filter.

The low-pass filter is depicted in Figure 5. Cut off frequency is around 10kHz. Relation 2 described the cut off frequency by circuit passive elements.

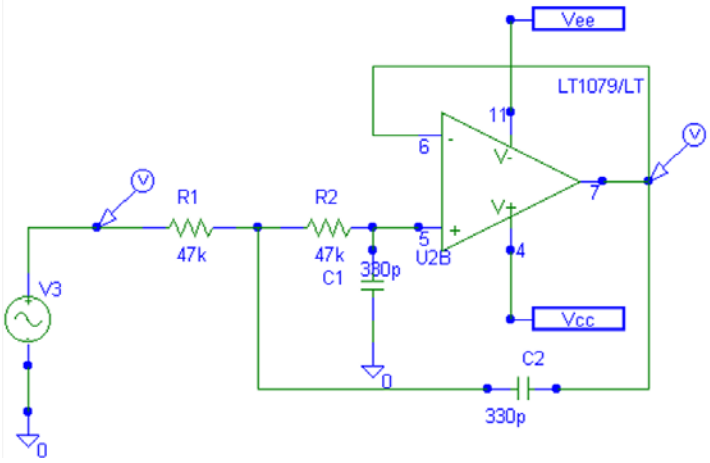

Figure 5. Low-pass filter.

$$2 \cdot \pi \cdot f = \frac{1}{\sqrt{R1 \cdot R2 \cdot C1 \cdot C2}}$$
$$f = \frac{1}{2 \cdot \pi \cdot \sqrt{R1 \cdot R2 \cdot C1 \cdot C2}} \quad (2)$$

R1=R2=47 kΩ and C1=C2= 330 pF => f= 10261 Hz.

For experimental purposes, we designed two different schematics, but with the same structure. The first schematic has bipolar power supply and inverted amplifier stage and the second use unipolar power supply and non-inverted amplifier stage. Figure 6 shows the complete schematics for bipolar power supply.

Obviously, this schematic can be changed and adapted to different requests. Thus, it can be removed, or bridging, some stages and modify amplification until 10000. The only preliminary phase of this device is the calibration phase of a convenable amplifier, for a specified signal.

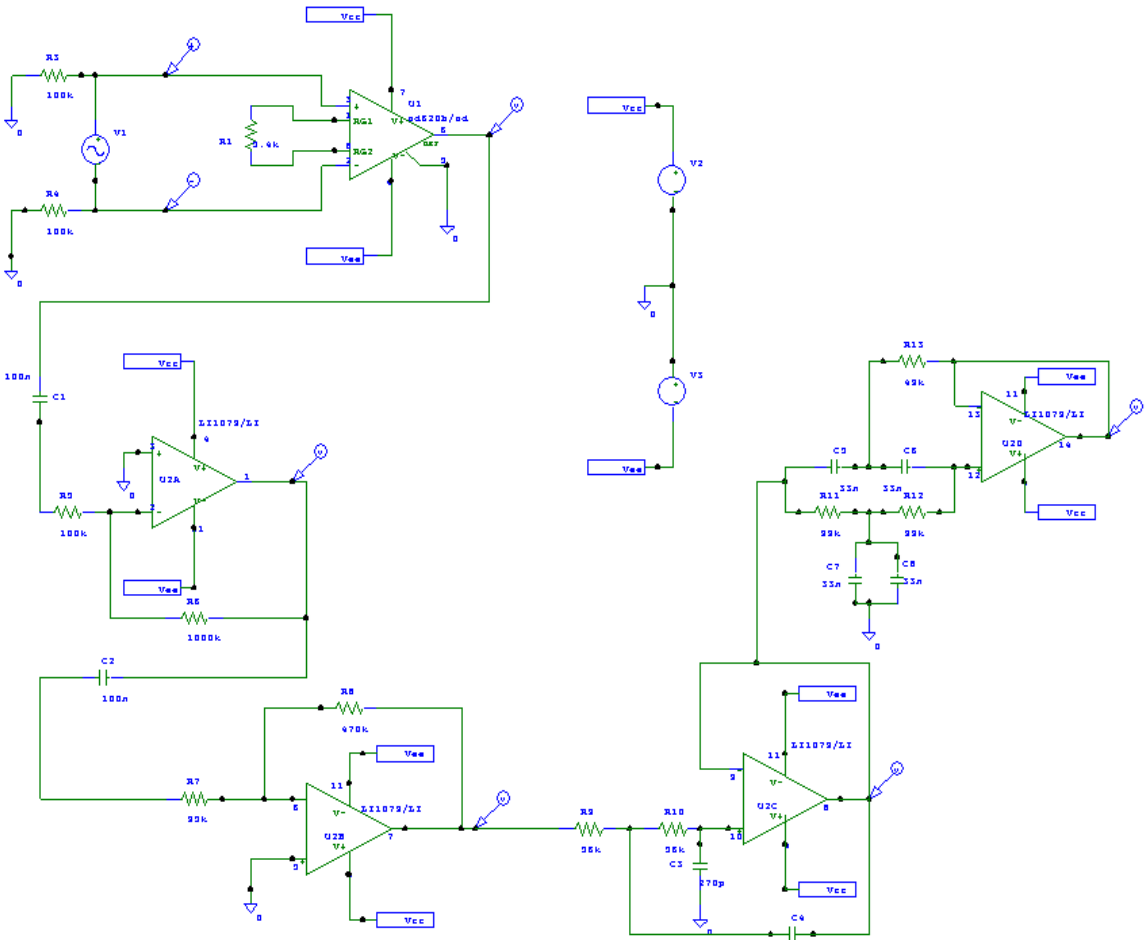

Figure 6. Bipolar power supply, full schematics.

Complete schematic of unipolar power supply is in Figure 7 and has some particular aspects. To make a translation of signal, which became with only one polarity, it is used a reference voltage connected to REF terminals of instrumentation amplifiers LT1920. The intermediary amplifier stage is connected directed (DC coupled) and are non-inverted type. This was enforced by unipolar signal. Schematics are very flexible and can be changed to different signal sources. Filtered stages are unchanged because they are made in non-inverted configuration.

Practical aspects of the device must be according to problems with this type of very low signal device. To shield regarding noise, all printed circuit board must be in metallic box. It is preferable to use connection terminals, because of easy use of connection elements. To select the gain of the device the back panel has a three-position switch. The input in device is done by shielded cable with a minimum length. On the front panel is another three-position switch to select clean signal or filtered signal [15].

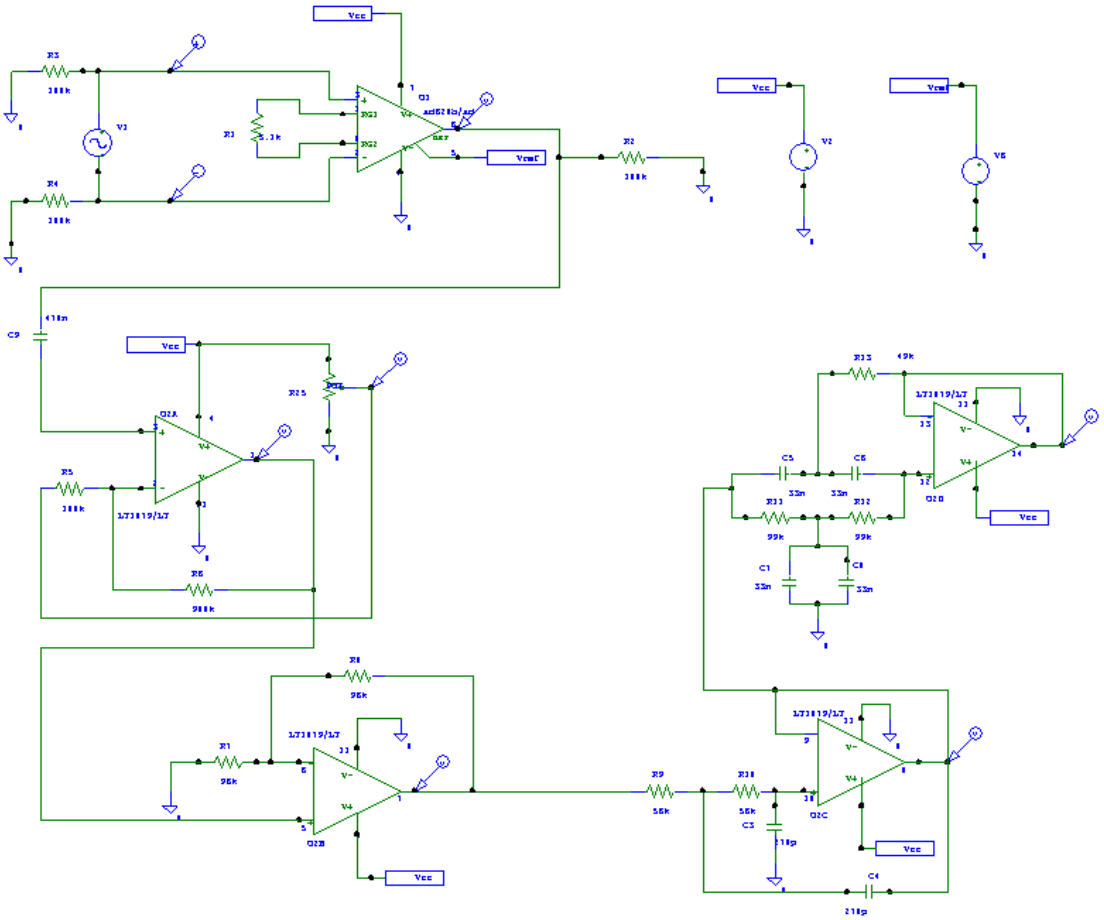

Figure 7. Unipolar power supply, full schematics.

It must be considered that the power supply should be made from chemical sources of continuous current to eliminate any additional interference.

3. Results and Discussion

The amplifier made was tested in signal simulation condition and real condition. One of the first tests is to see the input-output functionality and to determine the characteristics of amplifier. A signal generator and an oscilloscope can be useful at this time. If the generator does not permit low level signals, a signal generator and amplifier is inserted into a voltage divider. Two resistors make it. Oscilloscope must have sensitivity, to represent low level signal. Experiments are made using a non-filtered and filtered signal. Notch filters stage (50 Hz) affects the signal, and the experiment reveals this.

Input signal has a convenient value to oscilloscope (5-10 mV). To avoid clipped mode, at this stage, the gain is reduced to acceptable value. For example, a value of 100 times to gain is enough. Other criterion that must handle are internal noise and common mode rejection rate. Internal noise can be measured connected to the differential input some resistors (0 Ω, 100 kΩ and 1 MΩ). Theoretically, the output must have 0 V. For CMRR the

procedure is to apply both inputs through 100 kΩ two resistors a sinusoidal signal with 1 V amplitude and 50 Hz frequency and follow the output. For this test notch filters (50 Hz) are not used.

For real physiological signals here, sciatic nerves were used from rat or frog. The starting procedure consists of a biological tissue preserve solution. Along with experiments it was finding lose the physiological signal after 1-2 hours (because of nerve fiber drying).

Because of multiple configurations possibilities, this amplifier can be used to ECG or EMG type of signal.

For every working condition, is necessary to modify the amplification, cut off frequency of filters and input configurations.

Signals can be processed after using a plug-in or stand-alone acquisition system. Data from acquisition is saved in file. The software is a simple date transfer from an oscilloscope display and computer. The main component is an oscilloscope. For signal acquisition here there was used serial interface of an oscilloscope. Statistical processing and mathematical transformers can be used to extract utility information from the waveform.

Experiments are done using rat sciatic nerves. Using signal stimulator, the experimental results are present in waveform from Figures 8 and 9. Stimulation is done by one or two pulses. Informative, parameters of these are 0.5 – 5mV amplitude and a pulse width of 1-10 ms.

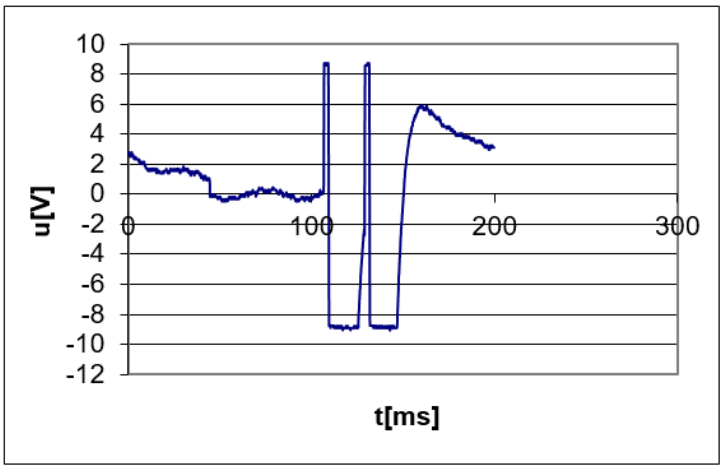

Figure 8. Stimulus signal.

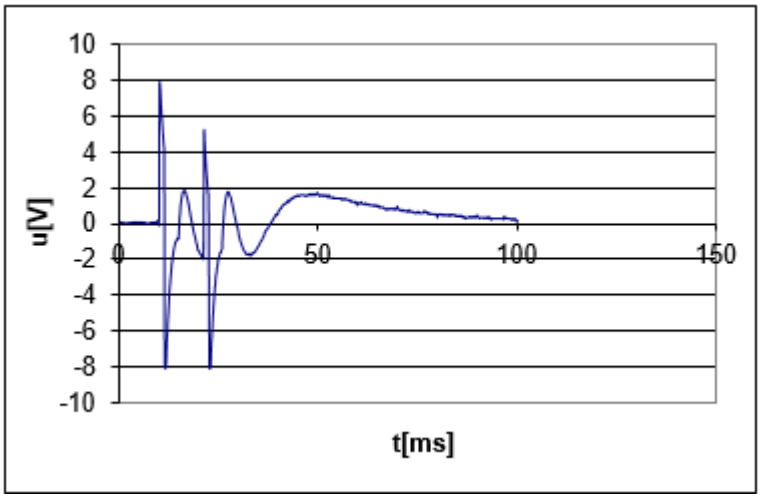

Figure 9. Sciatic nerve signal, excited by stimulus signal.

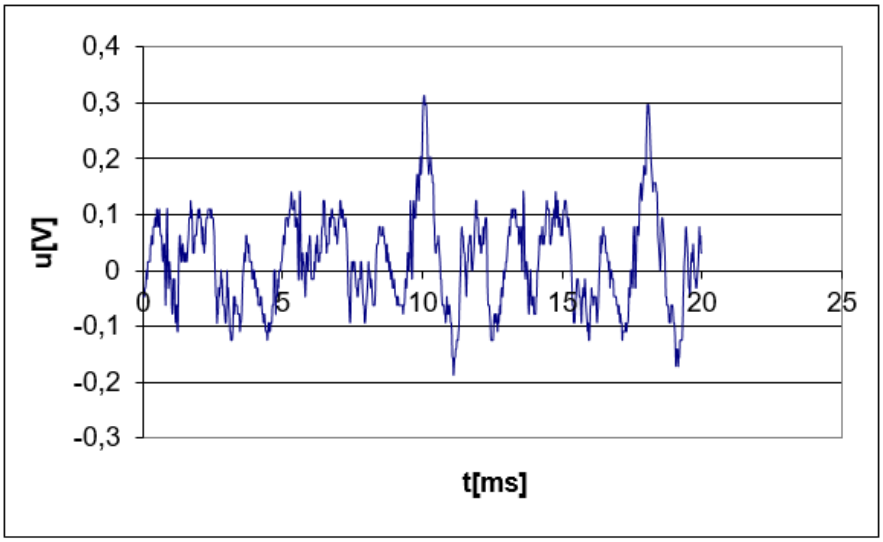

Figure 10. Sciatic nerve signal, without stimulus.

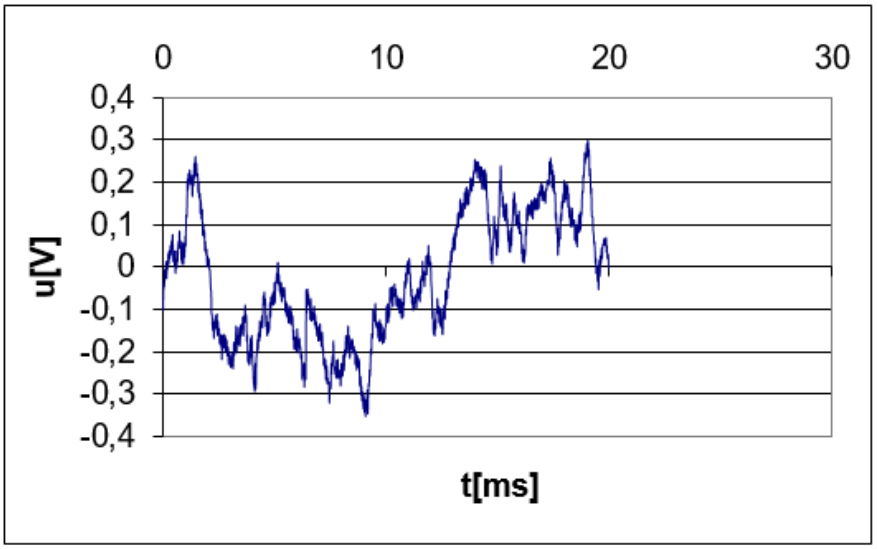

Figure 11. Frequency of 50Hz influence, signal unfiltered.

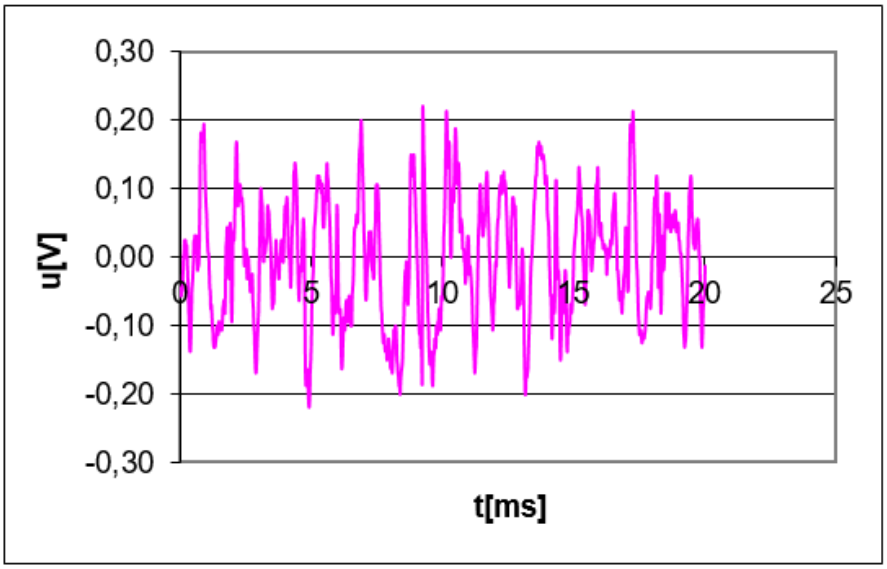

Figure 12. Signal filtered (50 Hz rejected).

Avoid using filters has the result of signal distortion, things shown in Figure 11, where is not use notch filter 50 Hz. The useful signal is modulated by 50 Hz frequency. To compare, in Figure 12 is shown the same signal but filters (50 Hz rejected). The experimental device is depicted in Figure 13.

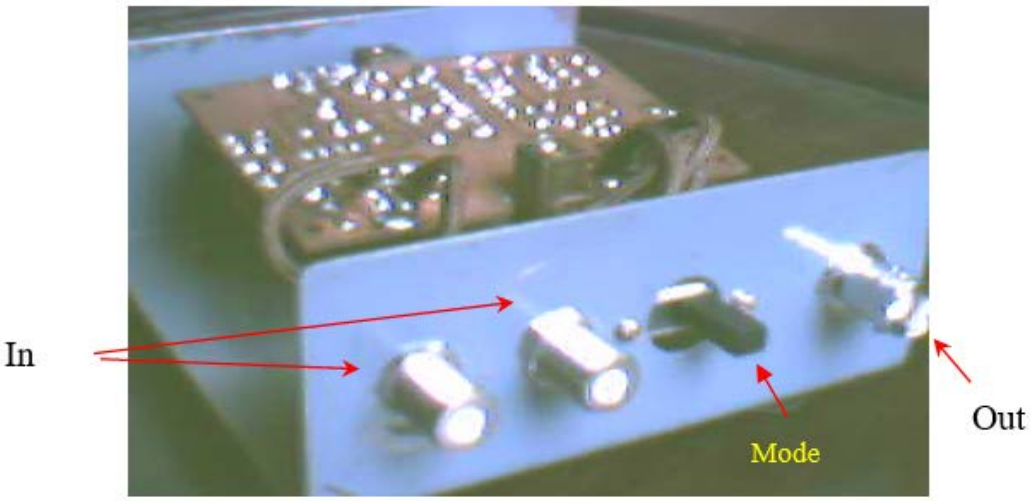

Figure 13. Overview of experimental device.

Considering the results obtained, the designed device, for amplifying low-level signals of a biomedical nature, works according to the proposed objective. Although it is a purely analog implementation, using quality components and considering appropriate technological design of printed circuit board rules, the results confirm a realistic approach.

4. Conclusions

Briefly, the mains accomplish of this paper are:

- Documentation steps consisting in distinguishing parameters of physiological signal amplifiers, displaying some types of this device, which are used in specialty laboratories, research/processing signal methods, using filters and importance of that.
- Designing, according to the block diagram of a physiological signal amplifier, in two alternatives: bipolar and unipolar power supply.
- Schematics functionality by simulation and by experimentation.
- Practical implementation of amplifier, Figure 13.
- Experimental diagram of filters.
- Experimental diagrams of device and reveal unusual state like amplifier saturation.
- Using this device to real physiological signals, from rat nerve.

On all experimental work signals had prevailed through non polarized capacitors. This can affect the output characteristic on the failing edge at very low frequency.

The experiment was done using signal waveform generator and an oscilloscope to determine the output characteristic and using rat sciatic nerve for real physiological signal. Tests can be extended by external signal, for example skin surface. Contact surface must be very clean for a steady connection (using silver electrodes is a good idea).

All connection elements are shielded to avoid additional noise sources. On the front panel of the box are F connector for input signal, BNC coupling for output signal, switch to select type of signal in three steps (only amplifier, low pass filtered signal and notch filtered signal 50 Hz).

In opposite side are gain selection switch (three steps) and power supply connectors. Using power supply from battery instead of real DC power supply. It has no ripple over DC component.

This paper was presented at the scientific event the International Conference on Electronics, Communications, and Computers (ECCO 2024), October 17-18, 2024, Technical University of Moldova, Chisinau.

Conflicts of Interest: The author declares no conflict of interest.

References

1. Radwan, A.; Mohammed, M.; Mahmoud, H. Review of Biometric Sensors for Assessing Human Emotional Responses in Virtual Reality Architectural Studies. *JES Journal of Engineering Sciences* 2025, 53(3), pp. 288-305. doi: 10.21608/jesaun.2025.354434.1415
2. PLUGSYS Microelectrode Amplifier Module (MEA). Available online: https://www.hugo-sachs.de/plugsys-microelectrode-amplif-er-mea.html (accessed on 20 March 2024).
3. Easysnap Electrodes for Compex Muscle Stimulators. Available online: https://www.compex.com/en/accessories/electrodes (accessed on 20 March 2024).
4. PLUGSYS Microelectrode Amplifier Module (MEA). Available online: https://www.harvardapparatus.com/plugsys-microelectrode-amplif-er-mea.html (accessed on 20 March 2024).
5. Counts, L.; Kitchen, C. *A Designer's Guide to Instrumentation Amplifiers*, 3rd ed.. Analog Devices Inc., USA, 2006, 130 p.
6. Abdel-Hafez, I.; Khalaf, Y.; Farag, F. High linearity cmos variable gain amplifier for UWB applications. *JES Journal of Engineering Sciences* 2013, 41(2), pp. 577-591. doi: 10.21608/jesaun.2013.114750
7. Wu, R.; Huijsing, J.H.; Makinwa, K.A.A. *Dynamic offset cancellation techniques for operational amplifiers in precision instrumentation amplifiers and read-out integrated circuits*. Springer Printing House, New York, SUA, 2013, pp. 21-49.
8. Gree, S. Design notes for a 2-pole filter with differential input. *Cirrus Logic* 2003, 6 p.
9. Williams, A. *Analog Filter and Circuit Design*. McGraw-Hill Education Publisher, NY, USA, 2013, 640 p.
10. Lacanette, K. A *Basic Introduction to Filters – Active, Passive and Switched-capacitor*. National Semiconductor, Dallas, USA, 1991, 24 p.
11. Winder, S. *Analog and Digital Filter Design*. Second Edition, Newnes Publishing, Boston, USA, 2002, 456 p.
12. El-Saady, G.; Hemeida, A.; Nasrallah, M. Voltage and current harmonic suppression by shunt active filter feeding dc load on dc link. *JES. Journal of Engineering Sciences* 2013, 41(2), pp. 558-576. doi: 10.21608/jesaun.2013.114749.
13. Pactitis, S.A. *Active Filters: Theory and Design*. CRC Press Publisher, Boca Raton, USA, 2007, 274 p.
14. Su, K. *Analog Filters*, Second Edition. Springer Publisher, New York, USA, 2010, 421 p.
15. The Axon Guide. A guide to Electrophysiology and Biophysics Laboratory Techniques. 3rd Edition, 2012. Available online: http://ala-laurila.biosci.helsinki.fi/content/refs/axon_guide_3rd_edition.pdf (accessed on 20 March 2024).

Citation: Oancea, C.-D. Interface adaptation design for extracellular recordings from excitable tissue. *Journal of Engineering Science*. 2025, XXXII (2), pp. 46-57. https://doi.org/10.52326/jes.utm.2025.32(2).04.

Submission of manuscripts: jes@meridian.utm.md

Journal of Engineering Science *Vol. XXXII, no. 2 (2025), pp. 58 - 67*
Fascicle *Electronics and Computer Science* *ISSN 2587-3474*
Topic *Biomedical Engineering* *eISSN 2587-3482*

https://doi.org/10.52326/jes.utm.2025.32(2).05
UDC 615.47:005.6

ENSURING EFFECTIVE MANAGEMENT OF MEDICAL DEVICES THROUGH SAFE USE OF MEDICAL DEVICES AND EVIDENCE-BASED MANAGEMENT

Gheorghe Gorceag *, ORCID: 0000-0002-4470-8014

Technical University of Moldova, 168 Ștefan cel mare Blvd., Chisinau, Republic of Moldova
* Corresponding author: Gheorghe Gorceag, *gheorghe.gorceag@mib.utm.md*

Received: 06. 07. 2025
Accepted: 06. 28. 2025

Abstract. To ensure effective management of medical devices, it is imperative that medical devices must be safe and inoffensive, and their management must be based on evidence. Thus, to help enhance the safety of medical devices, a new mechanism for the periodic compliance assessment of medical devices has been developed. The mechanism involves the assessment of general safety, electrical safety and performance parameters in line with international best practice. At the same time, the effective management of medical devices requires data and information related to medical devices and their lifecycle events, which can be obtained through the medical device management information system. The establishment and implementation of efficient management of medical devices, involves strengthening the capacities of medical devices' management, in order to be able to respond to the current requirements of the health system, in such a way as to ensure the functionality of medical devices and the safe and efficient use of medical devices. Accordingly, the implementation of efficient management of medical devices is fundamental for providing qualitative, safe and efficient medical devices, which contributes to increasing the quality of medical services.

Keywords: *medical devices, information system, medical device management, periodic verification, security, performance, records, safety, efficiency.*

Rezumat. Pentru asigurarea unui management eficient a dispozitivelor medicale, este imperial necesar ca dispozitivele medicale să fie sigure și inofensive, iar gestionarea acestora să fie bazată pe evidență și dovezi. Astfel, pentru a contribui la sporirea siguranței dispozitivelor medicale, a fost elaborat un nou mecanism de evaluare periodică a conformității dispozitivelor medicale. Mecanismul presupune evaluarea parametrilor de securitate generală, de securitate electrică și parametrilor de performanță în conformitate cu cele mai bune practici internaționale. În același timp, pentru gestionarea eficientă a dispozitivelor medicale sunt necesare date și informații aferente dispozitivelor medicale și a evenimentelor ciclului de viață a acestora, care pot fi obținute prin intermediul sistemului informațional de management a dispozitivelor medicale. Stabilirea și implementarea unui management eficient al dispozitivelor medicale necesită fortificarea capacităților de gestionare a dispozitivelor medicale, pentru a putea răspunde cerințelor actuale ale sistemului de sănătate, astfel încât să se asigure funcționalitatea dispozitivelor medicale și

utilizarea sigură și eficientă a acestora. Drept rezultat, punerea în aplicare a unui management eficient al dispozitivelor medicale este fundamentală pentru utilizarea dispozitivelor medicale calitative, sigure și eficiente, ceea ce contribuie la creșterea calității serviciilor medicale.

Cuvinte-cheie: *dispozitive medicale, sistem informațional, management a dispozitivelor medicale, verificare periodică, securitate, performanță, evidență, siguranță, eficiență.*

1. Introduction

Currently, at the international and national level, it is certain that medical devices have become indispensable in the performance of medical acts.

At the same time, international experience shows us that the involvement of the necessary resources and the implementation of an efficient management of medical devices increase the performance of medical devices. Meanwhile, qualitative, efficient and safe medical devices, used at their maximum performance, contribute to increasing the quality and safety of medical services [1].

Accordingly, the streamlining of the medical device management system is an essential element in order to ensure the quality and safety of medical acts, and this must be in relation to the best international practices, as well as in accordance with the current requirements of the health system. The establishment of an efficient management of medical devices also involves strengthening management capacities in the field of medical devices by recording and ensuring the security and performance parameters of medical devices [2].

2. Medical device management information system

One of the basic conditions for efficient management of medical devices is the record of medical devices, in order to manage them correctly and efficiently. This involves the development and implementation of a national database, with the purpose of recording and managing data related to medical devices and their life cycle events, monitoring the traceability of medical devices, as well as planning the procurement and maintenance processes of medical devices.

Thus, in order to create the medical device management information system (MDMIS) in the field of medical devices, it was established that it must ensure:

- ✓ creating a secure information environment regarding medical devices in use;
- ✓ delivering truthful information in an operational manner;
- ✓ quick access to data and information regardless of location;
- ✓ continuous information of users and decision-makers in the management of medical devices;
- ✓ homogenization and totalization of information at local and national levels in the health system.

The MDMIS must be a tool designed to collect, store and report information about medical devices. And, the information must be provided to the users of the system, but also to the competent public authorities, such as the Ministry of Health, the Medicines and Medical Devices Agency (MMDA), etc., according to Figure 1.

According to Figure 1, Technical University of Moldova provides qualified personnel to medical institutions, which are users of the information system and are obliged to enter information about medical devices into the MDMIS. The Ministry of Health is the central public authority that develops and promotes policies in the field of medical devices.

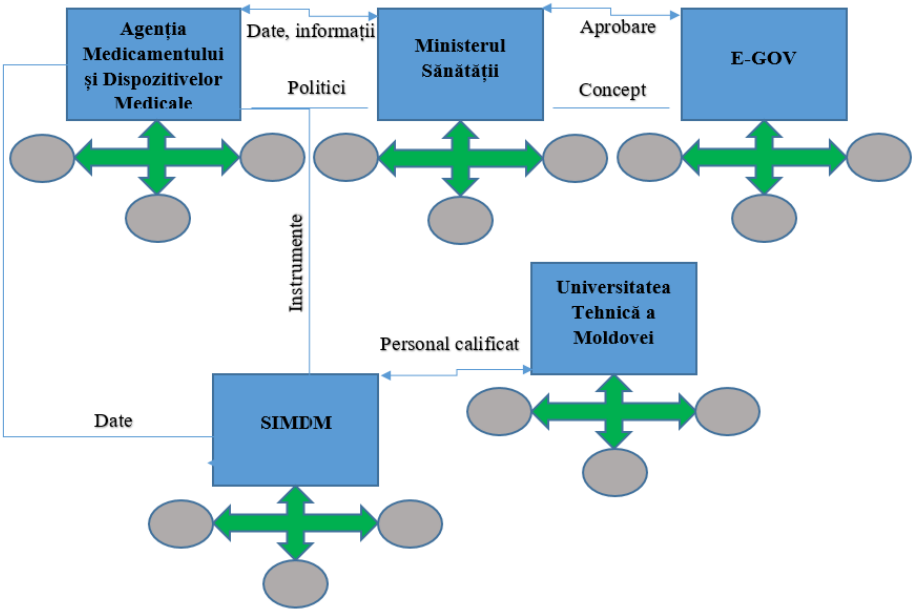

Figure 1. Organizational structure and correlation with MDMIS.

Based on the principles of the proper functioning of information systems, the Medical Devices Management Information System was developed [3,4]. According to the Order of the Ministry of Health No. 200 of 14.03.2017, its implementation became mandatory for all public medical institutions in the health system and will later be implemented in private medical institutions as well [5]. MDMIS was placed on the MMDA website (Figure 2).

Figure 2. Access to MDMIS on the MMDA website.

MDMIS stores all information about medical devices, based on which reports can be generated for users of the information system, but also for the competent public authorities, in order to improve policies in the field of medical devices, and to facilitate decision-making within the management of medical devices. After receiving the login data from MMDA, the MDMIS page is accessed and the login data is entered, according to Figure 3 [6]. The next step consists of entering all the medical device data in the open window.

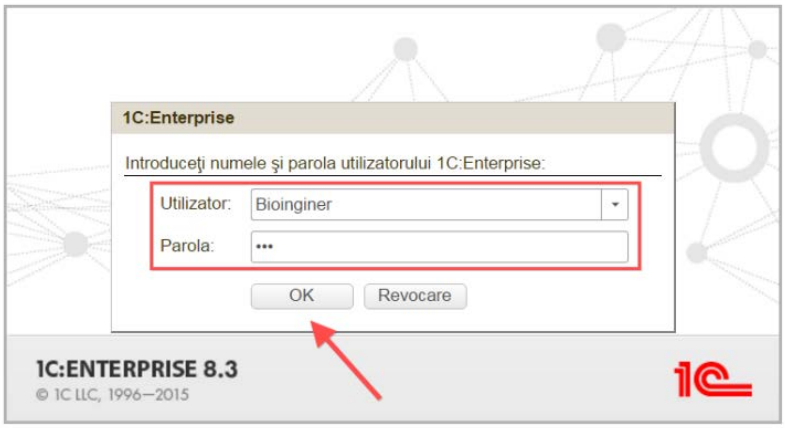

Figure 3. MDMIS login window.

In MDMIS, the following modules were provided, namely: the "Medical Devices" module; the "Consumables" module; the "Contacts" module; the "Employees" module; the "Maintenance" module; the "Periodic Check" module; the "Reports" module; the "Configuration" module; the "Tools" module; the "Vigilance" module; the "Security Subsystem" module.

All MDMIS users can access any of the 9 implemented functional modules, for example: medical device management, according to Figure 4.

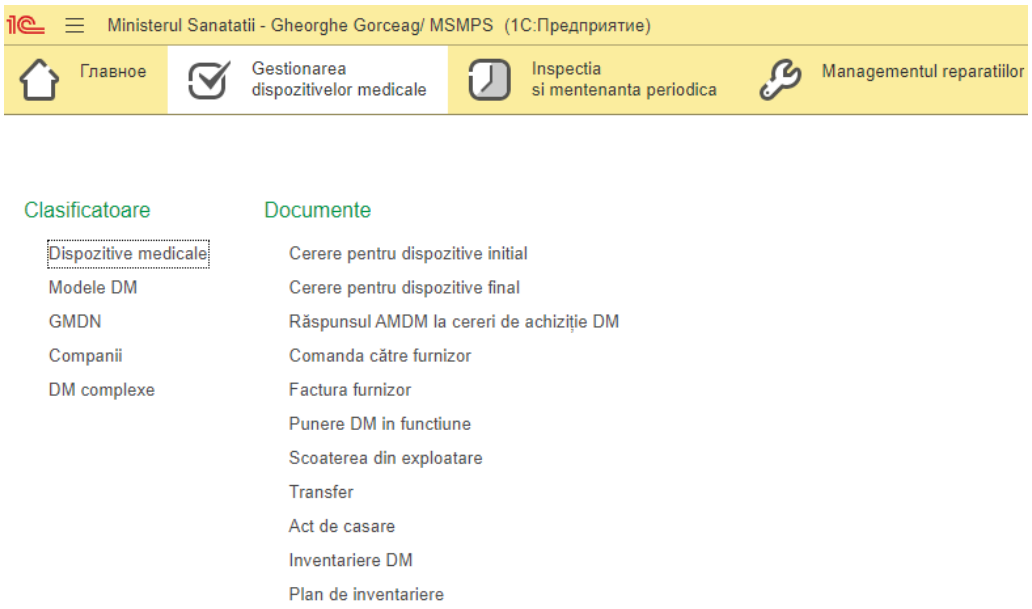

Figure 4. Medical Device Management module.

Accordingly, after entering information into the MDMIS about medical devices and related activities, data analysis reports or standard documents can be generated and provided based on predefined templates. This module can deliver the following types of reports:

- maintenance and testing report;
- engineer activity report;
- reporting of reaction time, repair time (downtime), type of defect;
- repair and activity report (medical department, bioengineers, repair time, response time, etc.);
- device report by (model, department, year of production, manufacturer, manager, price, serial number or inventory);
- report by years of receipt;

- report of hours of repairs, maintenance and inspection;
- report of available and used consumables and spare parts stock;
- report of consumables, used spare parts;
- incident reports;
- periodic verification, metrological reports;
- reports on medical devices by status (settled, intensively used, unused, defective);
- report by funding source.

With the development and implementation of MDMIS, by having a clear record of medical devices and data related to medical devices and their life cycle events, traceability of medical devices, data-driven decisions can be made regarding the replacement of certain medical devices, and the procurement and maintenance processes of medical devices can be planned. This constitutes an extremely important step in the efficient management of medical devices, and respectively, their efficient management [7].

Currently, MDMIS is implemented and can be used by all medical health facilities of the health system in the Republic of Moldova. At the same time, there is an opportunity to expand it also to private medical facilities.

3. Regulation of the mechanism for periodic verification of medical devices put into service and in use

At the same time, for efficient management and ensuring the use of safe, harmless and qualitative medical devices, it is imperative to ensure the compliance of the security, electrical safety and performance parameters of medical devices. The most appropriate and proper procedure by which the compliance of the security, electrical safety and performance parameters of medical devices can be confirmed is periodic verification.

In this regard, following the study and analysis of international practice with reference to the periodic verification of medical devices, in countries such as: Italy, France, the Netherlands, Romania, Japan, Switzerland, Germany, with the exception of the countries of the former USSR, for medical devices put into service and in use, periodic verifications are carried out through tests by laboratories/conformity assessment bodies (Figure 5) [8,9].

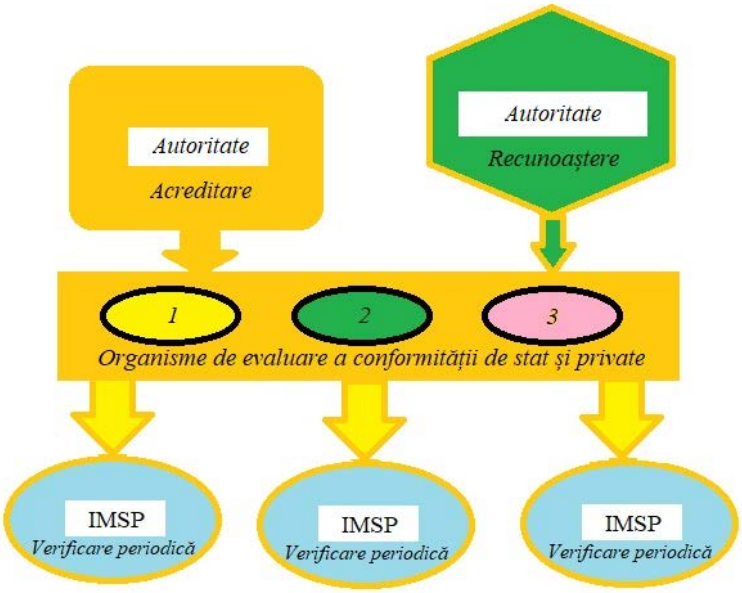

Figure 5. Model 1 of periodic verification practiced internationally.

At the same time, in some more developed countries, the same type of periodic verifications are practiced through tests, but these are carried out by bioengineers within medical institutions, who have their own testing equipment (Figure 6).

This implies that the medical institution must have the financial possibility to purchase and own the testing devices, including the instruments necessary for carrying out the periodic verification. At the same time, it is necessary to ensure the appropriate conditions for carrying out the periodic verifications, as well as the human resources (bioengineers, engineers) qualified and trained to be able to carry out the periodic verifications of the medical devices in the institution [10].

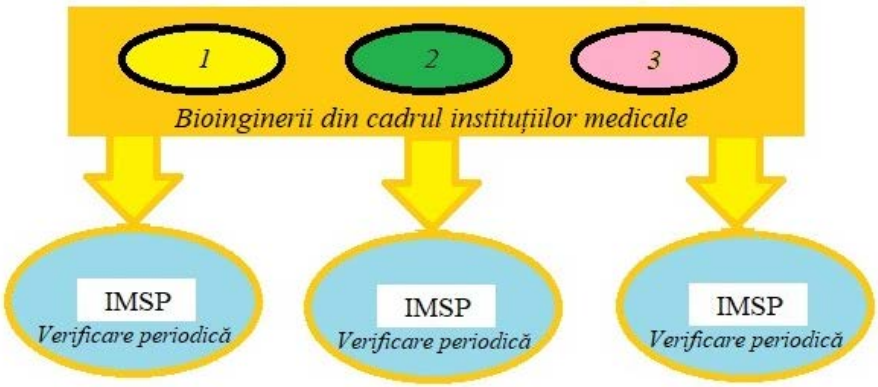

Figure 6. Model 2 of periodic verification practiced internationally.

At the national level, until 2017, medical devices that were qualified as measuring instruments were actually subject to metrological verifications that could not guarantee the conformity or the level of conformity of the safety parameters and, in particular, of the performance parameters. While, in the healthcare system, a wider variety of types of medical devices were exploited and used, important in terms of the intended purpose, with safety and performance parameters that required to be subject to periodic assessment through examination and laboratory tests. Respectively, on the one hand, the medical devices that were subject to metrological verification were insufficiently verified in terms of confirming the conformity of the safety and performance parameters. And, on the other hand, only a few types of medical devices, from the wide range of those used in the healthcare system, were subject to metrological verification (Figure 7).

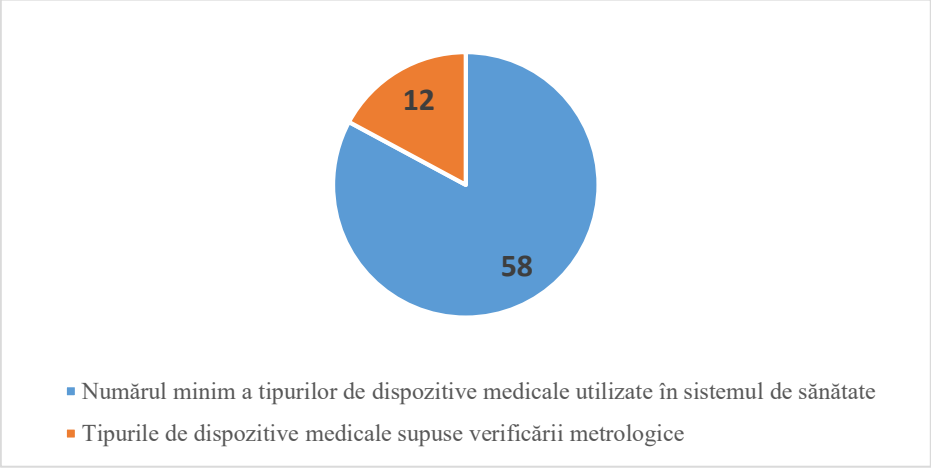

Figure 7. Ratio between medical devices subject to metrological verification and those used in the healthcare system that required periodic verification.

Accordingly, following the research and analysis carried out to develop the concept of periodic verification of medical devices put into service and in use in the healthcare system of the Republic of Moldova, we have identified several options or conceptual models for carrying out periodic verification, namely:

- by an accredited and recognized state laboratory;
- by bioengineers within medical institutions;
- by state and private conformity assessment bodies.

Considering the need for investments, as well as the allocation of human resources and appropriate spaces for carrying out periodic verification activities, conceptual model 3 (Figure 8) was identified as the most viable option, which involves carrying out periodic verifications by both state and private conformity assessment bodies [11-13]. In order for conformity assessment bodies to be admitted to carry out periodic verifications of medical devices put into service and in use, they must be accredited under the terms of Law no. 235/2011 on accreditation and conformity assessment activities, and subsequently recognized by the authority in the field, which is the Ministry of Health.

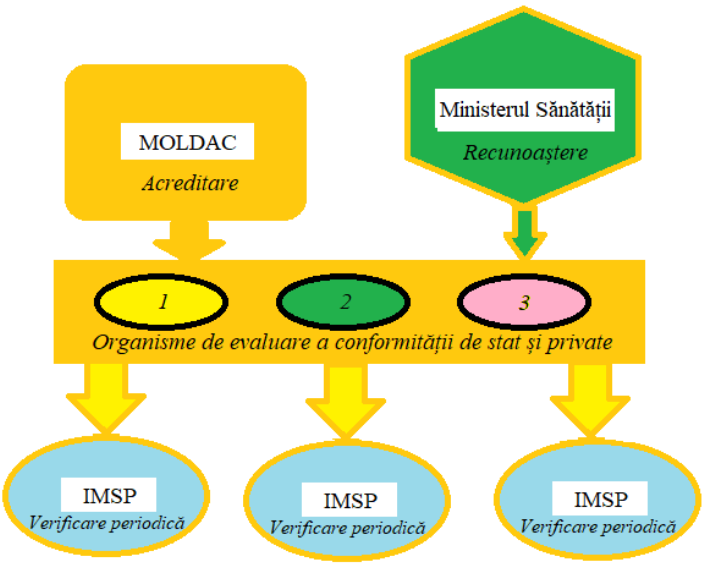

Figure 8. Conceptual model 3. Periodic verification of medical devices by state and private conformity assessment bodies.

The following step is the regulation of the mechanism for periodic verification of medical devices. Based on the provisions of Law No. 102 of June 9, 2017 on medical devices, we have developed and submitted for approval, the draft Government Decision for the approval of the Regulation on the periodic verification of medical devices put into service and in use, which was approved and became: Government Decision No. 966 of November 14, 2017, for the approval of the Regulation on the periodic verification of medical devices put into service and in use [14].

And, based on the approved Regulation, a draft order was developed regarding the specific procedures for periodic verification of medical devices (Figure 9), subsequently approved according to the Order of the Ministry of Health, Labor and Social Protection [15].

With the approval of the specific procedures for periodic verification of medical devices, we can say that the creation and implementation of a new system for periodic verification of medical devices has been achieved, which is an important step for the healthcare system of the Republic of Moldova, today the full regulatory framework is applicable to be able to carry out such periodic verifications of medical devices, at the national level.

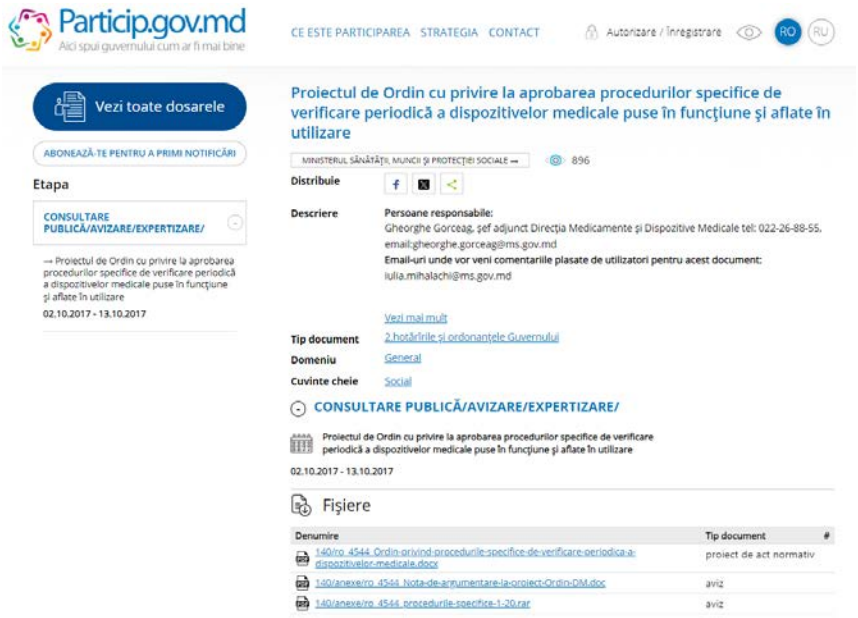

Figure 9. Draft order on specific verification procedures.

4. Discussions

MDMIS contains and provides data and information related to medical devices and their lifecycle events which is necessary for effective medical device management.

The information system has been developed following the Swiss model and is currently functional and implemented in all public health care institutions in the Republic of Moldova. It can also be extended to private medical facilities.

At the same time, the new mechanism for periodic conformity assessment of medical devices, which involves periodic assessment of general safety, electrical safety and performance parameters, is functional and implemented at national level. Respectively, all public health care institutions in the Republic of Moldova are obliged to ensure the periodic verification of medical devices.

Such types of periodic verification by laboratory tests are applied in the countries of the European Union, as well as in the USA, Japan, Australia, Ukraine, etc. In the ISC countries (countries of the ex-Soviet Union), metrological verification is still applied to medical devices, but not periodic verification by laboratory tests.

5. Conclusions

The Medical Device Management Information System is an extremely important step in the efficient management of medical devices, which together with the new system for periodic verification of medical devices contributes to the implementation of efficient management of medical devices. It allows a data-driven decisions making regarding the replacement of certain medical devices, or the procurement and maintenance of medical devices, as well as ensuring the health system with safe, high-quality and effective medical devices.

Acknowledgments Thanks to prof. univ., dr. Șontea Victor, for support and guidance, as well as for the constructive recommendations.

Conflict of interest: The author declares no conflict of interest.

References

1. World Health Organization. Available online: https://www.who.int/health-topics/medical-devices#tab=tab_1 (accessed on 10 June 2025).
2. Effective Management of Medical Technologies for A Functional Health System. In: *Electronics, Communications and Computing IC ECCO 2022*, 20-21 octombrie 2022, Tehnica-UTM, Chisinau, Republic of Moldova, 2023, p. 35. https://ibn.idsi.md/vizualizare_articol/176082.
3. Regulation (EU) 2017/745 of the European Parliament and of the Council of 5 April 2017 on Medical Devices, Amending Directive 2001/83/EC, Regulation (EC) No 178/2002 and Regulation (EC) No 1223/2009 and Repealing Council Directives 90/385/EEC and 93/42/EE (accessed on 10 June 2025).
4. Regulation (EU) 2017/746 of the European Parliament and of the Council of 5 April 2017 on in vitro diagnostic medical devices and repealing Directive 98/79/EC and Commission Decision 2010/227/EU (Text with EEA relevance.). *Official Journal* 2017, pp. 176–332.
5. Law no. 102/2017 on medical devices. Official Gazette of the Republic of Moldova, 2017, 244-251, 389.
6. Agency for Medicines and Medical Devices, Medical Devices. Available online: https://amdm.gov.md/ro (accessed on 10 June 2025).
7. Essential Principles of Safety and Performance of Medical Devices and IVD Medical Devices. Available online: https://www.imdrf.org/sites/default/files/2024-04/IMDRF GRRP WG N47 %28Edition 2%29.pdf (accessed on 10 June 2025).
8. Technical Guidance Series (TGS) for WHO Prequalification Diagnostic Assessment Guidance on Test Method Validation for in Vitro Diagnostic Medical Devices. Available online: https://iris.who.int/bitstream/handle/10665/258971/WHO-EMP-RHT-PQT-TGS4-2017.04-eng.pdf?sequence=1.
9. Best Practice Guidance for the Submission of Technical Documentation under Annex II and III of Medical Device Regulation (EU) 2017/745. Available online: https://www.team-nb.org/wp-content/uploads/2022/10/Team-NB-PositionPaper-BPG-TechnicalDocEU-MDR-2017-745-V1-20221005.pdf (accessed on 20 May 2025).
10. Laboratory for Periodic Verification Through Testing Within the "Grigore T. Popa" University of Medicine and Pharmacy in Iași, Romania. Available online: https://www.umfiasi.ro/ro/cercetare/Centre-si-platforme/Pagini/Laborator-de-instrumenta%C5%A3ie-%C8%99i-m%C4%83sur%C4%83ri-biomedicale.aspx (accessed on 20 May 2025).
11. Medical Device Coordination Group Document MDCG 2022-2 Guidance on General Principles of Clinical Evidence for In Vitro Diagnostic Medical Devices 2022. Available online: https://health.ec.europa.eu/system/files/2022-01/mdcg_2022-2_en.pdf (accessed on 20 June 2025).
12. International Electrotechnical Commission IEC 60601-2-21 Consolidated Version: Medical Electrical Equipment - Part 2-21: Particular Requirements for the Basic Safety and Essential Performance of Infant Radiant Warmers; 2023; ISBN 9782832278062. Available online: https://cdn.standards.iteh.ai/samples/102636/36e1a33589d24879b3e48f002a2d232c/IEC-60601-2-21-2020.pdf (accessed on 20 May 2025).
13. International Electrotechnical Commission IEC 60601-1-8 Consolidated Version: Medical Electrical Equipment - Part 1-8: General Requirements for Basic Safety and Essential Performance - Collateral Standard: General Requirements, Tests and Guidance for Alarm Systems in Medical Electrical Equipment; 2020; ISBN 9782832287200. Available online: https://www.iso.org/standard/41986.html (accessed on 20 May 2025).
14. Draft Government Decision for the Approval of the Regulation on the Periodic Verification of Medical Devices. Public Consultations. Available online: https://www.cna.md/public/files/rapoarte_expertiza/Proiect-verif-dispoz-medic5877d.pdf (accessed on 10 May 2025).
15. Draft Order Regarding the Approval of Specific Procedures for Periodic Verification of Medical Devices Put into Operation and in Use. Available online: https://particip.gov.md/ro/document/stages/proiectul-de-ordin-cu-privire-la-aprobarea-procedurilor-specifice-de-verificare-periodica-a-dispozitivelor-medicale-puse-in-functiune-si-aflate-in-utilizare/4544. (accessed on 10 May 2025).

Citation: Gorceag, Gh. Ensuring effective management of medical devices through safe use of medical devices and evidence-based management. *Journal of Engineering Science*. 2025, XXXII (2), pp. 58-67. https://doi.org/10.52326/jes.utm.2025.32(2).05.

Submission of manuscripts: jes@meridian.utm.md

Journal of Engineering Science *Vol. XXXII, no. 2 (2025), pp. 68 - 74*
Fascicle *Electronics and Computer Science* *ISSN 2587-3474*
Topic *Computers and Information Technology* *eISSN 2587-3482*

https://doi.org/10.52326/jes.utm.2025.32(2).06
UDC 530.145:519:539.1

QUANTUM COMPUTING FOR MULTI-QUBIT SYSTEMS USING SCHWINGER REPRESENTATION OF ANGULAR MOMENTUM

Ion Geru *, ORCID: 0000-0003-1320-3889

Institute of Chemistry of the State University of Moldova, 3 Academiei Str., Chisinau, Republic of Moldova
* Corresponding author: Ion Geru, *iongeru11@gmail.com*

Received: 05. 25. 2025
Accepted: 06. 24. 2025

Abstract. This paper deals with the features of quantum computing for a system containing a relatively large number of qubits n, which is characterized by a half-integer effective spin S in the Schwinger representation of paired bosons. It was shown that for n = 70, the number of boson states corresponding to lowest 2S + 1 excited energy levels of each of the two harmonic oscillators implementing the two-boson representation of the effective spin S is N = 10^{70} = 1.18 x 10^{21}. Under such conditions, it can be assumed with great precision that for n ≥ 70 all boson states of both harmonic oscillators participate in the implementation of the two-bo**so**n representation of the effective spin S. This allows one to apply the quantum field theory methods when performing quantum computations for multi-qubit systems. Another advantage of the Schwinger representation of paired bosons compared to the spinor representation when performing quantum computations for multi-qubit systems is that in the first case the form of the spin projection operators of the effective spin S does not depend on the number of qubits n.

Keywords: *effective spin, harmonic oscillators, bosons, spin projection operators, logical elements.*

Rezumat. Au fost studiate particularitățile calculului cuantic pentru un sistem cu un număr relativ mare de qubiți n, care este caracterizat prin spinul efectiv semiîntreg S în reprezentarea lui Schwinger a bosonilor perechi. S-a demonstrat că pentru n = 70 numărul de stări bosonice care corespund celor mai de jos 2S + 1 niveluri energetice excitate ale fiecăruia dintre cei doi oscilatori armonici, care implementează reprezentarea spinului efectiv S prin intermediul a doi bosoni, ecte N = 10^{70} = 1.18 x 10^{21}. În astfel de condiții, se poate considera cu precizie inaltă că pentru n ⩾ 70 toate stările bosonice ale ambilor oscilatori armonici participă la reprezentarea spinului efectiv S prin intermediul a doi bosoni. Această situație permite aplicarea metodelor teoriei cuantice a câmpului atunci, când se efectuează calcule cuantice pentru sisteme multi-qubit. Un alt avantaj al reprezentării spinului efectiv S prin intermediul bosonilor perechi, în comparație cu reprezentarea spinorică, este că în primul caz forma operatorilor priiecțiilor spinului efectiv S nu depinde de numărul de qubiți n.

Cuvinte cheie: *spin efectiv, oscilatori armonici, bosoni, operatorii proiecțiilor spinului, elemente logice.*

1. Introduction

The first report on the possibility of building a quantum computer as a calculating machine based on quantum-mechanical laws was proposed by Feynman [1]. The fundamental difference between calculations performed quantum and classical computers is that unlike a bit, a quantum bit (cubit) is a linear combination of quantum states |1/2, 1/2> = |0> and |1/2, -1/2> = |1> corresponding to real or effective spin S = 1/2 [2]:

$$|\psi> = \alpha|0> + \beta|1>, \quad (1)$$

where: α and β are complex coefficients satisfying the equality

$$|\alpha|^2 + |\beta|^2 = 1. \quad (2)$$

In the case of real coefficients α and β, the wave function $|\psi>$ is considered as a vector in a linear space in which the orthogonal wave functions |0> and |1> ($<0|0> = 1$, $<1|1> = 1, <0|1> = 0$) play the role of a basis of this space. In the case of complex coefficients α and β, the qubit $|\psi>$ geometrically is presented by the unit vector, which has its origin in the center of the Bloch sphere and the end on its surface. There is an infinite set of points on the surface of Bloch sphere and correspondingly any qubit would be in an infinite set of states. It would seem that from one qubit it would be possible to obtain a set of clones of one arbitrary state $|\psi>$ and carry out measurements of the state of each copy. Then with the probability $|\alpha|^2$ the qubit would be found in the state |0> and with the probability $|\beta|^2$ it would be found in the state |1>. Since $|\alpha|^2$ and $|\beta|^2$ can have infinitely many values, it would be possible to obtain infinitely many information in one qubit. However, in fact it is not so, because during the measurement of the qubit state it can be found only in one from two possible states $|0>$ or $|1>$. Therefore, the scenario described above cannot be implemented due to existence of no-cloning theorem of Nootters and Zurek [3].

Despite the restrictions caused by the no-cloning theorem, the number of publications in the field of quantum computing continues to grow, especially after the discovery of Deutsch-Jozsa [4, 5], Shor [6] and Grover [7,8] algorithms. Practically in all these studies the spinor algebra formalism is used [2] in view of the fact that a system consisting of one or more qubits can be characterized by an effective spin S.

Along with the spinor representation, there are the representations of spin projection operators via creation and annihilation Bose operators, such as Holstein-Primakoff [9] and Dyson-Maleev [10,11] representations. However, these representations are not very convenient in applications. Precisely, in the Holstein-Primakoff representation the spin projection operators S_x and S_y depend on Bose operators in such a way that the last are found under the square root. On the other hand, the use of S_x and S_y operators in the Dyson-Maleev representation leads to the non-Hermitian Hamiltonian. Unlike such behavior of spin projection operators in Holstein-Primakoff and Dyson-Maleev representations, exists the Schwinger representation of angular momentum by means of paired bosons [12]. This representation is free from the deficiencies mentioned and can be successfully applied to quantum computing [13,14]

This paper shows how to simplify quantum computations for n-qubit system ($n \geqslant 70$) using features of the Schwinger representation of paired bosons for the effective spin S characterizing such a system. Two features of this representation allow us to simplify the implementation of quantum computations. One of them is that the Pauli matrices that define quantum logic elements NOT (or X), Y, Z, and Hadamard gate for a single qubit with effective

spin S = 1/2 will also define quantum logic elements for n-qubit systems. This is due to the fact that in the case of these n-qubit systems the spin projection operators of the effective spin S do not depend on the number of qubits n. Another feature of the Schwinger paired bosons representation for the effective spin S is that, starting from some very large number of qubits n, it can be stated with great precision that all boson states of both harmonic oscillators take part in the implementation of this representation. Under these conditions, the quantum field theory methods [15] can be used to perform quantum computations. These methods cannot be used for performing the quantum computing in the case of a small number of qubits n.

2. Features of a n-qubit system due to an effective spin S in the Schwinger paired bosons representation at large values of n

Each multi-qubit system can be characterized by some effective spin S, the value of which depends on the number of cubits n [16]. For n cubits the basis vectors correspond to the eigen states of the spin projection operator S_z related to spin S = 2^{n-1}- 1/2. The value S at different n is presented in Table 1 [16, p. 201].

Table 1

Values of the effective spin S for different numbers n of cubits

n	1	2	3	4	5	6	7	8	9	10	n
S	1/2	3/2	7/2	15/2	31/2	63/2	127/2	255/2	511/2	1023/2	$2^{n-1} - \frac{1}{2}$

According to Table 1, with an increasing number of qubits the effective spin S quickly increase. For example, when n increases from 2 to 3, the effective spin S increases from 3/2 to 7/2, while when n increases from 9 to 10, the effective spin S increases from 511/2 to 1023/2. As a consequence of this, there is also a sharp increase in the dimensionality of the spin projection operator matrices in the spinor representation. For example, the dimensionality of each of the three spin projection operator matrices of the spin S = 1023/2 is 1024 x 1024.

The 2S + 1 spin wave functions related to the effective spin S = 2^{n-1} - 1/2, which characterizes the n-qubit system, is usually given in the spinor representation. However, for quantum computations it is convenient to express these wave functions in the Schwinger paired bosons representation [12]:

$$|S, M_S> = [(S + M_S)!\ (S - M_S)!\ ]^{-1/2}\ (a_1^+)^{S+M_S}(a_2^+)^{S-M_S}\ |0>, \quad (3)$$

where $a_i^+ (i = 1, 2)$ and a_i (i = 1, 2) are the operators of creation and annihilation of the bosons related to harmonic oscillators 1 and 2; $|0> = |0>_1 \cdot |0>_2$, $|0>_1$ and $|0>_2$ are the vacuum states related to harmonic oscillators 1 and 2, M_S is the eigen value of the spin projection operator S_z. The spin wave functions $|S, M_S>$ (M_S = S, S-1, S-2, ..., 2-S, 1-S, -S) from (3) can be presented as

$$|S, M_S> = |S + M_S> \cdot |S - M_S>, \quad (4)$$

where:

$$|S + M_S> = [(S + M_S)!\ ]^{-1/2}\ (a_1^+)^{S+M_S}|0>_1, |S - M_S> = [(S - M_S)!\ ]^{-1/2}\ (a_2^+)^{S-M_S}|0>_2. \quad (5)$$

The spin projection operators in the Schwinger paired bosons representation using a system of units, in which Planck constant is equal to one, have the form [12]:

$$S_x = (1/2)\ (a_1^+ a_2 + a_2^+ a_1),\ \ S_y = (i/2)\ (a_2^+ a_1 - a_1^+ a_2),\ \ S_z = (1/2)\ (a_1^+ a_1 - a_2^+ a_2). \quad (6)$$

3. Results and Discussion

The formulas (6) can be obtained in the different way that it is done in the original Schwinger's work [12]. For this we introduce a unitary spinor operator U_S [14]:

$$U_S = \left(\frac{1}{\sqrt{(2S)!}} a_1^{2S} \ \frac{1}{\sqrt{(2S-1)!}} a_1^{2S-1} a_2 \ \cdots \ \frac{1}{\sqrt{(S+M_S)!(S-M_S)!}} a_1^{S+M_S} a_2^{S-M_S} \ \cdots \ \frac{1}{\sqrt{(2S-1)!}} a_1 a_2^{2S-1} \ \frac{1}{\sqrt{(2S)!}} a_2^{2S}\right), \quad (7)$$

which satisfies the unitarity condition $U_S^+ U_S$ = **1,** where **1** is the unit operator corresponding to the unit (2S+1) x (2S+1)-matrix. Under the action of the unitary spinor operator U_S, the spin projection operators S_x, S_y, and S_z are transformed as follows:

$$U_S^+ S_x U_S = (1/2)\ U_S^+ \sigma_x U_S = (1/2)\ (a_1^+ a_2 + a_2^+ a_1)\cdot O_x, \quad (8)$$

$$U_S^+ S_y U_S = (1/2)\ U_S^+ \sigma_y U_S = (i/2)\ (a_2^+ a_1 - a_1^+ a_2)\cdot O_y, \quad (9)$$

$$U_S^+ S_z U_S = (1/2)\ U_S^+ \sigma_z U_S = (1/2)\ (a_1^+ a_1 - a_2^+ a_2)\cdot O_z, \quad (10)$$

where: σ_x , σ_y and σ_z are Pauli operators, O_x, O_y and O_z are so-called operator loads. In the Ref. [14] it has been proven that $O_x = O_y = O_z$ = **1**.

Taking these equalities into account, formulas (8) – (10) represent a transition from the spinor representation to the Schwinger paired bosons representation using the unitary operator U_S. The right-hand sides of formulas (8) – (10) exactly coincide with the expressions for the spin projection operators S_x, S_y and S_z in the Schwinger paired bosons representation [12]. In the Springer paired bosons representation of an effective spin S the explicit form of the spin projection operators S_x, S_y and S_z should not depend on the value of S. Therefore, taking into account the Table 1, the explicit form of the spin projection operators should also not depend on the number of qubits n. This should lead to a significant simplification of quantum computations for multi-qubit systems. In this case all specific features of multi-qubit systems compared to single-qubit system are determined only by the |S, $M_S >$ spin wave function of a multi-qubit system in the paired bosons representation.

It may be questionable whether in the paired boson representation the quantum logic elements of single- and multi-qubit systems coincide. In the spinor representation such a coincidence is impossible, since in this case any quantum logic element of an n-qubit system is a direct product of n logic elements of a single-qubit systems. However, despite the fact that in the Schwinger paired bosons representation the quantum logic elements do not depend on the number of qubits, the results of the action of these operators on the self functions related to single- and multi-qubit systems are different. This is due to the fact that the eigen vectors of single- and multi-qubit systems are different. Let us demonstrate this with a simple example of a quantum logic element Z = $2S_z$. In the spinor basis, the quantum logic element Z for one qubit has the form

$$Z^{(1)} = (1\ 0\ 0\ -1), \quad (11)$$

while, for example, for a three-qubit system the following relation holds:

$$Z^{(3)} = Z_1^{(1)} \otimes Z_2^{(1)} \otimes Z_3^{(1)}. \quad (12)$$

In the Schwinger paired bosons representation, the quantum logic element Z is determined by the operator

$$Z = a_1^+ a_1 - a_2^+ a_2, \quad (13)$$

which retains its form for both a single qubit and in the general case for an n-qubit system. We especially note the absence in this case of the need to calculate the direct product of quantum logic elements, as is required in the case of the spinor representation. In the spinor representation, the eigen functions $|S, M_S>$ and eigen values M_S of the operator S_z are determined by simple equation:

$$S_z\ |S, M_S> = M_S\ |S, M_S>. \tag{14}$$

In this case, the type of the operator S_z, the type of eigen functions $|S, M_S>$ and the eigen values M_S depend on the number of qubits. In contrast to this, in the Schwinger paired bosons representation, the equation (14) has the form:

$$(1/2)\ (a_1^+ a_1 - a_2^+ a_2)\ |S, M_S> = M_S\ |S, M_S>, \tag{15}$$

which does not depend on the number of qubits. Although the operator $(a_1^+ a_1 - a_2^+ a_2)$ does not depend on the number of qubits n, the spin wave functions $|S, M_S>$ and eigen values M_S depend on n. In the particular case S = 3/2, the equations for determining the eigen values M_S have the form:

$$(1/2)\ (a_1^+ a_1 - a_2^+ a_2)\ (a_1^+)^3\ |0>_1 = M_S\ (a_1^+)^3\ |0>_1, \tag{16}$$

$$(1/2)\ (a_1^+ a_1 - a_2^+ a_2)\ (a_1^+)^2 a_2^+\ |0> = M_S\ (a_1^+)^2 a_2^+\ |0>, \tag{17}$$

$$(1/2)\ (a_1^+ a_1 - a_2^+ a_2)\ a_1^+\ (a_1^+)^2 |0> = M_S\ a_1^+ (a_1^+)^2\ |0>, \tag{18}$$

$$(1/2)\ (a_1^+ a_1 - a_2^+ a_2)\ (a_2^+)^3\ |0>_2 = M_S\ (a_2^+)^3\ |0>_2. \tag{19}$$

It is easy to show that the solutions of equations (16)-(19) are M_S = 3/2, 1/2, -1/2, -3/2, which, as they should be, coincide with the solutions of equation (14) given in the spinor representation. This particular example demonstrates that although in the Schwinger paired bosons representation the operator S_z does not depend on the number of qubits n, its eigen functions $|S, M_S>$ and eigen values M_S depend on n. Since the quantum logic elements NOT (or X), Y, Z, and Hadamard gate H are defined via Pauli matrices that do not depend on the number of qubits, then in the Schwinger paired bosons representation these logic elements have the form

$$\begin{aligned} X &= a_1^+ a_2 + a_2^+ a_1, \\ Y &= i\ (a_2^+ a_1 - a_1^+ a_2), \\ Z &= (a_1^+ a_1 - a_2^+ a_2), \\ H &= \frac{1}{\sqrt{2}}\ [\ a_1^+ (a_1 + a_2\ ) + a_2^+ (a_1 - a_2)]. \end{aligned} \tag{20}$$

Logic elements (20) have the same form both for one qubit and for multi-qubit systems. The same applies to the quantum logic elements T (or $\pi/8$), S (not to be confused with spin) and Φ with the corresponding phase factors in the second term of the first and third of these logic elements:

$$\begin{aligned} T &= a_1^+ a_1 + \exp\ (i\ \pi/8) \cdot a_2^+ a_2\ , \\ S &= a_1^+ a_1 + i\ a_2^+ a_2\ , \\ \Phi &= a_1^+ a_1 + \exp\ (i\ \Phi_0/8) \cdot a_2^+ a_2\ . \end{aligned} \tag{21}$$

The result of the action of operators (20) and (21) on the eigen functions of these operators depends on the number of qubits. This statement is confirmed by the fact that in the case of one qubit, instead of equations (16) - (19) for a three-qubit system, it is necessary to consider the equations

$$(1/2)\ (a_1^+ a_1 - a_2^+ a_2)\ a_1^+\ |0>_1 = M_S\ a_1^+\ |0>_1,$$

$$(1/2)\ (a_1^+ a_1 - a_2^+ a_2)\ a_2^+\ |0>_2 = M_S\ a_2^+\ |0>_2, \quad (22)$$

whose solutions are M_S = 1/2, -1/2.

The two-boson representation of the effective spin S involves 2S + 1 states corresponding to the lowest energy levels of each of the harmonic oscillators 1 and 2. For a small number of qubits n, this number of states is negligible compared to the infinite number of states of each of the two harmonic oscillators. For example, for n = 2 (S = 3/2) only the four lowest excited states of each of two harmonic oscillators are involved in the implementation of paired bosons representation of the effective spin:

$$|3/2, 3/2> = |3>_1\ |0>_2,\ |3/2, 1/2> = |2>_1\ |1>_2,$$

$$|3/2, -1/2> = |1>_1\ |2>_2,\ |3/2, -3/2> = |0>_1\ |3>_2. \quad (23)$$

All other energy levels of harmonic oscillators 1 and 2 must be excluded from consideration.

In the general case, the exclusion of boson states of both harmonic oscillators that do not participate in the implementation of the Schwinger paired bosons representation of the effective spin S is performed using the relationship [17] (p. 267):

$$a_1^+ a_1 + a_2^+ a_2 = 2S \cdot \mathbf{1}, \quad (24)$$

where: **1** is the unit operator represented by the unit (2S+1) x (2S+1)-matrix.

With an increase in the number of cubits n, there is a sharp increase in the number of boson states of each of the quantum harmonic oscillators 1 and 2 participating in the two-boson representation of 2S+1 spin states $|S, M_S>$ (M_S = S, S-1, ..., 1-S, -S). Particularly, for n = 70 we obtain 2S+1 = 1.18 x 10^{21}. Therefore, at n ≥ 70 the number of boson states of each of the quantum harmonic oscillators 1 and 2 participating to the paired boson representation of spin states can be considered with high precision equal to infinity. In this case, the methods of quantum field theory [15] can be used to perform quantum computations.

The possibilities of simplifying quantum computing in the case of multi-qubit systems considered in this paper may prove useful in connection with the development of quantum computer technology and the expansion of the range of problems solved with their help. Particularly, the IBM Corporation plans to demonstrate a quantum supercomputer in 2025 by linking together three 1386-qubit "Kookaburra" processors into a 4,158-qubit system [18]. At n = 4,158, the number of boson states of each of the two harmonic oscillators implementing the Springer paired bosons representation of the effective spin S is infinitely large number $2^{4,158}$, which allows the use of quantum field theory methods to perform quantum computations.

4. **Conclusions**

1. Any n-qubit system can be characterized by an effective spin S = $2^{n-1} - \frac{1}{2}$.

2. In the paired bosons Schwinger representation, the spin projection operators S_x, S_y S_z do not depend on the spin value S and, accordingly, on the number of qubits n.

3. The explicit forms of logical elements NOT (or X), Y, Z, H, T (or $\pi/8$), S (not to be confused with spin) and Φ do not depend on the number of qubits n.

4. At a high number of qubits n (n ≥ 70), the quantum computations for n-qubit systems can be performed using the quantum field theory methods.

Conflicts of Interest: The authors declare no conflict of interest.

References

1. Feynman, R.P. Simulating physics with computers. *Int J Theor Phys* 1982, 21, pp. 467–488.
2. Stolze, J.; Suter, D. *Quantum Computing: A Short Course from Theory to Experiment*. Wiley-Vch GmbH & Co. KGaA, Weinheim, Germany, 2004, 244 p.
3. Wootters, W.K.; Zurek, W.H. A single quantum cannot be cloned. *Nature* 1982, 299, pp. 802–803.
4. Deutsch, D. Quantum theory, the Church-Turing principle and the universal quantum Computer. *Proc. R. Soc. Lond. A* 1985, 400, pp. 97-117.
5. Deutsch D.; Josza R. Rapid solutions of problems by quantum computations. *Proc. R. Soc. Lond. A* 1992, 439, pp. 553-558.
6. Shor, S. Algorithms for quantum computation: discrete logarithms and factoring. In: *Proceedings of 35th Annual Symposium on Foundation of Computer Science,* IEEE, 1994, pp. 124–134.
7. Grover, L.K. A fast quantum mechanical algorithm for database search. In: *Proceedings of 28th Annual ACM Symposium on the Theory of Computation*, 1996, p. 212.
8. Grover, L.K. Quantum Mechanics Helps in Searching for a Needle in a Haystack. *Phys. Rev. Lett.* 1997, 79, pp. 325-328.
9. Holstein, T.; Primakoff, H. Field Dependence of the Intrinsic Domain Magnetization for a Ferromagnet. *Phys. Rev.* 1940, 58, pp. 1098-1113.
10. Dyson, F. J. Quantum Thery of Spin-Wave Interactions. *Phys. Rev.* 1956, 102 (5), pp. 1217-1230.
11. Maleev, S.V. Scattering of Slow Neutrons in Ferromagnets. *Soviet Journal of Experimental and Theoretical Physics* 1958, 6(4), pp. 776-784 [in Russian].
12. Schwinger, J. Angular Momentum. In: *Quantum Theory of the Angular Momentum*, Biedenharn, L.C.; Vam Dan, H. (eds), Academic Press, New York, SUA, 1965, p. 229.
13. Geru, I. I.; Geru, V. Bosonization of Angular Momentum. *Rom. Journ. Phys*. 1999, 44 (1-2), pp. 97-115.
14. Geru, I. I. Non-traditional Approach to Quantum Computing. *Appl. Magn. Reson.* 2014, 45, pp. 1427–1439.
15. Zee, A. *Quantum Field Theory, as Simple as Possible*. Princeton University Press, Princeton, SUA, 2023, 392 p.
16. Geru, I. I.; Suter, D. *Resonance Effects of Excitons and Electrons: Basics and Applications*. Springer-Verlag, Berlin, Heidelberg, Berlin, Germany, 2013, 283 p.
17. Geru, I. I. *Time-Reversal Symmetry: Seven Time-Reversal Operators for Spin Containing Systems*. Springer Nature Switzerland AG, 2018, 281, 362 p.
18. Jay, G. Expanding the IBM Quantum roadmap to anticipate the future of quantum-centric supercomputing (Updated 2024). Available online: https://ibm.com/quantum/blog/ibm-quantum-roadmap-2025 (accessed on 29. 05. 2020).

Citation: Geru, I. Quantum computing for multi-qubit systems using Schwinger representation of angular momentum. *Journal of Engineering Science*. 2025, XXXII (2), pp. 68-74. https://doi.org/10.52326/jes.utm.2025.32(2).06.

Submission of manuscripts: jes@meridian.utm.md

Journal of Engineering Science *Vol. XXXII, no. 2 (2025), pp. 75 - 86*
Fascicle *Electronics and Computer Science* *ISSN 2587-3474*
Topic *Computers and Information Technology* *eISSN 2587-3482*

https://doi.org/10.52326/jes.utm.2025.32(2).07
UDC 004.056.5:334.72(478)

SECURING MOLDOVAN SMALL AND MEDIUM-SIZED BUSINESSES: STRATEGIES BASED ON IT INFRASTRUCTURE DOMAINS

Anatol Alexei *, ORCID: 0000-0002-0570-4854,
Victor Moraru, ORCID: 0000-0002-5454-8341,
Arina Alexei, ORCID: 0000-0003-4138-957X

Technical University of Moldova, 168, Stefan cel Mare Blvd., Chisinau, Republic of Moldova
* Corresponding author: Anatol Alexei, *anatolie.alexei@adm.utm.md*

Received: 03. 28. 2025
Accepted: 05. 04. 2025

Abstract. The digitization of small and medium-sized enterprises (SMEs) has accelerated in recent years, increasing their reliance on information systems to support core business operations. ENISA's 2021 report showed an important growth in SME dependence on IT, while the World Economic Forum ranked cybersecurity failure among the top five global risks. Although digital transformation brings competitive advantages, it also exposes SMEs to cyber threats. A comparative analysis of scientific studies from the UK, Australia, the EU, Malaysia, and the USA identified social engineering, Denial of Service (DoS) / Distributed Denial of Service (DDoS), and Man-in-the-Middle (MitM) attacks as the most frequent threats. This article analyzes the main barriers preventing SMEs from implementing information security frameworks and identifies the lack of national-level regulations in the Republic of Moldova. Based on a structured model developed by the authors, the paper proposes tailored recommendations for improving information system security in Moldovan micro-enterprises. The findings emphasize the need for contextualized, cybersecurity solutions and public policy support targeting risk management and awareness.

Keywords: *cybersecurity, information system; framework, risk, SME.*

Rezumat. Digitalizarea întreprinderilor mici și mijlocii (IMM-uri) s-a accelerat în ultimii ani, crescând dependența acestora de sistemele informaționale pentru susținerea operațiunilor esențiale. Raportul ENISA din 2021 a evidențiat o creștere semnificativă a dependenței IMM-urilor de tehnologiile IT, iar Forumul Economic Mondial a clasat eșecul în materie de securitate cibernetică printre primele cinci riscuri globale. Deși transformarea digitală aduce avantaje competitive, ea expune IMM-urile la amenințări cibernetice. O analiză comparativă a studiilor științifice din Regatul Unit, Australia, Uniunea Europeană, Malaysia și Statele Unite a identificat ingineria socială, atacurile DoS/DDoS și atacurile de tip MitM drept cele mai frecvente amenințări. Acest articol analizează principalele bariere care împiedică IMM-urile să implementeze cadre de securitate informațională și evidențiază lipsa unor reglementări naționale în Republica Moldova. Pe baza unui model structurat elaborat de autori, lucrarea propune recomandări specifice pentru îmbunătățirea securității sistemelor informaționale în

micro-întreprinderile din Moldova. Concluziile subliniază necesitatea unor soluții de securitate cibernetică adaptate contextual, precum și sprijinul politicilor publice orientate spre gestionarea riscurilor și creșterea nivelului de conștientizare.

Cuvinte-cheie: *securitate cibernetică, sistem informațional, cadru, risc, IMM.*

1. Introduction

Small and medium-sized enterprises (SMEs) play a very important role in the global economy, accounting for 90% of businesses worldwide [1]. In Australia, for example, SMEs represent 98% of all Australian enterprises, generate one-third of the total Gross Domestic Product (GDP), and employ 4.7 million people, while in the United Kingdom, SMEs account for approximately 99.9% of all businesses [1]. In the Republic of Moldova, it was reported in 2020 that 98.6% of the enterprises active in the national economy are SMEs [2].

The digitization of SMEs is no longer regarded as an option, but rather as a key driver of sustainable development in the context of a global digital economy. Digital transformation can enhance the competitiveness, efficiency, and adaptability of SMEs to emerging challenges, offering benefits such as:

- improved operational efficiency and reduced costs through the automation of various processes, minimization of human errors, and time savings;
- expanded access to new markets and customers, regardless of the company's geographical location, through digital marketing and e-commerce;
- the ability to make informed decisions based on the analysis of large volumes of data using a variety of Business Intelligence tools;
- increased innovation and market competitiveness through the implementation of new business models and personalized services based on customer behavior analysis.

The digitization of small and medium-sized enterprises (SMEs) has been progressing in recent years. SMEs carry out various business processes that rely on information systems [3], such as: e-commerce; the exchange of information between employees, business partners, and customers [4]; as well as informing and promoting companies through websites and social media platforms. Information systems are defined as the complete set of software, hardware, data, people, and procedures that enable the use of a company's informational resources [5]. The 2021 report of the European Union Agency for Cybersecurity (ENISA) indicated a growing dependence of small and medium-sized business operations on information technology systems [6].

What is certain is that technological progress adds competitiveness and can contribute to the increase of annual business revenues, but it also leads to heightened cyber risks associated with information systems security. In the 2019 report published by the World Economic Forum, cyber risks were ranked among the top 10 global risks [7], while in the 2021 report, cybersecurity failure was assessed as the 4th major global risk [4]. The analysis of scientific studies revealed that SMEs are frequently targeted by cyberattacks. For instance, 39% of SMEs in the United Kingdom reported having been targeted by cyberattacks in the past 12 months [8], while in Australia, statistics indicated that 66% of SMEs had fallen victim to cyberattacks [1]. In developing countries such as Malaysia, the percentage of SMEs affected by cyberattacks is even higher, reaching 85% [4]. In the Republic of Moldova, such statistics are lacking due to the immaturity of the field, making it very difficult to assess the real state of affairs [9].

The main challenges SMEs face in ensuring the security of information systems stem from insufficient allocated budgets, lack of awareness regarding information security issues, lack of support from top management who are unaware of the consequences of cyberattacks, the absence of processes and tools to improve security practices [8], and, of course, the employees' cybersecurity culture, with the human factor representing the greatest vulnerability in the information system [10].

According to a survey conducted by ENISA in 2021 [11], which involved 16 SMEs from 14 European Union countries, European SMEs face the following issues: low staff awareness of information security, inadequate protection of critical and sensitive data, budget limitations, a shortage of Information and Communication Technologies (ICT) cybersecurity specialists, lack of appropriate cybersecurity guidelines tailored to SMEs, poor IT management, ICT-related work shifting beyond SME control, and low support from company management [7].

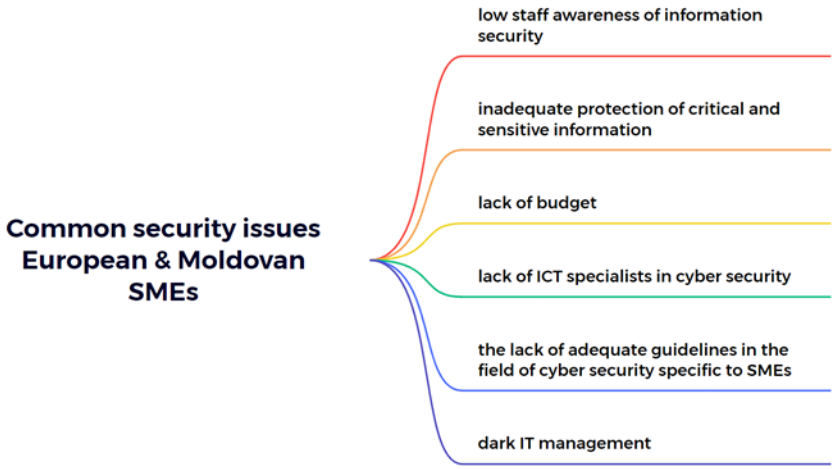

Figure 1. Common security issues in European and Moldovan SMEs – synthesized from ENISA 2021 survey data and national context.

The scope is to analyze the current state of cybersecurity readiness among SMEs, identify common vulnerabilities, and propose tailored security measures that are both effective and feasible within the specific constraints of small and medium-sized businesses. The central hypothesis explored in this study is that the implementation of a structured, cost-effective cybersecurity framework adapted to the SME context can reduce exposure to cyber threats, even in environments with limited institutional maturity in the field. To support this analysis, a review of key academic and institutional publications was conducted, including reports from ENISA, the World Economic Forum, Ponemon Institute, Check Point Research, Verizon and various country-specific studies focused on cybersecurity in the SME sector.

2. Materials and Methods

This research was conducted based on a systematic review of specialized literature, with a focus on both international and national studies concerning information security in small and medium-sized enterprises (SMEs). Primary sources included ENISA reports [12-14], studies by Verizon [15,16], Ponemon Institute [17], Check Point Research [18], as well as peer-reviewed scientific articles and governmental reports relevant to the context of the Republic of Moldova.

The methodology consisted of the following steps:

- Thematic bibliographic analysis, which allowed the identification of key threats, vulnerabilities, and reported security practices in SMEs at both international and national levels. Reference management and citation consistency were ensured using Mendeley Reference Manager.
- Identification and systematization of IT infrastructure domains in SMEs, structured into seven core components: users, workstations, LAN (local area network), LAN-to-WAN, WAN (wide area network), remote access, and system/application domains. This structure was based on the security framework proposed by Kim & Solomon [19], which provides a logical mapping of organizational IT assets for targeted risk analysis and protection strategies.
- Logical risk modelling, by correlating identified threats and vulnerabilities with the seven IT infrastructure domains, a domain-specific exposure. The conceptual design of this correlation process was supported using Xmind (version 25.01.01061) for visual mapping and clarity.

Adaptation and refinement of ENISA's recommendations to the national SME context by formulating a set of feasible policies, processes, and technological measures tailored to Moldovan SMEs. These included low-cost yet effective security practices and awareness-building initiatives focused on the human factor, considered the most vulnerability.

The methods applied were predominantly qualitative and descriptive, given the objective of synthesizing existing knowledge and tailoring it to a specific socio-economic and technological environment.

3. Results

The structured analysis of the scientific literature and the synthesis of relevant data for SMEs in the Republic of Moldova have led to the following results, which are described in detail below.

3.1. Aspects of Information Systems in SMEs

From a technical perspective, the implementation of information systems (IS) in SMEs can be structured into seven key domains of IT infrastructure [19]. These domains are summarized in Figure 2 and briefly described below.

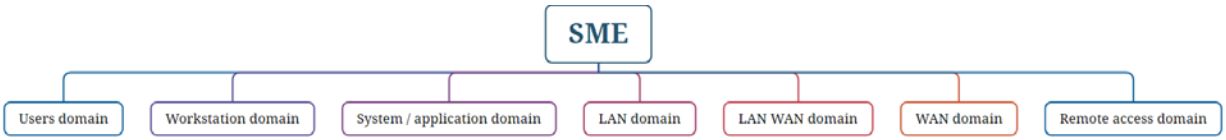

Figure 2. Key domains of the information systems infrastructure in SMEs.

(1) *User Domain* – covers SME personnel who access and operate the organizational IS.
(2) *Workstation Domain* – includes all connected devices (PCs, laptops, tablets, smartphones). It distinguishes between thin clients (limited local resources, rely on network) and thick clients (fully equipped for local processing).
(3) *LAN Domain* – comprises local networks built with Network Interface Cards (Media Access Control - based), Ethernet standards (Institute of Electrical and Electronics Engineers Standard 802.3), Unshielded Twisted Pair cabling (Cat 5/6), switches (Layer 2 and 3), file/print servers, and wireless access points. Logical elements include user authentication, shared directories, IP configurations, and VLANs.

(4) *LAN-WAN Domain* – connects LANs to the Internet via TCP/UDP protocols. Common logical ports include HTTP (80), FTP (20), TFTP (69), Telnet (23), and SSH (22).
(5) *WAN Domain* – enables interconnection between distant sites and Internet access.
(6) *Remote Access Domain* – ensures connectivity for remote users through mobile access, Virtual Private Network (VPN), Wi-Fi, and secure Internet links, used more post-COVID.
(7) *System/Application Domain* – includes mission-critical systems such as Transaction Processing Systems (TPS), Enterprise Resource Planning (ERP), Customer Relationship Management (CRM), and Management Information Systems (MIS) platforms.

This structural view serves as the basis for mapping security vulnerabilities and associated threats across each domain.

3.2. Security Threats Facing SMEs

Analyzing and publishing data on security threats affecting SMEs is important, particularly for raising awareness among top management regarding the importance of securing the information systems they oversee. SMEs are attractive targets for cyber attackers due to the relatively weak security measures they implement—unlike large organizations, which invest in good protection systems to safeguard sensitive business data, including personal, financial, and commercial information [20].

Academic and industry reports identify the most common threats to SMEs as social engineering attacks, credential and data theft, misuse of organizational assets, malicious software - especially ransomware - web application attacks, and e-commerce supply chain breaches [1,17,21,22]. These threats can be grouped into six major categories, as illustrated in Figure 3.

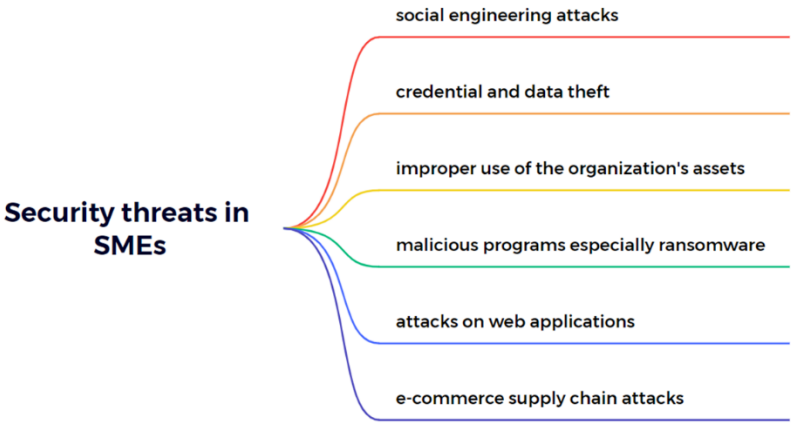

Figure 3. Major categories of security threats in SMEs.

These threats can be analyzed by examining vulnerabilities across five key components: software, hardware, communication networks, data, and users. Among these, the human factor remains the most exploitable - 84% of cyberattacks leverage social engineering to manipulate individuals [7].

Software-related threats include ransomware, which can lock down organizational systems until a ransom is paid. ENISA's 2021 report [13] describes an incident where attackers exploited the Remote Desktop Protocol (RDP) to gain unauthorized access to corporate servers. Other malware types - viruses, trojans, worms, rootkits, and downloaders—pose serious risks. Web applications are also frequently targeted through vulnerabilities such as cross-site scripting (XSS), buffer overflows, XML injection, and SQL injection [3].

Network security is a critical aspect of information system protection. Both wired and wireless networks are vulnerable to attacks such as Denial of Service/Distributed Denial of Service (DoS/DDoS) [11,22,23], man-in-the-middle (MitM) attacks [23,24], and identity spoofing [25], where attackers impersonate legitimate devices to infiltrate networks. Wireless networks, although widely adopted for their convenience, are inherently less secure than wired ones and susceptible to authentication weaknesses and rogue access points [26].

Social engineering attacks, particularly phishing and spear phishing, are increasing in frequency. ENISA reports that 41% of attacks on SMEs fall into this category [11], often targeting top executives. These attacks succeed not by exploiting technical flaws but by manipulating human behavior. The lack of awareness and training in this area is an emerging challenge for effective cybersecurity in SMEs.

Based on this classification, the specific threats and vulnerabilities identified for each IT domain are summarized in Table 1.

Table 1

Security threats and risks in SME IT domains [19]

IT Domain	Security Threats and Risks
User Domain	Unauthorized access; lack of awareness; security policy violations; use of removable media; unauthorized web downloads; system or application damage; sabotage; unauthorized actions
Workstation Domain	Unauthorized access to workstations, systems, applications, or data; OS vulnerabilities; software vulnerabilities; missing updates; malware infections; use of personal devices; use of removable media; unauthorized content downloads
LAN Domain	Unauthorized LAN access; unauthorized access to systems, applications, or data; server OS vulnerabilities; vulnerable server applications; unauthorized WLAN access; compromised wireless transmission; difficult network administration
LAN-WAN Domain	Unauthorized network and port scanning; unauthorized access; DoS/DDoS attacks; router/firewall firmware vulnerabilities; misconfigurations; remote access threats; unverified content downloads; access to malicious URLs; access to unrelated/non-business content
WAN Domain	Open access; unencrypted traffic; malware infections; data corruption; use of insecure protocols
Remote Access Domain	Brute-force and password attacks; multiple unauthorized access attempts; remote data compromise; data loss; theft of remote employees' devices; theft of employee credentials
System/Application Domain	Unauthorized access to data repositories; server unavailability due to maintenance; server OS vulnerabilities; insecure virtual environments; unauthorized access; vulnerable applications; data loss or corruption; loss of backup copies; IT system unavailability

The security risks faced by SMEs are substantial. A previous study showed that approximately 60% of SMEs that suffer a cyberattack go out of business within six months [27]. Several factors contribute to the limited implementation of cybersecurity frameworks, models, or standards in SMEs [1]:

- Underestimation of cyber risk and the complexity of modern threats.
- Lack of expertise and domain knowledge [17,28,29] leading to poor understanding by management regarding the importance of information security.
- Limited financial resources, as managers tend to prioritize product or service development over security investments.
- The steady stream of new digital tools (e.g. Internet of Things, Artificial Intelligence), which further complicate understanding and implementation.
- Excessive and ambiguous information in the field, increasing uncertainty for decision-makers.
- Lack of perseverance due to the indirect or delayed visibility of returns from security investments.

These limiting factors are summarized in Figure 4, which reflects the most common barriers preventing SMEs from adopting cybersecurity frameworks.

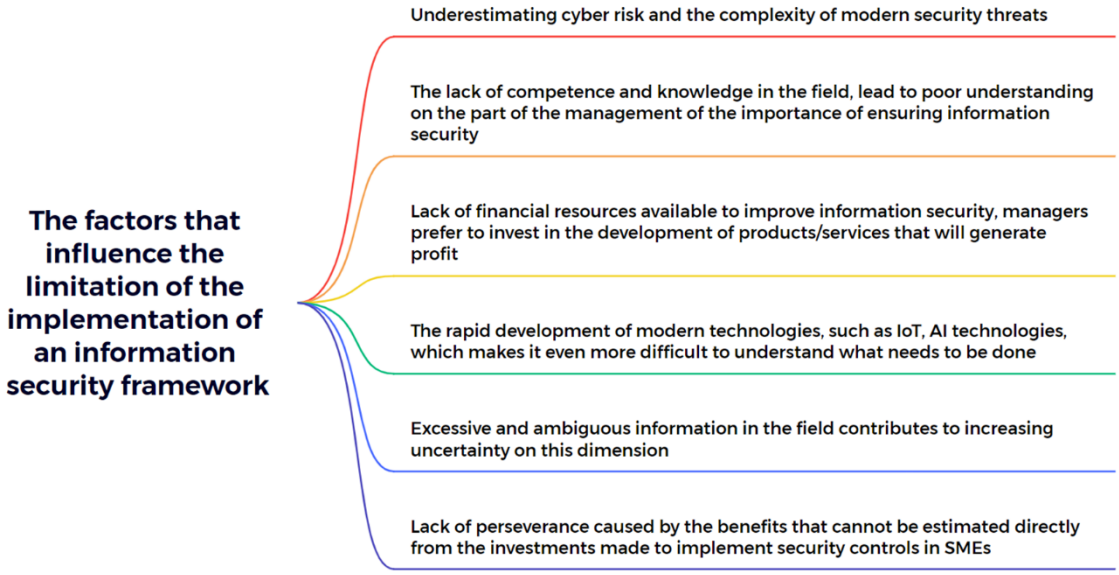

Figure 4. Key factors limiting the implementation of information security frameworks in SMEs.

One of the most critical risks for SMEs is business failure [1], in addition to loss of competitiveness, financial damages, or legal issues resulting from compromised customer data. Moreover, the cost of recovery after a major incident can be extremely high, including equipment upgrades, implementation of security controls, and staff training. An additional concern is the recurrence of attacks - studies show that 28% of SMEs affected by cyberattacks are targeted again within two years. The range and severity of consequences that SMEs face following a cyber incident are illustrated in Figure 5.

Research has shown that most studies on information security in SMEs have focused on developed countries such as the United Kingdom, the United States, Australia, and European Union (EU) member states. However, information security is also highly important for developing countries, such as the Republic of Moldova.

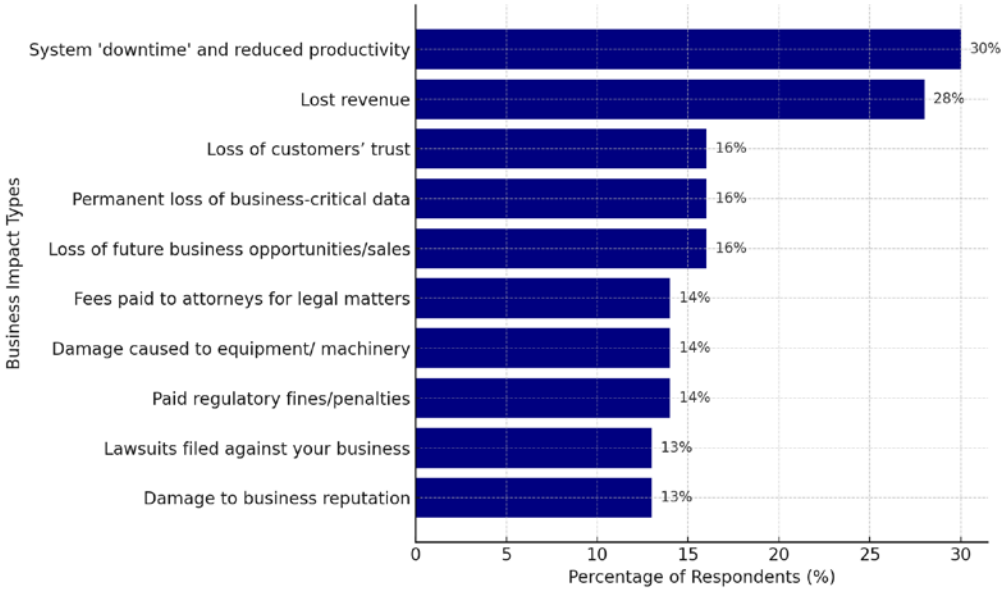

Figure 5. Main consequences of cyberattacks on SMEs.

The analysis of scientific studies revealed that SMEs are frequently targeted by cyberattacks. In the United Kingdom, 39% of SMEs reported being attacked within the last 12 months [8], while in Australia, statistical data showed that 66% had fallen victim to cyberattacks [1]. In developing countries such as Malaysia, the proportion is even higher, reaching 85% [4].

In the Republic of Moldova, such statistics are unavailable due to the immaturity of the field, making it very difficult to assess the actual state of cybersecurity among SMEs [9].

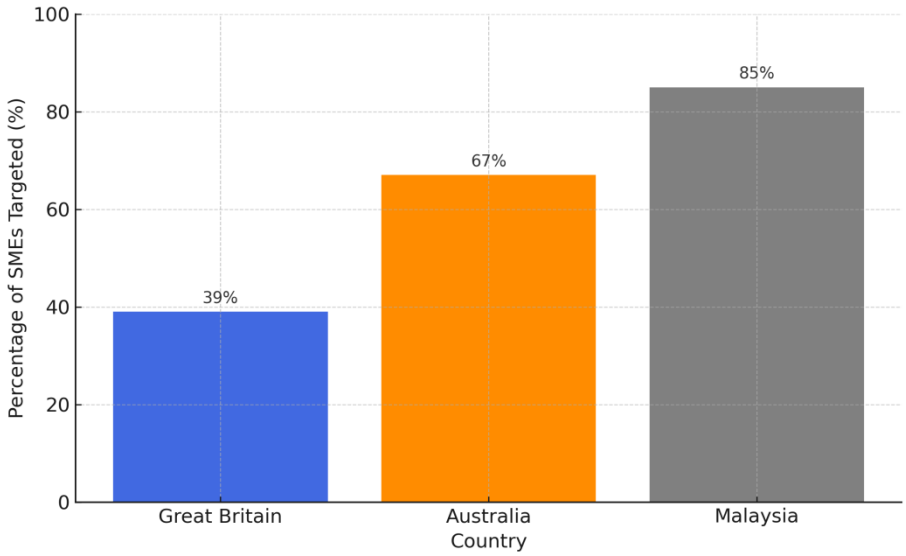

Figure 6. Percentage of SMEs targeted by cyberattacks in selected countries – United Kingdom, Australia, and Malaysia [1, 4, 8].

These results demonstrate not only the widespread nature of cyber threats across SMEs but also the pressing need for structured, context-aware cybersecurity policies - especially in underregulated environments like the Republic of Moldova.

4. Discussion

The results of this study confirm that SMEs are exposed to a wide range of cybersecurity threats across all layers of their IT infrastructure, from end-users to remote access and core applications. These vulnerabilities are not isolated or accidental but systemic, reflecting both structural weaknesses and a lack of organizational preparedness.

Compared to large enterprises, SMEs face disproportionate risks due to limited financial and human resources, minimal formalization of security processes, and low awareness at the management level. These findings are consistent with prior studies conducted in the UK [8], Australia [1], and Malaysia [4], which emphasize the lack of cybersecurity culture as a critical barrier.

In the case of Moldovan SMEs, the situation is more severe due to the immaturity of national cybersecurity frameworks, a low adoption rate of digital technologies, and the absence of structured support mechanisms. Although international bodies such as ENISA provide valuable recommendations, this study shows that global guidelines must be contextualized to meet local needs.

According to 2020 statistics, EU countries and the UK have mostly implemented security measures such as network access control, regular backups, software updates, and strong password policies. However, they show a low level of implementation of risk management practices, security testing, and secure remote access [7,8]. In a study referring to security practices among SMEs in the United States [30], several issues were identified regarding information system security: although SMEs use antivirus software, updates - considered a key element - are performed by only a portion of respondents. Firewall programs used both at endpoint devices [31,32] and at network nodes are deployed by only one-third of the respondents and are updated even less frequently. Problems with password usage and management were also observed.

As for employee education, organizations in the UK implement awareness activities to a limited extent [8], which may be due to a lack of commitment from top management in this area. As shown in a study conducted in France [33], managers are typically occupied with entrepreneurial tasks and dedicate little time to data protection concerns.

The ENISA report outlines the EU's recommendations for implementation within SMEs, as well as priority areas in this domain (Figure 7).

Figure 7. EU recommandations for SMEs [3].

As demonstrated in Table 1 and Figures 5 - 6, the impact of cyberattacks is huge and recurring, while the mitigation efforts remain fragmented.

A notable limitation of this research is the lack of empirical data from Moldovan SMEs, caused by low transparency and reluctance to report incidents. This constrained the analysis to secondary sources and comparative literature. Future research should focus on empirical

validation through surveys, interviews, or incident analysis to assess the actual implementation of cybersecurity measures.

Nevertheless, the findings show the urgent need for tailored, low-cost, and effective cybersecurity solutions that can be adopted even by microenterprises. Public-private partnerships, state-backed education programs, and regulatory incentives are needed for improving cyber resilience across the SME sector.

These recommendations build upon a prior study by the authors [3], where a framework aligned with ENISA principles was adapted to the specific needs and constraints of SMEs in the Republic of Moldova. The proposed framework structures security measures into three categories: People, Processes, and Technology. It shows the need for security policies, staff training, and managerial involvement (People); incident response planning, password and patch management (Processes); and antivirus, encryption, access control, and secure backups (Technology).

Building on this foundation, the underlying research problem addressed by the authors is the identification of security policies and practices that are both effective and realistically implementable in the SME environment, particularly within the Republic of Moldova. The study was guided by three core objectives:

(1) to analyze the current challenges, security behaviors, and managerial attitudes within national SMEs;
(2) to design a sustainable information system model aligned with SME capabilities; and
(3) to develop a support platform with implementation guidelines, risk management tools, and clearly defined mappings of vulnerabilities, threats, and controls.

These components form the basis for a cybersecurity reference model tailored to the needs of local SMEs.

5. Conclusions

This study emphasizes the need to strengthen information system security in small and medium-sized enterprises, especially in countries such as the Republic of Moldova. The analysis showed that SMEs are exposed to a wide variety of cybersecurity threats affecting multiple layers of IT infrastructure, from users and devices to networks and business applications.

Despite their economic importance, SMEs in developing countries often give priority to immediate business needs, while information security remains a secondary concern. This approach increases exposure to cyber threats, especially in the context of digitalized and technology-driven operations. Security should not be seen as optional, but as a necessary component of business continuity.

The results indicate that SMEs are limited by reduced financial and human resources, insufficient awareness at the managerial level, and the absence of a coordinated approach to risk. While international recommendations, such as those from ENISA, provide useful guidance, they need to be adapted to local conditions to be effective in practice.

Further research is needed to collect empirical data from SMEs in the Republic of Moldova. A national-level survey would help assess the current state of information security, including:

- security measures applied in practice;
- types of threats encountered;
- employee and manager awareness levels;

- and how risks are perceived and managed.

The long-term objective is to design a support platform tailored to the local SME environment, offering practical tools and guidance for improving resilience against cyber incidents.

Conflicts of Interest: The authors declare no conflict of interest.

References

1. Chidukwani, A.; Zander, Z.; Koutsakis, P. A Survey on the Cyber Security of Small-to-Medium Businesses: Challenges, Research Focus and Recommendations. *IEEE Access* 2022, 10, pp. 85701–85719. DOI: 10.1109/ACCESS.2022.3197899.
2. NBSRM. The activity of small and medium enterprises in the Republic of Moldova in 2020. Available online: https: // statistica. gov.md /ro/activitatea-intreprinderilor-mici-si-mijlocii-in-republica-moldova-in-anul-9557_ 50055.html (accessed on 05.04.2025).
3. Alexei, An.; Alexei, Ar. The problem of information systems security in SME. In: *Central and Eastern European eDem and eGov Days 2023*, ACM, NY, USA, 2023, pp. 101–105.
4. Wallang, M.; Shariffuddin, M. D. K.; Mokhtar, M. Cyber security in small and medium enterprises (SMEs). *Journal of Governance and Development* 2022, 18(1), pp. 75–87.
5. Whitman, M. E.; Mattord, H. J. Principles of Information Securit, 7th ed. Cengage Learning, Boston, SUA, 2021, 658 p.
6. ENISA. Threat Landscape 2021. Available online: https://www.enisa. europa. eu/publications/ enisa-threat-landscape-2021 (accessed on 05.05.2025).
7. Falch, M.; Olesen, H.; Skouby, K. E.; Tadayoni, R.; Williams, I. Cybersecurity Strategies for SMEs in the Nordic Baltic Region. *Journal of Cyber Security and Mobility* 2023, 11(6), 727–754. https://doi.org/10.13052/jcsm2245-1439.1161.
8. Erdogan, G.; Halvorsrud, R.; Boletsis, R.; Tverdal, S.; Pickering, J. Cybersecurity Awareness and Capacities of SMEs. In: *Proceedings of the 9th International Conference on Information Systems Security and Privacy, SCITEPRESS - Science and Technology Publications* 2023, pp. 296–304.
9. Bolun, I.; Ciorbă, D.; Zgureanu, A.; Bulai, R. Informatics security assessment in the Republic of Moldova. *Journal of Engineering Science* 2020, 27(4), pp. 103–119.
10. Boletsis, C.; Halvorsrud, R.; Pickering, J.; Phillips, S.; Surridge, M. Cybersecurity for SMEs: Introducing the Human Element into Socio-technical Cybersecurity Risk Assessment. In: *Proceedings of the 16th International Joint Conference on Computer Vision, Imaging and Computer Graphics Theory and Applications, SCITEPRESS - Science and Technology Publications* 2021, pp. 266–274
11. Sarri, A.; Paggio, V.; Bafoutsou, G. *Cybersecurity for SMEs – Challenges and Recommendations*. Heraklion, European Union Agency for Cybersecurity, Greece, 2021, 61 p.
12. ENISA threat landscape for ransomware attacks 2022. Available online: https://www.enisa. europa.eu/ publications/enisa-threat-landscape-for-ransomware-attacks/@@download/fullReport (accessed on 06.05.2025).
13. ENISA. Cybersecurity for SMES Challenges And Recommendations, 2021. Available online: https://www.enisa.europa.eu/publications/enisa-report-cybersecurity-for-smes (accessed on 08.05.2025).
14. ENISA. Cybersecurity Maturity Assessment for Small and Medium Enterprises. Available online: https://www.enisa.europa.eu/cybersecurity-maturity-assessment-for-small-and-medium-enterprises#/ (accessed on 08.05.2025).
15. Verizon. Data Breach Investigations Report, 2024. Available online: https://www.verizon.com/business/resources/reports/dbir/2024/industries-intro/healthcare-data-breaches/ (accessed on 09.05.2025).
16. Verizon. Data Breach Investigations Report, 2023. Available online: https://www.verizon.com/business/resources/reports/dbir/2023/small-business-data-breaches/?mkt_tok= MTU3LUlQVy04NDYAAAGP51ZU5rx9mZgDjn1I6bznDT1j-OutdGDM2wlWO_wNe3RNqr87MTdVGu_Pn LvBiUFzCodL2mCHf9cRYDk7zNfejzmKlZe_bcHGhu9bR339nWz0NKSG /(accessed on 09.05.2025).
17. Cost of a Data Breach Report 2021. Available online: https://www.ibm. com /downloads/cas/3R8N1DZJ (accessed on 06.05.2025).
18. Check Point Research. Cyber Security Report, 2022. Available online: https://www.checkpoint.com (accessed on 06.05.2025).

19. Kim, D.; Solomon, M. Fundamentals of Information Systems Security (4th ed.). Jones & Bartlett Learning, Burlington, MA, USA, 2023, 550 p.
20. Alexei, A; Platon, N.; Bolun, I.; Alexei, A. Smart and Digital Healthcare. Advanced Technologies and Security Issues. In: *Proceedings of the Central and Eastern European eDem and eGov Days 2024,* New York, USA, 2024, pp. 288–294.
21. Keller, S.; Powell, A.; Horstmann, B.; Predmore, C.; Crawford, M. Information Security Threats and Practices in Small Businesses. *Information Systems Management* 2005, 22(2), pp. 7–19.
22. Alexei, A. Network security threats to higher education institutions. *CEE e|Dem and e|Gov Days* 2021, pp. 323–333. DOI: 10.24989/ocg.v341.24.
23. Alexei, A.; Alexei A. Cyber Security Threat Analysis in Higher Education Institutions as a Result of Distance Learning. *International Journal of Scientific & Technology Research* 2021, 10(3), pp. 128–133.
24. Javeed, D.; Mohammedbadamasi, U.; Ndubuisi, C. O.; Soomro, F.; Asif, M. Man in the Middle Attacks: Analysis, Motivation and Prevention. *International Journal of Computer Networks and Communications Security* 2020, 8(7), pp. 52–58.
25. Ramesh, P.; Bhaskari, D.L. A Comprehensive Analysis of Spoofing. *International Journal of Advanced Computer Science and Applications* 2010, 1(6), pp. 157–162. DOI: 10.14569/IJACSA.2010.010623.
26. Wu, D.; Hu, G. Research and improve on secure routing protocols in wireless sensor networks. In: *International Conference "Circuits and Systems for Communications 2008, IEEE",* 2008, pp. 853–856.
27. Galvin, J. 60 Percent of Small Businesses Fold Within 6 Months of a Cyber Attack Here's How to Protect Yourself. Available online: https://www.Inc.com/joe-galvin/60-percent-of-smallbusinesses- fold-within-6-months-of-a-cyber-attack-heres-how-to-protectyourself. html (accessed on 17.05.2025).
28. What's New in the 2019 Cost of a Data Breach Report. Security Intelligence. Available online: https://securityintelligence.com/posts/whats-new-in-the-2019-costof-a-data-breach-report/ (accessed on 20.05.2025).
29. Cost of a Data Breach Report 2020. Available online: https://www.ibm. com /downloads/cas/3R8N1DZJ (accessed on 16.05.2025).
30. Berry, C. T.; Berry, R. L. An initial assessment of small business risk management approaches for cyber security threats. *International Journal of Business Continuity and Risk Management* 2018, 8(1), pp. 1-10.
31. Alexei, A. Laboratory Guidelines for the Course "Information Security Technologies". Tehnica-UTM, Chisinau, Republic of Moldova, 2024, 94 p.
32. Alexei, A. Course Support "Fundamentals of Cybersecurity". Tehnica-UTM, Chisinau, Republic of Moldova, 2024, 120 p. ISBN 978-9975-64-464-8.
33. Barlette, Y.; Gundolf, K.; Jaouen, A. CEOs' information security behavior in SMEs: Does ownership matter? *Systèmes d'information & management* 2017, 22(3), pp. 7–45.

Citation: Alexei, A.; Moraru, V.; Alexei, A. Securing Moldovan small and medium-sized businesses: strategies based on it infrastructure domains. *Journal of Engineering Science*. 2025, XXXII (2), pp. 75-86. https://doi.org/10.52326/jes.utm.2025.32(2).07.

Submission of manuscripts: jes@meridian.utm.md

Journal of Engineering Science *Vol. XXXII, no. 2 (2025), pp. 87 - 98*
Fascicle *Electronics and Computer Science* *ISSN 2587-3474*
Topic *Computers and Information Technology* *eISSN 2587-3482*

https://doi.org/10.52326/jes.utm.2025.32(2).08
UDC 331.108.4:159.9:004.056.5(478)

CYBER SECURITY PROFESSIONAL DEVELOPMENT WITHIN CYBERCOR

Dinu Țurcanu, ORCID: 0000-0001-5540-4246,
Ludmila Peca *, ORCID: 0000-0002-4394-2933,
Adrian Prisacaru, ORCID: 0000-0001-7809-0868,
Tatiana Țurcanu, ORCID: 0000-0002-8972-8262

Technical University of Moldova, 168, Stefan cel Mare Blvd., Chisinau, Republic of Moldova
* Corresponding author: Ludmila Peca, *ludmila.peca@isa.utm.md*

Received: 04. 12. 2025
Accepted: 05. 17. 2025

Abstract. One of the main development challenges facing the Republic of Moldova is its vulnerability to state security threats and risks. In the context of the objectives for developing the digital economy and digitalizing public services, measures to counter cyber threats and risks become imperative. Law No. 48/2023 on cyber security stipulates the implementation of requirements, measures, and mechanisms to ensure a sufficiently high level of security for networks and information systems in the Republic of Moldova, capable of guaranteeing the protection of the vital interests of individuals and legal entities, society, and the state, as well as the national interests of the Republic of Moldova. In this regard, the human resources' preparation level plays a primary role and is a priority. Developing cybersecurity skills among staff is an indispensable part of the process of ensuring the cybersecurity of systems and information resources. The creation of the National Institute for Cybersecurity Innovation CYBERCOR aims ultimately to ensure the necessary level of cybersecurity competencies among personnel, strengthening the security of networks and information systems. The appropriate professional development of public authority staff at any level and employees of other legal entities, public or private, will enable the prevention and counteraction of cyber threats and risks.

Keywords: *cybersecurity, personal development, training programs, professional development, cybersecurity training exercises.*

Rezumat. Una dintre principalele provocări de dezvoltare cu care se confruntă Republica Moldova este vulnerabilitatea sa la amenințări și riscuri la adresa securității statului. În contextul obiectivelor de dezvoltare a economiei digitale și digitalizării serviciilor publice, măsurile de contracarare a amenințărilor și riscurilor cibernetice devin imperios necesare. Legea nr. 48/2023 privind securitatea cibernetică prevede implementarea cerințelor, măsurilor și mecanismelor necesare pentru a asigura un nivel suficient de ridicat de securitate a rețelelor și sistemelor informatice din Republica Moldova, capabil să garanteze protecția intereselor vitale ale persoanelor fizice și juridice, ale societății și ale statului, precum și a intereselor naționale ale Republicii Moldova. În acest sens, nivelul de pregătire a resurselor umane joacă un rol esențial și reprezintă o prioritate. Dezvoltarea competențelor în domeniul

securității cibernetice în rândul personalului este o componentă indispensabilă a procesului de asigurare a securității sistemelor și resurselor informaționale. Crearea Institutului Național de Inovații în Securitatea Cibernetică CYBERCOR are ca obiectiv final asigurarea nivelului necesar de competențe în domeniul securității cibernetice în rândul personalului, consolidând securitatea rețelelor și a sistemelor informatice. Formarea profesională adecvată a angajaților autorităților publice, indiferent de nivel, precum și a salariaților altor entități juridice, publice sau private, va permite prevenirea și contracararea amenințărilor și riscurilor cibernetice.

Cuvinte-cheie: securitate cibernetică, dezvoltare personală, programe de formare, dezvoltare profesională, exerciții de instruire în domeniul securității cibernetice.

1. Introduction

In a global context dominated by rapid digitalization, the Republic of Moldova is rapidly developing its information and communication technology (ICT) sector, significantly contributing to economic growth and providing a solid foundation for IT innovation and outsourcing. The launch of Moldova's Digital Transformation Strategy 2023–2030 reflects the country's ambition to build a robust digital economy and strengthen cybersecurity culture [1]. However, in this process, cyber threats have become a major challenge, putting pressure on the digital security of both public and private infrastructures. The COVID-19 crisis highlighted the vulnerability of essential digital services to cyberattacks, emphasizing the need for a robust cybersecurity culture at all levels of society.

The ICT sector has grown rapidly due to high market demand, dynamic competition, and coordinated support from all involved stakeholders. Contributing approximately 7% to the national GDP and generating annual revenues of around 15 billion MDL (approximately 900 million USD), the ICT sector has become a key pillar of the Moldovan economy. Between 2015 and 2020, information technology (IT) became the primary growth driver, surpassing telecommunications, with a 3.6% contribution to GDP in 2020, compared to only 0.8% in 2013, when IT was first prioritized as a national policy focus.

This growth has been supported by competitive costs, advantageous location, and the availability of skilled professionals in Moldova, as well as by fiscal incentives offered to residents of the Virtual Moldova IT Park. International and national reports on digitalization (such as the UN DESA e-Government Index, the Networked Readiness Index, and reports from ANRCETI) reflect progress in internet access, IT device usage, and the implementation of e-government platforms.

However, ICT development and digital transformation have contributed to a substantial growth in cyber risks. The acceleration of digitalization has attracted numerous cyber threats, further amplified by the pandemic, which highlighted the vulnerability of digital services and the economy to these constantly evolving risks.

For example, the assessment report [2] conducted by the International Telecommunication Union (ITU) provides an overview of cyber threats in the Republic of Moldova. Like other countries, Moldova is affected by various types of cyberattacks that target government entities, the private sector, and the general population. Although authorities monitor cyber threats related to government entities, achieving a holistic understanding of cyberattacks at the national level remains challenging This issue is also highlighted in the *Moldova Cybersecurity Governance Assessment* developed by DCAF, which outlines persistent challenges in institutional coordination, clarity of roles, and the visibility of cyber risks at the

national level [3]. Common types of cybersecurity incidents include online scams, phishing (including smishing and vishing), ransomware, web defacement, and denial of service attacks.

Since 2015, Moldova has faced attacks such as DDOS, phishing, brute force attacks on government information systems, and hijacking of official websites. The private sector is equally exposed, with small and medium-sized enterprises (SMEs) representing approximately 98.6% of all businesses in the country as of 2019 [4]. These SMEs are particularly vulnerable due to their limited capacity to implement robust cybersecurity measures. According to ODIMM data, fewer than 17% of SMEs have effectively integrated digital technologies into their operations, revealing both a significant untapped potential and an urgent need to adopt standardized cybersecurity protocols [5].

According to the 2020 Global Cybersecurity Index (GCI) published by the International Telecommunication Union (ITU), the Republic of Moldova ranks 33rd in Europe and 63rd globally. The GCI serves as a benchmark for evaluating national commitment to cybersecurity across five key domains: legal, technical, organizational, capacity development, and cooperative measures.

2. Materials and methods

The methodological approach adopted for cybersecurity capacity development at CYBERCOR integrates theory with applied practice, combining formal instruction with hands-on simulations. A key element is the E-Academy platform, available through CYBERCOR's internal learning environment, which enables realistic training environments by simulating corporate networks and attack scenarios. These simulations are aligned with international frameworks such as ISO/IEC 27001 and ISO/IEC 31000, and cover all phases of cyber incident response—protection, detection, reaction, and recovery.

Additionally, the curriculum design process involves collaboration with industry partners (e.g., Cisco, Fortinet, Palo Alto), allowing the integration of certified training programs. Practical content includes structured exercises in computer networks and network security, developed by academic staff, and used across bachelor and master's levels. Training outcomes are monitored through performance assessments, SIEM tools, and feedback systems, ensuring the practical relevance and adaptability of content to current threats.

All methodological components aim to support the development of both individual skills and organizational readiness in the cybersecurity field.

3. Results and discussions

According to the 2020 Global Cybersecurity Index (GCI) published by ITU, the Republic of Moldova demonstrates varied performance across the assessed cybersecurity domains. In terms of legal measures, Moldova obtained a score of 16.73, reflecting a well-developed legal framework for cybersecurity. Technical measures also registered a strong performance, with a score of 16.86, indicating the presence of robust digital protection tools and infrastructure.

In contrast, organizational measures scored 13.21, suggesting that improvements are needed in the strategic planning and governance of cybersecurity at the institutional level. Capacity development scored 13.09, highlighting the urgent need to expand training, education, and workforce development programs in cybersecurity. For cooperative measures, Moldova scored 15.89, reflecting active participation in international partnerships and collaborative initiatives.

Overall, Moldova achieved a GCI score of 75.78, ranking 33rd in Europe and 63rd globally. These results underscore the country's strengths in legal and technical dimensions

while also revealing areas for further development - particularly in organizational maturity and capacity building. Figure 1 presents Moldova's scores across the five core areas of cybersecurity, as assessed in the 2020 GCI.

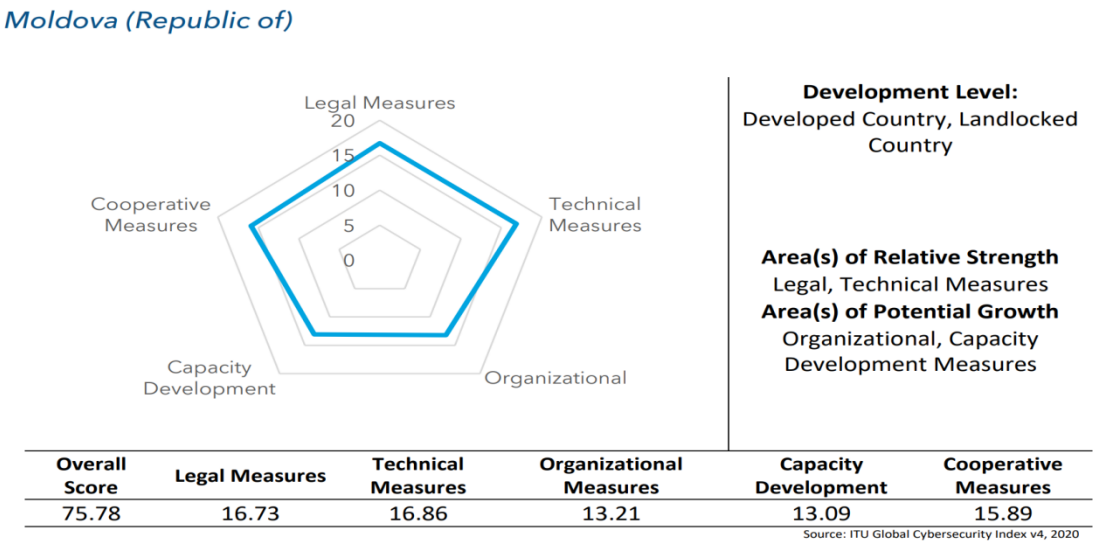

Overall Score	Legal Measures	Technical Measures	Organizational Measures	Capacity Development	Cooperative Measures
75.78	16.73	16.86	13.21	13.09	15.89

Source: ITU Global Cybersecurity Index v4, 2020

Figure 1. Moldova's scores across evaluation domains as reflected in the 2020 Global Cybersecurity Index (GCI) report [6].

According to the ITU's assessment report aimed at supporting the establishment of a national Computer Incident Response Team (CIRT-MD), the slight decline in Moldova's performance in 2020 compared to previous years was primarily attributed to changes in the GCI methodology and question weighting. Nevertheless, Moldova has made steady progress since 2015, particularly in adopting national policies and cooperation agreements designed to enhance the protection of critical information infrastructure.

In response to these challenges, the National Institute for Cybersecurity Innovation – CYBERCOR – was established to serve as a key driver for national cybersecurity progress. The institute plays a fundamental role in professional development, acting as a platform for advanced training, capacity building, and the consolidation of a national network of cybersecurity specialists.

4. The role of CYBERCOR in professional development

The primary objective of the Institute for Innovation in Cybersecurity CYBERCOR is to enhance cybersecurity competencies, contributing to the formation of a network of specialists equipped to address today's information security challenges. CYBERCOR's mission is to provide advanced training and support the development of organizational capabilities through a combination of educational programs and applied exercises that ensure comprehensive, up-to-date training for personnel involved in protecting digital infrastructures.

CYBERCOR is dedicated to fostering professional development in information security, aiming to build competencies at all levels of society, from technical staff to decision-makers. It offers both analytical and implementation services for security systems, as well as specialized training designed to strengthen organizational resilience against cyber incidents.

A fundamental objective of CYBERCOR is to train specialists to secure a high standard of theoretical and practical readiness in the protection of informational assets. These training sessions are designed to help organizations develop monitoring, management, and incident

resilience capacities. Following training, organizations are expected to autonomously identify and eliminate the primary causes of attacks and implement effective corrective measures to prevent future incidents. The training also encompasses processes for acquiring, developing, and maintaining ICT systems, ensuring data confidentiality, integrity, and availability in line with organizational protection standards.

CYBERCOR offers a variety of programs and workshops that adhere to international standards, such as the ISO 2700X and 3100X families, relevant for information security and risk management. These workshops are essential for the efficient management of organizational continuity and for improving information security standards. During these sessions, essential recommendations are provided that organizations should implement to ensure strong cybersecurity governance and to develop robust risk assessment and management processes.

CYBERCOR promotes the establishment of a robust IT governance system that ensures effective cyber risk management at the organizational level. This includes developing a clear information security policy and strategy as an integral part of the company's overall development strategy. Key objectives of this governance system include:

1. **Implementing an IT governance structure**. Ensures efficient management of IT and cybersecurity risks through a governance system focused on analyzing and mitigating cyber risks.
2. **Information security policy and strategy**. As part of the organization's overarching strategy, the security policy should define objectives and necessary measures for information protection.
3. **Determining an acceptable risk level**. Each organization should establish a risk tolerance level, integrating it into the risk strategy and providing regular reports on risks across processes and applications.
4. **Information security audits.** IT governance and security processes should undergo regular audits as per a set plan to identify vulnerabilities and evaluate compliance with security standards.
5. **Introducing the role of information security officer**. Creating a dedicated information security role with well-defined responsibilities and boundaries supports centralized and effective security management.
6. **Monitoring and evaluating security measures**. Involves assessing the effectiveness of implemented measures and regularly reviewing security policies through penetration testing and other practical evaluations.
7. **Education and awareness programs**. Raising employee awareness of the importance of information security is essential for reducing risks associated with the improper use of systems.
8. **Security incident management**. Organizing processes for prompt and effective responses to security incidents at the organizational level and assigning responsibilities for information security.
9. **Long-term acquisition and development plan**. Establishing a security systems acquisition and development plan for 1, 3, and 5-year periods ensures strategic security planning.
10. **Business continuity and disaster recovery plans**. Organizing a continuity and post-incident recovery plan is crucial for maintaining operational continuity in case of disasters.

11. Incident impact analysis and implementation of intervention plans. Involves assessing the impact of incidents and planning quick interventions, including periodic testing of systems and crisis communication plans.

12. National and international cooperation. CYBERCOR aims to ensure effective cooperation at both national and international levels, disseminating relevant information, alerts, and international best practices to organizations in critical sectors.

Moldova's national commitment to cybersecurity is also reflected in the National Security Strategy adopted in December 2023. This document places cybersecurity among the country's top strategic priorities and calls for stronger institutional resilience and broader cooperation across all sectors [7]. At the organizational level, applying concrete measures helps build the capacity to prevent and respond effectively to cyber threats, while also ensuring continuity of operations. In this broader context, aligning Moldova's legislation with European Union standards is a necessary step, especially given the country's current status as an EU candidate.

A critical step in aligning Moldova's cybersecurity framework with European standards is the transposition of the NIS2 Directive, the Directive (EU) 2022/2555 of the European Parliament and of the Council, which sets out measures for a high common level of cybersecurity across the Union. This process also involves amending Regulation (EU) No. 910/2014 and Directive (EU) 2018/1972, while repealing the earlier Directive (EU) 2016/1148 [8]. The implementation of NIS2 is a national priority and plays a key role in strengthening Moldova's cyber defense capabilities. It supports both institutional alignment with EU standards and the development of a more robust and coordinated cybersecurity ecosystem in the country [9,10].

5. Initiatives and training activities

The National Institute for Cybersecurity Innovation plays a crucial role in professional development by organizing specialized courses and workshops in cybersecurity. Through the simulation platform „E-Academy", CYBERCOR provides participants with an integrated experience that combines theory with applied practice, enabling them to strengthen their skills in a realistic environment. This platform is designed for both professionals and individuals responsible for security within small and medium-sized companies, where practical training opportunities have previously been limited due to resource constraints.

Key focus areas of the cybersecurity training platform

1. **Realistic simulation of cyber threats**. The „E-Academy" platform offers participants a virtual environment that faithfully replicates a corporate network. It is equipped with a full range of security tools and devices (firewalls, routers, IPS/IDS, and SIEM products) that enable complex simulations, including sophisticated attacks like ransomware and malware. All activities are recorded for later analysis and performance assessment. This customizable environment allows participants to learn how to detect, investigate, and respond effectively to current cyber threats.

2. **Network versatility**. The adaptability of the platform allows for simulations of diverse configurations tailored to the needs and profile of each participating organization. A variety of attack scenarios, including simulations of complex threats such as trojans, exploits, and DDoS attacks, helps trainees identify specific vulnerabilities and better understand the need for investments in cybersecurity.

3. **Diversity of simulated threats**. A key feature of „E-Academy" is its ability to simulate a wide range of attacks tailored to different types of organizations. This includes both common and advanced threats, reflecting the complexity of modern cyber threats and preparing participants to handle incidents that could disrupt a company's operational continuity.

4. **Adaptable curriculum**. The platform offers specialized courses, such as Fileless Attack, Ransomware and Encryption, and Corporate Espionage. Each course is structured to cover all phases of the incident response cycle, including protection, detection, reaction, and recovery. In addition to simulation-based courses, CYBERCOR's curriculum incorporates practical resources developed by local academic staff, including collections of solved exercises designed to support hands-on learning in core areas such as computer networks [13] and network security [14]. These materials are widely used in undergraduate and master's programs, helping students consolidate their technical understanding through real-world examples.

5. **Advanced learning, analysis, and feedback tools.** The platform includes a complex set of tools for vulnerability scanning and SIEM exercises, providing real-time feedback to participants. Instructors can monitor participants' progress, offering personalized guidance and discussing results in detail during evaluation sessions. Additionally, participants can revisit specific stages through video recordings to analyze decisions made and improve their response strategies.

To address the cybersecurity skills gap, CYBERCOR collaborates with external partners such as Cisco, Fortinet, and Palo Alto. These partnerships support the continuous development of training programs, ensuring that the content and technologies used remain aligned with international best practices. This approach also reflects broader trends identified in recent reports, such as Fortinet's global overview of workforce challenges in cybersecurity [11], as well as ENISA's recommendations for advancing cybersecurity education and skills across the European Union [12]. Additionally, these collaborations enable the provision of internationally recognized courses and certifications, preparing participants to meet the increasingly rigorous demands of the cybersecurity field.

Figure 2. Simulation of the „Dragonfly" Cyber Attack (exercise).

The „E-Academy" platform includes advanced simulations of persistent and sophisticated attacks, such as „Dragonfly". This type of advanced persistent cyber threat is

known for targeting critical infrastructure, including government entities, essential sectors like energy, water, aviation, and industrial manufacturing. Attacks in the "Dragonfly" family focus on compromising industrial control systems, with the ultimate goal of gaining unauthorized access to organizational networks and disrupting their operations.

During the simulation, participants are trained to detect suspicious activities associated with attacks like „Dragonfly", investigate targeted components and vulnerabilities, and implement response measures.

The simulation covers complex attack scenarios, including network exploitation techniques and unauthorized access to control systems, reflecting the disruptive potential of such attacks on the operation of critical infrastructures. This model provides trainees with practical experience in identifying, analyzing, and mitigating threats that impact sectors essential to national security.

The „E-Academy" platform is designed to meet the specific needs of trainees and the cybersecurity market in the Republic of Moldova. The objective of CYBERCOR and the „E-Academy" platform is to contribute to the preparedness of Moldovan IT specialists by promoting a solid understanding of security incidents and attacks, as well as an effective response capability.

Through the realistic and immersive learning environment of „E-Academy", the platform offers trainees not only technical knowledge but also essential practical skills, such as configuring security systems and understanding the risks associated with improperly implemented measures. This enables organizations to develop long-term security strategies, multi-year security plans, and prioritized investments in systems and dedicated personnel. These skills are crucial for preparing companies to withstand cyberattacks and protect critical infrastructure effectively.

To ensure high-quality and continuously updated cybersecurity skills, the platform also functions as a research and development laboratory. This center enables the team to develop and validate new cybersecurity tools and techniques, test security architectures, and analyze malware for a better understanding of attack mechanisms.

CYBERCOR provides continuous and solid cybersecurity education to partner organizations, ensuring a practical and adaptable approach to current threats. CYBERCOR's training approach is also grounded in modern e-learning methodologies, combining theoretical instruction with interactive, digital environments that support independent learning and experimentation. Previous research has emphasized the value of e-learning in developing ICT skills and its role in shaping effective engineering education strategies [15,16].

The National Institute for Cybersecurity Innovation, established at the Technical University of Moldova supported through the Future Technologies Project (FTA), sponsored by USAID and the Government of Sweden, was created in response to the shortage of specialized cybersecurity personnel, both nationally and internationally. In Moldova, cybersecurity is an underpromoted field and is rarely addressed within the traditional education system (secondary, high school, and university), lacking sufficient integration into the curriculum.

The founding of the Institute aims not only to train a new generation of cybersecurity professionals but also to increase awareness and integrate this essential field into youth education.

6. Objectives and actions of the National Institute for Cybersecurity Innovation

Founded to address the shortage of cybersecurity specialists, CYBERCOR at the Technical University of Moldova aims to accomplish the following objectives and measurable actions in its first year of operation:

1. **Research and studies**
   - Conduct studies on methods for ensuring the cybersecurity of networks and digital services, with a focus on preventing attacks and enhancing the cyber resilience of information systems.
   - Develop software resources to protect data managed within cyber infrastructures.
   - Implement and test advanced security architectures and protocols.
2. **Professional development and continuous training**
   - Support theoretical and practical training for students, master's candidates, doctoral students, and professors, stimulating creativity and innovation in cybersecurity.
   - Organize cyber exercises and simulations within the Academy to prepare specialists for realistic cyberattack scenarios.
   - Offer training and workshops for IT personnel in the public and private sectors to strengthen national cyber defense capabilities.
3. **Partnerships and cooperation**
   - Collaborate with public institutions to develop cybersecurity skills in line with the state's plan for enhancing public sector personnel.
   - Participate in working groups to develop cybersecurity curricula at all educational levels.
4. **Dissemination and publicity**
   - Disseminate academic results and research to increase interest in cybersecurity and expand the market.
   - Publish scientific articles, patent technical innovations, and participate in national and international conferences.
5. **Technical support and infrastructure**
   - Provide technical and informational support for conducting cybersecurity workshops and training sessions.
   - Establish a specialized lab equipped with cutting-edge technologies and tools provided by global leaders in cybersecurity solutions (Cisco Systems, BitDefender, Palo Alto, MicroFocus, Fortinet, etc.).

In addition to building technical capacity, CYBERCOR places emphasis on cultivating a sense of mission and shared purpose among trainees and educators. This perspective aligns with modern approaches to leadership and organizational development, which highlight the importance of understanding "why" behind every professional action [17]. Hosted from the Technical University of Moldova, with support from the Information Technology and Cybersecurity Service (STISC), the Electronic Governance Agency (AGE) and the Cybersecurity Agency (ASC), CYBERCOR will contribute to strengthening national security infrastructure and support the government's digital transformation processes.

The National Institute for Cybersecurity Innovation offers multi-dimensional education in cybersecurity, including undergraduate and master's programs at the Technical University of Moldova, as well as executive education tailored to professionals and managers in the field. CYBERCOR is also actively involved in training teachers in schools and high schools,

disseminating best practices in cybersecurity among students, and contributing to the modernization of the school curriculum in cybersecurity.

7. Strategic development directions of CYBERCOR

The National Institute for Cybersecurity Innovation CYBERCOR aims to unify and coordinate cybersecurity initiatives within the Technical University of Moldova, consolidating a strategic action plan to advance this essential field. The new entity welcomes collaboration with international partners and top cybersecurity solution providers, fostering a high-quality educational environment that aligns with market needs.

In its first year of operation, CYBERCOR plans to implement the following measurable actions:

1. **Faculty training**. Training and certifying at least 20 faculty members from the FCIM and FET faculties through advanced programs provided by industry leaders, supported by Pearson VUE Testing Center.
2. **Student Training**. Including cybersecurity courses for 200 students annually within the undergraduate and master's programs at FCIM and FET. Developing micro-master programs in cybersecurity.
3. **Enhancing teaching capacity**. Integrating at least five industry trainers to improve the quality of the academic teaching process alongside university faculty.
4. **Providing practical training**. Offering internships for students at STISC, AGE, and private cybersecurity companies, ensuring hands-on training.
5. **Organizing competitions and events**. Hosting at least two national competitions in cybersecurity, with a minimum of 100 student participants. Organizing a roundtable with at least 50 participants from the public and private sectors to discuss current cybersecurity challenges and the role of academia.
6. **Training for educational institution staff**. Collaborating with the General Directorate of Education, Youth, and Sports in Chișinău to provide training for school directors on online safety, reaching an audience of at least 100 participants.
7. **Training public sector employees**. Organizing cybersecurity training for at least 600 public sector employees, subject to the approval of mandatory retraining through government decision.
8. **Inviting international trainers**. Collaborating with international trainers, especially from Romania, to enhance education quality and overcome potential language barriers.
9. **Establishing educational partnerships**. Forming at least three partnerships with leading cybersecurity providers to implement authorized courses and utilize software resources and educational tools in the training process.

The National Institute for Cybersecurity Innovation „CYBERCOR” is committed to developing a qualified workforce and strengthening national capabilities in cybersecurity, thereby supporting digital transformation and the resilience of critical infrastructures in the Republic of Moldova.

8. Conclusions

The results of the GCI reveal Moldova's partial progress in strengthening digital resilience. While the legal and technical measures are relatively strong, the organizational dimension and capacity development remain underdeveloped. In response to this need, the CYBERCOR Institute was created to strengthen national capacities through advanced training. Through partnerships with industry leaders and simulation-based learning, CYBERCOR

contributes to the consolidation of a skilled cybersecurity workforce. The human-centered approach supports the development of practical abilities and institutional readiness to respond to cyber threats, thus contributing to improving the overall national cybersecurity posture. Continued investment in such structured professional development initiatives is essential to ensure Moldova's resilience against emerging cyber threats.

A version of these results was initially presented at the International Conference on Electronics, Communications and Computing (ECCO 2024), held on 17–18 October 2024 in Chișinău.

Conflicts of interest. The authors declare no conflicts of interest.

References

1. Government of the Republic of Moldova. Announcement regarding the initiation of the development of the Digital Transformation Strategy of the Republic of Moldova for the years 2023–2030 [in Romanian] 2023. Available online: https://particip.gov.md/ru/document/stages/anunt-privind-initierea-elaborarii-strategiei-de-transformare-digitala-a-republicii-moldova-pentru-anii-20232030-stdm-2030/9355. (accessed on 22 January 2025).
2. International Telecommunication Union (ITU). Assessment Report of Moldova National Computer Incident Response Team (CIRT-MD) 2022. Available online: https://moldova.un.org/sites/default/files/2023-01/CIRT-Assessment-Moldova-final.pdf. (accessed on 9 February 2025)
3. Geneva Centre for Security Sector Governance (DCAF). Moldova Cybersecurity Governance Assessment 2019. Available online: https://www.dcaf.ch/sites/default/files/publications/documents/MoldovaCybersecurity GovernanceAssessment.pdf (accessed on 21 May 2025).
4. National Bureau of Statistics of the Republic of Moldova. Total number of enterprises and the share of SMEs in Moldova [in Romanian] 2023. Available online: https://statistica.gov.md/newsview.php?l=ro&idc=168&id=6716. (accessed on 2 February 2025).
5. Organization for the Development of Small and Medium Enterprises (ODIMM). Digitalization of SMEs in the Republic of Moldova [in Romanian] 2023. Available online: https://www.odimm.md/ro/digitalizarea. (accessed on 19 February 2025)
6. International Telecommunication Union (ITU). Global Cybersecurity Index (GCI) Report 2021. Available online: https://www.itu.int/dms_pub/itu-d/opb/str/D-STR-GCI.01-2021-PDF-E.pdf (accessed on 12 January 2025).
7. Parliament of the Republic of Moldova. Decision No. HP391/2023 of 15.12.2023 on the approval of the National Security Strategy of the Republic of Moldova [in Romanian] Published in: Official Monitor No. 17–19, 17 January 2024. Available online: https://presedinte.md/app/webroot/uploaded/Proiect%20SSN_2023.pdf.
8. European Commission. Directive (EU) 2022/2555 of the European Parliament and of the Council on measures for a high common level of cybersecurity across the Union (NIS 2 Directive). *Official Journal of the European Union*, 27 December 2022. Available online: https://eur-lex.europa.eu/eli/dir/2022/2555/oj (accessed on 21 May 2025).
9. Dinu Țurcanu, Natalia Spinu, Serghei Popovici, Tatiana Țurcanu. Cybersecurity of the Republic of Moldova: a retrospective for the period 2015-2020.*In: Journal of Social Sciences*, Vol. IV, no. 1 (2021), pp. 74 – 83.
10. Peca, L.; Țurcanu, D. Reducing cyber risk through a human–centred approach. *Journal of Engineering Science,* 2025, 32(1), pp.18–31.
11. FORTINET. *Cybersecurity Skills Gap Report 2024*. Available online: https://www.fortinet.com/resources/reports/cybersecurity-skills-gap. (accessed on 5 January 2025).
12. ENISA. Cybersecurity Skills Development in the EU: An Overview. European Union Agency for Cybersecurity, 2023. Available online: https://www.enisa.europa.eu/publications/cybersecurity-skills-development-in-the-eu (accessed on 13 April 2025).
13. Peca, L.; Țurcanu, D. *Computer networks: Practical examples solved to be introduced in computer networks.* ; Tehnica-UTM, Chisinau, RM, 2022, 188 p.
14. Peca, L.; Țurcanu, D. Network security*: Practical examples solved to be introduced in network security*. Tehnica-UTM, Chisinau, RM, 2023, 243 p.

15. Dumbraveanu, R.; Peca, L. E-learning in Developing ICT Skills of Future Engineers. In: *1st International Online Scientific Conference ICT in Life*, August 2022, Osijek, Croația. 2022, pp. 86-95.
16. Peca, L. The power of eLearning from promises to practices applied in engineering. *Journal of Social Sciences* 2023, 6(1), pp. 69-80.
17. Sinek, S.; Mead, D.; Docker, P. *Find your why: A practical guide for discovering purpose for you and your team*. Portfolio, New York, SUA, 2017, 242 p.

Citation: Ţurcanu, D.; Peca, L.; Prisacaru, A.; Ţurcanu, T. Cyber security professional development within CYBERCOR. *Journal of Engineering Science*. 2025, XXXII (2), pp. 87-98. https://doi.org/10.52326/jes.utm.2025.32(2).08.

Publisher's Note: JES stays neutral with regard to jurisdictional claims in published maps and institutional affiliations.

Submission of manuscripts: jes@meridian.utm.md

Journal of Engineering Science *Vol. XXXII, no. 2 (2025), pp. 99 - 107*
Fascicle *Architecture, Civil and Environmental Engineering* *ISSN 2587-3474*
Topic *Environmental Engineering* *eISSN 2587-3482*

https://doi.org/10.52326/jes.utm.2025.32(2).09
UDC 662.63:620.952

THE EFFECT OF TORREFACTION ON PELLETS MADE FROM VEGETAL BIOMASS GENERATED BY FRUIT SHRUBS

Grigore Marian [1], ORCID: 0000-0002-9975-2522,
Alexandru Banari [1]*, ORCID: 0000-0001-9132-610X,
Teodor Marian [2], ORCID: 0000-0002-7859-385X

[1] *Scientific Laboratory of Solid Biofuels, Technical University of Moldova, 168 Stefan cel Mare Blvd., Chisinau, Republic of Moldova*
[2] *CC "BASADORO AGROTEH" LLC, 192 Alba-Iulia Str., 2071 Chisinau, Moldova*
* Corresponding author: Alexandru Banari, *alexandru.banari@sfc.utm.md*

Received: 03. 12. 2025
Accepted: 04. 28. 2025

Abstract. This study investigates the effects of torrefaction on the properties of pellets produced from vegetable biomass residues of fruit shrubs. The research focuses on two pellet formulations: (1) a blend of sea buckthorn (*Hippophae rhamnoides* L.) and blackberry (*Rubus fruticosus*) residues and (2) a mixture of sea buckthorn residues with wheat straw. The torrefaction process was conducted in an inert argon atmosphere at temperatures between 200 °C and 300 °C for durations ranging from 10 to 30 min. The study assessed the impact of these parameters on the net calorific value and ash content of the pellets. Results indicate that torrefaction significantly enhances the calorific value of the biomass, with optimal conditions identified at 250-280 °C and exposure times of 15-25 min. However, excessive temperature and duration lead to mass losses and increased ash content. These findings provide insights into optimizing torrefaction parameters for improving the quality of densified solid biofuels derived from agricultural residues.

Keywords: *torrefaction, fruit shrub biomass, solid biofuels, calorific value, ash content.*

Rezumat. Acest studiu investighează efectele torefierii asupra proprietăților peleților produși din reziduuri de biomasă vegetală provenite de la arbuști fructiferi. Cercetarea se concentrează pe două formulări de peleți: (1) un amestec de reziduuri de cătină albă (*Hippophae rhamnoides* L.) și mur (*Rubus fruticosus*) și (2) un amestec de reziduuri de cătină albă cu paie de grâu. Procesul de torefiere a fost realizat într-o atmosferă inertă de argon, la temperaturi cuprinse între 200 °C și 300 °C, pentru durate de expunere între 10 și 30 min. Studiul a evaluat impactul acestor parametri asupra valorii calorifice nete și conținutului de cenușă al peleților. Rezultatele indică faptul că torefierea îmbunătățește semnificativ valoarea calorifică a biomasei, condițiile optime fiind identificate la temperaturi de 250 - 280 °C și durate de expunere de 15 - 25 min. Totuși, temperaturile și timpii excesivi conduc la pierderi de masă și la creșterea conținutului de cenușă. Aceste constatări oferă informații utile pentru optimizarea parametrilor de torefiere în vederea îmbunătățirii calității biocombustibililor solizi densificați obținuți din reziduuri agricole.

Cuvinte cheie: *torefiere, biomasă de arbuști fructiferi, biocombustibili solizi, valoare calorifică, conținut de cenușă.*

1. Introduction

The cultivation of fruit shrubs is an essential sector of agriculture, contributing to the diversification of agricultural production and generating additional income for farmers [1]. In the Republic of Moldova, due to its geographical position and morphological characteristics, especially in the Northern and Central regions, the areas designated for these crops have seen significant growth, increasing from 698 ha in 2021 to 908 ha in 2023 [2].

The results obtained in our previous research demonstrate that fruit shrubs generate a significant amount of plant biomass, which can be successfully used for the production of densified solid biofuels, including pellets [3-6]. The use of these residues as raw material for pellet production holds significant potential for the development of renewable energy in the Republic of Moldova.

Wood pellets are successfully used for heating in both the residential and industrial sectors [7]. However, the production of pellets from agricultural residues, including plant biomass from fruit shrubs, has some disadvantages, such as hydrophilicity, low calorific value, and poor densification capacity [8,9].

Thermochemical treatment through torrefaction can eliminate or at least reduce these disadvantages by significantly modifying certain essential characteristics [10]. Torrefaction is a thermal treatment process in which biomass, before densification, or the final product is slowly heated in an inert or oxygen-deficient environment at temperatures ranging from 200 to 300 °C [11,12 pp. 30-31]. The specialized literature describes three types of torrefaction: wet torrefaction [13], dry torrefaction [14] and ionic torrefaction [15]. Among these, dry torrefaction is the most widely used thermochemical treatment method for producing solid biofuels [16].

Regardless of the method used, torrefaction consists of several distinct stages: initial heating, pre-drying, post-drying, and intermediate heating [17]. However, the torrefaction mechanism remains a subject of scientific and practical interest, as it is specific to each type of biomass. It is important to note that research in this field varies significantly depending on the technological solutions applied [18,19]. In this context, studies focused on specific cases have been a constant concern for many researchers.

For example, researchers in Canada analysed the effects of torrefaction on rice and peanut husks, wood sawdust, and bagasse in a nitrogen environment, depending on exposure duration and temperature. It was found that biomass torrefied at 300 °C achieved the highest heating value (HHV = 25.68 MJ/kg), comparable to the HHV of lignin [20]. Kumar demonstrated that densifying biomass torrefied at 225 °C reduces energy consumption and improves densification productivity [21]. Additionally, the positive effects of pre-processing torrefaction on cereal residues were highlighted by [22] for corn and cotton stalks.

Researchers in Thailand studied the effects of torrefaction on four types of agricultural waste (corn cobs, coconut husks, cassava rhizomes, and rice husks) in an inert environment at temperatures ranging from 200 to 300 °C for 30 min. The results demonstrated that torrefaction is a promising technology for converting agricultural waste into solid biofuels, which can be used as an alternative to coal [23].

Information on the effects of torrefaction on different types of agricultural biomass is also available in studies by researchers from Poland and Sweden, who investigated wheat, rice, and rye husks and straw [24, 25], corn cobs, cotton, and sunflower stalks [26], corn and cotton stalks [27], as well as soybean husks, corn cobs, rice straw, and grapevine branches [28].

The torrefaction of corn residue pellets with wet combustion gases highlighted that, at high steam concentrations, the decomposition reaction of hemicellulose occurs more rapidly, with the optimal torrefaction conditions being an exposure temperature of 260 °C and a duration of 20 minutes [29]. He efficiency of water vapor presence in the torrefaction atmosphere is also demonstrated in [30], due to its influence on the degradation kinetics of solid biomass.

The effect of torrefaction on pellets produced from wheat straw and wood residues was analyzed using a laboratory setup that simulates heating conditions in the absence of oxygen. Torrefaction was conducted at temperatures of 240 - 270 °C for 15 min [31].

The results indicated that the calorific value of woody biomass increased by approximately 16%, confirming the efficiency of the torrefaction process in the production chain of agricultural residue pellets. This finding is also supported by the research of Tumuluru et al. [11,32].

The possibility of using residues from poppy (*Papaver somniferum* L.) and buckwheat (*Fagopyrum esculentum*) in the pyrolysis process to improve energy performance and utilize biomass waste for biochar production was analyzed by Saletnik et al. [33]. In this study, samples were maintained in a nitrogen atmosphere with 99.99% purity and a gas flow rate of 2 min^{-1} at temperatures of 400, 450, and 500 °C for 2 - 18 min.

Although there are numerous studies on the torrefaction of agricultural residues, the specific characteristics of torrefying pellets made from biomass generated by fruit shrubs have been less explored. The aim of this study is to estimate the effect of torrefaction on pellets produced from mixtures of fruit shrub residues.

The methodology used is based on a multifactorial study of the effects of torrefaction regimes on the quality of pellets produced from mixtures of sea buckthorn, blackberry, and wheat straw residues. The results obtained allowed for the optimization of the technological parameters of torrefaction.

2. Material and Methods

The research was conducted in the Solid Biofuels Scientific Laboratory of the Technical University of Moldova and in the Surface Engineering Laboratory within the Faculty of Mechanics at the "Gheorghe Asachi" Technical University of Iași. The study focused on two types of pellet samples:

1. Mixture of sea buckthorn plant residues (SBPR) 30% and blackberry plant residues (BPR) 70%, called SBPR+BPR.
2. Mixture of SBPR 30% and wheat straw (WS) 70%, called SBPR+WS.

The torrefaction of the pellets was carried out in a Nabertherm N41/H thermal treatment oven, equipped with a separate chamber and controlled atmosphere, allowing the simulation of the torrefaction process in an argon environment within a closed space (Figure 1).

The research was based on a 2^2 multifactorial experimental design with three levels. The considered influencing factors were the torrefaction temperature, ranging from 200 to 300 °C, and the exposure duration, between 10 and 30 min. Statistical data analysis was performed using STATGRAPHICS Centurion version 18 software.

For all the analyzed samples, the calorific value and ash content were determined. The gross calorific value was measured using the IKA C6000 isoperibol calorimeter, used in a constant volume environment, according to the SM EN ISO 18125:2017 standard. In this study, the calorific value is expressed as the net calorific value, adjusted to 10% moisture.

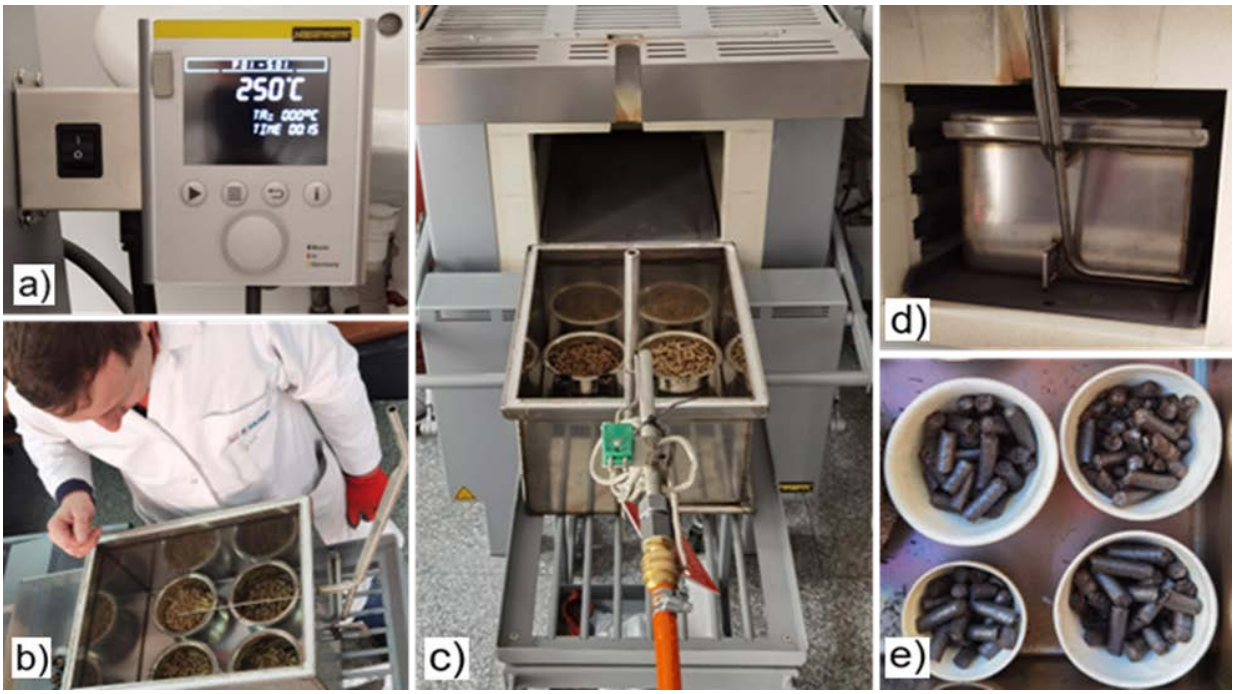

Figure 1. Sequences related to the torrefaction process of pellets from the Surface Engineering Laboratory at the Faculty of Mechanics, "Gheorghe Asachi" Technical University of Iași: a) electronic control panel for exposure time and temperature; b) and e) the samples investigated; c) Nabertherm N41/H thermal treatment oven before sample loading; d) protective box with gas inlet and outlet equipped with temperature sensors.

The ash content was determined according to the SM EN ISO 18122:2023 standard, using an LH 05/13 muffle furnace. The detailed procedure for determining the ash content is described in [4].

Before testing, the torrefied pellet samples were crushed using the Retsch SM 100 mill, equipped with a sieve with a mesh size of 1 mm. All tests were repeated five times, and the results were analyzed by determining the standard deviation and confidence interval.

3. Results and discussions

Following the statistical processing of the experimental data, the following regression equations were obtained, which adequately express the dependence of the examined factors on the torrefaction regimes:

$$Q = 6.46167+0.0471T+0.359583DE-0.000052T^2-0.000135T\cdot DE-0.00535DE^2 \quad (1)$$

$$A = 0.67333+0.0108T+0.052833DE-0.00002T^2+0.00002T\cdot DE-0.00105DE^2, \quad (2)$$

where: Q - calorific value; T - torrefaction temperature; DE - exposure duration; A - ash content.

The analysis of these equations allows for an understanding of the physico-chemical phenomena that occur during the torrefaction of the examined pellets.

Thus, the analysis of equation (1), the results of which are presented in Figure 2, shows that both the increase in torrefaction temperature and exposure duration lead to an increase in the net calorific value. At the same time, the second-order terms of the equation suggest a nonlinear behaviour, indicating that, at very high temperatures and durations, the calorific value begins to decrease. The interaction between temperature and exposure duration shows that their combined effects are not purely additive, meaning that, under certain conditions, they can negatively affect the efficiency of the process.

Analyzing the dynamics of the process (Figure 2), it is observed that the calorific value starts to increase from the first phase of the experiment. This can be explained by the fact that, in the temperature range of 200-250 °C, hemicellulose begins to degrade, releasing volatile compounds and improving the carbon-to-hydrogen ratio.

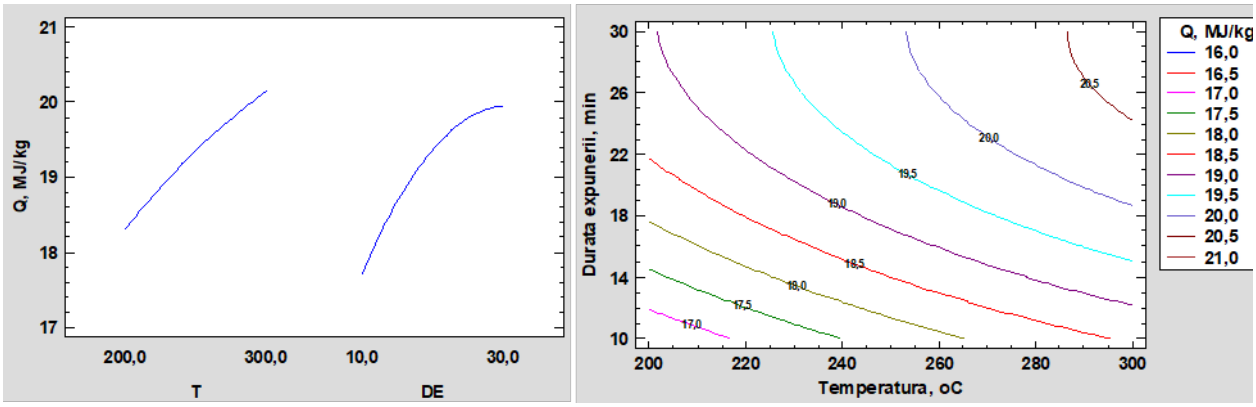

Figure 2. Diagram of the effects and response surface contours for the net calorific value (Q), adjusted to 10% moisture, of pellets obtained from SBPR+BPR, depending on the torrefaction temperature (T) and exposure duration (DE).

In the range of 250-300 °C, cellulose undergoes partial pyrolysis, leading to a reduction in mass and the formation of more carbonized structures. Lignin, due to its thermal stability, undergoes slower degradation, thus contributing to the increase in calorific value. However, at temperatures exceeding 300 °C, excessive mass loss occurs, resulting in a decrease in calorific value. When the temperature and exposure duration are too high, mass losses are amplified by the release of combustible gases (CO, CH_4, H_2), which negatively affect the energy efficiency of the final product. This phenomenon is reflected by the negative second-order terms of the regression equation.

These findings are consistent with the results obtained by the collaborators of the Scientific Laboratory of Solid Biofuels at UTM in studies on agricultural biomass, such as wheat straw and woody residues [31].

It is worth mentioning that the increase in torrefaction temperature and exposure duration leads to a slow increase in ash content (see equation 2 and Figure 3), indicating losses of organic mass. The second-order terms show that, after a certain threshold, the increase in temperature and duration may slow down the accumulation of ash.

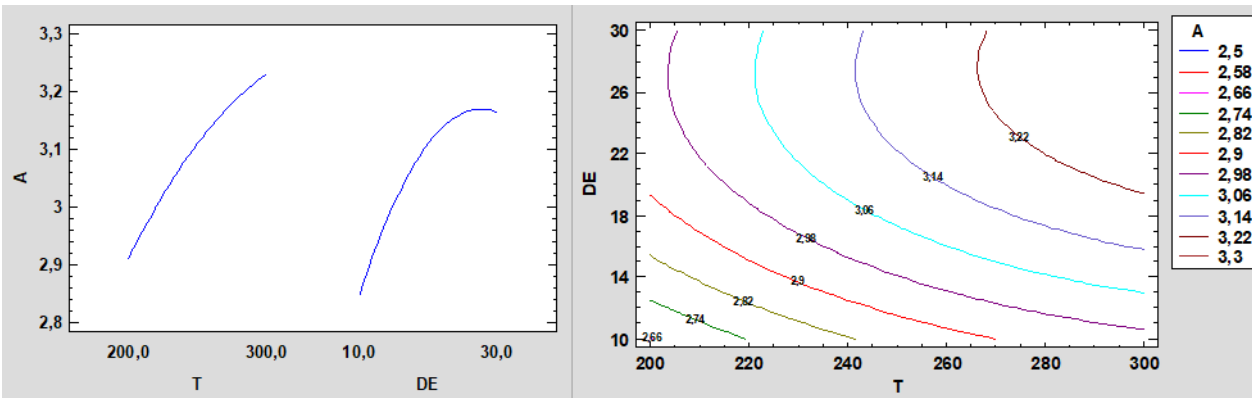

Figure 3. Diagram of the effects and response surface contours for the ash content (A) of pellets obtained from SBPR +BPR, depending on the torrefaction temperature (T) and exposure duration (DE).

The interaction between temperature and exposure duration is insignificant, suggesting that these two variables have an almost independent effect on the ash content. The increase in ash content can be explained by the fact that, as the temperature rises, volatile organic compounds are released, and the biomass becomes richer in fixed carbon and ash. At higher temperatures and longer durations, losses of organic matter accentuate the ratio between ash and total mass.

The negative higher-order terms suggest that, after a certain threshold, the increase in temperature no longer leads to a significant increase in ash content, as the mineral components reach a stable state.

Next, the changes in the net calorific value (Q) and ash content (A) of pellets obtained from SBPR + WS are presented, depending on the torrefaction temperature (T) and exposure duration (DE). The regression equations describing these dependencies are:

$$Q = 4.53333+0.05187T+0.34767DE - 0.00006T^2-0.00014T\cdot DE-0.0054DE^2 \quad (3)$$

$$A = 4.45278+0.0112T+0.05458DE-0.00002T^2+0.00002T\cdot DE-0.00107DE^2 \quad (4)$$

The Pareto diagram and the response surface contours (Figures 4 and 5) provide a clear visualization of the influence of temperature and exposure duration on the studied parameters.

The positive coefficients of the linear terms in regression equations (3) and (4) indicate that both the increase in temperature and exposure duration contribute to the initial increase in calorific value and ash content. At the same time, the negative coefficients in equation (3) suggest a nonlinear relationship, indicating that after a certain value, the increase in temperature and duration begins to have a negative effect on the calorific value. Additionally, from equation (4), it can be observed that after a certain threshold, the effect of increasing temperature and duration on ash content becomes less pronounced, as confirmed by the negative coefficients of the higher-order terms.

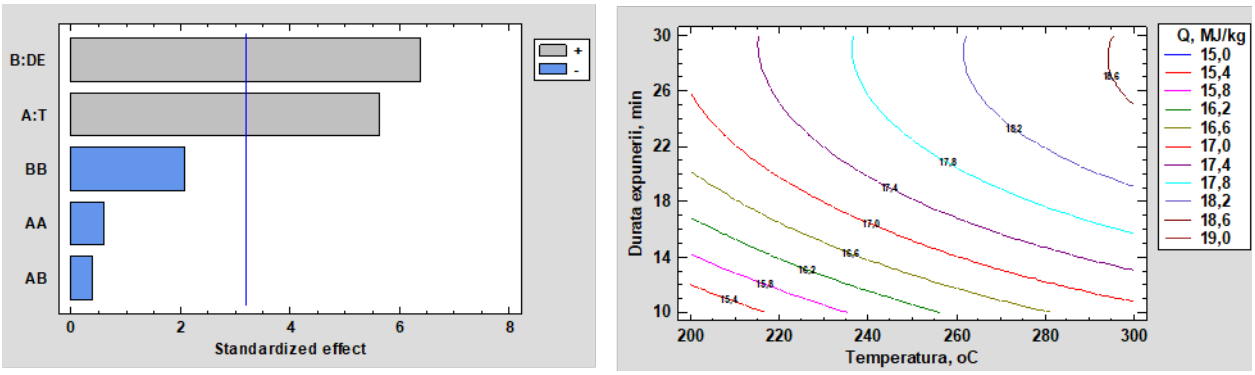

Figure 4. Pareto diagram and response surface contours for the net calorific value (Q), reported at 10% humidity of pellets obtained from SBPR +WS, depending on the torrefaction temperature (T) and exposure duration (DE).

It is also observed that the two parameters have an almost independent influence on the calorific value and ash content, and a simultaneous increase in both may insignificantly reduce the efficiency of the process.

The analysis of the diagrams in figures 2-5 highlights a high similarity between the dynamics of the torrefaction of SBPR +BPR pellets and that of SBPR +WS pellets, based on similar thermal processes. However, it should be noted that the torrefaction of mixtures containing wheat straw leads to a significant increase in ash content, reaching values over 7.14% for regimes that provide the highest calorific value of the pellets.

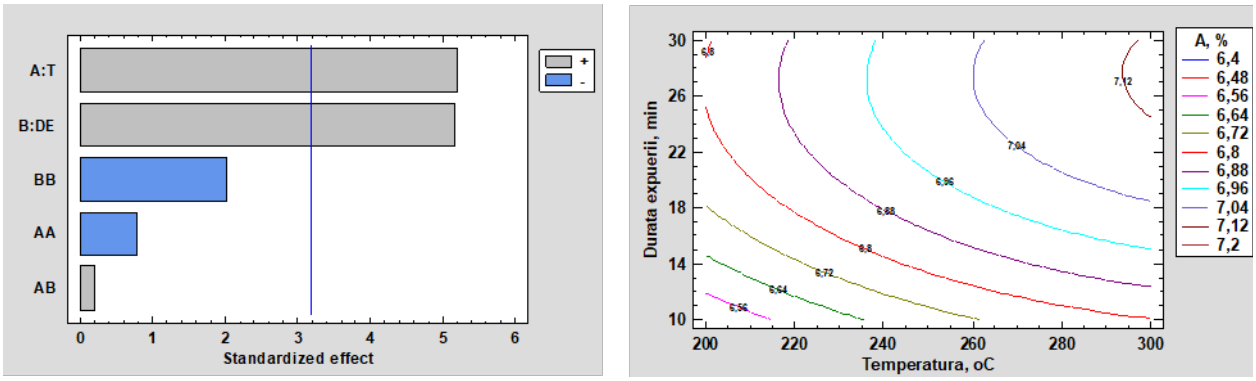

Figure 5. Pareto diagram and response surface contours for the ash content (A), reported at 10% humidity of pellets obtained from SBPR + WS, depending on the temperature and exposure duration (DE).

It is worth mentioning that the SM EN ISO 17225-6:2021 standard assigns this type of pellet to class B, which allows an ash content of up to 10%. To classify the pellets in category A, it is necessary to increase the proportion of SBPR or use other types of residues, while simultaneously reducing the percentage of WS.

5. Conclusions

Based on the findings, it can be concluded that:

1. The optimal torrefaction temperature for pellets made from SBPR + BPR is between 250 and 280 °C, where the calorific value is maximized and the increase in ash content is moderate.

2. The effective exposure duration for SBPR + BPR is between 15-25 min, as the increase in calorific value becomes insignificant after this point, while mass losses may become too large.

3. To prevent uncontrolled mass losses and a reduction in energy efficiency, temperatures above 300 °C and excessive durations (>30 min) should be avoided.

4. The obtained information can be used by solid biofuel producers to maximize the quality of pellets made from fruit shrub residues.

Acknowledgment: The authors gratefully acknowledge the financial support provided by the Government of the Republic of Moldova and the National Agency for Research and Development under project no. 23.70105.7007.08, contract no. 7/08R. This work was also supported by the technical and logistical assistance of project no. 20.80009.5107.15, "Development and implementation of good practices for sustainable agriculture and climate resilience / GREEN/020407."

Conflicts of interest: The authors declare no conflict of interest.

References

1. Enes, T.; Lousada, J.; Fonseca, T.; Viana, H.; Calvão, A.; Aranha, J. Large scale shrub biomass estimates for multiple purposes. *Life* 2020, 10 (4), pp. 1–12. https://doi.org/10.3390/life10040033.
2. National Statistical Office of the Republic of Moldova. Available online: https://statbank.statistica.md/PxWeb/pxweb/ro/40%20Statistica%20economica/40%20Statistica%20economica__16%20AGR__AGR020/AGR020070.px/table/tableViewLayout2/ (accessed on 16.02.25).
3. Marian, G.; Banari, A.; Gudima, A.; Nazar, B.; Pavlenco, A. Improving the quality of pellets produced from white buckchin biomass through the formation of blends. *The Agri-Food Sector – Achievements and Perspectives*

2022, pp. 119-121. Available online: https://ibn.idsi.md/sites/default/files/imag_file/119-121_35.pdf [in Romanian].
4. Marian, G.; Banari, A.; Gudîma, A.; Daraduda, N.; Pavlenco, A. Characterization of residues from the sea buckthorn production chain. *Ştiinţa agricolă* 2020, 2, pp. 91–96. https://doi.org/10.5281/zenodo.4321228. [in Romanian].
5. Marian, G.; Banari, A.; Nazar, B.; Gudima, A.; Daraduda, N.; Pavlenco, A. Prospects for the use of Seabuckthorn residues in the production of densified solid biofuels. *Scientific Papers. Series E. Land Reclamation, Earth Observation & Surveying, Environmental Engineering* 2021, 10, pp. 60–63.
6. Banari, A.; Marian, G.; Nazar, B.; Gudima, A. Study of the densification process of pellets produced from white buckchin biomass. *The Agri-Food Sector – Achievements and Perspectives* 2022, pp. 156-157 [in Romanian].
7. Sarker, T.R.; Nanda, S.; Meda, V.; Dalai, A. K. Densification of waste biomass for manufacturing solid biofuel pellets: a review. *Environmental Chemistry Letters* 2023, 21, pp. 231-264. https://doi.org/10.1007/s10311-022-01510-0.
8. Sarker, T.R.; Nanda, S.; Dalai, A.K.; Meda, V. A Review of Torrefaction Technology for Upgrading Lignocellulosic Biomass to Solid Biofuels. *Bioenergy Research* 2021, 14 (2), pp. 645–669. https://doi.org/10.1007/s12155-020-10236-2.
9. Ranzi R.; Ferro T. D.; Torres, A.; Beaton, P.; Björnbom, E. Biomass Torrefaction. In: *2nd World Conference on Biomass for Energy, Industry and Climate Protection*, 2004, pp 859-862.
10. Sarker, T. R.; German, C. S.; Borugadda, V. B.; Meda, V.; Dalai, A. K. Techno-economic analysis of torrefied fuel pellet production from agricultural residue via integrated torrefaction and pelletization process. *Heliyon* 2023, 9, e16359. https://doi.org/10.1016/j.heliyon.2023.e16359.
11. Tumuluru, J.S.; Ghiasi, B.; Soelberg, N.R.; Sokhansanj, S. Biomass Torrefaction Process, Product Properties, Reactor Types, and Moving Bed Reactor Design Concepts. *Frontiers in Energy Research* 2021, 9, pp 1–20. https://doi.org/10.3389/fenrg.2021.728140.
12. Dumitru E.; Bădan, D.; Turek-Rahoveanu, P.; Berevoianu R.; Găceanu I. *Identification of biomass energy conversion techniques*. Terra Nostra, Iași, Romania, 2020, 40 p. [in Romanian].
13. Onsree, T.; Tippayawong, N.; Williams, T.; McCullough, K.; Barrow, E.; Pogaku, R.; Lauterbach, J. Torrefaction of pelletized corn residues with wet flue gas. *Bioresource Technology* 2019, 285, 121330. https://doi.org/10.1016/j.biortech.2019.121330.
14. Lasek, J.A.; Kopczyński, M.; Janusz, M.; Iluk, A.; Zuwała, J. Combustion properties of torrefied biomass obtained from flue gas-enhanced reactor. *Energy* 2017, 119, pp. 362–368. https://doi.org/10.1016/j.energy.2016.12.079.
15. Sarvaramini, A.; Gravel, O.; Larachi, F. Torrefaction of ionic-liquid impregnated lignocellulosic biomass and its comparison to dry torrefaction. *Fuel* 2013, 103, pp. 814–826. https://doi.org/10.1016/j.fuel.2012.09.037.
16. Olugbade, T.O.; Ojo, O.T. Biomass Torrefaction for the Production of High-Grade Solid Biofuels: a Review. *Bioenergy Research* 2020, 13, pp. 999–1015. https://doi.org/10.1007/s12155-020-10138-3.
17. Mochizuki, Y.; Ma, J.; Kubota, Y.; Uebo, K.; Tsubouchi, N. Production of high-strength and low-gasification reactivity coke from low-grade carbonaceous materials by vapor deposition of tar. *Fuel Processing Technology* 2020, 203, 106384. https://doi.org/10.1016/j.fuproc.2020.106384.
18. Cremers, M.; Koppejan, J.; Middelkamp, J.; Witkamp, J.; Sokhansanj, S.; Melin, S.; Madrali, S. Status overview of torrefaction technologies A review of the commercialisation status of biomass torrefaction. Available online: https://www.ieabioenergy.com/wp-content/uploads/2015/11/IEA_Bioenergy_T32_Torrefaction_update_2015b.pdf (accessed on 29.01.25).
19. Devaraja, U.M.A.; Dissanayake, C.L.W.; Gunarathne, D.S.; Chen, W.H. Oxidative torrefaction and torrefaction-based biorefining of biomass: a critical review. *Biofuel Research Journal* 2022, 35, pp. 1672–1696. https://doi.org/10.18331/BRJ2022.9.3.4.
20. Pimchuai, A.; Dutta, A.; Basu, P. Torrefaction of agriculture residue to enhance combustible properties. *Energy and Fuels* 2010, 24 (9), pp. 4638–4645. https://doi.org/10.1021/ef901168f.
21. Kumar, E. Y. Torrefaction of Agricultural Residues. *International Journal of Multidisciplinary Approach and Studies* 2014, 01 (5), 138–147.
22. Chen, Y.; Yang, H.; Yang, Q.; Hao, H.; Zhu, B.; Chen, H. Torrefaction of agriculture straws and its application on biomass pyrolysis poly-generation. *Bioresource Technology* 2014, 156, pp. 70–77. https://doi.org/10.1016/j.biortech.2013.12.088.

23. Nakason, K.; Pathomrotsakun, J.; Kraithong, W. Torrefaction of Agricultural Wastes: Influence of Lignocellulosic Types and Treatment Temperature on Fuel Properties of Biochar. *International Energy Journal* 2019, 19, pp. 253–266.
24. Jagodzińska, K.; Czerep, M.; Kudlek, E.; Wnukowski, M.; Yang, W. Torrefaction of wheat-barley straw: Composition and toxicity of torrefaction condensates. *Biomass and Bioenergy* 2019, 129, 105335. https://doi.org/10.1016/j.biombioe.2019.105335.
25. Jagodzińska, K.; Czerep, M.; Kudlek, E.; Wnukowski, M.; Pronobis, M.; Yang, W. Torrefaction of agricultural residues: Effect of temperature and residence time on the process products properties. *Journal of Energy Resources Technology, Transactions of the ASME* 2020, 142 (7), 070912.
26. Akhtar, J.; Imran, M.; Ali, A. M.; Nawaz, Z.; Muhammad, A.; Butt, R. K.; Jillani, M. S.; Naeem, H. A. Torrefaction and thermochemical properties of agriculture residues. *Energies* 2021, 14 (14), 1–13. https://doi.org/10.3390/en14144218.
27. Chen, W.H.; Lin, B.J.; Lin, Y.Y.; Chu, Y.S.; Ubando, A.T.; Show, P.L.; Ong, H.C.; Chang, J.S.; Ho, S.H.; Culaba, A.B.; Pétrissans, A.; Pétrissans, M. Progress in biomass torrefaction: Principles, applications and challenges. *Progress in Energy and Combustion Science* 2021, 82, 100887.
28. Park, S.; Kim, S. J.; Oh, K. C.; Kim, S. Y.; Kim, H. E.; Kim, D. H. Utilising Torrefaction to Determine the Fuel Characteristics of Forestry and Agricultural Biomass for Solid Biofuel. *Journal of Biosystems Engineering* 2024, 49, pp. 167–185. https://doi.org/10.1007/s42853-024-00225-0.
29. Onsree, T.; Tippayawong, N. Analysis of reaction kinetics for torrefaction of pelletized agricultural biomass with dry flue gas. *Energy Reports* 2020, 6, pp. 61–65. https://doi.org/10.1016/j.egyr.2020.10.038.
30. Martínez, M.G.; Hélias, E.; Ratel, G.; Thiéry, S.; Melkior, T. Torrefaction of woody and agricultural biomass: Influence of the presence of water vapor in the gaseous atmosphere. *Processes* 2021, 9(1), 30.
31. Marian, G.; Pavlenco, A.; Gudîma, A.; Gorobeț, V. Torrefaction – a new direction for enhancing the quality of fire pellets produced from local biomass. *Știința Agricolă* 2017, (1), pp 74–81 [in Romanian].
32. Tumuluru, J.S.; Wright, C.T.; Hess, J.R.; Kenney, K.L. A review of biomass densification systems to develop uniform feedstock commodities for bioenergy application. *Biofuels, Bioproducts and Biorefining* 2011, 5(6), pp. 683–707. https://doi.org/10.1002/bbb.324.
33. Saletnik, B.A.; Fiedur, M.; Saletnik, A.; Bajcar, M.; Zaguła, G.; Puchalski, C.; Lipa, T.; Dobrzański, B.Jr. Pyrolysis as a method of refining plant biomass residues from poppy (*Papaver somniferum* L.) and buckwheat (*Fagopyrum esculentum*) crops. *Int. Agrophys.* 2025, 39(2), pp. 113-124. https://doi.org/10.31545/intagr/197319.

Citation: Marian, G.; Banari, A.; Marian, T. The effect of torrefaction on pellets made from vegetal biomass generated by fruit shrubs. *Journal of Engineering Science*. 2025, XXXII (2), pp. 99-107. https://doi.org/10.52326/jes.utm.2025.32(2).09.

Submission of manuscripts: jes@meridian.utm.md

Journal of Engineering Science *Vol. XXXII, no. 2 (2025), pp. 108 - 121*
Fascicle *Architecture, Civil and Environmental Engineering* *ISSN 2587-3474*
Topic *Environmental Engineering* *eISSN 2587-3482*

https://doi.org/10.52326/jes.utm.2025.32(2).10
UDC 528.8:004:574.4:63:629.735

ADVANCED DRONE-BASED MONITORING OF AGRICULTURAL, FORESTRY, AND AQUATIC ECOSYSTEMS: TECHNICAL FRAMEWORK

Maria Gutu*, ORCID: 0000-0002-2820-393X,
Lilia Rotaru, ORCID: 0000-0002-6578-418X,
Victoria Alexei, ORCID: 0000-0003-4560-3131,
Maxim Kapusteanski, ORCID: 0009-0004-5009-6503

Technical University of Moldova, 168 Stefan cel Mare Blvd., Chisinau, Republic of Moldova
* Corresponding author: Maria Gutu, *maria.gutu@iis.utm.md*

Received: 04. 06. 2025
Accepted: 05. 14. 2025

Abstract. The rapid advancement of drone technology has significantly transformed environmental monitoring, enhancing capabilities for observing and managing agricultural, forestry, and aquatic ecosystems. This paper presents a comprehensive technical framework for implementing advanced drone-based systems into ecosystem monitoring, focusing on integrating high-resolution sensors, data processing, and artificial intelligence-based analytics. The framework incorporates modern technologies, including drones from Da-Jiang Innovations or First-Person View drones equipped with metric cameras for aerial photogrammetry. These can be further enhanced with multispectral and Light Detection and Ranging sensors to acquire real-time data, enabling more effective analysis. Furthermore, the Proxmox Virtual Environment is the core of the system's architecture, increasing effective virtualisation and deployment. Core data processing technologies include Python scripts, Quantum Geographic Information System, and Pix4D software for photogrammetric reconstruction, as well as Elasticsearch for database management, acquisition, and storage. The Kibana platform ensures interactive data visualisation and supports evidence-based decision-making. The service-oriented structure and system modularity enable the rapid integration of new analytical tools that are adaptable to diverse ecological contexts. Validation in operational environments confirms the framework's ability to address challenges in ecosystem management, particularly in remote areas. This integrated approach contributes to more sustainable and adaptive ecosystem monitoring and management practices.

Keywords: *drone-based monitoring, ecosystem management, real-time data processing, ai-driven analytics, precision agriculture.*

Rezumat. Evoluția accelerată a tehnologiei dronelor a transformat semnificativ procesul de monitorizare a mediului, extinzând capacitățile de observare și gestionare a ecosistemelor agricole, forestiere și acvatice. Lucrarea prezintă un cadru tehnico-științific complex pentru implementarea sistemelor avansate de monitorizare ecologică bazate pe drone, cu accent pe

integrarea senzorilor multispectrali și a tehnologiei de detectare și măsurare a distanței prin lumină, precum și a analiticii avansate asistate de inteligență artificială. Arhitectura este fundamentată pe mediul virtual Proxmox, care permite virtualizarea scalabilă și implementarea modulară a componentelor. Fluxurile de achiziție și procesare a datelor utilizează scripturi automatizate în Python, sistemul geografic de informații Quantum pentru analiză geospațială, Pix4D pentru reconstrucție fotogrammetrică și Elasticsearch pentru stocare și indexare performantă. Platforma Kibana asigură vizualizarea interactivă a datelor și sprijină procesul decizional bazat pe dovezi. Structura orientată pe servicii și modularitatea sistemului permit integrarea rapidă a noilor instrumente analitice, adaptabile diverselor contexte ecologice. Validarea experimentală în medii operaționale confirmă eficiența metodologiei propuse în depășirea constrângerilor geografice, promovând astfel o guvernanță ecologică sustenabilă și adaptativă, bazată pe tehnologii de teledetecție de generație nouă.

Cuvinte-cheie: *monitorizare bazată pe drone, managementul ecosistemelor, procesarea datelor în timp real, analize bazate pe inteligență artificială, agricultură de precizie*.

1. Introduction

The swift advancements in drone technology have dramatically reshaped the field of environmental monitoring, offering innovative solutions for efficiently managing agricultural, forestry, and aquatic ecosystems. Unmanned Aerial Vehicle (UAV) imagery has become a crucial data source for Geographic Information Systems (GIS), providing high-resolution visual data that is essential for spatial analysis and informed environmental decision-making [1]. Equipped with advanced sensors and real-time data processing capabilities, drone systems have become essential instruments for better resource management and improved ecosystem care practices. The increasing preference for UAVs can be attributed to their affordability, ease of use, and ability to minimise fieldwork. Their efficiency in rapidly collecting photogrammetric data, combined with the high accuracy and detail of the resulting analyses, has made them a preferred option in environmental studies [2].

The foundation of the digital photogrammetry technique lies in image processing and analysis, enabling the generation of precise data [3,4]. Integrating low-cost UAVs with digital cameras provides a viable and cost-effective alternative for documenting surface structures and generating 3D models from collected data [4,5]. High-resolution drone imagery enables the creation of detailed terrain maps, which are valuable in urban planning, land-use management, and environmental monitoring. These maps, derived from UAV data, deliver accurate and comprehensive representations of various landscapes, enabling informed decision-making [6].

GIS-integrated drone technology is a notable application in disaster management and emergency response. UAVs equipped with thermal cameras can detect and monitor wildfires or other natural disasters, providing real-time data that is crucial for timely intervention. Additionally, drones can assess post-disaster damage and pinpoint areas that require immediate attention. The integration of GIS enables the analysis of this data, the production of maps that illustrate the extent of damage, and the pinpointing of critical areas for emergency response efforts [1,6].

UAV-supported remote sensing techniques have been effectively employed across several environmental domains. Notable examples include forest monitoring [7–10], agricultural assessments [11–13], and studies of aquatic ecosystems [14–16]. UAV

technology presents a time- and cost-efficient framework, enhancing data resolution and offering new perspectives on observed objects and phenomena. This approach is especially advantageous for monitoring settings such as remote or complex underwater habitats, where conventional techniques may be insufficient.

This paper outlines a comprehensive technical architecture for a drone-based monitoring system, highlighting the incorporation of advanced sensors and artificial intelligence (AI) algorithms for effective data analysis. The proposed system utilises drones manufactured by Da-Jiang Innovations (DJI) and First-Person View (FPV) drones equipped with multispectral cameras to collect and process data in real-time, ensuring an accurate and detailed visualisation of the monitored ecosystems. The primary objective of this framework is to enhance environmental monitoring techniques and provide effective approaches for sustainable resource management.

The primary objective of this project is to develop an adaptable system for overseeing and controlling agricultural lands, forests, and water environments using drones and advanced data processing technologies. This study focuses on establishing UAV-based data acquisition protocols alongside GIS-based image processing guidelines to enhance the monitoring and management of these ecosystems. Specifically, the research addresses critical applications across three environmental domains: the agricultural, forestry, and aquatic systems.

For the agricultural system, the guidelines are customised to assist with various monitoring tasks, such as spraying field crops [17] and overseeing irrigation practices, while evaluating crop conditions during different growth stages, including winter wheat seeding. Identifying and diagnosing diseased areas is a crucial process for preventing plant disease outbreaks and safeguarding both public health and the economy [6,18]. In the forestry system, the project aims to facilitate the monitoring of deforestation, landslides, and other natural disasters that threaten forested areas. Lastly, for the aquatic system, the guidelines are geared towards monitoring the health of lakes and rivers, providing insights into water quality and detecting ecological disturbances.

Through the implementation of this comprehensive monitoring solution, the project pursues the following key goals:

1. Real-time monitoring of crop and forest health and water quality using multispectral sensors and high-resolution cameras. This feature facilitates interventions and well-informed resource management decisions.
2. Data processing and analysis using AI to detect and mitigate ecological issues, such as soil degradation, illegal deforestation, and water pollution. AI-driven analysis enhances the precision and speed of data interpretation, providing actionable insights to effectively prevent and manage environmental challenges.
3. Integration and management of real-time data through a scalable and efficient platform. The proposed system utilises Proxmox Virtual Environment for virtualisation alongside open-source software solutions for data storage and visualisation. This approach ensures that the platform is flexible, easily adaptable, and capable of handling large volumes of data while maintaining high performance and reliability.

The project is designed to create a robust framework that leverages UAV technology and GIS-based data processing to optimise the monitoring and management of various ecosystems. By advancing the capabilities of environmental monitoring, this research aims to support sustainable practices and promote the efficient use of natural resources.

2. Materials and Methods

2.1. Platform Architecture

The technical architecture of the proposed monitoring and management system (Figure 1) is founded on a Service-Oriented Architecture, which ensures the modularity and scalability necessary for integrating emerging technologies. The system utilises Docker containers to deploy and manage individual services, including data storage and processing, within the Proxmox Virtual Environment. This virtualisation infrastructure facilitates efficient resource allocation and the streamlined execution of services.

The platform is designed to exhibit a high degree of flexibility, facilitating the seamless integration of new functionalities as the needs of its users evolve. This flexibility is demonstrated through the ease with which additional features, such as advanced image analysis algorithms or the incorporation of external data sources, can be added to enhance the system's capabilities. The architecture's modular design ensures that these integrations do not disrupt existing functionalities but complement and expand the system's operational scope.

This adaptability is particularly beneficial in addressing the diverse requirements of various end-users, including researchers, decision-makers, and agricultural managers. Each of these groups has distinct needs for data analysis, monitoring, and reporting, and the platform's design allows it to provide tailored solutions accordingly. The platform can facilitate detailed and customizable analyses for researchers, supporting scientific investigations and data-driven discoveries. Conversely, decision-makers may benefit from real-time data processing and visualisation capabilities, enabling informed and timely decisions that are critical in dynamic environments. Agricultural managers can leverage the platform to precisely monitor plantations and aquatic surfaces, utilising the insights generated to optimise resource management and improve productivity.

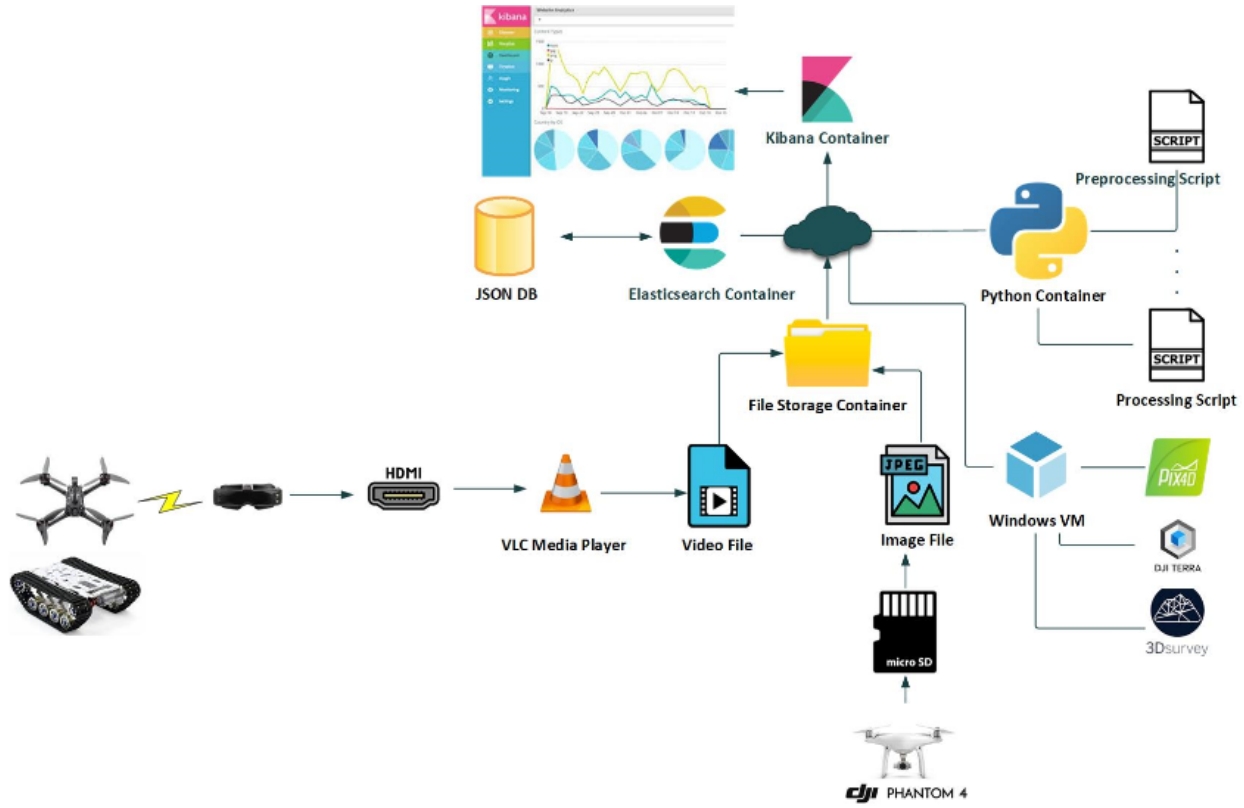

Figure 1. Architecture of the monitoring and management platform for plantations and aquatic surfaces.

The platform is versatile and robust because it supports a wide range of use cases. It is capable of meeting both current monitoring needs and anticipating future requirements, ensuring long-term utility and relevance across various fields of application. The system's inherent flexibility promotes innovation and the integration of cutting-edge technologies, ensuring that the platform remains responsive to the continuously evolving landscape of user demands and technological advancements [19].

The system is designed using the open-source Proxmox Virtual Environment, which optimises the management and utilisation of hardware resources. Proxmox is a powerful and flexible virtualisation platform that facilitates the deployment, operation, and oversight of both virtual machines and containers. This capability ensures a highly robust, efficient, and scalable infrastructure that meets the demands of modern virtualised environments.

The system's hardware configuration is based on multiple Lenovo ThinkCentre mini PCs, specifically models M700, M73, and M710Q. These devices have been upgraded with more powerful Intel i3 and i5 processors to boost performance. Additionally, the storage capacity has been significantly enhanced by integrating solid-state drives and hard disk drives, providing a balance between speed and storage capacity.

These mini PCs are integrated into a cluster environment, which allows them to function as a cohesive unit managed through a single, centralised web interface. This configuration simulates the operational framework of a traditional data centre. The system ensures streamlined management, optimised resource allocation, and enhanced reliability by leveraging the cluster capabilities. This infrastructure provides a comprehensive and scalable solution, ideally suited for efficient and centralised hardware resource management scenarios.

Within this architectural framework, services are strategically developed and deployed using either containers or virtual machines, selected based on criteria such as resource efficiency and software compatibility requirements. Containers, known for their lightweight design and reduced overhead, are generally the preferred method for deploying services when optimal resource utilisation is essential. Their efficiency arises from sharing the host operating system's kernel, which reduces the duplication of system resources and accelerates the deployment and scalability of applications.

Nonetheless, virtual machines are employed when specific platform services require an operating system different from Linux, which containers predominantly support. Virtual machines offer the flexibility to run a completely isolated operating system, complete with its kernel, thereby accommodating software environments and dependencies that are not natively compatible with the Linux-based container ecosystem. This dual deployment strategy ensures that the platform remains versatile and capable of supporting a broad spectrum of software environments, from container-optimised applications to services that demand a more traditional virtualised infrastructure.

Moreover, the architecture facilitates the seamless integration of additional hardware components or external workstations. This adaptability is enabled through robust connectivity options, supporting communication and data exchange over local networks or the Internet. Such integration capabilities enhance the system's extensibility, allowing both internal and external resources, including specialised software applications and web-based services, to be efficiently incorporated into the platform. By enabling smooth communication between disparate hardware and software components, the architecture ensures that the

system can expand and evolve to meet diverse operational demands, fostering an adaptable and future-proof environment.

Considering the diverse requirements and the dynamic conditions during system design and development, a microservice-based architectural approach was selected as the foundational framework. This architectural paradigm, rooted in Service-Oriented Architecture (SOA) principles, effectively organises software components into a collection of independent and self-contained services. Each microservice performs a specific function and operates autonomously. Therefore, all services within the system communicate seamlessly using standardised protocols, such as HTTP, SOAP (Simple Object Access Protocol), or REST (Representational State Transfer).

A Service-Oriented Architecture framework ensures that each microservice has well-defined interfaces, such as HTTP APIs or messaging systems, that facilitate smooth communication and data exchange between services. This decoupling of services is a crucial feature, as it significantly reduces the direct dependencies that often complicate software systems. Consequently, this modular design enables the modification, enhancement, or updating of individual services without compromising the overall system's functionality or performance.

Moreover, this microservice-based approach provides substantial flexibility in addressing varying performance and usage demands. Since each service operates independently, scaling can be performed per service, ensuring efficient resource utilisation. For instance, services experiencing high loads can be scaled to accommodate increased demand, while other services that require fewer resources can remain unaffected. This scalability ensures the system remains robust and responsive, even under fluctuating workloads or expanding functionalities.

Adopting a microservice architecture also enhances the system's ability to adapt to evolving requirements. As new features or services become necessary, they can be integrated seamlessly into the existing architecture without necessitating a comprehensive redesign. This capacity to incorporate changes efficiently is particularly advantageous in environments subject to rapid technological advancements or shifting user needs, ensuring that the system remains relevant and future-proof. Overall, the microservice-based design promotes maintainability, scalability, and continuous system improvement, making it a highly effective and sustainable architectural choice.

2.2. Technologies Used

The proposed monitoring platform is designed to integrate a diverse array of technologies, providing comprehensive support for data collection, processing, and visualisation. The foundational infrastructure is built upon the Proxmox Virtual Environment, an open-source platform that delivers a robust and efficient solution for container virtualisation and the optimal management of hardware resources. Proxmox’s virtualisation capabilities are instrumental in efficiently handling multiple workloads, enabling the seamless deployment and management of virtual machines and containers on a unified platform.

By leveraging the Proxmox Virtual Environment, the monitoring platform effectively optimises the performance of servers and Lenovo ThinkCentre mini-PCs, which serve as key hardware components. The integration of these hardware resources is streamlined, with Proxmox ensuring efficient resource allocation and load balancing, thereby enhancing the overall system's performance and reliability. This optimization extends to data storage and

analysis processes, where Proxmox's advanced features facilitate the efficient management and processing of large datasets, reducing latency and improving throughput.

Furthermore, the architecture's inherent scalability is a significant advantage. As the platform's data processing and analysis requirements grow, the Proxmox Virtual Environment allows for the seamless addition of new resources, such as servers or containers, without compromising system stability or performance. This scalability is crucial for adapting to growing data volumes and evolving monitoring requirements, offering a future-proof solution that accommodates advancements in data analysis technologies.

The performance and scalability benefits of this architecture are illustrated in Figure 2, which depicts how Proxmox's efficient virtualisation framework enhances the platform's capacity to handle complex and data-intensive operations. By integrating these technologies, the platform meets current operational demands and remains adaptable to future developments, ensuring long-term sustainability and effectiveness in diverse monitoring applications.

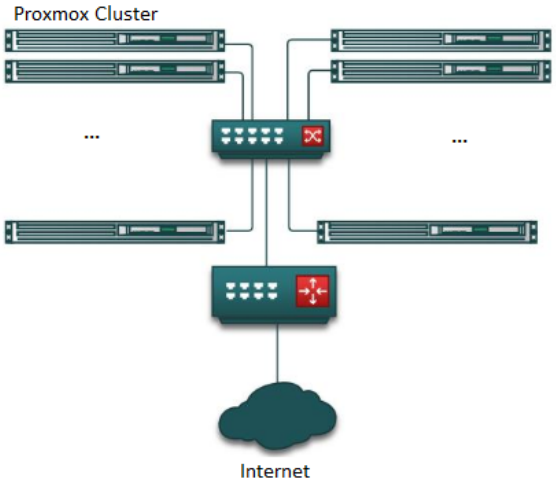

Figure 2. Universal development and deployment infrastructure.

For data collection, the proposed monitoring platform utilises advanced unmanned aerial vehicles, specifically DJI and FPV drones [20, 21], equipped with high-precision metric cameras and state-of-the-art multispectral sensors. These sophisticated sensing devices can capture high-resolution images and generate extensive datasets, providing detailed and accurate visual representations of the monitored ecosystems. Integrating metric cameras ensures that spatial data is collected with high accuracy. At the same time, multispectral sensors enable the acquisition of spectral information essential for analysing vegetation health, water quality, and other ecological indicators.

The drones are engineered to transmit collected data in real-time, thereby facilitating immediate analysis and rapid response in dynamic monitoring situations. For scenarios where instantaneous data analysis is not required, the drones are also equipped to store captured information on SD cards, enabling subsequent data processing at a more convenient time. This dual capability ensures the system is flexible and can be adapted to various monitoring scenarios, from emergency response and rapid environmental assessment to more comprehensive and in-depth post-mission analyses.

Once the images and datasets have been acquired, they are subjected to rigorous analysis using Geographic Information System (GIS) software, such as QGIS and Pix4D. These advanced geospatial tools are crucial for interpreting the collected data, as they support the

creation of accurate and detailed maps and models of the monitored ecosystems. QGIS, an open-source GIS application, facilitates the analysis and visualisation of spatial data through various geoprocessing tools [6], while Pix4D specialises in photogrammetry and 3D mapping, enabling precise modelling and measurement of environmental features.

Integrating drone-based data acquisition with GIS technologies significantly enhances the overall efficiency and precision of the monitoring process. The platform can generate high-quality geospatial information that informs and improves decision-making processes by leveraging these advanced analytical tools. This integration is valuable for real-time environmental management, allowing stakeholders to respond quickly and effectively to changing conditions. Moreover, combining high-resolution data collection and sophisticated GIS analysis contributes to a more holistic understanding of ecosystem dynamics, supporting immediate interventions and long-term environmental monitoring and management strategies.

2.3. Platform Functionality

The data processing framework embedded within the proposed monitoring platform is designed to be highly robust and capable of managing and analysing the complex, high-volume information collected from diverse ecosystems, such as forests, agricultural landscapes, and aquatic environments. This framework employs state-of-the-art software solutions and sophisticated algorithms to ensure that data is efficiently processed, securely stored, and effectively visualised, all aimed at facilitating proactive and informed ecosystem management.

At the core of the data processing pipeline are Python scripts, which are strategically deployed within dedicated containers to optimise performance and scalability. These scripts harness advanced artificial intelligence and machine learning algorithms to analyse the high-resolution images and comprehensive datasets that drones capture. The primary objective of these algorithms is to automate the detection and classification of various environmental anomalies, including critical issues such as deforestation, soil erosion, forest fires, water pollution, and other forms of ecological disturbance. The framework's capability to conduct real-time analysis ensures that significant environmental threats are rapidly identified, enabling swift intervention and enhancing the responsiveness of monitoring operations.

Regarding data management, the platform employs a sophisticated multi-layered storage and retrieval system that ensures both the security and efficiency of data handling. Raw data, which includes live video streams and high-resolution image files collected by drones, is initially stored in a secure File Storage Container. This setup provides a scalable and organised repository for large volumes of unprocessed data, facilitating efficient data access and retrieval for subsequent analysis. After data processing, the refined and analysed datasets are transferred into a JSON-based database managed by Elasticsearch.

Elasticsearch is a high-performance, scalable database system that supports rapid data querying and is essential for conducting in-depth data analysis. Implementing Elasticsearch streamlines data retrieval and enhances the system's ability to recognise complex patterns and environmental trends. This capability is especially crucial for effective ecosystem monitoring and management. Furthermore, Elasticsearch's integration with the platform enables the deployment of advanced, machine learning-driven mechanisms that monitor infrastructure for potential anomalies [22]. These mechanisms can automatically generate alerts, notifying managers or administrators when environmental or infrastructural issues are

detected, ensuring that timely and informed decisions are made. This integration supports efficient and accurate environmental monitoring, empowering stakeholders to make data-driven decisions and implement rapid response measures to mitigate ecological threats.

The data processing workflow within the proposed monitoring platform is structured into two primary stages: image pre-processing and advanced analysis. During the image pre-processing phase, raw data captured by drones and sensors is converted into formats optimised for integration and compatibility, such as GeoJSON. This conversion step ensures that the data are standardised and seamlessly interact with the broader monitoring system. By establishing a uniform and optimised data structure, this phase lays a critical foundation for the detailed and complex analysis that follows.

In the subsequent stage, advanced machine learning algorithms are employed to conduct in-depth analyses and generate comprehensive maps of the monitored ecosystems. These algorithms process pre-formatted data to produce high-resolution, geospatially accurate maps that visually delineate areas at risk of ecological degradation. These detailed maps serve as an essential resource for researchers and policymakers, visually representing environmental vulnerabilities and enabling targeted intervention strategies for ecological preservation and sustainable management.

PostgreSQL is integrated as the primary relational database management system to further augment the platform's analytical capabilities. PostgreSQL's robust architecture allows it to efficiently handle complex queries and manage extensive datasets, organising the data to facilitate seamless access, refinement, and analysis. This integration is particularly valuable for supporting high-precision data analysis tasks, as it provides a stable and efficient foundation for managing the large volumes of information generated by the monitoring activities.

Data visualisation constitutes a vital component of the overall data processing framework and is accomplished using Kibana, an open-source analytics and visualisation tool. Kibana enables the creation of dynamic and interactive dashboards that allow stakeholders to explore and interpret data patterns through intuitive graphical representations. These dashboards highlight critical findings and trends, making it easier for environmental managers, researchers, and decision-makers to gain actionable insights and engage in data-driven decision-making. By offering a user-friendly interface, Kibana enables stakeholders to make informed decisions regarding resource allocation, environmental protection, and ecosystem management.

Additionally, the platform extends its data processing and analysis capabilities through a dedicated Windows Virtual Machine. This virtual environment hosts specialised software tools, such as DJI Terra and 3DSurvey, for photogrammetric analysis and generating three-dimensional models from drone imagery. Integrating these tools is crucial for conducting detailed structural assessments of ecosystems and creating advanced topographical maps. The addition of this 3D modelling capability significantly enhances the platform's analytical potential, allowing for a more nuanced understanding of ecosystem structures and landscape changes, which is indispensable for advanced environmental studies and management efforts [4].

Overall, the data processing system is characterised by a modular design, further strengthened by a containerised architecture. This approach ensures that the platform is both scalable and adaptable, enabling it to evolve in response to the changing needs of research and monitoring initiatives. By combining state-of-the-art artificial intelligence algorithms,

efficient data storage solutions, and intuitive visualisation tools, a comprehensive and highly effective framework for modern environmental monitoring is provided. This integration of advanced technology ensures that the platform can deliver accurate, timely, and actionable insights, making it a powerful tool for addressing complex environmental challenges and promoting sustainable resource management.

3. Results

Comprehensive empirical results are currently unavailable, as the research remains in the development and local testing phase. Nevertheless, preliminary observations have highlighted the proposed platform's significant potential for enhancing environmental monitoring and management practices. Integrating advanced technologies, including drone-based data collection and artificial intelligence-driven data processing, presents a promising framework that could substantially improve real-time ecosystem analysis and facilitate more effective environmental interventions.

Initial testing efforts have primarily focused on evaluating the functionality and interoperability of the platform's integrated hardware and software components. The system's modular architecture, which leverages Docker containers for efficient resource management within the Proxmox Virtual Environment, has demonstrated noteworthy flexibility and adaptability. These preliminary tests have validated the seamless operation of individual components, such as Python-based data processing scripts and the Elasticsearch database utilised for high-performance data storage and retrieval. Specifically, the Python scripts are responsible for executing machine learning algorithms designed to analyse and interpret drone-captured imagery, while Elasticsearch ensures that processed data is organised and accessible for subsequent analysis and decision-making.

Further assessments have examined the platform's capacity to manage diverse data formats and support rapid data retrieval, which is critical for applicability in real-world environmental monitoring scenarios. The system's ability to process and store data efficiently is crucial for generating timely insights, especially in dynamic ecological contexts where prompt responses are necessary. Additionally, the performance of data visualisation tools, such as Kibana, has been preliminarily evaluated. Early results suggest that Kibana's intuitive and interactive dashboards effectively translate processed data into graphical insights, making complex environmental information more accessible to researchers and decision-makers. The platform's visualisation capabilities have shown promise in identifying and highlighting potential ecological risks, which could be instrumental in guiding informed management strategies.

Moreover, the deployment of machine learning algorithms for anomaly detection is undergoing rigorous validation. These algorithms are designed to identify environmental disturbances, such as deforestation, soil erosion, or water contamination, and their accuracy and efficiency are being closely monitored. Early testing indicates that these algorithms have the potential to automate the detection process effectively, enabling proactive responses to environmental threats. However, further validation is necessary to ensure these machine-learning models perform reliably across various ecological conditions.

As the project advances, comprehensive validation in various environmental settings will be crucial to fully assess the platform's scalability and overall effectiveness. The research aims to produce detailed, high-resolution maps and generate actionable insights to inform sustainable resource management practices. Future testing phases will be crucial to evaluate the platform's impact across various ecosystems, spanning from terrestrial to aquatic

environments. The research will assess the system's capacity to deliver real-world benefits and contribute meaningfully to global environmental conservation and management efforts through extensive field trials. The ongoing development and testing are expected to yield a robust and adaptable monitoring solution that addresses complex environmental challenges.

4. Discussion

The development and initial deployment of the proposed UAV-integrated environmental monitoring platform underscore a paradigm shift in ecosystem observation methodologies, facilitated by the convergence of edge sensing, containerised data processing, and geospatial intelligence. Rather than merely automating existing workflows, the system redefines the spatial and temporal resolution at which ecological phenomena can be captured, interpreted, and acted upon. This advancement is particularly pertinent in the context of increasingly volatile environmental conditions, where real-time, high-fidelity data are essential for evidence-based intervention [9].

A salient observation from the preliminary phase pertains to the system's architectural agility. The microservice-driven deployment model, underpinned by the Proxmox virtualisation layer and Docker containerisation, enables the dynamic orchestration of analytic services. Such decoupling of functionalities enhances system resilience and facilitates rapid, iterative development, a crucial feature in ecological domains characterised by unpredictable and heterogeneous data influxes. Moreover, this design promotes cross-disciplinary extensibility, allowing the platform to incorporate emerging technologies (e.g., edge AI, semantic geospatial reasoning) without necessitating structural overhauls.

The application of machine learning models to drone-derived datasets reflects a broader movement toward predictive environmental analytics [17]. Thus, it also exposes foundational challenges related to model generalizability and data representativeness. While the initial anomaly detection outcomes suggest promise, particularly in identifying biophysical stressors such as vegetation chlorosis or aquatic turbidity gradients, these models remain constrained by the limited scope of training data and the absence of longitudinal environmental baselines. A rigorous validation campaign involving multi-seasonal, multi-ecosystem deployments is required to mitigate overfitting and establish model robustness across ecological gradients.

From a human-systems integration perspective, the visualisation layer, anchored by Kibana dashboards, functions not only as an interpretive interface but also as a cognitive scaffold for decision-makers. The ability to synthesise volumetric spatial-temporal data into actionable insights represents a key advantage of the system [4]. However, the epistemological implications of relying on algorithmically filtered representations must be acknowledged. Future development cycles should prioritise transparency and explainability in the AI modules to foster trust and accountability in high-stakes ecological decision-making.

Another dimension warranting attention is operational sustainability. While the mini-PC cluster approach provides an energy-efficient and cost-effective computing backbone for localised deployments, its efficacy in field conditions subject to environmental stressors (e.g., humidity, temperature extremes, network intermittency) remains to be empirically evaluated. Additionally, the current reliance on Windows-based photogrammetric suites introduces heterogeneity in the software ecosystem, which could complicate long-term maintainability and integration [5, 7]. Migrating critical photogrammetric functionalities to containerised, platform-agnostic services would enhance systemic coherence and reduce operational friction.

Finally, the platform's capacity for synergistic integration with external environmental data sources (e.g., satellite imagery, IoT sensor networks, citizen science inputs) opens compelling avenues for hybrid data fusion and multiscale modelling. These capabilities would enable the system to transcend its current diagnostic function and evolve into a forecasting and simulation tool, supporting anticipatory governance of environmental resources.

Therefore, the proposed architecture lays a foundational framework for next-generation environmental monitoring—one that is modular, scalable, and poised for intelligence augmentation. The implications extend beyond technical efficacy to questions of ecological epistemology, technological sovereignty, and the ethics of automated environmental stewardship. Advancing this system from a functional prototype to a broadly deployable monitoring infrastructure will require not only technological refinements but also a sustained commitment to interdisciplinary co-design, empirical validation, and critical reflection.

5. Conclusions

The proposed monitoring and management system enables the comprehensive assessment of forests, agricultural lands, and aquatic ecosystems. It provides an effective environmental monitoring and exploration structure by integrating advanced technology and software elements. The system features are divided into services stored in containers, each designed for a particular purpose, such as storing data, conducting analysis, or processing information. This architecture ensures the efficient use of resources, thereby improving the overall management of different ecosystems.

Central to the platform's functionality is its capability to handle high volumes of data collected by drones and other monitoring devices. The data flow begins with ingesting raw images and sensor readings, which are then pre-processed and stored in a structured format. Using dedicated containers for tasks such as Python-based data processing and Elasticsearch for data management allows for the rapid and efficient handling of complex datasets. The processed data are subsequently analysed using machine learning algorithms, which detect patterns and anomalies, providing valuable insights for environmental monitoring.

Moreover, integrating visualisation tools like Kibana enables users to interact with the processed data through intuitive and customizable dashboards. These visualisations support data-driven decision-making by highlighting critical areas, such as regions susceptible to ecological disturbances or needing immediate intervention. The platform's modular design ensures that additional functionalities, such as new data analysis techniques or external data integrations, can be easily incorporated without disrupting the existing system.

Therefore, the platform's structured and scalable data management and analysis approach enhances its effectiveness in monitoring complex ecosystems. The platform is a valuable tool for researchers, policymakers, and environmental managers dedicated to sustainable ecosystem management, providing real-time insights and a high degree of adaptability.

Acknowledgements: This research was conducted as part of the project titled "Satellite Systems and a Monitoring Platform for Plantations and Aquatic Areas Using Space Technologies and Drones", under project number 020401, with an implementation period from January 1, 2024, to December 31, 2027.

Conflicts of Interest: The authors declare that they have no conflicts of interest.

References

1. Colpaert, A. Satellite and UAV Platforms, Remote Sensing for Geographic Information Systems. *Sensors* 2022, 22(12), 4564.
2. Kovanic, L.; Topitzer, B.; Petovsky, P.; Blistan, P.; Gergelova, M. B.; Blistanova, M. Review of Photogrammetric and Lidar Applications of UAV. *Appl. Sci.* 2023, 13(11), 6732.
3. Zhang, D.; Zhang, Y.; Cheng, T.; Meng, Y.; Fang, K.; Garg, A.; Garg, A. Measurement of Displacement for Open Pit to Underground Mining Transition Using Digital Photogrammetry. *Measurement* 2017, 109, pp. 187–199.
4. Kovanic, L.; Blistan, P.; Stroner, M.; Urban, R.; Blistanova, M. Suitability of Aerial Photogrammetry for Dump Documentation and Volume Determination in Large Areas. *Appl. Sci.* 2021, 11(14), 6564.
5. Krsak, B.; Blistan, P.; Paulikova, A.; Puskarova, P.; Kovanic, L.; Palkova, J.; Zeliznakova, V. Use of Low-Cost UAV Photogrammetry to Analyse the Accuracy of a Digital Elevation Model in a Case Study. *Measurement* 2016, 91, pp. 276–287.
6. Quamar, M.; Al-Ramadan, B.; Khan, K.; Shafiullah, M.; El Ferik, S. Advancements and Applications of Drone-Integrated Geographic Information System Technology – A Review. *Remote Sens.* 2023, 15(20), 5039.
7. Goodbody, T.; Coops, N.; White, J. Digital Aerial Photogrammetry for Updating Area-Based Forest Inventories: A Review of Opportunities, Challenges, and Future Directions. *Curr. For. Rep.* 2019 5(2), pp. 55–75.
8. Ecke, S.; Dempewolf, J.; Frey, J.; Schwaller, A.; Endres, E.; Klemmt, H.-J.; Tiede, D.; Seifert, T. UAV-Based Forest Health Monitoring: A Systematic Review. *Remote Sens.* 2022, 14(13), 3205.
9. Srivastava, S.; Seng, K.; Ang, L.; Pachas, A; Nahuel, A.; Lewis, T. Drone-Based Environmental Monitoring and Image Processing Approaches for Resource Estimates of Private Native Forest. Sensors 2022, 22(20), 7872.
10. Krause, S. UAV Applications for Intensive Forest Monitoring. Ph.D. Thesis, University of Bonn, Bonn, Germany, 2024.
11. Trappey, A.; Lin, J.; Chen, K.; Chen, M. Global Patent Technology Portfolio Study of Agricultural UAV Innovations. *Adv.Transdiscip. Eng.* 2023, 41, pp. 761-770.
12. Yang, X.; Gao, F.; Yuan, H.; Cao X. Integrated UAV and Satellite Multi-Spectral for Agricultural Drought Monitoring of Winter Wheat in the Seedling Stage. *Sensors* 2024, 24(17), 5715.
13. Kovalev, I.; Kovalev, D.; Astanakulov, K.; Podoplelova, V.; Borovinsky, D.; Shaporova, Z. Productivity Analysis of Agricultural UAVs by Field Crop Spraying. *IOP Conf. Ser. Earth Environ. Sci.* 2023, 1284(1), 012026.
14. Nishi, R.; Kawamori, A.; Tsurunari, Y. UAV Potential for Aquatic and Sub-Aquatic Environmental Monitoring. *J. Jpn. Soc. Civ. Eng. Ser. B3 Ocean Eng.* 2018, 74(2), I_1006-I_1011.
15. Novkovic, M.; Cvijanovic, D.; Mesaros, M.; Pavic, D.; Dreskovic, N.; Milosevic, D.; Andelkovic, A.; Damnjanovic, B.; Radulovic, S. Towards UAV Assisted Monitoring of Aquatic Vegetation within Large Rivers – The Middle Danube (Serbia). *Carpathian J. Earth Environ. Sci.* 2023, 18(2), pp. 307–322.
16. Vivaldini, K.; Pazelli, T.; Rocha, L.; Santos, I.; Caldas, K.; Soler, D.; Benevides, J.; Simplício, P.; Hernandes, A.; Andrade, K.; Kim, P.; Alvarez, I.; Nascimento, E.; Santos, M.; Almeida, A.; Cavalcanti, L.; Inoue, R.; Terra, M.; Becker, M. Multi-UAV Collaborative System for the Identification of Surface Cyanobacterial Blooms and Aquatic Macrophytes, *J. Intell. Robot. Syst.* 2024, 110(1), 40.
17. Bah, M.; Hafiane, A.; Canals, R. Deep Learning with Unsupervised Data Labelling for Weed Detection in Line Crops in UAV Images. *Remote Sens.* 2018, 10(11), 1690.
18. El Sakka, M.; Mothe, J.; Ivanovici, M. Images and CNN Applications in Smart Agriculture. *Eur. J. Remote Sens.* 2024, 57(1), 2352386.
19. Rajak, P.; Ganguly, A.; Adhikary, S.; Bhattacharya, S. Internet of Things and Smart Sensors in Agriculture: Scopes and Challenges. *J. Agric.Food Res.* 2023, 14, 100776.
20. Ahmed, F.; Mohanta, J.; Keshari, A.; Yadav, P. Recent Advances in Unmanned Aerial Vehicles: A Review. *Arab. J. Sci. Eng.* 2022, 47(7), pp. 7963–7984.
21. Mohsan, S.; Othman, N.; Alsharif, M.; Khan, M. Unmanned Aerial Vehicles (UAVs): Practical Aspects, Applications, Open Challenges, Security Issues, and Future Trends. *Intell. Serv. Robot.* 2023, 16, pp. 109-137.
22. Zamfir, V.; Carabas, M.; Carabas, C.; Tapus, N. Systems Monitoring and Big Data Analysis Using the Elasticsearch System. In: *Proceedings of the 2019 22nd International Conference on Control Systems and Computer Science (CSCS)*, Bucharest, Romania, 28-30 May 2019, IEEE, NY, USA, 2019, pp. 188-193.

Citation: Gutu, M.; Rotaru, L.; Alexei, V.; Kapusteanski, M. Advanced drone-based monitoring of agricultural, forestry, and aquatic ecosystems: technical framework. *Journal of Engineering Science*. 2025, XXXII (2), pp. 108-121. https://doi.org/10.52326/jes.utm.2025.32(2).10.

Submission of manuscripts: jes@meridian.utm.md

Journal of Engineering Science *Vol. XXXII, no. 2 (2025), pp. 122 - 132*
Fascicle *Food Engineering* *ISSN 2587-3474*
Topic *Biotechnologies, Food Chemistry and Food Safety* *eISSN 2587-3482*

https://doi.org/10.52326/jes.utm.2025.32(2).11
UDC 631.46:57.083:635.6

MOLECULAR DIAGNOSTICS OF SOIL-BORNE PATHOGENIC FUNGI IN SEVERAL AGRICULTURAL CROPS

Angela Deaghileva *, ORCID 0000-0003-3659-2450

Moldova State University, IGPPP, 20 Padurii Str., Chisinau, Republic of Moldova
* Corresponding author: Angela Deaghileva, *angela.deaghileva@sti.usm.md*

Received: 05. 13. 2025
Accepted: 06. 18. 2025

Abstract. Modern requirements for product quality provide for expanding the competence in sectors of producing and managing agricultural products by investigating the cause-effect relationships in the transmission of diseases between species through host-pathogen interactions. Monitoring and accurate identification of pathogens in agriculture products are essential for successful implementation of an integrated pest management program. Among the pathogens that have a serious impact on agricultural production, micromycetes outnumber all other species. Diagnostics of fungal pathogens using traditional methods can be difficult due to the similarity of their morphological traits, the lack of the ability to study non-culturable genotypes. In this regard, molecular detection methods based on polymerase chain reaction (PCR) were used in the study, which allow specific detection of any microorganisms. Analysis of the species composition of pathogenic fungi of *Fusarium, Penicillium* and *Aspergillus* genera in the genotypes of some vegetable crops of local selection was conducted based PCR-assay. The efficiency of molecular technique for the species-specific detection of pathogenic fungi that can affect agricultural crops was demonstrated. Molecular diagnostic assessment of the phytosanitary status of seeds of different storage periods was done. Development of some fungal infection during plant ontogenesis using *nested*-PCR assay was monitored.

Key-words: *PCR, Fusarium, Aspergillus, Penicillium, bell pepper, eggplant, beans.*

Rezumat. Cerințele contemporane pentru asigurarea unei calități înalte a produselor agricole impun o extindere a competențelor în domeniul producției și gestionării acestora, prin investigarea relațiilor cauză-efect ce determină transmiterea bolilor între specii, în contextul interacțiunii gazdă-patogen. Monitorizarea precisă și identificarea corectă a agenților patogeni din produsele agricole sunt esențiale pentru implementarea cu succes a unui program de management integrat al dăunătorilor. Printre agenții patogeni cu un impact major asupra producției agricole, micromicetele se disting prin prevalența lor comparativ cu alte specii. Diagnosticul agenților patogeni fungici prin metode tradiționale poate fi dificil datorită asemănării morfologice a acestora și a imposibilității studierii genotipurilor necultivabile pe medii nutritive. În acest context, studiul a utilizat metode de detecție moleculară bazate pe reacția de polimerizare în lanț (PCR), tehnică ce permite determinarea specifică a diverselor microorganisme. Pe baza testului PCR, a fost realizată o analiză detaliată a compoziției speciilor de patogeni din genurile *Fusarium*, *Penicillium* și *Aspergillus*

în genotipurile unor culturi agricole de selecție locală. Rezultatele obținute au demonstrat eficiența tehnicii PCR pentru diagnosticul specific a speciilor fungice patogene care pot afecta culturile agricole. De asemenea, s-a realizat o evaluare moleculară a stării fitosanitare a semințelor, pe parcursul diferitelor perioade de depozitare. A fost monitorizată răspândirea infecției fungice în timpul ontogenezei plantelor, utilizând metoda *nested*-PCR.

Cuvinte-cheie: *PCR, Fusarium, Aspergillus, Penicillium, ardei, vinete, fasole.*

1. Introduction

Providing the growing population with foodstuffs and preserving the environment is a huge problem that humanity encounters on a global scale. Human activity and stressed ecosystems have created new conditions for the emergence and spread of pathogen-induced diseases in the food industry and agricultural sectors, posing a threat to food security. Sustainable production of goods and managing ecosystems are of paramount importance and require a "One Health" approach. "One Health" concept implies that human, animal, plant and environmental health are inextricably connected, which requires interconnection of the respective sectors and not their separation [1].

An integral part of this concept is controlling the pathogenic microorganisms in the environment, monitoring diseases at local, regional, national and global levels. Modern requirements for product quality provide for expanding the competence in sectors of producing and managing agricultural products by investigating the cause-effect relationships in the transmission of diseases between species through host-pathogen interactions.

Plant pathogenic diseases pose a serious threat for crop yield and cause significant economic losses. Most of the strategies for their combating focus on soil. Intensive tillage has a negative impact on soil functioning and, as a consequence, on plant productivity. Long-term use of pesticides leads to loss of their effectiveness and promotes pathogen adaptation and the emergence of new, more aggressive genotypes resistant to antimicrobial agents [2]. To improve soil quality and preserve biodiversity, finding safe approaches for pathogen control is a priority. Integrated pest control requires specific solutions in each particular case. Monitoring and accurate identification of pathogens are essential for successful implementation of an integrated pest management program.

Among the pathogens that have a serious impact on agricultural production, micromycetes outnumber all other species. They are an important component of soil microbiota. However, from a practical point of view, they pose a major problem for agrosystems, causing up to 80% yield losses [3, 4]. In particular, soil fungi of *Fusarium, Penicillium* and *Aspergillus* genera are among the most harmful pathogens that reduce crop yield worldwide [5]. Species of *Fusarium* genus cause various types of wilts, rots, tissue necrosis and vascular diseases during plant vegetation [6]. In addition, most *Fusarium, Penicillium* and *Aspergillus* species produce mycotoxins that are hazardous to human and animal health, the content of which in plant products is strictly regulated [7].

Soil fungal pathogens can survive latently in soil for a long time in the absence of a host plant, forming stable structures. As a result, the diseases they cause are particularly difficult to forecast and successfully control. Screening of pathogenic microbiomes for identifying causal agents of diseases is the first step towards revealing direct and indirect links between the plant and the pathogen. Diagnostics of fungal pathogens using traditional microbiological methods can be difficult due to the similarity of their morphological features, the lack of the ability to study slow growing or non-culturable genotypes. In this regard,

molecular detection methods based on PCR are used in the practice of phytopathology, which allow specific detection of any microorganisms. They accelerate the identification of pathogens, including the cases of complex infection, allow the differentiation of pathogens with identical symptoms, and provide the ability to detect the pathogen at the pre-symptomatic stage. These minimize the risks of dissemination of pathogens.

A PCR-based technology was optimized for identifying various soil-born plant pathogens [8]. This approach was used to analyze species composition of fungi of *Fusarium, Penicillium* and *Aspergillus* genera in the genotypes of some vegetable crops of local selection. Monitoring of causal agents of fungal infections was performed in seeds of different storage periods and in plants at different phases of ontogenesis.

2. Material and methods

2.1. Plant material

The seeds of common bean, bell pepper and eggplant of different storage periods of the collection of Laboratory of Plant Genetic Resources (IGPPP) were analyzed. In the study were used following genotypes, Tabel 1:

Table 1

Description of seeds genotypes

Taxon	Genotype name	Year of preservation	Originator
Common bean (*Phaseolus vulgaris*)	MDS202, MDS204, MDS209	2015, 2020	Local forms from subsistence farms
Bell pepper (*Capsicum annuum*)	Fildes, Caolin, Excelent	2015, 2020	Varieties of Moldavian selection
Eggplant (*Solanum melongena*)	Rada, Magda	2011, 2018	Varieties of Moldavian selection

Eggplant genotypes of local selection cultivated on the experimental plots of the IGPPP served as objects of the field study in current research. Four eggplant genotypes of the collection of Laboratory of Plant Genetic Resources were studied: 'Laura', 'Forma 92', 'Magda' and 'Sucleischii' varieties. Different organs of plants during ontogenesis were tested. The asymptomatic leaves and fruits were selected randomly from 10-12 plants and bulk samples were prepared.

Prior to extraction of nucleic acids, seeds, leaves or fruits were thoroughly washed to remove impurities and surface microflora.

2.2. Desoxyribonucleic acid (DNA) extraction

The PCR reaction requires a pure DNA template in optimal quantities to ensure correct amplification of the target sequence. Nucleic acids were extracted from 0.2 – 0.5 g of seeds or 1 g of plant material and were purified according to the combination of several protocols from ISO 21571:2005 [9,10].

2.3. Primers

The specificity of PCR depends on the correct design of highly specific primers. Primers must be carefully designed to amplify only the genetic sequences of interest and to eliminate the possibility of false positive or negative results.

PCR primer design was done based on species-specific sequences of each pathogen from NCBI nucleotide collection presented in GenBank database using Primer-BLAST designing tool [11,12]:

- Translation elongation factor 1-alpha (*tef1*) gene sequences of *Fusarium verticillioides, Fusarium oxysporum, Fusarium solani, Fusarium avenaceum*.
- Beta-tubulin (*tub2*) gene sequences of *Fusarium equiseti, Fusarium sporotrichioides, Penicillium chrysogenum, Penicillium expansum, Penicillium citrinum*.
- Oxygenase (*fum6*) gene sequences of *Fusarium proliferatum*.
- RNA polymerase II subunit (*RPB2*) gene of *Fusarium nivale*.
- O-methyltransferase A (*aflP*) gene, partial cds; and *aflP-aflQ* intergenic region, genomic sequence of *Aspergillus flavus, Aspergillus parasiticus*.

A theoretical analysis of primer selection and conditions for their use in PCR was performed.

2.4. Polymerase chain reaction (PCR)

PCR is an experimental method of molecular biology suitable for detecting pathogens in DNA extracted from infected plant material excluding the step of their isolation and cultivation.

This highly specific technique allows rapid amplification of a specific DNA fragment of interest in biological material, permitting its detection and visualization. Methods of the molecular diagnostics present the possibility of identifying pathogens that cause diseases with the similar symptoms in mixed infections, as well as before the appearance of visible symptoms. PCR-assay is much faster than conventional culture-based methods, so the results can be obtained within a few hours.

PCR was performed in a 25 µL mix containing 66 mM Tris-HCl (pH 8.4), 16 mM $(NH4)_2SO_4$, 2.5 mM $MgCl_2$, 0.1% Tween 20.7% glycerol, 100 µg/ml-1 BSA, 0.2 mM of each dNTPs, 0.2 U Taq DNA polymerase (Thermo Fisher Scientific), 5 pM of each primer and 10 ng of DNA.

2.5. One-step PCR

The amplification conditions were as follows: in the first cycle, denaturation was carried out at 95^0C for 3 min; annealing – at 60 °C, 40 s, elongation – at 72 °C, 40 s, followed by 34 cycles: 95 °C – 40 s, 60 °C – 40 s, 72 °C – 40 s, final elongation - 7 min. Amplification was carried out using MiniAmp™ Thermal Cycler, 96 wells, Thermo Fisher Scientific.

2.6. Nested-PCR

Nested-PCR is a variant of conventional PCR and consists of two rounds, in which two pairs of primers are used in consecutive reactions. The second pair of primers amplify the DNA region within the product of the first reaction. It is applied to reduce nonspecific amplification and dramatically increases the sensitivity, productivity and specificity of the analysis.

The first round of *nested*-PCR included 1 cycle at 95 °C for 3 min (denaturation), 60 °C – 40 s (annealing), 72 °C – 40 s (elongation) followed by 29 cycles: 95 °C – 40 s, 60 °C – 40 s, 2 °C – 40 s, final elongation - 7 min. The conditions of the second round for *nested*-PCR were: 95 °C – 40 s, 60 °C – 40 s, 72 °C – 40 s, final elongation - 7 min (30 cycles). Amplification was carried out using MiniAmp™ Thermal Cycler, 96 wells, Thermo Fisher Scientific.

2.7. Results processing

The quality analysis of the isolated DNA and separation of the amplification products was performed in 1.5-2% agarose gel in the presence of 100 bp DNA ladder (Thermo Fisher Scientific molecular marker) with the addition of ethidium bromide, 1xTBE (pH 8.0) migration buffer, for approximately 1 h at 6V/cm. Visualization was performed in UV rays at a wavelength of 312 nm and photographed. The target fragments were compared with commercial molecular markers.

3. Results and discussion

3.1. Assessment of DNA quality

The integrity and quantity of total DNA extracted from plant material was carried out by electrophoresis in 1.5% agarose gel in the presence of coliphage λ DNA of known concentration (0.1 μg/10 μL). The results of the assessment of DNA quality are selectively presented in Figure 1.

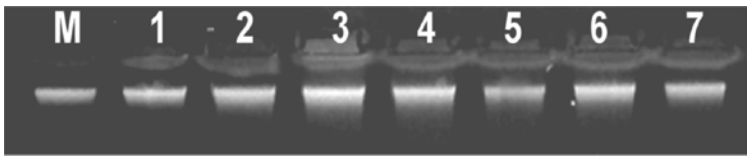

Figure 1. Electropherogram of total DNA extracted from seeds (1-3) and leaves (4-7) of eggplant. **M** - λ DNA - 0.1 μg/10 μL; **1-7** - 10 μL plant DNA per line.

Excessive amounts of DNA in a PCR reaction can suppress amplification. This can also lead to false priming and decreased PCR efficiency. As described in Material and methods (2.4. Polymerase chain reaction), 10 ng of DNA per sample was required for the PCR reaction mix. Based on the electrophoresis results, visually the amount of applied plant DNA (10 μL) is comparable to the amount of coliphage λ DNA (0.1 μg/10 μL). Thus, no more than 1 μL of DNA from each sample was used in subsequent molecular analysis.

The amplification capacity of DNA was validated by one-step PCR using primers designed based on the sequences of plant housekeeping genes, in particularly - 18S ribosomal RNA genes (18SrDNA) [13]. An example of PCR amplification of a target fragment of total DNA isolated from plant material using primers to the 18SrDNA is shown in Figure 2.

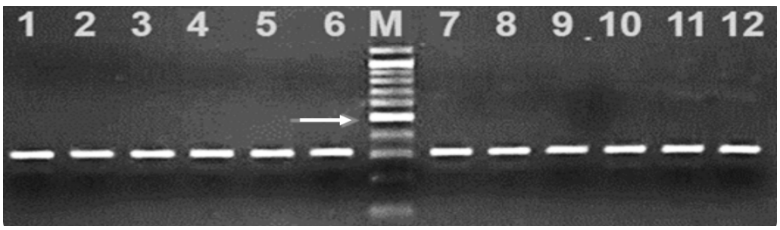

Figure 2. Electropherogram of the PCR products obtained on total DNA extracted from eggplant leaves (**1-12**) using primer to 18SrDNA. **M** - marker (100 bp DNA ladder). The arrow points at a 500 bp marker fragment.

As a result of one-step PCR using the specified primers, a fragment of 315 bp should be synthesized. The presence of amplicons of the expected length indicated that all tested DNA samples were free of PCR inhibitors and suitable for subsequent molecular analysis.

3.2. Validation of primers

Correct detection of fungal pathogens in plant material by molecular methods depends on highly specific primers for each taxon and suitable PCR protocol. Successful amplification is determined by obtaining amplicons corresponding to the target sequence of

certain pathogens and the absence of synthesis of non-specific products. The use of *nested*-PCR significantly improves the efficiency of pathogen detection.

This variant of PCR reduces the risk of non-specific amplification, which can lead to false negative or false positive results. But the sensitivity and specificity of PCR analysis should always be validated in each individual case. Therefore, initially the primers were tested using DNA extracted from different plant objects and *nested*-PCR conditions were optimized.

The results of molecular detection of pathogenic fungi of genus *Fusarium* in plant material are shown in Figure 3.

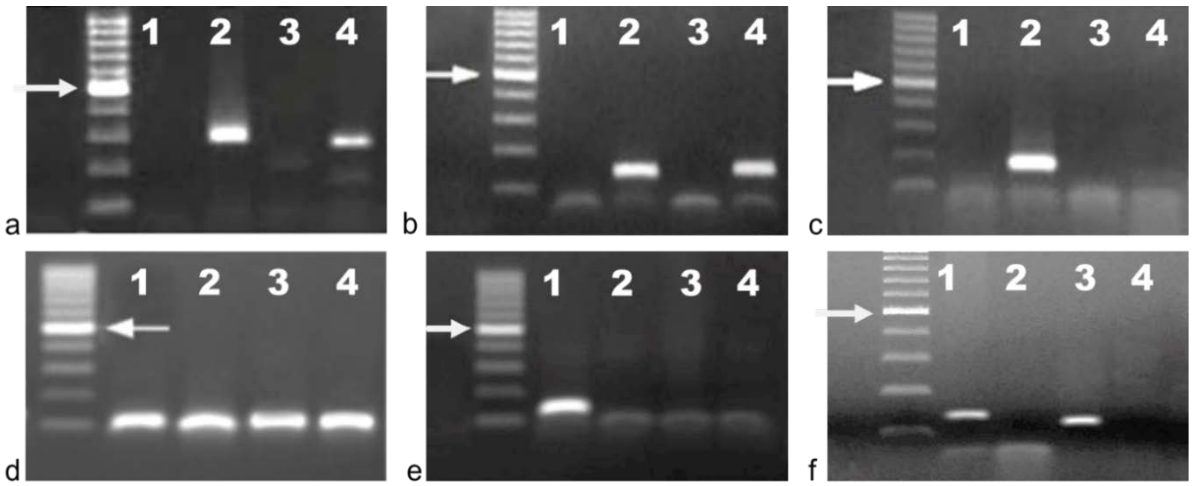

Figure 3. Electropherogram of the amplicons obtained in the second round of *nested*-PCR on total DNA extracted from plant material using primer pairs to *Fusarium* spp.
a) *Fusarium oxysporum* (line 2), *Fusarium solani* (line 4), b) *Fusarium avenaceum* (lines 2, 4), c) *Fusarium verticillioides* (line 2), d) *Fusarium equiseti* (lines 1-4), e) *Fusarium nivale* (line 1), f) *Fusarium sporotrichioides* (line 1), *Fusarium proliferatum* (line 3).
The arrow points at a 500 bp marker fragment.

The positive signals in the second round of *nested*-PCR for *Fusarium spp*. are marked with the presence of amplicons of following length: *Fusarium oxysporum* – 292 bp (Figure 3a, line 2), *Fusarium solani* – 275 bp (Figure 3a, line 4), *Fusarium avenaceum* - 140 bp (Figure 3b, lines 2, 4), *Fusarium verticillioides* - 160 bp (Figure 3c, line 2), *Fusarium equiseti* – 104 bp (Figure 3d, lines 1-4), *Fusarium nivale* – 127 bp (Figure 3e, line 1), *Fusarium sporotrichioides* – 135 bp (Figure 3f, line 1), *Fusarium proliferatum* – 123 bp (Figure 3f, line 3). The sizes of specific amplicons obtained by *nested*-PCR correspond to the parameters calculated using the BLAST software.

The results of testing primers for the identification of *Penicillium* spp. and *Aspergillus* spp. in plant material are presented in Figure 4. The presence of specific amplicons is marked of following length: *Penicillium citrinum* – 248 bp (Figure 4a, lines 1-4), *Penicillium chrysogenum* – 174 bp (Figure 4b, lines 1, 4), *Penicillium expansum* – 251 bp (Figure 4c, line 3), *Aspergillus flavus* – 144 bp (Figure 4d, lines 1, 3). The length of all fragments obtained as a result of amplification also corresponds to the parameters specified in the BLAST analysis.

It should be noted that the melting temperature of all primers is close to 60 °C and the length of the amplification products does not exceed 300 bp, which allows them to be used under the same PCR conditions. This set of primers was used for screening some crops to determine the qualitative composition of pathogenic fungi that affect plants.

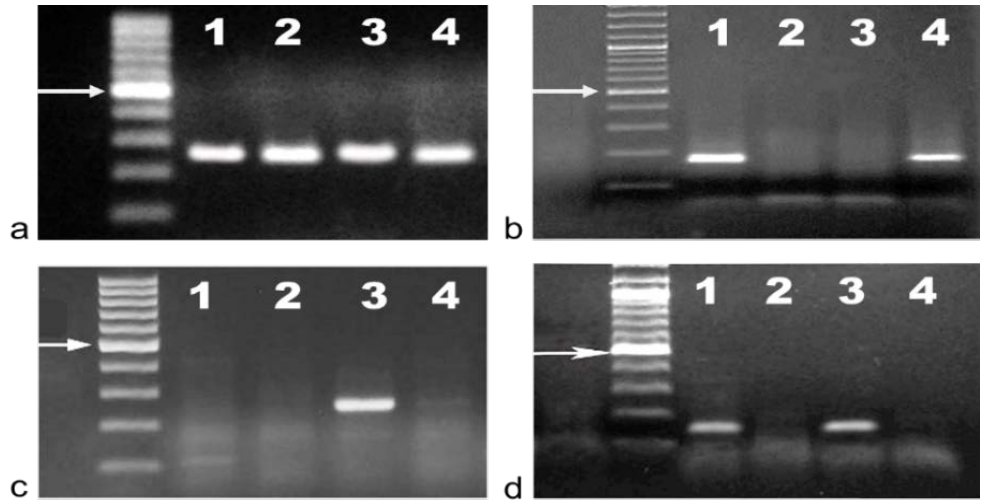

Figure 4. Electropherogram of the *nested-PCR* results obtained on total DNA extracted from plant material using primer pairs to *Penicillium* spp. and *Aspergillus* spp.: a) *Penicillium citrinum* (lines 1-4), b) *Penicillium chrysogenum* (lines 1, 4), c) *Penicillium expansum* (line 3), d) *Aspergillus flavus* (lines 1, 3). The arrow points at a 500 bp marker fragment.

3.3. Study of phytopathogenic load of seeds at different storage periods

Seed storage is associated with a number of problems. The main negative impact is caused by pathogenic microflora. Fungal infections affect stored seeds, reducing their viability and, as a result, leading to yield losses. The presence of minor amounts of pathogens in tissues or on the surface of seeds can cause mold growth when temperature and humidity fluctuations exceed admissible levels during storage. Propagation of pathogenic soil-born fungi in seeds cause their decay, necrosis, suppression of germination. Infections transmitted via seeds provoke the development of systemic plant diseases and a decrease in yield quantity and quality [14]. To prevent seed spoilage during storage, it is necessary to monitor their phytosanitary condition before preservation and during storage.

The results of molecular detection of fungal pathogens of *Fusarium, Penicillium* and *Aspergillus* genera in seeds of common bean, bell pepper and eggplant are presented in Figure 5.

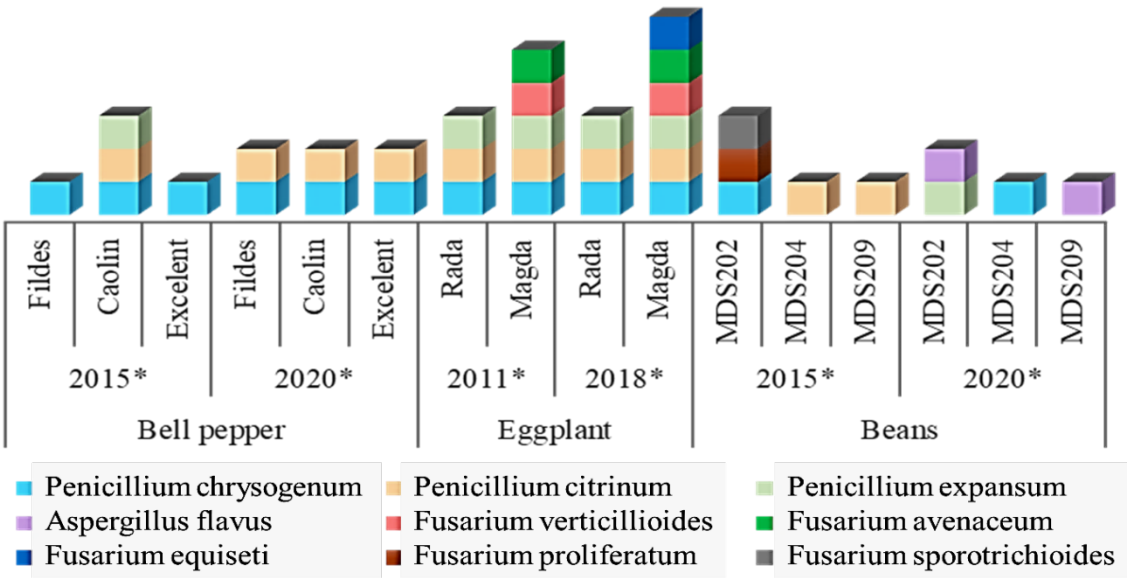

Figure 5. Species composition of pathogenic fungi in seeds of different storage periods. * - year of seeds preservation.

Fungi of the genus *Penicillium* were the predominant pathogens for all plant genotypes. *Penicillium chrysogenum* and *Penicillium citrinum* were the most detected in the seeds of eggplant and bell pepper. *Penicillium expansum* was found once in beans (MDS202, 2020 harvest) and bell pepper (Caolin, 2015). All eggplant varieties from 2011 and 2018 years of harvest were infected by *Penicillium chrysogenum, Penicillium expansum* and *Penicillium citrinum,* including bell pepper variety Caolin (2015 harvest). In beans, *Penicillium chrysogenum* (MDS204, 2020 harvest) and *Penicillium citrinum* (MDS204, MDS209, 2015 harvest) were detected. *Aspergillus flavus* was found twice in beans MDS202 and MDS209 (2020 year of seeds preservation).

Fungi of the genus *Penicillium* most often affect seeds and fruits of various crops in the post-harvest period, especially during long-term storage. During plant ontogenesis, *Penicillium* spp. and *Aspergillus* spp. behave predominantly as saprotrophs. Some species have been shown to act as pathogen antagonists by secreting antimicrobial active substances. Atoxigenic *Penicillium* and *Aspergillus* species can exhibit antifungal activity against some phytopathogenic fungi and suppressed their penetration into the host plant [15]. There are known species that are promote plant growth and resistance (PGPF - plant growth promotes fungi) and are used as biofertilizers [16,17]. However, their pathogenic potential manifests itself during harvest storage. They cause spoilage of fruits, their presence in seeds can lead to a significant decrease in germination, weakening of resistance to other factors, and even death [18]. There is a danger of the spread of pathogens to new areas when moving across international borders for trade or research purposes, as a consequence – their acclimatization, the emergence of new strains or physiological races [19]. Some species manifest phytotoxigenic activity that inhibit seed germination and plant development. Seed and fruit rots caused by filamentous *Penicillium* spp. fungi are hazardous storage diseases as they can cause huge yield losses and yield contamination with secondary metabolites called mycotoxins – a case of primary importance [20]. Therefore, control of these pathogens during crop storage is very important.

Molecular analysis demonstrated a low incidence of *Fusarium* species in studied seeds. They are absent in the bell pepper, and were detected in only one common bean genotype – MDS202 (2015 harvest). In the DNA sample of this genotype*, Fusarium proliferatum* and *Fusarium sporotrichioides* were identified. The eggplant variety 'Magda' showed increased sensitivity to *Fusarium* spp. pathogens. Thus, *Fusarium verticillioides* and *Fusarium avenaceum* were detected in the seeds of this genotype preserved in 2011 and 2018. *Fusarium equiseti* was found in the seeds of 2018 harvest.

Fusarium not only causes direct crop losses, but also reduces seed germination to the point of complete loss. Some common species of the genus *Fusarium* produce toxic metabolites – mycotoxins, the presence of which in seeds makes them unsuitable for food and feed purposes [21,22]. Therefore, monitoring of these pathogens in agricultural products is very important.

3.4. Monitoring of fungal infections during plant ontogenesis

The development of some fungal infections in plants during vegetative season was assessed: in seeds before planting, at the phase of 4-5 leaves, at the flowering phase, at the phase of fruit formation and growth, and in fresh seeds. The results of molecular analysis of eggplant genotypes during ontogenesis using primers for detection of *Fusarium* spp. and *Penicillium* spp. are presented in Figure 6.

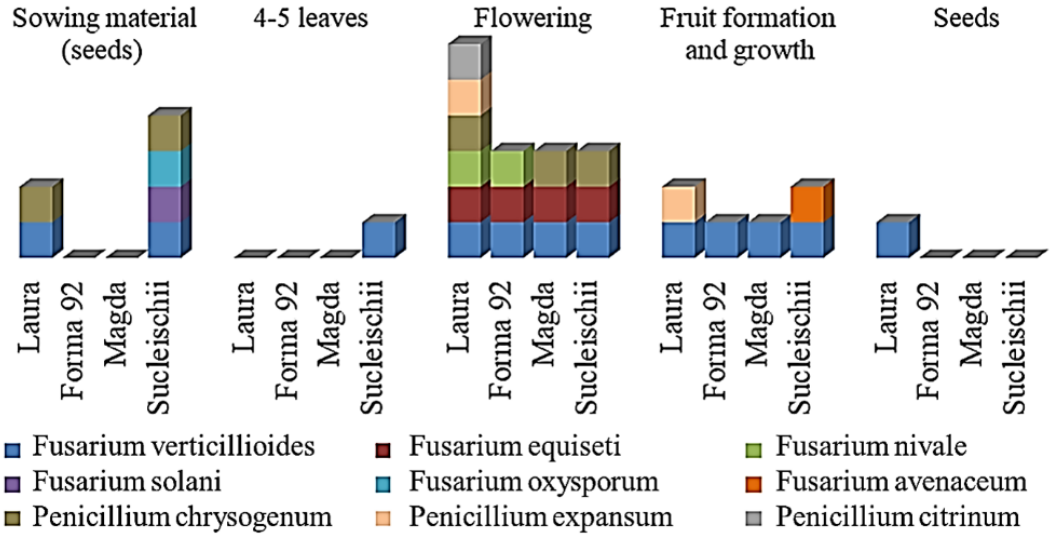

Figure 6. Distribution of *Fusarium* spp. and *Penicillium* spp. during eggplant ontogenesis.

PCR analysis revealed that the sowing material (seeds of the 2020 harvest) of two genotypes, 'Laura' and 'Sucleischii', was infected with *Fusarium verticillioides* and *Penicillium chrysogenum*, in addition, *Fusarium oxysporum* and *Fusarium solani* were detected in 'Sucleischii'. None of the pathogens were identified in the genotypes 'Magda' and 'Forma 92'. Molecular detection showed that plants are most prone to pathogenic fungi during the flowering phase. Eggplant genotypes at the phase of 4-5 leaves and "new" seeds show less vulnerability to pathogens.

The most cases of infection were noted in the 'Laura' variety during its ontogenesis. The following species of fungi were detected in this genotype: *Fusarium verticillioides, Fusarium equiseti, Fusarium nivale, Penicillium chrysogenum, Penicillium expansum, Penicillium citrinum*. 'Sucleischii' also showed increased susceptibility to *Fusarium* spp. and *Penicillium* spp. In this genotype *Fusarium verticillioides, Fusarium oxysporum, Fusarium solani, Fusarium equiseti, Fusarium avenaceum* and *Penicillium chrysogenum* were found throughout all development phases, with the exception of "new" seeds. The highest number of positive signals during vegetative season was observed for *Fusarium verticillioides*. The PCR analysis showed that fresh-harvested seeds are free of the listed pathogens, with the exception of a single incidence in the 'Laura' variety. Therefore, the eggplant seeds of this growing season are of good quality and can be used both for further reproduction and for long-term storage.

The presence of *Fusarium verticillioides, Fusarium equiseti, Fusarium proliferatum, Fusarium sporotrichioides, Penicillium expansum*, *Aspergillus flavus* in studied seeds and plants should be closely monitored, since these species of fungi belong to the group of mycotoxin producers that are dangerous to human and livestock health. This is especially relevant to agricultural products intended for storage.

Plant diseases pose a serious threat to agricultural production and food security. Factors such as climate change, changes in agricultural practices, loss of resistant varieties and loss of biodiversity provoke the risk of plant disease outbreaks. This situation not only directly leads to reduced yields, but also reduces the quality and value of agricultural products and increases agricultural costs. So, monitoring of plant diseases at local levels is necessary to improve global food security. Identification of genotypes with reduced sensitivity to fungal pathogens is of interest in terms of their further use to study the relationship between their genetic characteristics and diseases.

4. Conclusions

The efficiency of molecular technique for the effective species-specific detection of pathogenic fungi that can affect agricultural crops was demonstrated.

Molecular identification of *Fusarium spp., Penicillium spp*. and *Aspergillus spp*. in seeds of vegetable crops of different storage periods was carried out. Fungi of the genus *Penicillium* were the predominant pathogens in all plant genotypes. *Penicillium chrysogenum, Penicillium citrinum* and *Penicillium expansum* were the most detected in eggplant and bell pepper seeds regardless of the year of seed preservation. It was found that the studied eggplant seeds are the most vulnerable to pathogens of the genus *Fusarium*. Molecular diagnostic assessment of the phytosanitary status of seeds is necessary to ensure effective plant protection from a complex of seed-borne pathogens. Thus, it is not advisable to use infected seeds for long-term storage due to the risk of accumulation of metabolic products of pathogenic fungi - mycotoxins, which greatly reduces their quality.

The development of the fungal infection in some eggplant genotypes during ontogenesis was studied. Based on *nested*-PCR assay, predominant fungal pathogen in the tested plants was *Fusarium verticillioides,* which is one of the important producers of the mycotoxins. As a result of molecular analysis, studied eggplant genotypes showed varying susceptibility to fungal infections. The genotype 'Laura' demonstrated the greatest vulnerability to *Fusarium spp*. and *Penicillium spp*., the genotypes 'Magda' and 'Forma 92' showed the least susceptibility.

The species composition of *Fusarium, Penicillium* and *Aspergillus* genera affecting some vegetable crops plantings in the experimental plots of the IGPPP was shown.

Acknowledgments: This study was supported by the research project 011101 "Genetic and biotechnological approaches of management of agroecosystems under climate change conditions", funded by the Ministry of Education and Research.

Conflicts of Interest: The author declares no conflicts of interest.

References

1. Garcia, S.N.; Osburn, B.I.; Jay-Russell, M.T. One Health for Food Safety, Food Security, and Sustainable Food Production. *Front. Sustain. Food Syst.* 2020, 4, 1. https://doi.org/10.3389/fsufs.2020.00001
2. Miller, S.A.; Ferreira, J.P.; Lejeune, J.T. Antimicrobial Use and Resistance in Plant Agriculture: A One Health Perspective. *Agriculture* 2022, 12, 289. https://doi.org/ 10.3390/agriculture12020289
3. Gai, Y.; Wang, H. Plant Disease: A Growing Threat to Global Food Security. *Agronomy* 2024, 14, 1615. https://doi.org/10.3390/ agronomy14081615
4. Panth, M.; Hassler, S.; Baysal-Gurel, F. Methods for Management of Soilborne Diseases in Crop Production. *Agriculture* 2020, 10, 6. doi:10.3390/agriculture10010016.
5. Zakaria, L. An Overview of Aspergillus Species Associated with Plant Diseases. *Pathogens* 2024, 13, 813. https://doi.org/10.3390/ pathogens13090813.
6. Srinivas, C.; Nirmala Devi, D.; Narasimha Murthy K. Fusarium oxysporum f. sp. lycopersici causal agent of vascular wilt disease of tomato: Biology to diversity – A review. *Saudi J. of Biol. Sci.* 2019, 26(7), pp. 1315-1324. https://doi.org/10.1016/j.sjbs.2019.06.002
7. Abdelmotilib, N.; Abdel-Azeem, D.; Sheir, D. Fungal Mycotoxins. In: *Fungi in Sustainable Food Production*, Dai, X., Sharma, M., Chen, J. (Eds.); Springer Nature, Switzerland, 2021, pp. 197-226.
8. Grajdieru C.; Mitina I.; Tumanova L.; Mitin V. Assessing several fungal contaminants and their associated mycotoxins in maize cultivated on cornfields of Republic of Moldova. *Food Additives & Contaminants*: 2024, 41(6), pp. 675-687.
9. Aboul-Maaty, N.A.-F.; Oraby, H.A.-S. Extraction of high-quality genomic DNA from different plant orders applying a modified CTAB-based method. *Bulletin of the National Research Centre* 2019, 43(1), pp. 1–10.

10. ISO 21571:2005. Foodstuffs — Methods of analysis for the detection of genetically modified organisms and derived products - Nucleic acid extraction. International Organization for Standardization 2015, pp. 1-50.
11. NCBI. National Center for Biotechnology Information. U.S. National Library of Medicine. Available online: https://www.ncbi.nlm.nih.gov/genbank/ (accessed on 05.02.2025)
12. NCBI. National Center for Biotechnology Information. Primer-blast. Available online: https:// www.ncbi.nlm.nih.gov/tools/primer-blast/ (accessed on 05.02.2025)
13. Deaghileva, A.; Mitin, V.; Pasha, L.; Tumanova, L. Molecular examination of tomato plants with TYLCV-like symptoms. *Buletinul AŞM. Ştiinţele vieţii* 2016, 3(330), pp. 104-108.
14. FAO. ISPM 38. International movement of seeds, 1th ed. FAO, Rome, Italy, 2021, 22 p. ISBN 978-92-5-109748-9.
15. Mejdoub-Trabelsi, B.; Rania Aydi Ben, A.; Nawaim, A.; Mejda Daami R. Antifungal Potential of Extracellular Metabolites from Penicillium spp. and Aspergillus spp. Naturally Associated to Potato against Fusarium species Causing Tuber Dry Rot. *J Microb Biochem Technol*. 2017, 9, pp. 181-190. doi: 10.4172/1948-5948.1000364
16. Adedayo, A.A.; Babalola, O.O. Fungi That Promote Plant Growth in the Rhizosphere Boost Crop Growth. *J. Fungi* 2023, 9, 239. https://doi.org/10.3390/jof9020239
17. Ye, M.; Feng, H.; Hu, J.; Yu, Q.; Liu S. Managing tomato bacterial wilt by suppressing Ralstonia solanacearum population in soil and enhancing host resistance through fungus-derived furoic acid compound. *Front. Plant Sci*. 2022, 13, 1064797. doi: 10.3389/fpls.2022.1064797
18. Martín, I.; Gálvez, L.; Guasch, L.; Palmero, D. Fungal Pathogens and Seed Storage in the Dry State. *Plants* 2022, 11, 3167. https://doi.org/10.3390/ plants11223167
19. Tsedaley, B. Review on Seed Health Tests and Detection Methods of Seedborne Diseases. *J. of Biol., Agri. and Healthcare* 2015, 5(5), pp. 176-184.
20. Zhang, C.; Qu, Z.; Hou, J.; Yao, Y. Contamination and Control of Mycotoxins in Grain and Oil Crops. *Microorganisms* 2024, 12, 567. https://doi.org/10.3390/microorganisms 12030567
21. Bryła, M.; Pierzgalski, A.; Zapa´snik, A.; Uwineza, P.A.; Ksieniewicz-Wo´zniak, E.; Modrzewska, M.; Wa´skiewicz, A. Recent Research on Fusarium Mycotoxins in Maize - A Review. *Foods* 2022, 11, 3465, 5. https:// doi.org/10.3390/foods11213465.
22. Qu, Z.; Ren, X.; Du, Z.; Hou, J.; Li, Y.; Yao, Y.; An, Y. Fusarium mycotoxins: The major food contaminants. *mLife* 2024, 3(2), pp. 176–206. https://doi.org/10.1002/mlf2.12112

Citation: Deaghileva, A. Molecular diagnostics of soil-borne pathogenic fungi in several agricultural crops. *Journal of Engineering Science*. 2025, XXXII (2), pp. 122-132. https://doi.org/10.52326/jes.utm.2025.32(2).11.

Submission of manuscripts: jes@meridian.utm.md

Journal of Engineering Science *Vol. XXXII, no. 1 (2025), pp. 133 - 145*
Fascicle *Food Engineering* *ISSN 2587-3474*
Topic *Biotechnologies, Food Chemistry and Food Safety* *eISSN 2587-3482*

https://doi.org/10.52326/jes.utm.2025.32(2).12
UDC 664.34.09:665.1/.2:547-326:54.06

FATTY ACID METHYL ESTERS GC/FID ANALYSIS USING ICHIHARA-FUKUBAYASHI MODYFIED METHOD

Alexei Baerle, ORCID: 0000-0001-6392-9579,
Angela Gurev *, ORCID: 0000-0001-8493-5257,
Veronica Dragancea, ORCID: 0000-0002-5938-0410,
Iurie Subotin, ORCID: 0000-0002-5570-4713,
Raisa Druta, ORCID: 0000-0001-5301-6055

Technical University of Moldova, 168 Stefan cel Mare Blvd., Chisinau, Republic of Moldova
* Corresponding author: Angela Gurev*: angela.gurev@chim.utm.md*

Received: 04. 22. 2025
Accepted: 05. 27. 2025

Abstract. The method for preparing fatty acid methyl esters (FAMEs) from lipids for gas-liquid chromatography, developed by K. Ichihara and Y. Fukubayashi, was optimized as a result of research on the influence of mild (45 °C, for 14 h) and fast (100 °C, for 1 h) methanolysis-methylation conditions on the FAMEs yield. Based on the minor impact on the final products and the good FAMEs yields, the optimized mild methanolysis/methylation method was applied to eight vegetable oil samples and two types of fish oil dietary supplements. The FAMEs compositions were analyzed by gas chromatography with flame ionization detector (GC/FID). On the recorded chromatograms, 16 types of fatty acids with majority content were identified and their mass fractions were calculated. The modified Ichihara-Fukubayashi method allowed the conversion of ester-bound fatty acids and free acids to FAMEs in a single step. The accuracy, accessibility and convenience of the method, the use of low concentrations of samples and reagents were noted.

Keywords: *coelution, fish oil, methylation, omega-3, omega-9, oily seeds, toluene.*

Rezumat. Metoda de preparare a esterilor metilici ai acizilor grași (EMAG) din lipide pentru cromatografia gaz-lichid, elaborată de K. Ichihara și Y. Fukubayashi, a fost optimizată în rezultatul cercetării influienței condițiilor de metanoliza/metilare lentă (45 °C, timp de 14 h) si rapidă (100 °C, timp de 1 h) asupra randamentelor EMAG. Reieșind din impactul minor asupra produselor finale si randamentul EMAG bun, a fost aplicată metoda optimizata de metanoliza/metilare lentă la opt tipuri de uleiuri vegetale și două tipuri de suplimente alimentare de ulei de pește. Compozițiile EMAG au fost analizate prin cromatografia gaz-lichid cu detector de ionizare cu flacără (GC/FID). În cromatogramele înregistrate au fost identificați 16 tipuri de acizi grași cu conținut major și calculate părțile de masa ale acestora. Metoda Ichihara – Fukubayashi modificata a permis convertirea acizilor grași cu legături esterice și acizii liberi în EMAG într-o singură etapă. A fost remarcata acuratețea, accesibilitatea si comoditatea metodei, folosirea de concentrații mici de probe și reagenți.

Cuvinte cheie: *coeluție, metilare, omega-3, omega-9, semințe oleaginoase, ulei de pește, toluen*

1. Introduction

Lipids are the basic components of the human diet, important sources of energy (9 kcal/g), micro- and macronutrients for the human body. Lipids are classified into simple lipids, which are fats and oils (triglycerides of fatty acids) and compound lipids, such as phospholipids, cholesterol, phytosterols, sphingolipids etc. [1].

The physical, chemical and physiological properties of lipids are largely determined by the composition of the fatty acids (FA) they contain. FA are most often found in the form of glycerol esters, such as triglycerides (TG), phospholipids (PhL), but also in free form (FFA). FA are carboxylic acids with unbranched carbon chains and can be saturated, monounsaturated or polyunsaturated (fatty acids with multiple double bonds (PUFA), also called essential acids). Depending on the position of the double bonds, unsaturated fatty acids are divided into omega-9, omega-6 and omega-3 acids, such as oleic acid C18:1, linoleic acid C18:2 and linolenic acid C18:3, respectively [2,3]. Lipids from vegetable sources (sunflower, olive, flax, rapeseed, walnut, coconut, cocoa), animals (butter, lard, beef), fish oil and others, differ in the type and variety of fatty acids they contain. Thus, the identification of lipids is based on the qualitative and quantitative analysis of the FA in their composition. For this purpose, globally, gas-liquid chromatography (GC) analysis method that can be coupled with mass spectrometry (GC-MS) [4] is predominantly applied, due to its efficiency and affordable cost [5]. GC methods are also widely used to analyze the quality of lipids and identify their contaminants [6,7].

1.1 Lipid Sample Preparation Procedures for GC Analysis

Before analyzing lipids from various food samples, the following preparation steps are required: 1. lipid extraction; 2. lipid fractionation by polarity into neutral fats (TG) and polar lipids (PhL, glycolipids, sphingolipids) including FFA; 3. derivatization or conversion of FA into FAMEs; 3. separation of FAMEs and their analysis by GC.

Vegetable oils do not require many preparation steps, if they contain moisture, they are dried with anhydrous sodium sulfate (1 g of Na_2SO_4 per 10 g of sample) at room temperature or in vacuum ovens (at 45…50 °C) [8]. In the case of food products, the fatty matter is extracted with different solvents, depending on the properties and composition of the lipids. It is important that the food samples are well dried at low temperatures in a vacuum oven or by freeze-drying, to prevent lipid oxidation [9]. After drying, the samples are finely ground to increase the contact surface with the solvent. The method of extraction of the ground sample with the appropriate solvent follows, the fatty matter will be entrained by the solvent. Triglycerides and other non-polar compounds can be extracted with *n*-hexane, petroleum ether, diethyl ether and others [10,11]. Mixtures of polar solvents - methanol, ethanol, *n*-butanol, isobutyl alcohol, with non-polar solvents - chloroform, diethyl ether, *n*-hexane, petroleum ether will extract all types of lipids, polar and non-polar, fatty acids, *etc*. from the matrix [12-14]. Folch and Bligh methods [15] and the Dyer method [16] use the chloroform: methanol : water mixture in various proportions.

1.2 Derivatization of Fatty Acids

FA in their free form cannot be analyzed by GC because they are polar compounds, form hydrogen bonds, and have high boiling points. Typically, fatty acid methyl esters, which are much more volatile, are analyzed by GC [17]. Several processes are known for derivatizing or converting FA to FAMEs, which include cleavage of ester bonds from lipids under alkaline (saponification) or acidic conditions, followed by methylation of the fatty acids [18,19].

Derivatization in basic media is most often performed with sodium methoxide ($NaOCH_3$) or potassium methoxide ($KOCH_3$). Typically, 0.5 M $NaOCH_3$ in anhydrous methanol is added to the lipids, and the mixture reacts at 45 °C for 5 min. Sodium hydrogen sulphate, $NaHSO_4$ (15%) is added to neutralize the mixture. Finally, the FAMEs are extracted with an organic solvent and analyzed by GC [17,20]. The advantages of the method are short time, low rate of isomerization of double bonds from *cis*- to *trans*-, fewer oxidative reagents [21]. The disadvantage is that FFA are not converted to FAMEs under these conditions [22]. Acid derivatization is suitable for both esterified and free fatty acids. This method uses the reagents: hydrochloric acid (HCl), acetyl chloride (CH_3COCl), sulfuric acid (H_2SO_4), and boron trifluoride (BF_3) [23]. Hydrochloric acid (HCl) is the most widely used catalyst for lipid derivatization reactions, as it is a milder reagent and gives very good yields. However, the use of anhydrous methanolic HCl, prepared by mixing acetyl chloride with methanol, is a harmful process [17,24]. The disadvantage of the method is the danger that can be caused by the exothermic reaction with acetyl chloride; in addition, some polyunsaturated fatty acids are unstable at the high temperatures (90-95 °C) applied [4]. Sulphuric acid H_2SO_4 is a strong oxidizing agent and is not recommended in the analysis of PUFA [25]. Although the BF_3 method provides efficient derivatization, its instability and artifact formation have been concerns in several studies [26].

1.3 Ichihara-Fukubayashi method

Japanese researchers K. Ichihara and Y. Fukubayashi developed an accessible and efficient method for preparing FAMEs from FFA, TG, PhL and cholesterol for GC analysis [27]. The method uses a reagent mixture composed of commercial concentrated HCl, methanol and toluene, these reagents being superior in terms of convenience, safety, and cost. Researchers developed two processes for derivatization: methanolysis/methylation by slow reaction under mild conditions (45 °C) and methanolysis/methylation by rapid reaction (100 °C) [27].

The mild methanolysis/methylation conditions at 45 °C and the duration of up to 14 h ensure the conversion of almost all fatty acids from different types of lipids into methyl esters, both those resulting from the cleavage of ester bonds and FFA. FAMEs are formed at a rate of 98-99%. Researchers Ichihara, K. and Fukubayashi, Y. determined that FFA are methylated rapidly, at a concentration of 1.2% HCl, being converted to FAMEs after 20 min, almost quantitatively. TG and PhL follow, which were converted to FAMEs after 8 h under the same conditions (HCl 1.2%, 45 °C). Cholesterols and phytosterols need 14 h to be converted to methyl esters.

1.4 Rapid methanolysis/methylation at 100 °C

The reaction conditions of HCl 1.2% at 100 °C for 90 min are required to convert all fatty acids and FFA from sterol-containing lipids to FAMEs, while 30 min is a sufficient reaction time to give good yields of FAMEs for lipid samples that do not contain sterol esters. FFA are methylated after 15 min, and triglycerides are converted to FAMEs and glycerol after 30 min. The FAMEs yield is almost 97% [27]. The authors report that ester-linked fatty acids and free acids from all lipid types were converted almost quantitatively to FAMEs in a single step by both methods. The mild methanolysis/methylation conditions were applied to blood lipids that contain considerable amounts of cholesterol, and FAMEs were prepared from a drop of blood spotted on a filter paper [27].

The aim of the research was to optimize Ichihara-Fukubayashi method for derivatization of lipids and fatty acids into methyl esters for GC/FID analysis, by elucidating the influence of methanolysis/methylation conditions on the yield of FAMEs, as well as identifying the qualitative and quantitative composition of FA from simple lipids.

2. Materials and Methods

2.1. Materials

Commercial vegetable oils: coconut oil (CoO), avocado oil (AvO), chia seeds oil (ChO), quinoa seeds oil (QuO), flaxseeds oil (FSO), refined, deodorized sunflower oils: "ordinary" (SFO) and "high oleic" (SFHO), olive oil (OO). Dietary supplements from enriched fish oil EFO_1 („Solgar Inc.", NJ-07605, USA) and EFO_2 („Balkan Pharmaceuticals Ltd.", Republic of Moldova) fortified with ethyl esters of eicosapentaenoic (EPA) and docosahexaenoic (DHA) fatty acids. HCl (35%, *w/w*), *n*-hexane, toluene, methanol – all of GC grade ("Merck", USA).

Standards of methyl palmitate and methyl stearate were synthesized from the corresponding free fatty acids. The identification of other FAMEs was based on column polarity, retention time, molar mass and comparative bibliographic data – after the injections and the analysis of all samples.

2.2. Methods

2.2.1. Preparation of lipid samples

Commercially purchased vegetable oils were dried with anhydrous sodium sulfate (1 gram of Na_2SO_4 per 10 g of sample) for 2 h at room temperature. Dried and ground chia, flax and quinoa seeds were extracted with *n*-hexane in a sample:solvent ratio of 1:3 (*m/v*) at room temperature in the dark for 24 h. This was followed by filtration, evaporation of the solvent from the lipophilic extract at 55 °C and drying of the oil with anhidrous Na_2SO_4 at room temperature for 2 h. The oil layer was decanted into stoppered glass test tubes.

The contents of the fish oil dietary supplement capsules were poured into glass test tubes, from which the fatty matter was extracted with *n*-hexane in a ratio of 3:1 (*v/v*) by shaking for 2 min and left to stand for 4-5 min. The upper lipophilic extract layer was aspirated, from which the hexane was evaporated. EFO1 and EFO_2 were dried with anhydrous sodium sulfate for 2 h.

Immediately after drying, the lipid samples were weighed and subjected to methanolysis/methylation reactions as follows.

2.2.2. Preparation of fatty acid methyl esters (FAMEs)

Standard FAMEs - methyl palmitate and methyl stearate - were synthesized from palmitic and stearic acids. A total of 0.01 mol of the acid was dissolved in 1.25 mol of methanol and 0.02 mol of sulfuric acid was added as a catalyst. The reaction mixture was boiled with reflux for 1 h., then cooled and poured into 500 mL of ice-cold distilled water. The resulting esters were filtered and dried (18-20 °C). Identification of FA content in lipids was made according to FAMEs polarity, retention time, molar mass and by comparison with bibliographic data. The high content of lauric and myristic acids predominating exclusively in cocoa butter among the studied samples - facilitated their assignment.

FAMEs from lipid samples were prepared according to the bibliographic method [27], with some modifications. The concentrated hydrochloric acid reagent in methanol was prepared as follows: 9.5 mL of commercial HCl (35%, *v/v*) was diluted with 41.5 mL of MeOH, to obtain 50 mL of 8.0% (*w/v*) HCl. This HCl reagent contained 85% MeOH (*v/v*) and 15% water

(*v/V*) came from the concentrated hydrochloric acid solution. The reagent was stored in a refrigerator.

The weighed lipid (or fatty acid) sample (100 mg) was dissolved in 10 mL of toluene, from this solution 0.202 mL (202 µL) were taken with a micropipette and transferred into a screw-capped glass test tube (16.5 × 105 mm), to which another 0.200 mL of toluene was added. Thus, the mass of lipid dissolved in the toluene solution was 2 mg. To this lipid solution in toluene, it is mandatory to add in the following order: 3.00 mL of methanol and 0.60 mL (600 µL) of 8.0% HCl solution in methanol prepared above. The final HCl concentration is 1.2% (*w/v*) or 0.39 M in the 4 mL of solution in the test tube. The addition of a mixed solution of 1.2% HCl/methanol/toluene to lipid samples should be avoided due to the low solubilities of lipids in the contained water. The tubes were tightly closed, shaken for 1 min and subjected to methanolysis/methylation reactions under mild or rapid conditions. Two types of tubes were used: glass test tubes with ground glass stoppers (G-stoppers) and glass test tubes with polypropylene screw plugs (PPS-plugs). For slow methanolysis/methylation under mild conditions, the tubes were incubated at 45 °C for 14 h. Rapid methanolysis/methylation was performed at 100 °C for 1 hour. After the reaction time expired, the samples were cooled to room temperature, then 2 mL of hexane and 2 mL of water were added to the test tubes for FAMEs extraction. The test tubes were shaken for 1 min, left to stand for 2-3 min, then the upper hexane layer was carefully aspirated with a micropipette, dried with anhydrous sodium sulfate and analyzed by GC/FID.

2.2.3. Gas-Liquid Chromatography (GC)

GC analysis was carried out according to [28] with same modifications. An "Agilent 8860" instrument, equipped with autosampler, flame ionization detector (FID) and non-polar column HP-5 (30 m × 0.32 mm × 0.25 µm) was used. Conditioning gas Nitrogen (99.99%). Work gas Helium (99.99%), split mode, split ratio 4:1, flow 0.8 mL/min. Injector chamber temperature: 190 °C. Initial oven temperature: 140 °C. Temperature program: 0…4 min: plateau 140°C; 4…18 min: heating from 140 °C to 210 °C; 18…41 min – plateau 210 °C; 41…42 min – column cooling to 140 °C.

2.2.4. Statistical analysis of the results

The method standard deviation, SD_{method}, was calculated for three independent replicates using a sample of high oleic sunflower oil, SFHO. The P = 0.95, q = 0.05 hypothesis ($\Delta X = \pm\ 2 \cdot SD$) was accepted. Relative method error was amounted 0.043 (4.3%). The relative sample errors ε_{sample}, were calculated taking in account the number of GC-chromatogram peaks, processed as FAMEs, $n_{standard}$ and n_{sample} respectively in the SFHO and in the sample. The graduated pipette error, $\varepsilon_{pippette} = 2 \cdot (2\mu L/202\mu L) = 0.02$, also was taken in account to calculate sample relative error:

$$\varepsilon_{sample} = \sqrt{\varepsilon_{standard}^2 \frac{n_{sample}-1}{n_{standard}-1} + 0.02^2} \quad (1)$$

3. Results and discussions

3.1. Optimization of methanolysis/methylation methods

In order to investigate the influence of methanolysis/methylation conditions on the results of the experiments, two vegetable oil samples SFHO and OO were placed in glass test tubes with glass ground stoppers (G-stoppers) and in glass test tubes with polypropylene screw plugs (PPS plugs) for

mild (45 °C, for 14 h) and rapid (100 °C, for 1 h) methanolysis/methylation, according to the Ichihara-Fukubayashi method. FAMEs obtained in both experiments were GC/FID analyzed, the fatty acids with major content were identified and their mass fractions (%) of the total FA in the samples were calculated (Table 1). It was noted that heating the samples in G-stoppers test tubes at 100 °C resulted in the evaporation of the content (chemicals). The data illustrated in Table 1 confirm that PPS plugs better preserve the concentration of components during mild and rapid methanolysis/methylation, but in the chromatograms of FAMEs non-specific peaks of artifacts originating from polypropylene were detected.

Fast methanolysis/methylation at 100 °C for 1 hour led to a decrease in the yield of FA with C8-C16 carbon atoms in the chain, as a consequence, the calculated ratio resulted in higher mass fractions in favor of C18 acids (Table 1).

Under fast methylation/methanolysis conditions Ichihara, K. and Fukubayashi, Y. detected artifacts formed from cholesteryl oleate, which could not be separated from methyl oleate by silica gel column chromatography as well as by GC.

The method owners did not detect artifacts under mild methanolysis/methylation conditions, except for conjugated linoleic acid (rumenic acid), which is less stable under acidic conditions and forms artifacts in a ratio of 5% in both methods. Conjugated linoleic acid has two conjugated double bonds, separated by a single single bond, with the *cis*- and *trans*-configuration, respectively [29].

The researches [27] mentioned that in both methods, in the process of the methanolysis reaction in acidic medium, which is reversible, the presence of water derived from HCL could favor the formation of FFA. However, the results obtained by the Japanese authors demonstrate that less than 1.4% of FAMEs hydrolyzes into FFA. The researchers found that methanol containing 2.0% and 10% toluene is almost equivalent to anhydrous methanol in terms of the solubility of glyceryl trioleate. In the absence of toluene, lipid methanolysis was slow and partial. The effect of water on hydrophobic compounds was thus diminished by the addition of toluene.

The data in Table 1 are within those indicated in the literature for the mass fractions of FA in SFHO and OO, confirming the efficiency of both methanolysis/methylation regimes. However, the results obtained in these studies showed the advantage of mild methanolysis/methylation conditions, which affect less the concentration of volatile short-chain FAMEs.

It was also established that GC-FID analysis of FAMEs on the used GC column and others specified GC parameters of the given experiment (see 2.2.2) unfortunately does not allow the separation of FAMEs of oleic (C18:1 *ω*9) and α-linolenic (C18:3 *ω3*) acids, which give a common peak, Figure 1. Common elution of oleic and α-linolenic acid also correlate with bibliographical data (Tables 1 and 3).

Table 1

The influence of methanolysis/methylation conditions on fatty acid esters yield, %

No	FA	Bibliography		Mild, 45 °C, 14 h				Rapid, 100°C, 1 h	
		SFHO	OO	SFHO		OO		SFHO	OO
		[30, 31]	[32, 33]	G-stoppers	PPS-plugs	G-stoppers	PPS-plugs	PPS-plugs	PPS-plugs
1	12:0	< 0.1		0.012±0.001	0.055±0.003	0.013±0.001	0.053±0.003	0.012±0.001	0.011±0.001
2	14:0	< 0.1	< 0.1	0.050±0.002	0.062±0.003	0.028±0.001	0.025±0.001	0.055±0.003	0.021±0.001
5	15:0			0.015±0.001	0.029±0.001	0.015±0.001	0.012±0.001	0.017±0.001	0.012±0.001

Continution Table 1

6	16:1 ω9	< 0.2	0.3 - 3.5	0.169±0.008	0.185±0.009	1.424±0.067	1.516±0.073	0.160±0.007	1.284±0.062
7	16:0	3.5 - 8	7.5 - 20	4.67±0.22	5.25±0.26	14.81±0.70	15.97±0.77	4.63±0.22	13.72±0.66
8	18:2 ω6	5.0 -17	3.5 - 21	7.00±0.33	7.05±0.34	10.50±0.50	10.40±0.50	6.94±0.33	10.40±0.50
9	18:1 ω9	75 - 90	55 - 83	82.4±3.9	81.8±4.0	66.3±3.2	64.9±3.2	80.8±3.8	65.6±3.2
10	18:3 ω3	< 0.2	< 1.0						
11	18:1 ω9		< 0.1	0.700±0.033	0.781±0.037	2.74±0.13	2.92±0.15	0.818±0.038	2.93±0.15
12	18:0	3.0 - 7.0	0.5 - 5.0	3.01±0.15	3.03±0.15	2.64±0.13	2.68±0.13	3.09±0.15	2.79±0.14

Note: FA – fatty acid; SFHO - sun flower "high oleic" oil; OO - olive oil; G-stoppers – ground-stoppers; PPS-plugs - polypropylene screwed plugs.

3.2. Identification of the FAMEs composition from lipid samples

Based on the minor impact on the final products and the good FAMEs yield, the optimized Ichihara-Fukubayashi method of slow methanolysis/methylation (at 45 °C, for 14 h) of lipid samples, placed in G-stoppers test tubes, was applied in the research of this study. The resulting FAMEs were analyzed by GC/FID (Figures 1-3), the structural formulas of the identified FA are shown in Table 2. On the Y axis is represented the relative response of the detector (rel. Response), and on the X axis – the retention time (t_R).

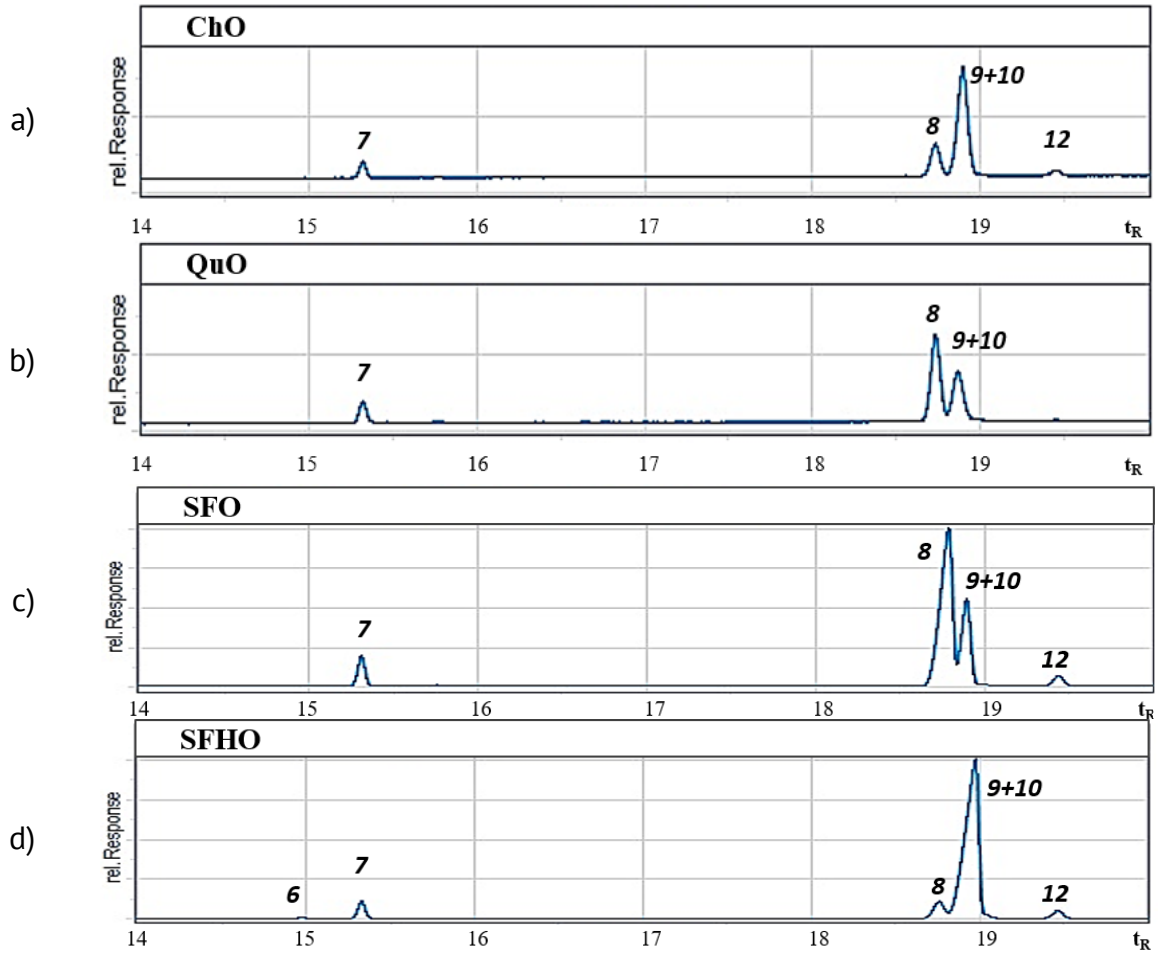

Figure 1. FAMEs C16 – C18 of a) Chia oil (ChO), b) Quinoa oil (QuO), c) Sunflower oil (SFO), d) Sunflower "high-oleic" oil (SFHO): 6 – palmitoleic; 7 – palmitic; 8 – linoleic; (9+10) – common peak of oleic and alpha-linolenic; 12 – stearic.

The FAMEs components identified on the chromatograms (Figure1a-d) are: 6 – palmitoleic acid (C16:1), visible in the SFHO sample; 7 – palmitic acid (C16:0), present in all samples, but with significant variations in intensity; 8 – linoleic acid (C18:2); 9+10 – co-eluent mixture of oleic acid (C18:1) and linolenic acid (C18:3); 12 – stearic acid (C18:0), detected in ChO, SFO and SFHO (Figure 3a, c, d), but less visible in QuO (Figure 3b). The common peak 9+10 is dominant in all samples, reflecting the high content of unsaturated fatty acids (oleic and/or linolenic).

All chromatograms of the seed oils show a moderate content of saturated acids and an unsaturated composition dominated by linoleic, oleic and α-linolenic acids. Although C18:1 and C18:3 acids give a common peak (9+10), the retention time of this peak is influenced by the ratio of the FAMEs concentration - linoleic:oleic:α-linolenic (Figure 1).

According to bibliographic sources, oil from different sunflower hybrids is classified into three groups: „ordinary" low oleic acid (10-29%), medium oleic acid (30-59%) and high oleic acid (60-90%) [34]. It is also known that sunflower oil contains a small amount (less than 0.2-0.5%) of α-linolenic acid [30,31], from which it follows that the major peak in the SFHO chromatogram belongs to oleic acid. These results are in accordance with the data indicated on the label of "high oleic" sunflower oil by the manufacturer, containing over 68.92 g of oleic acid per 100 mL of oil.

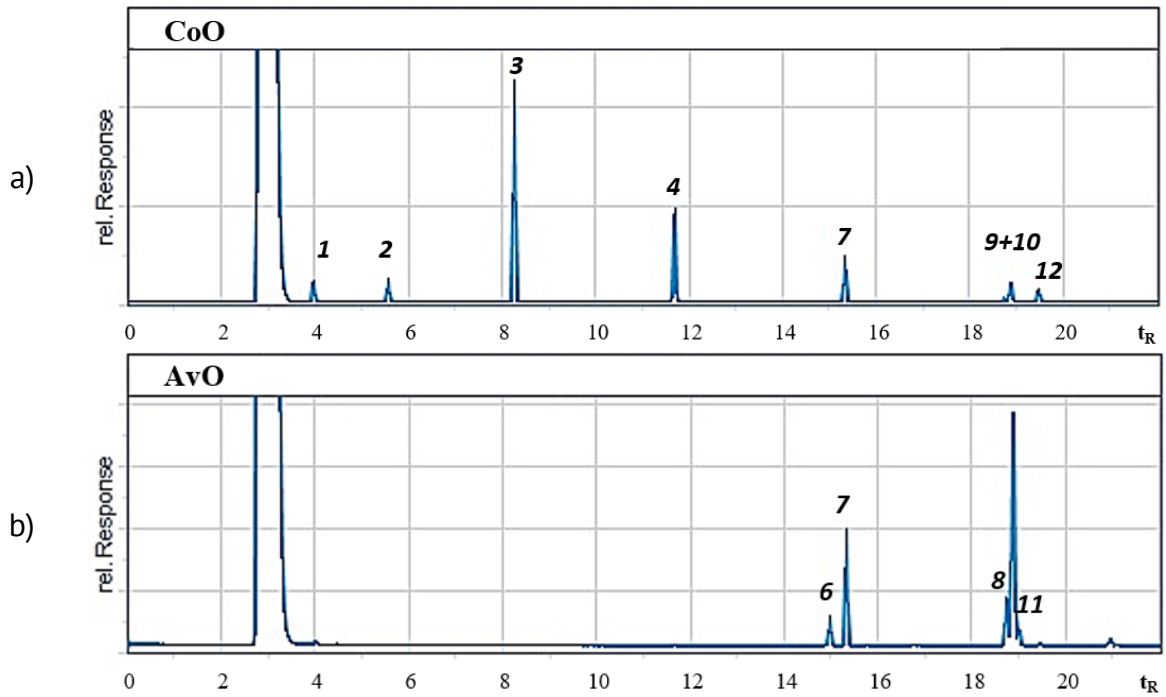

Figure 2. Nuts' FAMEs of: a) Cocoa oil (CoO), b) Avocado oil (AvO): 1 – caprylic; 2 – capric; 3 – lauric; 4 – myristic; 6 – palmitoleic; 7 – palmitic; 8 – linoleic; (9+10) – mixture of oleic and alpha-linolenic (common peak); 11 - elaidic; 12 – stearic.

The chromatograms in Figure 2 show the compositions of the CoO and AvO samples in methylated fatty acids. For coconut oil (Figure 2a), a profile dominated by short and medium chain FA results: caprylic acid (C8:0), capric acid (C10:0), lauric acid (C12:0), myristic acid (C14:0), palmitoleic acid (C16:1) and palmitic acid (C16:0). The majority peak is 3 (lauric acid) – typical for coconut oil [35]. In avocado oil (Figure 2b), the series of short and medium chain fatty acids is completely absent, the profile is rich in unsaturated FA: oleic/linolenic

(9+10) and linoleic (8) are dominant. The content of palmitoleic acid (6) is also notable, a signal specific for avocado oil [36,37].

The characteristic peaks of methyl esters of long-chain essential fatty acids with retention times more than 20 minutes were found in fish oil EFO_1 and EFO_2 (Figure 3a, b) The intensity of peaks 14 and 16 confirms the presence of increased amounts of EPA and DHA, respectively, which goes beyond the characteristics of regular fish oil. A typical fish oil provides 180 mg of EPA and 120 mg of DHA per 1000 mg of fish oil, but dosages can vary widely [38,39].

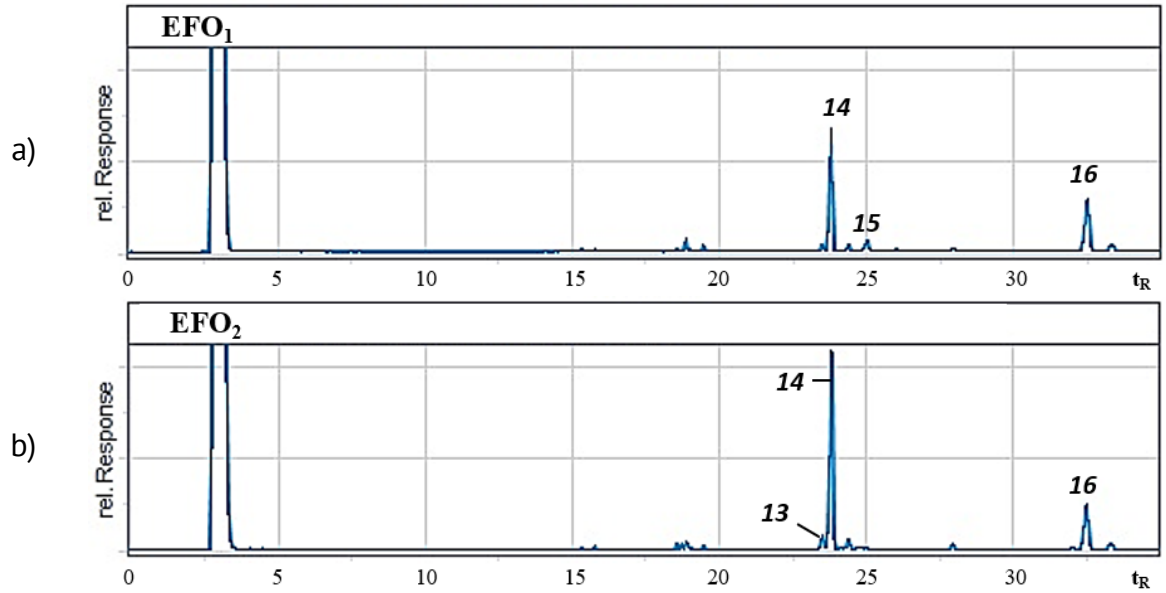

Figure 3. Fish Oil FAMEs C20 – C22 of: a) Dietary supplements from enriched fish oil "Solgar Inc" (EFO_1), b) Dietary supplements from enriched fish oil "Balcan Pharmaceutical Ltd" (EFO_2): 13 – arachidonic; 14 – eicosapentaenoic; 15 – eicosenoic; 16 – docosahexaenoic.

Table 2 represents the skeletal structural formulas of FA which were identified in all investigated samples. Only one trans-acid, C18:1-t *ω*9, called elaidic (or *trans*-oleic,) was detected in all of samples studied.

Table 2

Fatty acids detected by GC/FID

No	Fatty Acid	Code	Structure
1	Caprylic	8:0	COOH
2	Capric	10:0	COOH
3	Lauric	12:0	COOH
4	Myristic	14:0	COOH
5	Pentadecanoic	15:0	COOH
6	Palmitoleic	16:1 *ω*9	COOH
7	Palmitic	16:0	COOH
8	Linoleic	18:2 *ω*6	COOH
9	Linolenic	18:1 *ω*9	COOH
10	Oleic	18:3 *ω*3	COOH

Continution Table 2

11	Elaidic	18:1-t ω9	COOH
12	Stearic	18:0	COOH
13	Arachidonic	20:4 ω6	COOH
14	Eicosapentaenoic	20:5 ω3	COOH
15	Eicosenoic	20:1 ω9	COOH
16	Docosahexaenoic	22:6 ω3	COOH

The calculated FA mass fractions (%) of the total fatty acids contained in the analyzed samples are within the bibliographic data. Table 3 presents the values determined for the major FA identified in the research. Thus, according to literature data, CoO contains up to 7% caprylic acid, 5-8% capric acid, 48-55% lauric acid, 21-16% myristic acid, 9-10% palmitic acid, 3% stearic acid, 5-6.5% oleic acid and less than 0.01% linolenic acid [35], these data are similar to those in Table 3.

The values recorded for AvO and ChO fit into bibliographic data, which show that AvO contains 13-28% palmitic acid, 16% linoleic acid, 55-60% oleic acid and less than 1% α -linolenic acid [36,37]. ChO is rich in 6-8% palmitic acid, 18-21% linoleic acid, 4-10% oleic acid and up to 63% α -linolenic acid [40].

The recorded data correspond to those in the literature for linseed oil, containing 5-8% palmitic acid, 12-17% linoleic acid, 2-5% stearic acid, 17-19% oleic acid and 40-60% α-linolenic acid [41,42]. Also, the results in Table 3 are in line with those recorded by other researchers for QuO, rich in 60% linoleic acid, 20.5% oleic acid and 6.5% α-linolenic acid [43]. SFO contains 48-74% linoleic acid, 2.7-6.5% stearic acid, 14-39% oleic acid and less than 0.5% α-linolenic acid, according to the literature data [30,31].

Table 3

The composition of fatty acids in the form of methyl esters, %, determined in lipid samples by the modified Ichihara-Fukubayashi method

FA	CoO	AvO	ChO	FSO	QuO	SFO	EFO_1	EFO_2	t_R
8:0	4.98±0.19								3.97
10:0	5.05±0.19								5.57
12:0	47.2±1.8	0.20±0.01							8.26
14:0	20.72±0.76	0.71±0.03	0.05±0.01	0.06±0.01	0.14±0.01	0.09±0.01			11.69
15:0			0.02±0.01	0.03±0.02	0.07±0.01	0.02±0.01			13.50
16:1 ω9	0.21±0.01	5.31±0.19	0.09±0.01	0.16±0.01	0.23±0.02	0.12±0.01	0.21±0.02	0.04±0.01	14.96
16:0	10.56±0.39	20.06±0.71	7.09±0.38	6.41±0.32	10.02±0.53	6.93±0.34	0.45±0.03	0.35±0.02	15.33
18:2 ω6	1.18±0.05	11.62±0.41	18.66±0.98	16.16±0.80	49.5±2.6	61.4±3.1	0.38±0.03	1.12±0.07	18.77
18:1 ω9 18:3 ω3	6.06±0.23	55.2±2.0	68.9±3.6	70.8±3.5	32.2±1.7	26.0±1.3	2.82±0.18	1.88±0.11	18.94
18:1-t ω9	0.07±0.01	4.23±0.15			0.68±0.04	0.68±0.04	0.14±0.01	0.17±0.01	19.05
18:0	4.01±0.15	1.02±0.04	3.48±0.19	5.12±0.26	0.69±0.04	3.22±0.16	1.74±0.11	0.72±0.05	19.45
20:4 ω6							2.32±0.14	3.94±0.23	23.50
20:5 ω3							41.3±2.4	58.4±3.3	23.81
20:1 ω9				0.11±0.01	1.59±0.09		4.40±0.26	0.59±0.04	25.00
22:6 ω3							27.8±1.7	20.22±1.6	32.49
Others		1.62±0.06	1.71±0.09	1.12±0.06	4.86±0.26	1.56±0.08	18.5±1.1	5.11±0.29	4-42

Continution Table 3

N_{id}/N_{proc}	10/10	8/9	7/23	8/20	9/23	8/20	11/29	11/27	---
ε_{sample}	0.0367	0.0352	0.0522	0.0491	0.0522	0.0491	0.0580	0.0562	---
Bibliographic data about contain of Oleic and α-Linolenic acids [34-42]									
18:1 ω9	5 – 6.5	55 – 60	4 – 10	17 – 19	20.5	14 – 39	< 15.1	< 15.1	---
18:3 ω3	0.01	< 1.0	< 63	40 - 60	6.5	< 0.5	n/d	n/d	---
Sum	5 – 6.5	55 – 61	< 73	57 – 79	27	14 – 40	< 15.1	< 15.1	---

Note: FA – fatty acid; CoO - coconut oil;AvO - avocado oil; ChO - chia oil; QuO - quinoa oil; FSO - flax seed oil; SFO - sunflower oil; EFO_1 and EFO_2 - dietary supplements from enriched fish oil "Solgar Inc" and "Balcan Pharmaceutical Ltd"; t_R- retention time, min; N_{id} – identified FAMEs; N_{proc} – processed peaks; ε_{sample} – relative error for each oil sample.

Traditional fish oil typically contains 9.6% palmitoleic acid, 17.1% palmitic acid, less than 15% oleic acid, 2.7% stearic acid, 2.1% arachidonic acid, up to 18.6% EPA, and on average 14% DHA [38,39]. The EFO_1 and EFO_2 fish oil supplements analyzed in this study have increased EPA (41.3 and 58.4%) and DHA (27.8 and 20.22%), respectively, values indicated by manufacturers for fish oil supplements fortified with ethyl esters of the mentioned acids.

4. Conclusions

A convenient modification of Ichihara-Fukubayashi analysis method is pre-dilution of the oil sample with toluene in a ratio of 0.1:10.0 and further analysis of 202 microliters of the resulted solution, now containing 2 mg of oil. Heating the samples in test tubes with glass ground stoppers at 100°C result analysis failure. Test tubes with polypropylene screw plugs preserve the components better, but non-specific peaks or artifacts, probably originating from polypropylene, were detected in the FAMEs chromatograms. At the same time, fast methanolysis/methylation (100 °C, 1 h) led to a decrease in the yield of FA with C12-C16 chains. Therefore, only mild slow methanolysis/methylation at 45 °C for 14 h is optimal for FAMEs analysis. Because of the minor impact on the final products and the good yield of FAMEs, the optimized mild methanolysis/methylation method was applied to 8 types of vegetable oils and two types of fish oil dietary supplements. In the analyzed lipid samples, 16 fatty acids were identified qualitatively and quantitatively (from which linolenic and oleic as a sum, due to used column parameters) obtaining good correlation with bibliographical data. The modified Ichihara-Fukubayashi method is accessible and convenient because it uses reasonable quantities of samples and reagents.

Acknowledgements: The publication of this manuscript was supported by Institutional Project, subprogram 020405 "Optimizing food processing technologies in the context of the circular bioeconomy and climate change", Bio-OpTehPAS, being implemented at the Technical University of Moldova.

Conflicts of Interest: The authors declare that they have no conflicts of interest.

References

1. Benjamins, J.A.; Murphy, E.J; Seyfried, T.N. Chapter 5 – Lipids. Editors: Scott, T. B.; George, J. Siegel, G.J.; Wayne, R.A., Price, D.L. *Basic Neurochemistry* (Eighth Edition), Academic Press, 2012, pp. 81-100.
2. Gurev, A.; Dragancea, V. Organic Chemistry. Course Material . Tehnica-UTM, Chisinau, Republic of Moldova, 2023, 155 p. [in Romanian].
3. Coniglio, S.; Shumskaya, M.; Vassiliou, E. Unsaturated Fatty Acids and Their Immunomodulatory Properties. *Biology* 2023, 12, 279.
4. Chiu, H.H.; Kuo, C.H. Gas chromatography-mass spectrometry-based analytical strategies for fatty acid analysis in biological samples. *J. Food Drug Anal.* 2020, 28 (1), pp. 60–73.

5. Krone, N.; Hughes, B.A.; Lavery, G.G.; Stewart, P.M.; Arlt, W.; Shackleton, C.H. Gas chromatography/mass spectrometry (GC/MS) remains a pre-eminent discovery tool in clinical steroid investigations even in the era of fast liquid chromatography tandem mass spectrometry (LC/MS/MS). *J. Steroid Biochem. Molecular Biol.* 2010, 121 (3–5), pp. 496–504.
6. He, P.; Aga, D.S. Comparison of GC-MS/MS and LC-MS/MS for the analysis of hormones and pesticides in surface waters: advantages and pitfalls. *Anal. Methods* 2019, 11 (11), pp. 1436–1448.
7. Gurev, A.; Dragancea, V.; Druta, I. Health risks from toxic contaminants formed during the processing of vegetable oils and fats. *Journal of Engineering Science* 2024, 31(2), pp. 105-122. https://doi.org/10.52326/jes.utm.2024.31(2).10
8. Oils and Fats. Manual of Methods of Analysis of Foods. *AOAC 17th ed., 2015,* 96 p.
9. Nielsen, S.S. *Food Analysis*. Springer International Publishing, Switzerland, 2014, 602 p.
10. AOAC Official Method 2003.05. Crude fat in feeds, cereal grains, and forages. Randall/Soxtec/diethyl ether extraction-submersion method. Official Methods of Analysis of AOAC International 2003. International, Gaithersburg, MD, USA.
11. AOAC Official method 2003.06. Crude fat in feeds, cereal grains, and forages. Randall/Soxtec/hexanes extraction-submersion method. Official Methods of Analysis of AOAC International 2003. AOAC International, Gaithersburg, MD, USA.
12. AOAC Official Method 938.06. Fat in butter. Official Methods of Analysis of AOAC International. AOAC International 2013, Gaithersburg, MD, USA.
13. Matyash, V.; Liebisch, G.; Kurzchalia, T.V.; Shevchenko, A.; Schwudke, D. Lipid extraction by methyl-tert-butyl ether for high-throughput lipidomics. *J. Lipid Res.* 2008, 49 (5), pp. 1137–1146.
14. Amores, G.; Virto, M. Total and Free Fatty Acids Analysis in Milk and Dairy Fat. *Separations* 2019*, 6*, 14.
15. Folch, J.; Lees, M.; Stanley, G.H.S. A simple method for the isolation and purification of total lipides from animal tissues. *J. Biol. Chem.* 1957, 226, pp. 497–509.
16. Bligh, E.G.; Dyer, W.J. A rapid method of total lipid extraction and purification. *Can. J. Biochem. Phys.* 1959, 37, pp. 911–917.
17. Christie, W.W. *Lipid Analysis: Isolation, Separation, Identification and Structural Analysis of Lipids,* 3rd ed.; Bridgwater, England: Oily Press, 2005, 207 p.
18. Carrapiso, A. I.; Garcia, C. Development in lipid analysis: some new extraction techniques and in situ transesterifi cation. *Lipids* 2000, 35, pp. 1167 – 1177.
19. Nielsen, S.S.; Qian, M.C. Food Analysis Laboratory Manual. Gas-Chromatography 2017, Springer International Publishing, Switzerland, 2017, 244 p.
20. Ostermann, A.I.; Müller, M.; Willenberg, I.; Schebb, N.H. Determining the fatty acid composition in plasma and tissues as, fatty acid methyl esters using gas chromatography–a comparison of different derivatization and extraction procedures. Prostaglandins Leukot. *Essent. Fatty Acids* 2014, 91 (6), pp. 235–241.
21. Kramer, J.K.; Fellner, V.; Dugan, M.E.; Sauer, F.D.; Mossoba, M. M.; Yurawecz, M.P. Evaluating acid and base catalysts in the methylation of milk and rumen fatty acids with special emphasis on conjugated dienes and total trans fatty acids. *Lipids* 1997, 32 (11), pp. 1219–1228.
22. Koohi Kamali, S.; Tan, C.P.; Ling, T.C. Optimization of sunflower oil transesterification process using sodium methoxide. *Sci. World J.* 2012, pp. 1–8.
23. Carvalho, A. P.; Malcata, F. X. Preparation of Fatty Acid Methyl Esters for Gas-Chromatographic Analysis of Marine Lipids: Insight Studies. *J. Agric. Food Chem.* 2005, 53 (13), pp. 5049-5059. doi: 10.1021/jf048788i
24. Liu, K-S. Preparation of fatty acid methyl esters for gas chromatographic analysis of lipids in biological materials. *J. Am.Oil Chem. Soc.*1994, 71, pp. 1179 – 1187.
25. Kuksis, A. *Advances in Lipid Methodology – Two*. The Oily Press, Dundee, 1994, 71, pp. 115-116.
26. Knittelfelder, O.L.; Kohlwein, S.D. Derivatization and gas chromatography of fatty acids from yeast. *Cold Spring Harbor Protocols* 2017, 1 (5), 28461653.
27. Ichihara, K.; Fukubayashi, Y. Preparation of fatty acid methyl esters for gas-liquid chromatography. *J. Lipid Res.* 2010, 51 (3), pp. 635–640.
28. Dulf, F.V.; Pamfil, D.; Baciu, A.D.; Pintea, A. Fatty acid composition of lipids in pot marigold (*Calendula officinalis* L.) seed genotypes. *Chemistry Central Journal* 2013, 7 (1), 8. doi: 10.1186/1752-153X-7-8.
29. Weiss, M.F.; Martz, F.A.; Lorenzen, C.L. REVIEWS: Conjugated Linoleic Acid: Historical Context and Implications". *The Professional Animal Scientist* 2004, 20 (2), pp. 127–135. doi:10.15232/S1080-7446(15)31287-0

30. Harun, M. Fatty Acid Composition of Sunflower in 31 Inbreed and 28 Hybrid. *Biomed J Sci & Tech Res*. 2019, 16(3), pp. 12032-12038.
31. Ali, M.A.; Najmaldien, A.H.A.; Latip, R.A.; Othman, N.H.; Majid, F.A.A.; Salleh, L.M. Eff ect of heating at frying temperature on the quality characteristics of regular and high-oleic acid sunflower oils. *Acta Sci. Pol*., *Technol. Aliment*. 2013, 12(2), pp. 159-167.
32. Beltrán, P.C.; del Rio, C.; Sánchez, S.; Martínez, L. Influence of Harvest Date and Crop Yield on the Fatty Acid Composition of Virgin Olive Oils from Cv. Journal of Agricultural and Food Chemistry **2004***, 52 (*11), pp. 3434-3440.
33. Boskou, D. *Olive Oil. Chemistry and Technology*, Second Edition. AOCS Publishing, New York, USA, 2006, 288 p.
34. Lacombe, S.; Souyris, I.; Bervillé, A.J. An insertion of oleate desaturase homologous sequence silences via siRNA the functional gene leading to high oleic acid content in sunflower seed oil. *Mol Genet Genomics* 2009, 281(1), pp. 43-54. doi: 10.1007/s00438-008-0391-9. PMID: 18956214.
35. Handayani, U.F.; Wizna, Suliansyah I; Rizal, Y.; Mahata, M.E. The Evaluation of Dietary Addition of Palm and Coconut Oils in Steaming Tomato (*Lycopersicon esculentum*) Waste Powder on Digestibility of Crude Fiber and Retention of Lycopene and Nitrogen in Broiler Chickens. *J. World Poult. Res.* 2019*,* 9 (4), pp. 187-195.
36. Galvão, M.D.S.; Narain, N.; Nigam, N. Influence of different cultivars on oil quality and chemical characteristics of avocado fruit. *Food Sci. Technol*. 2014, 34, pp. 539–546. doi: 10.1590/1678-457x.6388.
37. Flores, M.; Reyes-García, L.; Ortiz-Viedma, J.; Romero, N.; Vilcanqui, Y.; Rogel, C.; Echeverría, J.; Forero-Doria, O. Thermal Behavior Improvement of Fortified Commercial Avocado (*Persea americana Mill.*) Oil with Maqui (*Aristotelia chilensis*) Leaf Extracts. *Antioxidants* 2021, 10, 664.
38. Matías, J.; Rodríguez, M.J.; Granado-Rodríguez, S.; Cruz, V.; Calvo, P.; Reguera, M. Changes in Quinoa Seed Fatty Acid Profile Under Heat Stress Field Conditions. *Front. Nutr.* 2022, 9, 820010.
39. Irnawati, I.; Nadia, L.O.M.H; Windarsih, A.; Riswanto, F.D.O.; Putri, A.R.; Rohman, A.; Ambardini, S. Fatty acid composition, biological activity and authentication of marine fish oil. *Food Research* 2023, 7(6), pp. 187-196.
40. Ayerza, R.; Coates, W. Composition of chia (*Salvia hispanica*) grown in six tropical and subtropical ecosystems of South America. *Trop. Sci.* 2004, 44, pp. 131–135.
41. Gandova, V.; Teneva, O.; Petkova, Z.; Iliev, I.; Stoyanova, A. Lipid Composition and Physicochemical Parameters of Flaxseed Oil (Linum usitatissimum L.) from Bulgaria. *Appl. Sci.* 2023, 13, 10141.
42. Guimaraes, R.D.C.A.; Macedo, M.L.R.; Munhoz, C.L.; Filiu, W.; Viana, L.H.; Nozaki, V.T.; Hiane, P.A. Sesame and flaxseed oil: nutritional quality and effects on serum lipids and glucose in rats. *Food Sci Technol.,* (Campinas) 2013, 33(1), pp. 209–217.
43. Matías, J.; Rodríguez, M.J.; Granado-Rodríguez, S.; Cruz, V.; Calvo, P.; Reguera, M. Changes in Quinoa Seed Fatty Acid Profile Under Heat Stress Field Conditions. *Front. Nutr.* 2022, 9, 820010.

Citation: Baerle, A.; Gurev, A.; Dragancea, V.; Subotin, Iu.; Druta, R. Fatty acid methyl esters GC/FID analysis using Ichihara-Fukubayashi modyfied method. *Journal of Engineering Science*. 2025, XXXII (2), pp. 133-145. https://doi.org/10.52326/jes.utm.2025.32(2).12.

Submission of manuscripts: jes@meridian.utm.md